International Conference

On

Futuristic Trends in Engineering, Science, Humanities, and Technology
FTESHT-16

January 23 – 24, 2016

VOLUME-1

Editor

Dr. P.S. Chauhan

Convener, FTESHT-2016

Organised by

IPS College of Technology & Management
Gwalior, Madhya Pradesh (India)
in
Association with
TRO INDIA

Preface

It gives us immense pleasure to present the proceeding of the International Conference on Futuristic Trends in Engineering, Science, Humanities, and Technology (FTESHT-2016) to be held during January 23-24, 2016 in the IPS College of Technology & Management.

One of the major objectives of the present International Conference is to provide a platform for Scientists, Technocrats and Researchers to share and exchange views on the opportunity and challenges offered by the ever increasing technological advancement taking place in the world.

There has been excellent response from various sections which is evident from the contributions received through valuable articles. We sincerely acknowledge and express our gratitude to the reviewers for their great contribution in selecting the worthy articles and facilitating the process of publication.

We take this opportunity to thank International and National Advisory Committee members and reviewers for their guidance and timely help. We also appreciate the efforts of my colleagues, members of the staff and students to make this event successful. We hope that the proceedings gets your appreciation.

Place: Gwalior, M.P., India   Dr. P. S. Chauhan
Date: January 23, 2016   Convener

Shivraj Singh Chouhan

Chief Minister

Government of Madhya Pradesh
BHOPAL - 462 004
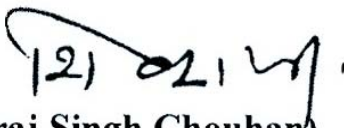
S.No. - **20, January 14, 2016**

Message

I am delighted to know that IPS College of Technology and Management, Gwalior is organizing an international conference on Futuristic Trends in Engineering, Science, Humanities and Technology (FTESHT-2016).

Innovations in science and technology aiming at human welfare need encouragement. The State Government is promoting scientific temperament among the masses so that optimum benefits of scientific advancement could be harnessed in an enthusiastic fashion.

I hope the conference will be a grand success with the renowned professionals sharing their insights on the subject.

Regards.

(Shivraj Singh Chouhan)

Shri Anoop Mishra
Hon'ble Member of Parliament (Morena)
Government of India

January 12, 2016

<u>Message</u>

With the advent of new technologies, new avenues are opening up. Emergence of new Technology is also throwing up new challenges. In the context of the new challenges educational Institutions need to constantly review, update knowledge and adopt technology driven skills. This is possible through mutual exchange of thoughts and sharing of knowledge and skills.

I am quite sure that this International Conference on "Futuristic Trends in Engineering, Science, Humanities & Technology" will provide a unique opportunity of sharing and equipping trends and latest research works.

It is my heart-felt wish that this event becomes a successful forum of exchange of ideas and knowledge for one and all.

Regards.

Anoop Mishra

Prof. Piyush Trivedi
Vice Chancellor

राजीव गांधी प्रौद्योगिकी विश्वविद्यालय, म.प्र.
(मध्यप्रदेश का तकनीकी विश्वविद्यालय)

Rajiv Gandhi Proudyogiki Vishwavidyalaya, M.P.
(State Technological University of Madhya Pradesh)

DO Letter No. : vc/ps/2016/693

दिनांक / Date : 12/01/2016

MESSAGE

I am happy to learn that the **IPS College of Technology & Management, Gwalior** is organizing the International Conference on **"Futuristic Trends in Engienering, Science, Humanities & Technology (FTESHT-2016"** on January 23-24, 2016.

I hope this Internationl Conference will provide an excellent platform for developmental and research activities in the field of Science, Humanities and Engineering.

I am sure that deliberations made by the experts will be beneficial for advancement of science and technology.

It is a laudable effort of the organizers for choosing a very relevant and active field of research. Conducting the Conference as above, are vital part of quality improvement activities for all the stake holders viz a viz researchers, faculty, academecia and Students community.

I extend my warm greetings to the organizers and hope that the Conference will attain its desired goals.

Prof. Piyush Trivedi 12/01/16

Smt. Shobha Mishra
Chairperson
IPS Group of Colleges

January 11, 2016

<u>Message</u>

"Vision looks inward & becomes duty

Vision looks outward & becomes aspiration

 Vision looks upward & becomes faith"

When the vision of duty, aspiration and faith become a reality, it becomes a proud moment for me and my team to see professionals, students and researchers come together to work collectively towards a better society.

The International Conference on "Futuristic Trends in Engineering, Science, Humanities & Technology" is being organized with a view to provide a platform to the professionals, scientists and students to work together for a just and better society.

I extend warm greetings to all those associated with the conference and wish the conference a grand success.

Shobha Mishra

Dr. Arun K. Tyagi
Director
IPS Group of Colleges

January 11, 2016

<u>Message</u>

Education is simply the soul of the society as it passes from one to another.

G.K. Chesterton

The world is moving very fast & new technologies are coming every week. We need to be proactive & enthusiastic in learning about these cutting edge tools and research.

New technology is bringing opportunities along with new set of skills and new challenges. Interaction in person is the best mode of communication to know the development taking place in Science, Technology & Engineering.

IPS constantly strives to meet challenges of future by fostering education and technical advancement. This conference is an effort in the similar direction. It aims at keeping pace with technological development taking place globally and bridging the technology gaps.

I am quite optimistic about the success of the conference and wish it gives a qualitative outcome for global educational growth and development.

Best wishes….!!!

Dr. Arun K. Tyagi

Mr. Ashwini Mishra
Deputy Director
IPS Group of Colleges

January 11, 2016

<u>Message</u>

I am delighted to know that the IPS is organizing an International Conference on "Futuristic Trends in Engineering, Science, Humanities & Technology."

Knowledge is a liberating force which helps in removing the barriers of prejudices and ignorance and facilitates eliminating the various disparities between human beings. Knowledge has also come a long way, from being power to becoming powerful vision.

I am sure this conference will prove a step-ahead in the same direction and achieve the ultimate target of global academic success.

I offer my best wishes and greetings to all the participants and wish good luck and grand success.

Ashwini Mishra

Mr. P. K. Ghosh
CAO
IPS Group of Colleges

January 11, 2016

Message

It is a matter of great happiness for me to know about the initiative being taken by the teaching community and students of IPS College of Technology & Management for having conceived and organize an International Conference.

The theme of the International Conference is appropriate in the present context. I am sure the conference will bring Engineers, Technocrats and Professional on a common platform, for exchange of views and sharing updated knowledge which will go a long way as a value addition to the education system.

I wish the organizers and participants the very best in their endeavor and am confident that the event will be a great success.

 I extend my sincere greetings.

P. K. Ghosh

International Advisory Committee

Dr. M. Rahman. Professor, National University of Singapore
Dr. Madhavi Singh, Penn State Hershley Medical Group Park Avenue, USA
Dr. Dariusz Jacek Jakóbczak, Professor, Technical University of Koszalin, Poland
Dr. Khalid Mahmoud Abd Elghany, Director of CAD/CAE and RPM Lab, CMRDI, Egypt

National Advisory Committee

Dr. V. K. Jain, Professor, IIT Kanpur
Dr. Rabi Pradhan, Associate Professor, IIT Kharagpur
Dr. Uday S. Dixit, Associate Professor & Head, IIT Guwahati
Dr. R. S. Jadon, Professor, G. B. Pant University, Pant Nagar
Dr. Manpreet Singh Manna, Director, AICTE, New Delhi
Mr. Alok Mathur, General Manager- Production, JK Tyre, Banmore
Dr. A. Lakshmi Devi, Professor, SVU College of Engineering, Sri Venkateswara University
Prof. Shravani Badiganchala, Shirdi Sai Institute of Science and Engineering
Dr. Bhasker Gupta, Jaypee University of Information Technology, Himachal Pradesh, India
Prof Amit R. Wasnik, Sinhgad Institute of Technology, Lonavala, Pune Maharashtra (SIES Group)
Prof. M. K. Sharma Amrapali Institute, Haldwani
Dr. Arjun Pralhad Ghatule, Sinhgad Institute of Computer Sciences (SICS), Korti
Prof. Abhay Saxena Sanskrit Vishavvidyalaya, Haridwar
Dr. G.Suresh Babu, Professor, CBIT, Hyderabad, Andhra Pradesh
Prof. Sanjay Ramchandra Kumbhar, Rajarambapu Institute of Technology, Rajaramnagar, Maharashtra
Dr. Punyaban Patel, Chhatrapati Shivaji Institute of Technology, Durg
Prof. Dipak S.Bajaj, Amrutvahini College of Engineering, Sangamner
Dr. Rajeev Agrawal, Birla Institute of Technology (Deemed University), Ranchi, Jharkhand
Dr. Hansa Jeswani, Sardar Patel College of Engineering, Mumbai, Maharashtra
Dr. S. P. Anandaraj, Sr. Asst. Professor, Dept. of Computer Science, SR Engineering College
Dr. Chandrakant R. Sonawane, Dyanganga College of Engineering & Research, Pune
Prof. Deepika Vodnala, Assistant Professor, SREC, Warangal
Prof. Subzar Ahmed Bhat, Assistant Professor, GLA University
Mr. I. Hameem Shanavas, Department of ECE, M.V.J College of Engineering, Bangalore
Mr. K. Maheshkumar, Bannariamman Institute of Technology, Sathy
Mr. B. Sudheer Kumar, Placement Officer, Vaagdevi Institute of Technology & Science
Mr. Krishna Nand Pandey, Galgotias College of Engineering & Technology, Greater Noida
Mr. Vishal J. Deshbhratar, Assistant Professor, ITM COE, Kamptee, Nagpur
Mr. Ram Indrajit Chavan, BITS Pilani, K. K. Birla Goa Campus, Goa
Mr. Sanjith J, P.G. Coordinator, Adhichunchanagiri Institute of Technology, Karnataka
Mr. Jeetendra Bhawsar, Medi-Caps Institution of Technology and Management, Indore

Organizing Committee
Patrons

Mrs. Shobha Mishra	Chairperson, IPS GOC
Dr. Arun K. Tyagi	Director, IPS GOC
Mr. Ashwani Mishra	Deputy Director, IPS GOC
Mr. P. K. Ghosh	CAO, IPS GOC

Convener

Dr. P.S. Chauhan	Principal, IPS College of Technology & Management

Secretary

Dr. Jagat Mishra	Director, TRO India
Dr. R.K. Dwivedi	Associate Professor, MANIT, Bhopal

Reception Committee

Dr. Atul Kaushik	Principal, IPS College of Pharmacy
Dr. Rama Tyagi	Principal, Institute of Professional Studies
Dr. P.S. Chauhan	Principal, IPS College of Technology & Mgmt
Dr. Ashutosh Trivedi	Dean, Research & Development
Prof. Ramesh Kumar Batra	Head, Dept. of Civil Engineering
Prof. V. K. Jain	Head, Dept. of Mechanical Engineering
Dr. Jyoti Mishra	Head, Dept. of Applied Sciences & Humanities
Prof. Anurag Garg	Head, Dept. of Electronics & Comm. Engineering
Prof. Karunendra Verma	Head, Dept. of Computer Science &Engineering
Prof. Alok Pathak	Head, Dept. of Electrical Engineering
Prof. Anil Singh	Head, Dept. of Management
Prof. Rajeev Shrivastava	Head, Dept. of Finishing School

Conference Coordinators

Mr. Anurag Garg	Head, Dept. of Electronics & Comm. Engineering
Mr. R.P. Singh	Faculty, Dept. of Mechanical Engineering
Mr. Karunendra Verma	Head, Dept. of Computer Science &Engineering
Mr. Pankaj Agrawal	Faculty, Dept. of Electronics & Comm. Engineering
Mr. Sumit Tiwari	Faculty, Dept. of Computer Science &Engineering
Dr. Rajiv Dwivedi	Faculty, Dept. of Applied Sciences & Humanities
Mr. Ramani Ranjan Pandey	Junior Engineer, NSPCL
Mr. Santosh Mukerjee	Manager, TROINDIA

Functional Committees

Sr. No	Committee	Faculty Members
1	Registration Committee	Mr. Karunendra Verma (Coordinator) Mrs. Ritika Keswani Ms. Arti Vig
2	Welcome Committee	Mrs. Anupma Agrawal (Coordinator) Mr. Anurag Garg Mr. Sumit Tiwari Ms. Deepti Bhargava
3	Accommodation Committee	Mr. Pankaj Goyal (Coordinator) Mr. R. P. Singh Mr. Anand Bhatnagar Mr. Prabhu Dayal Mr. Maheshwari Prasad
4	Technical Session Committee	Mr. V.K. Jain (Coordinator) Mr. R. K. Batra Dr. Jyoti Mishra Mr. Anurag Garg Mr. Karunendra Verma Mr. Alok Pathak
5	Printing & Publication Committee	Mr. Pankaj Goyal (Coordinator) Mr. Shatrughan Mishra Mr. Ganesh P. S. Jadon Mr. Suresh Dixit
6	Logistics Committee (Venue)	Mr. Shatrughan Mishra (Coordinator) Mr. Juber Qureshi Mr. Ashutosh Bansal Mr. Hitendra Parhak
7	Food & Refreshment Committee	Mr. Sourabh Agrawal (Coordinator) Mr. Akash Agrawal Mr. Ravi Chourasia
8	Transportation Committee	Mr. Pankaj Goyal (Coordinator) Mr. Sumit Nigam Mr. Manvendra Gautam Mr. Maheshwari Prasad
9	Cultural Committee	Mr. Sudhir Sharma (Coordinator) Mrs. Anupama Agrawal Ms. Deepti Bhargava
10	Certification Committee	Dr. Rajeev Dwivedi (Coordinator) Mr. Manoj Sharma Mr. Sumit Pathak Mrs. Mukta Shrivastava
11	Invitation Committee	Dr. Jyoti Mishra (Coordinator) Dr. Snehika Shrivastava Dr. Alka Pradhan Mrs. Anupama Agrawal

12	Electrical Power Supply Committee	Mr. Alok Pathak (Coordinator)
		Mr. Sanjay Kulshreshtha
		Mr. Neeraj Pandey
13	Videography & Photography Committee	Mr. Ranjeet P. Singh (Coordinator)
		Mr. Suresh Dixit
14	Flex designing Committee	Mr. Kapil Keshwani (Coordinator)
		Mr. Vineet Raj Singh Kushwah
		Mr. Manvendra Gautam

For any assistance or clarification, contact Dr. P.S. Chauhan, Convener of this event.

Dr. Arun K. Tyagi
Patron – FTESHT 2016,
IPS College of Technology & Management,
Shivpuri Link Road, Gwalior,
Madhya Pradesh – India 474001

TABLE OF CONTENTS

SL NO	TITLE/AUTHOR	PAGE NO

Dr. Elammaran Jayamani
Faculty of Engineering, Computing and Science
Swinburne University of Technology Sarawak
Campus Malaysia
E-mail: ejayamani@swinburne.edu.my
Phone: +60-16-5774867

January 23, 2016

KEYNOTE SPEECH

Green Manufacturing

Abstract

Green Manufacturing is a challenge for today but as business opportunities for tomorrow. This work presents the importance of Green manufacturing. This concept focuses on both how the product is made as well as the product's attributes. Nowadays customers are environment conscious and also the environmental protection is a top agenda for them. They are thinking about the global issues such as global warming, depletion of the Ozone layer, running out of fossile fuel supply and loss of trees and forest.

The detailed discussion of the intersection of the environment and manufacturing been discussed related to Green manufacturing, clean technologies and Green products, this work also covers things such as making products with less energy and materials, producing less waste, and fewer hazardous materials as well as products that have greener attributes.

Dr. Joydip Dhar (PhD-IITK)
Associate Professor
Department of Applied Sciences
ABV-Indian Institute of Information Technology and Mgmt
Gwalior-474010, M.P., India
E-mail: jdhar@iiitm.ac.in
Phone: +91-751-2449829

January 23, 2016

KEYNOTE SPEECH

Fundamentals of Mathematical Model Development for Basic Sciences

Abstract

The problems that modelers wish to solve exist in the real world. First step is to simplify the real world to create a model world, i.e., the model world leaves out much of the complexity of the real world problem. The original question gets translated into a question involving the model world. Next, we construct a model of the problem in the model world using known mathematical tolls and techniques. The final step is to interpret the answer found for the model world problem back in the real world. "Every study must begin with a clear statement of the study's overall objectives and specific issues to be addressed; without such a statement there is little hope for success". Modeling is a way of thinking and reasoning about systems. The goal of modeling is to come up with a representation that is easy to use in describing systems in a mathematically consistent manner. Models based on good theory can compensate for lack of data, and models based on broad evidence can compensate for lack of theory, but models alone can hardly compensate for the lack of both. We often fail to realize how little we know about a thing until we attempt to simulate it on a computer.

Dr. Karmveer Arya
(M.Tech – IISc, Banglore, PhD-IITK)
Associate Professor
ABV-Indian Institute of Information Technology and Mgmt
Gwalior-474010, M.P., India
E-mail: kvarya@iiitm.ac.in
Phone: +91-751-2449830

January 23, 2016

KEYNOTE SPEECH

Restoration from Noisy and Motion Blurred Images
Abstract

Generally the images captured in uncontrolled environment have degraded quality as compared to the original images due to imperfections in the imaging and capturing process. The degraded images are classified into two major categories: (i) blurred imaged and (ii) noisy images. The factors responsible for blurring of images in general are: atmospheric turbulence, defocusing of the lens, aberration in the optical systems, relative motion between the camera and scene. The restoration of such blurred images sometimes becomes mandatory particularly in surveillance applications. The effectiveness of the restoration process mainly depends on the blurring system model. The motion blur system is characterized by two parameters, namely, blur direction and blur length. Various methods for the identification of blur parameters have been proposed in literature. The popular methods used for determination of point spread function (PSF) parameters in the spectral domain will be discussed. The talk will focus on the algorithms to determine motion blur PSF parameters, i.e., blur direction and blur length, in frequency domain. The blur direction is identified using Hough transform to detect the orientation of line in the log magnitude spectrum of the blurred image. The blur length is found by rotating the binarized spectrum of the blurred image in the estimated direction. These parameters are the used to restore the images. A modified Weiner filter is then employed for restoration of images.

REVIEW ON INFORMATION SECURITY MANAGEMENT

Madhavi Dhingra
Asst. Prof., Amity University Madhya Pradesh
Email: madhavi.dhingra@gmail.com

Abstract:
Currently, all organizations have to tackle the issue of information security. The paper deals with various aspects of Information Security Management (ISM), including procedures, processes, organizational structures, policies and control processes. Introduction of Information Security Management should be a strategic decision. The concept and implementation of Information Security Management in an organization are determined by the corporate needs and objectives, security requirements, the processes deployed as well as the size and structure of the organization. The implementation of ISM should be carried out to the extent consistent with the needs of the organization.

Keywords: information security; information security policy; asset management of organization; business continuity management; management of intrusion

1. Introduction

An information security management system (ISMS) is a set of policies concerned with information security management or IT related risks. Security management is becoming a strategic, tactical and operational objective of almost any enterprise or organization. In the public sector, the development of e-government applications becomes possible only if IT-risks are correctly managed.

2. Security Management

Security management involves user authentication and identity management, digital rights management and data integrity, certificate management for Public Key Infrastructures (PKI).

User authentication is the starting point of making IT-systems more secure. It is also one of the most critical weaknesses of many internet-based systems, since attackers often try to get access to the system by using the identity of another user. Password identification is no longer considered as being secure, so alternatives must be searched. Most of the present approaches rely on strong authentication, combining a secret the user knows, with something he holds (for instance some portable memory device). On the other hand, experiences in biometrics have not been fully satisfying until now. As a consequence, it is important to explore new means of authentication and to evaluate the efficiency of these approaches. Very often authentication is only done at the entry point of an IT-system. Today this is no longer sufficient, since an attacker could get access to any point of the IT-system; so it is important to generalize the authentication model to all interactions between hard- or software components. Therefore completely new approaches in system design and threat modelling are needed.

Authentication is only as strong as the user management processes and these rely on efficient identity policies. Identity management has become an active research topic since the events of 9-11 and the subsequent growing awareness of the dangers of terrorism. All countries now have the problem of correctly identifying each member of the society, as the old identification schemes are outdated. The Luxembourg national personal identity number for instance is based on the date of birth and the sex of the identified person. This is no longer in accordance with the modern requirements of protection of personal data, where there should

be no information leaking from the identification data.

One way of authentication and identity management relies on the use of a Public Key Infrastructure. Such a highly secure infrastructure requires very important investments and an excellent technical, organizational and legal know-how. Therefore it is essential to explore new business cases for these infrastructures, which cannot survive in selling only identity certificates.

3. Information Security Cycle

ISO/IEC 27001:2005 therefore incorporated the "Plan-Do-Check-Act" (PDCA), or Deming cycle, approach:
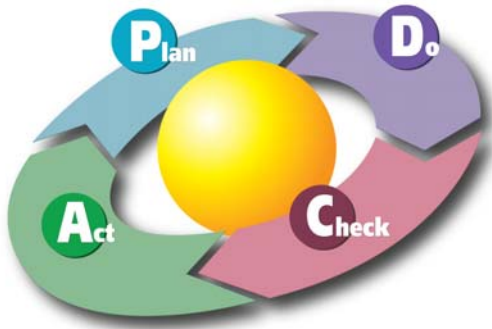

Figure 1: PDCA or Deming Cycle used by ISMS Standards

- The Plan phase is about designing the ISMS, assessing information security risks and selecting appropriate controls.
- The Do phase involves implementing and operating the controls.
- The Check phase objective is to review and evaluate the performance (efficiency and effectiveness) of the ISMS.
- In the Act phase, changes are made where necessary to bring the ISMS back to peak performance.

ISO/IEC 27001:2005 is a risk based information security standard, which means that organizations need to have a risk management process in place. The risk management process fits into the PDCA model given above.

4. Need for an Information Security Management System

Security experts say:

- information technology security administrators should expect to devote approximately one-third of their time addressing technical aspects. The remaining two-thirds should be spent developing policies and procedures, performing security reviews and analyzing risk, addressing contingency planning and promoting security awareness;
- security depends on people more than on technology;
- employees are a far greater threat to information security than outsiders;
- Security is like a chain. It is only as strong as its weakest link;
- the degree of security depends on three factors: the risk you are willing to take, the functionality of the system and the costs you are prepared to pay;
- Security is not a status or a snapshot, but a running process.

These facts inevitably lead to the conclusion that security administration is a management issue, and not a purely technical issue.

The establishment, maintenance and continuous update of an ISMS provide a strong indication that a company is using a systematic approach for the identification, assessment and management of information security risks.

5. Critical factors of Information Security Management System ISMS

Confidentiality: Protecting information from unauthorized parties.
Integrity: Protecting information from modification by unauthorized users.
Availability: Making the information available to authorized users.
A company will be capable of successfully addressing information confidentiality, integrity and availability (CIA) requirements which in turn have implications:

- business continuity;
- minimization of damages and losses;
- competitive edge;

- profitability and cash-flow;
- respected organization image;
- legal compliance

Large organizations, banks and financial institutes, telecommunication operators, hospital and health institutes and public or governmental bodies have many reasons for addressing information security very seriously. Legal and regulatory requirements which aim at protecting sensitive or personal data as well as general public security requirements impel them to devote the utmost attention and priority to information security risks.Under these circumstances, the development and implementation of a separate and independent management process - namely an ISMS - is the only alternative.

The development of an ISMS framework based on ISO/IEC 27001:2005 entails the following six steps:

- Definition of security policy,
- Definition of ISMS scope,
- Risk assessment (as part of risk management),
- Risk management,
- Selection of appropriate controls
- Statement of applicability

6. Issues in Information Security Management System

There are three main problems which lead to uncertainty in information security management systems (ISMS):

1. Dynamically changing security requirements of an organization -Rapid technological development raises new security concerns for organizations. The existing security measures and requirements become obsolete as new vulnerabilities arise with the development in technology. To overcome this issue, the ISMS should organize and manage dynamically changing requirements and keep the system up-to-date.

2. Externalities caused by a security system Externality is an economic concept for the effects borne by the party that is not directly involved in a transaction. Externalities could be positive or negative. The ISMS deployed in an organization may also cause externalities for other interacting systems. Externalities caused by the ISMS are uncertain and cannot be predetermined before the ISMS is deployed. The internalization of externalities caused by the ISMS is needed in order to benefit internalizing organizations and interacting partners by protecting them from vulnerable ISMS behaviors.

3. Obsolete evaluation of security concerns The evaluations of security concerns used in ISMS become obsolete as the technology progresses and new threats and vulnerabilities arise. The need for continuous security evaluation of organizational products, services, methods and technology is essential to maintain an effective ISMS. The evaluated security concerns need to be re-evaluated. A continuous security evaluation mechanism of ISMS within the organization is a critical need to achieve information security objectives. The re-evaluation process is tied with dynamic security requirement management process discussed above.

7. Conclusion

The chief objective of information security management is to implement the appropriate measurements in order to eliminate or minimize the impact that various security related threats and vulnerabilities might have on an organization. In doing so, information security management will enable implementing the desirable qualitative characteristics of the services offered by the organization (i.e. availability of services, preservation of data confidentiality and integrity etc.). By preventing and minimizing the impacts of security incidents, ISMS ensures business continuity, customer

confidence, protect business investments and opportunities, or reduce damage to the business.

References

1.   Humphreys, Edward (8 March 2011). "Information security management system standards". Datenschutz und Datensicherheit : 7–11.

2. Jo, Heasuk; Kim, Seungjoo; Won, Dongho (1 January 2011). "Advanced information security management evaluation system". KSII Transactions on Internet and Information Systems 5(6): 1192–1213.

3. Caballero, Albert. (2009). "14". Computer and Information Security Handbook. Morgan Kaufmann Publications. Elsevier Inc. p. 232. ISBN 978-0-12-374354-1.

4.Ma, Qingxiong; Schmidt, Mark B.; Pearson, Michael (2009). "An integrated framework for information security management". Review of Business 30 (1): 58–69. Retrieved 26 October 2013.

5. Abbas, Haider; Magnusson, Christer; Yngstrom, Louise; Hemani, Ahmed (1 January 2011). "Addressing dynamic issues in information security management". Information Management & Computer Security 19 (1): 5–24.

SHEAR DEFORMABILITY CHARACTERISTICS OF FRP (FIBER-REINFORCED POLYMER) STRENGTHENED RC BEAM

Shubham Kumar[1], Shilpa Pal[2], H. C. Arora[3]
[1]P.G Scholar, Civil Engineering, Gautam Buddha University
[2]Asst. Prof. Civil Engineering, Gautam Buddha University
[3]HOD, Asst. Prof., Civil Engineering, Gautam Buddha University, CSIR – CBRI
Email: Shubhamthakur22@gmail.com[1], Sh6281pa@gmail.com[2], hc.arora@rediffmail.com[3]

Abstract— Deterioration of concrete structures leading to its failure & collapse is most common problem of construction industry. Failures that can be predicted before actual collapse of structure are still safer than the failures which are difficult to predict accurately leading to sudden collapse of structure, called shear or diagonal tensional failure. Since complete replacement of structure takes huge amount of money, it is beneficial to strengthen such critical members in shear. The use of corrosion resistant, light weight and strong Fiber-Reinforced Polymer (FRP) is most beneficial method. This paper presents comprehensive review on Shear behavior of FRP strengthened beam. The review covers past efforts in FRP strengthening against shear failure using EBR method and also validates the literature by experimental programs done by investigators. Concept of shear failure, application of FRP in Civil Engineering and recommendations for future research are also presented.

Index Terms— Externally Bonded Reinforcement (EBR), Fiber-Reinforced Polymer (FRP), Shear failure, Shear resistance.

I. INTRODUCTION

In the rapid urbanization, reinforced concrete is widely used material. It has extensive use all over the world in construction industry. The main advantages that lead to increase in uses of reinforced concrete are chemical resistance, high modulus of elasticity, freeze thaw resistance and low permeability, creep and shrinkage. Besides these various advantages there are various types of failure modes that exist in reinforced concrete structures. The predominant failure in reinforced concrete beam and other critical structural components is diagonal tension failure or shear failure which is sudden and gives no pre attention and warning to his user. Various researches had been carried out an numerous experiments had been performed on beams with and without web reinforcement and found following factors that influences the behavior of beams in shear. Those factors are shear span to effective depth ratio (a_v/d), aggregate type, longitudinal steel ratio, loading type, concrete strength and support conditions of member.

The main objective of all researchers is to find the accurate judgment of shear failure or to predict the more accurate shear strength capacity of structure. When a beam is loaded, it is subjected to two main components shear force and bending moment. Variation of shear force is such that it will be maximum when bending moment is minimum and will be minimum when bending moment is maximum. These components when acts on a member can lead to its failure by following ways also shown in Fig. 1.

(1) Diagonal Tension Failure/Shear Failure
This failure occurs under large shear force and lesser bending moment resulting in formation of cracks at 45°.

(2) *Flexure Tension Failure*
This failure occurs under large bending moments and cracks are at 90°.

(3) Diagonal Compression Failure
This failure occurs under large shear force when beam is reinforced against heavy shear leading to crushing of concrete.
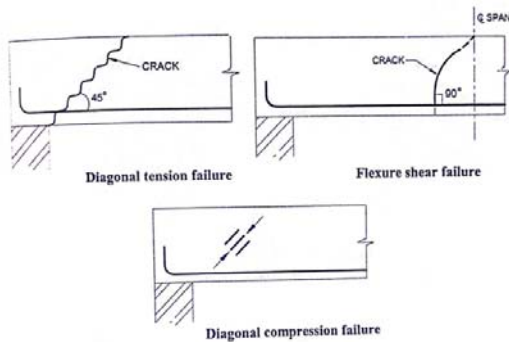

Fig. 1. Types of failure

II. SHEAR FAILURE

Shear failure of reinforced concrete beam more properly called diagonal tension failure is difficult to predict accurately[13]. These failure are undesirable because of their brittle nature which does not allow any warning or little warning. These failure occur under action of large shear force and less amount of bending moment and finally leading to development of cracks at 45° to the horizontal surface as shown in Fig. 2. When principal tensile stress reaches to tensile strength of concrete, cracks will occur and opens normal to the direction of principal tensile stress or in other words parallel to the direction of principal compressive stress. Therefore the shear forces generated at ultimate load in a member always results in inclined cracks called shear or diagonal cracks. So as to avoid shear failure, beams are provided with transverse reinforcement whose behavior is based on av/d ratio. The chances of shear failure are more when the value of av/d lies between 2.5 and 6.
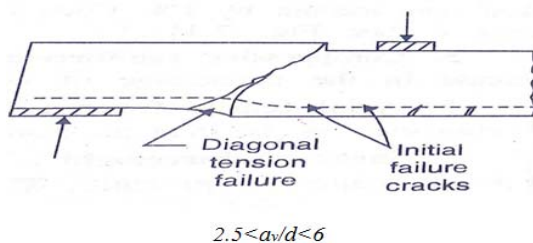

Fig. 2. Diagonal tension failure/shear failure

The provision of transverse reinforcement is still not enough so as to avoid this brittle and abrupt failure, the concept of FRP is used which is more effective in shear strengthening of member.

III. FACTORS AFFECTING SHEAR RESISTANCE OF CONCRETE

(1) *Grade of concrete*
Higher grade of concrete has higher characteristic strength which in turns results in higher tensile strength, greater dowel shear resistance, greater aggregate interlock capacity and greater concrete strength in compression zone.

(2) *Percentage and grade of longitudinal tensile reinforcement*
The increase in percentage of longitudinal tensile reinforcement results in increase in dowel shear. However higher grade of steel results in lesser shear resistance because percentage required of steel for high grade is less.

(3) *Ratio of shear span to effective depth*
Shear capacity decreases with decrease in av/d ratio.

(4) *Compressive force*
Presence of axial compressive force results in increase of shear capacity

(5) *Compressive reinforcement*
The shear resistance is found to increase with the increase in percentage of compressive steel.

(6) *Axial tensile force*
Axial tensile force marginally reduces the shear resistance of concrete.

(7) *Shear reinforcement*
The shear resistance of beam increases with increase in shear reinforcement ratio. It is because of two reasons, firstly the concrete gets confined between stirrup spacing and secondly the shear reinforcement itself provides shear resistance.

IV. FIBER-REINFORCED POLYMER (FRP)

FRP is a composite material which is made up and composed of polymer matrix and reinforced with fibers. The fibers define the type of FRP. The fibers are of carbon, glass, aramid and other fibers such as wood or asbestos have also been used. When the fibers that are used in production of FRP are of glass, the composite is called Glass Fiber-Reinforced Polymer (GFRP) and when the fiber used is carbon, composite is called Carbon Fiber-Reinforced Polymer (CFRP).

A. Application Of FRP In Civil Engineering

Due to properties like light weight, non corrosive, high specific strength and high specific stiffness, FRP are increasingly being considered as an enhancement or substitute for construction components namely concrete and steel. Because of these advantages, FRP is included in construction and rehabilitation of structures and have uses as reinforcement in concrete, bridge decks, form work, modular structure, external reinforcement for strengthening and seismic upgrade.

B. Methods Of Using FRP In Beams

Strengthening can be done as shown in Fig. 5. FRP can be used mainly by two methods which are

1. Near Surface Mounted (NSM) Method

In this method, FRP bars or strips are embedded into grooves made on concrete cover by elements to be strengthened [3] as shown in Fig. 3.

2. Externally bonded reinforcement (EBR) Method

In this method the FRP laminates plates or sheets are generally applied externally on surface of structural element to be strengthened using an adhesive as shown in Fig. 4. This adhesive is high strength epoxy resin used to bind the FRP sheets with concrete surface. This paper presents the effort of researchers in shear strengthening of FRP beams using EBR techniques.

Grooves made on the surface of the concrete

Strengthening by NSM method

Fig. 3. NSM Method [3]

Strengthening by EBR method

Fig. 4. EBR Method [3]
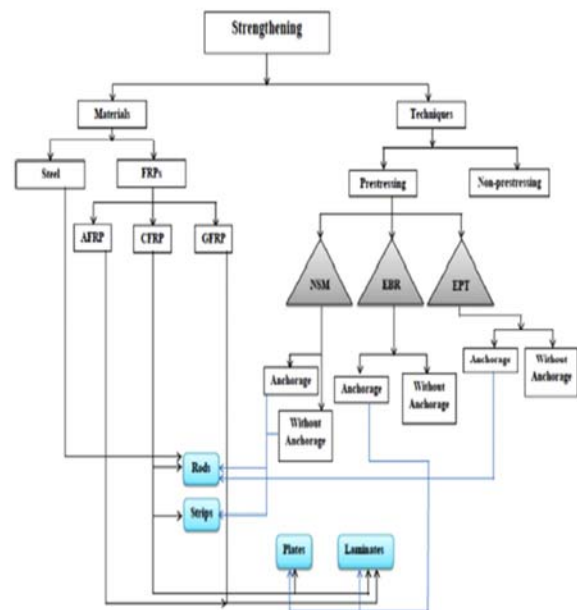
Fig. 5. Strengthening processes [9]

V. RESEARCH PROGRESS ON EXTERNALLY BONDED FRP REINFORCEMENT

The concept of using the EBR technique for shear strengthening of RC beams has been examined for many years by researchers. The use of FRP sheets to shear strengthen reinforced concrete beam has been studied and proven repeatedly since it started in 1982. However, numerous strengthening configurations and materials can be combined with FRP to maximize the increase in strength and repair.

Kotsovos [8] described the experimental evidence that causes shear failure exhibited by RC beams are associated with stress conditions in

region of path along which compressive force is transmitted. The behavior of concrete beam was compared according to that concept and found out that the studied behavior is compatible with cause of shear failure. Later Shibata and Goto [11] investigated on members that are subjected to shear with diagonal tension like as footing in beams in high rise buildings. The experimental study was carried out to investigate the shear behavior of such members and it was found that there was a remarkable reduction in shear cracking strength of almost 30% from the past proposed equation derived from compressive loading test results. Arathy and George [3] studied the properties of RC beams strengthened with glass fiber reinforced polymer with control beam. Beam was investigated with both types of failure which are flexure failure and shear failure. In first scheme, flexural strength was done by using both EBR and NSM methods. In second scheme shear strengthening is done by using both EBR and NSM methods. A two point loading was adopted an deflection was observed at end of each test. It was concluded that the load carrying capacity was increased by using GFRP and when number of GFRP sheets were increased.

Bousselham and chaallal [1] studied the shear strengthening of RC beams with EBR polymer (FRP) composites. They contributed to the understanding shear resistance mechanism involved in RC beams strengthened in shear. The results based on experimental program composed of 17 tests helped to establish the contribution of concrete, FRP an transverse steel under increasing load to shear resistance of beam. It was found that contribution of concrete to shear resistance starts from loading and attains constant value due to occurrence of first diagonal crack, contribution of FRP is activated after formation of first diagonal crack and does not vary linearly and is dependent upon strain in different regions. Also, contribution of transverse steel starts after formation of first diagonal crack and is not quite linear due to evolution of strain. Later Bousselham and Chaallal [2] again investigated for maximum shear strength of RC beams retrofitted in shear with FRP composites by developing an alternative equation as an upper limit for shear strength against web

FRP materials can be obtained by holistic approach which is concept of performance factor. Farooq and Bedi [13] studied the shear behavior of

crushing failures in such structures. The prediction of equations analytically were compared with those obtained from tests reported in literature and various other codes and was found out to be in well agreement.

Chen et al. [5] developed a new model for shear strengthening of beams with FRP by composing the adverse shear between the internal steel shear reinforcement and external FRP. It was found out that proposed shear strength model performs the best among model compared and performance of other shear strength model can be significantly improved by including the proposed shear interaction factor.

Later Sabol and Priganc [10] investigated the increase in shear capacity of beam by one of other methods called near surface mounted NSM method by using combination of epoxy and FRP system. It was concluded that based on experimental research, numerical analysis and analytical approach, NSM method is also an effective way of shear strengthening of concrete elements. Zhang et al. [12] proposed a mechanics based segmental approach, a generic closed form solution was derived for quantifying the shear capacity of RC beams without stirrups. The design recommendation shows a reduction to different degrees in measured to predicted shear strength ratio for proposed approaches.

Baggio, et al. [4] investigated the effectiveness of using commercially manufactured carbon FRP (CFRP), glass FRP (GFRP) and fiber reinforced cementitious matrix (FRCM) sheets to increase shear capacity RC beam. The experiment was carried out to investigate the maximum effectiveness of all of these sheets. Experimental results revealed that applying FRP sheets increased the overall shear capacity and full depth U wrapped FRP sheets performed better as compared to partial depth U wrapped sheets. Spadea, et al. [6] studied the composite action of externally bonded plate with a RC beam. The relevant aspects like increase in shear strength, ductility and ability to dissipate internal strain energy were illustrated by a extensive ongoing experimental investigation. It was shown that how a stable and controlled progressive failure of RC beams strengthened with RC beams with help of ATENA. ATENA is the new FEM based software that do nonlinear analysis of RCC structures. Study was carried out to

investigate the influence of span to depth ratio, percentage of longitudinal reinforcement and concrete grade on shear strength of beam. It was concluded that graph between load and deflection for experimental observation were well in agreement with values obtained with software ATENA.

Lately Yu et al. [7] investigated the efficiency of externally bonded L-shaped FRP laminates in strengthening seismically damaged RC joints. Retesting after retrofitting showed that average peak strength of CFRP strengthen specimen increased approximately by 20%.

VI. EXPERIMENTAL VALIDATION OF LITERATURE SHOWING EFFECTS OF EXTERNALLY BONDED FRP ON VARIOUS PROPERTIES OF BEAM

Spadea et al. [6] investigated the shear behavior of externally bonded FRP strengthened beam by experimenting on 7 beams (series B2 and B3) designed to be identical in every aspect expect for the test loading regime, internal shear reinforcement and external reinforcement in shear span. The beam B2 was provided with 6 mm diameter stirrups at 150 mm center to center, three under load and two over each support. The beam of series B3 had internal shear reinforcement of 3 mm diameter stirrups at 150 mm center to center. Beams B2 and B2.1 were used as control beams without any external reinforcement. B2 and B2.1 were tested with a_v/d ratio of 6.9 and 3.4 so they fail in bending and shear respectively. The details of external reinforcement are shown in Fig. 7. Strains in concrete, internal steel reinforcement and CFRP lamina were measured at various sections along the span using strain gauges. All beams were tested under displacement control regime and applied loads were measured by high accuracy load cell with load sensitivity of 0.1 kN.

VII. TEST RESULTS AND DISCUSSION

The load and deformation behavior of beams tested in shear is analyzed. The structural behavior of beams tested in shear is presented in terms of their load-central deflection at mid span section as shown in Fig. 6. The results drafted in Fig. 6 and Table 1 shows that the capacity for shear strength and deformability of control beams and of simply strengthen beam tested in shear were drastically reduced and their overall performance are also very much affected. On the other hand factor related to beams with an external anchorage system shows that an external anchorage system can significantly improve structural performance both in terms of strength and deformability.

VII. CONCLUDING REMARKS

The role of external shear reinforcement serves two purposes, firstly it increases the shear strength capacity of beams in all respect and secondly it protect the beams from adverse effects of environments, chemical actions etc. These FRP sheets are light weight, so do not increase the overall weight of structure and also increases the load carrying capacity and control the deflection of beam. Hence these lightweight, strong, durable and corrosion resistant FRP sheets are best effective way to strengthen a member against failure or to retrofit an already existing member. Scope for future research can be explored and broadened by experimenting on different combinations and orientations of externally bonded FRP plates and effects due to change in strip widths and strips spacing can be investigated.
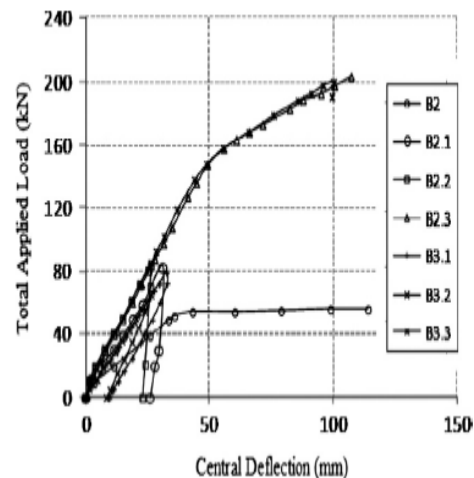

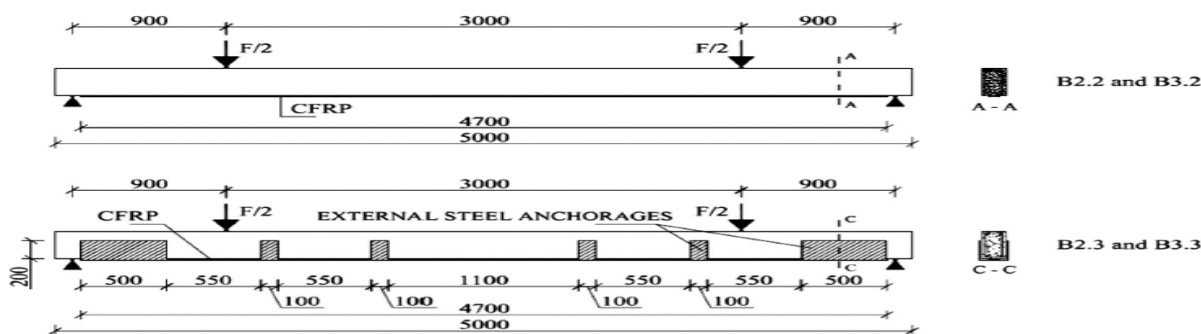Fig. 6. Load deflection diagram in shear [6]

Fig. 7. External strengthening of beams tested in shear [6]

Table 1. Summary of test results of beams tested in shear [6]

Tested beams shear loading regime (a/d = 3.4)	Beam label	First visible flexural crack		Tension steel yielding load		Failure load	Max concrete strain at failure	CFRP strain at failure	Mode of failure
		(kN)	(% FL)	(kN)	(% FL)	(kN)	(μm/m)	(μm/m)	
Control beams	B2.1	10.1	12.2%	No	Yield	82.5	871	–	SC
	B3.1	7.5	9.4%	No	Yield	80.1	893	–	SC
(a/d = 6.9)	B2	9.1	15.8%	48.8	84.9%	57.5	3667	–	CC
Beams with only CFRP	B2.2	10.4	12.7%	No	Yield	82.1	1063	1981	SC
	B3.2	9.0	10.9%	No	Yield	82.7	1020	1922	SC
CFRP + external links	B2.3	10.3	5.0%	134.9	65.4%	206.3	2706	8669	SCS
	B3.3	7.4	3.6%	120.2	59.1%	203.5	2735	8474	SCS

FL = Failure load.
SC = Shear crack.
CC = Concrete crushing.
SCS = Slice end concrete section.

REFERENCES

[1] Abdelhak Bousselham and Omar Chaallal, "Mechanism of shear resistance of concrete beams strengthened in shear with externally bonded FRP", Journal of Composites for Construction, vol. 12, no. 5, pp. 499-512, 2008.

[2] Abdelhak Bousselham and Omar Chaallal, "Maximum shear strength of RC beams retrofitted in shear with FRP composites", Journal of Composites for Construction, vol.13, no.4, pp. 302-314, 2009.

[3] Arathy A.R. and Tom George, "Strengthening of RC beam using GFRP with EBR and NSM techniques".

[4] Daniel Baggio and Khaled Soudki, "Strengthening of shear critical RC beams with various FRP systems", Construction and Building Materials, pp. 634-644, 2014.

[5] G. M. Chen, J. G. Teng and J. F. Chen, "Shear strength model for FRP-Strengthened RC beams", Journal of Composites for Construction, vol. 17, no. 1, pp. 50-66, 2013.

[6] Giuseppe Spadea, Francesco Bencardino and Fabio Sorrenti, "Structural effectiveness of FRP materials in strengthening RC beams", Engineering Structures, pp. 631-641, 2015.

[7] Jiangtao Yu, Xingyan and Zhoudao, "Efficiency of EB L-shaped Laminates", Journal of Composites for Construction, 2015.

[8] M. D. Kotsovos, "Shear failure of reinforced concrete beams", Eng. Struct., vol. 9, 1987.

[9] Muhammad Aslam, Payam Shafig, Zamin Jummat and SNR Shah "Strengthening of RC beams using PS FRP", Construction and building materials, vol. 82, pp. 235-256, 2015.

[10] Peter Sabol and Sergej Priganc, "Shear strengthening of concrete members using NSM method", Concrete And Concrete Structures, Procedia Engineering, pp. 364-369, 2013.

[11] T. Shibata, Y. Goto, " Shear failure of reinforced concrete beams subjected to diagonal tension", Eleventh World Conference On Earthquake Engineering, paper no. 1195, 1996.

[12] T. Zhang, D. J. Oehlers and P. Visintin, "Shear strength of FRP RC beams", Journal of Composites for Construction, vol. 18, no.5, 2014.

[13] Umer Farooq and K.S. Bedi, "Study of shear behaviour of RC beams", Guru Nanak Dev engineering college, 2015.

EFFECT OF MATCHING NETWORK ON AMBIENT RF ENERGY HARVESTING CIRCUIT FOR WIRELESS SENSOR NETWORKS

Pankaj Agrawal

Research Scholar, Mahatma Gandhi Chitrakoot Gramodaya Vishwavidyalaya Chitrakoot, India

Email: Pankajgate2000@gmail.com

Abstract— Limited battery life of wireless devices is encouraging companies and research groups to develop new technologies which operate these devices for an enhanced period of time. Transfer of Radio Frequency (RF) energy and its harvesting techniques have become an attractive and very promising alternatives for powering the wireless sensor networks and devices. In wireless sensor networks, low power consumption is a major challenge. From the point of view of system cost and lifetime, energy dissipation in wireless sensor networks has become an emerging and active research field For mobile and mini electronics or sensor devices, the best possible solution is to capture and store the energy from ambient energy sources, are the type of renewable energy. It holds a promising future for generating a required amount of electrical energy for operating wireless communicating electronics devices. In this paper we have reviewed the various Radio Frequency (RF) energy harvester circuits which utilized different rectifier and voltage boosting circuit. Simulation results represents that by using matching network of high-Q, output voltage of harvesting circuit increases and it becomes more sensitive with respect to input signal frequency and value of elements used.

Keywords – Radio frequency energy harvesting, matching network, RF to DC power conversion, diode's non linear behavior.

I. INTRODUCTION

In last decades the size and amount of power supply has been drastically reduced for many devices which require very less amount of power to recharge the battery. Wireless sensor networks (WSN) used in environment, agriculture and structures application demands continuous availability of power sources with long lifetime. With growing development of wireless communication, plenty amount of RF energy broadcasted through millions of public services signal sources like cell phone tower, handheld radios, Wi-Fi networks and television (T.V.) or radio broadcast stations. Hence it is very useful to collect this energy and may provide to different wireless devices such as wearable medical sensors, headsets, microcontrollers, cell phones and so on, which may increase their battery life or even may avoid the requirement of battery through this technique [1]. Since huge amount of ambient RF energy is available, spread over several frequency bands according to their application areas. Hence it is possible to receive them in combined form and converted into equivalent electrical energy by employing appropriate circuit.

Electromagnetic RF signals are omnipresent these days and they carry a tiny amount of energy employed for communication and other purposes like cellular mobile signals, TV transmitter, WiFi and DTH signals. Therefore, energy harvesting from these resources cannot be exploited for power hungry applications, and it is restricted only to small ultralow power applications. Specifically, a wireless sensor network (WSN) may include a large number of individual sensor nodes that may be difficult to access due to being implanted within a wall, a ceiling, or in a hostile

environment, where frequent human access is very difficult and replacement of their batteries become impractical. Therefore, powering these tiny sensor nodes remotely through RF energy harvesting may extend their existing battery life or even they can work satisfactorily without these batteries. This concept may also be extended for other purposes such as Internet of Things (IoT) etc. An IoT system having three essential elements sensors, connectivity and processor. The major objective of energy harvesting systems is to ensure uninterrupted (or on demand basis) supply of energy for the life time of these systems, which works on its own without any human intervention. The increasing use of wireless devices like wireless computing devices, cell phones and remote sensor networks resulted in an increased demand for self powered systems. Hence there is a need of development of system which extracts energy more efficiently from the ambient and converts it into electrical energy, used to charge-up a battery operated system.

Several research groups have selected to recycle ambient energy such as in Micro-electromechanical Systems (MEMS) [18]. The charging of mobile devices is much convenient and easy for the user, like for mobile phones. But for other equipments, like wireless sensor nodes which are located in inaccessible places, the charging of the batteries present a major challenge. This becomes major issue when the number of devices is large and are distributed in a wide area or located in difficult to access environments. The development on RF energy harvesting techniques provides reasonable solution of overcoming these problems. For charging of battery it is required that received RF signal is converted in to DC power through rectification. The process of rectification of microwave signals to DC power has been proposed and researched in the case of high-power signal. It has been proposed for helicopter powering [18], solar power satellite [11], the SHARP System [29]. The DC power depends on the available RF power, the choice of antenna and frequency band.

Ambient RF energy is freely available from RF transmitters which are not intended for transfer of RF energy. The transmitted RF power varies from 1Megawatt for TV transmitter, approx. 10 watt for cellular mobile system and 0.1 watt for mobile devices and WiFi systems.

The RF energy available from the wireless sources is much higher up to 30W for 10GHz frequency [19], but only a small amount can be propagated in the real environment. The remaining is dissipated as heat or absorbed by other materials. Maximum theoretical power available for RF energy harvesting is 7.0 μW for 2.4 GHz and 1.0 μW for 900 MHz band, for a free space distance of 40 m [19]. A great motivation behind the energy harvesting research and development is ultra-low-power applications.

The remainder of this paper is organized as follows. Section II illustrates circuit design of RF energy harvester. Section III explains the methods and techniques developed for implementing RF energy harvesting circuit. Section IV describes the effect of matching network on output voltage of harvesting circuit. Conclusion is given in Section V.

II. CIRCUIT DESIGN

Energy harvesting process is a method of conversion of the abundant available atmospheric energy into useful electrical energy. There are different forms of energy available in the atmosphere, as light and heat, solar, wind and vibration energy. Energy harvesting from RF signal is different from other sources and has following characteristics:

- Inexhaustible nature and abundant availability in the atmosphere.

- Energy scavenging process is not harmful and do not pollute the atmosphere.

- Constant RF energy available from distant RF sources can be easily controlled.

- The output energy available from harvester is predictable and stable for long time in a fixed RF energy harvesting network.

- Since the intensity of RF energy harvesting depends upon the distance between RF sources and harvesting device, the wireless sensor nodes at different location may have different amount of harvested RF energy.

- RF energy harvesting circuit provides non removable power source in biomedically implanted devices such as pacemaker, stimulator and drug

deliverer, which reduces the patient's risk of death.

- Work in perpetually dark and hazardous locations and eliminates the need of charging mats or charging stations for wireless devices.

This section introduces hardware devices of RF energy harvesting circuit. Here the main object is to provide the understanding of communication aspects of the energy harvesting network. Basic block diagram of RF energy harvesting circuit is shown in fig. 1. It contains
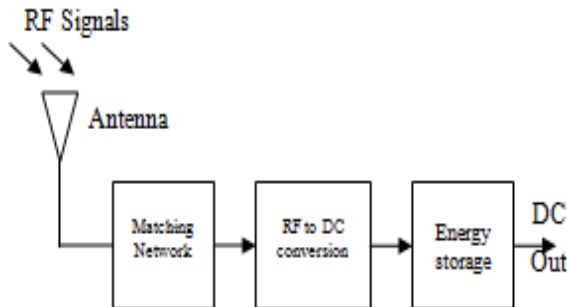

Fig. 1 Block diagram of RF energy harvesting circuit [21]

A. Antenna

Antenna receives RF energy of different frequency band from ambient [8][14][15][21] and converts it in to equivalent electrical signal through electromagnetic induction. It may be single band [27][29], dual bands [30] and triple bands [31] – [33]. A broadband antenna [13] receives RF power over wide frequency band with maximum 20% efficiency.

B. Matching Network

To deliver maximum received power from antenna to rectifier stage, it is necessary that antenna impedance must be matched to input impedance of diode used in rectifier stage, called impedance matching. It reduces transmission loss. For this purpose matching network [2],[9] is connected between antenna and rectifier stage which consist of inductive and capacitive element or LC network in 'L', 'T' or 'π' shape, according to which these are called 'L', 'T' or 'π' matching network.

C. RF to DC converter or Rectifier

To charge the battery of wireless devices or sensors, RF electrical signal supplied from matching network have to convert in DC power through rectifier circuit. Since signal strength depends upon distance between transmitter and receiver, power of RF sources, size / gain of receiving antenna and transmission frequency as given by Friis transmission equation [6], this arises a problem of low conversion efficiency, gives low output DC voltage. Hence to boost up the DC voltage we may use voltage multiplier circuit [4]. The Schottky barrier diode [28] is most commonly used device for this purpose due to lower built in voltage capable of providing high conversion efficiency at lower input power level.

D. Energy storage

To ensure smooth power delivery from RF to DC power converter stage to the load, the energy storage device is connected at output, which works as a reserve for durations when external energy is unavailable or insufficient.

III. METHODS

Energy harvesting circuits have been demonstrated for more than 50 years, but only a few have been able to harvest energy from freely available ambient (i.e., non-dedicated) RF sources. Several RF energy harvesters are implemented using various technologies such as CMOS, SMS and HSMS schottky diode. The authors in [10] proposed a resonant voltage boosting network followed by a two stage voltage doubler rectifier for RF energy harvesting. Since at low input RF levels, the peak voltage of the RF signal is much smaller than the diode threshold voltage, a resonant tank based voltage boosting network designed for a given frequency to maximize the boosted voltage amplitude. The authors in [5] proposes RF power harvesting through inductive coupling, which has proved efficient over a distance of up to 25 mm between coils, with the primary coil driven with an RF amplifier to create an electromagnetic field, and the secondary coil on the implanted device used to induce a current and hence a voltage depending on the coupling factor and the current through the primary coil. The study in [22] investigates the theoretical issues in the design of power harvesting systems in terms of the trade-off between matching network gain and bandwidth. C-MOS rectifier is designed for RFID application by using 0.5 μm and 0.18μm MOSFET based rectifier structure with 4 transistor cell operating around 950 MHz. The

work in [3] represents power harvester circuit for an RF identification transponder fabricated in a 0.18 μm CMOS (Complementary Metal Oxide Semiconductor) process operates at the UHF band of 920 MHz. The circuit employed an impedance transformation circuit to boost the input RF signal with optimum values for the circuit parameters. The authors in [23] design a RF-DC power conversion system in a 0.25 μm CMOS technology using floating gate transistors as rectifying diodes to efficiently convert far-field RF energy to DC voltages in low power sensor network with the 36-stage rectifier.

The work in [26] presents UHF 900-MHz RFID transponder front end implemented in a 0.35-μm CMOS technology, having zero-threshold MOS transistors which are particularly helpful for increasing the conversion efficiency of RF–DC rectifier in transponders. Instead of conventional Schottky diodes, diode-connected MOS transistors with zero threshold are used as a power supply generator in the on-chip RF–DC voltage rectifier to improve the compatibility with standard CMOS technology. The authors in [7] designed a compact dual polarized rectenna operating at 2.45 GHz consists of a square aperture coupled patch antenna with a cross shaped slot. The received signal from each slot output is rectified by using two stages, two voltage doubler circuits. The first stage is

formed by a series capacitor and a shunt Skyworks SMS7630 Schottky diode. The second stage uses a series SMS7630 diode and a shunt capacitor.

A new design for an energy harvesting device by using schottky diode HSMS – 2852 and one stage voltage doubler is presented in [17]. The authors in [12] present a 2.4 GHz RF energy harvester integrated into a low-power transceiver (TRx) operating at the same frequency. To keep performance degradation of the TRx low, an RF switch is used which decouples the harvester from the TRx and enable the harvester to operate without a DC power supply. The circuit is implemented in a 130 nm CMOS process, requires a minimum input RF power of -10 dBm.

A dual-band rectenna which can harvest ambient RF power of GSM-1800 and UMTS-2100 bands efficiently, based on a broadband Yagi antenna array with bandwidth from 1.8 to 2.2 GHz is designed in [8]. It used dual band matching network with a Schottky diode HSMS-2852 (Vth = 150 mV, Cj = 0.18 pF, Rs = 25 Ω) is inserted between the matching circuit and the DC-pass filter to convert the RF power into DC power. The DC-pass filter is realized by a simple stepped impedance microstrip line low pass filer,

TABLE I
Performance Comparison of various Circuit Techniques

S. No.	Reference	Technology Used	Maximum Conversion Efficiency with RF input power	Frequency
1	[22]	0.18 μm CMOS	37% with -17.7 dBm	950 MHz
2	[3]	0.18 μm CMOS	N. A.	920 MHz
3	[23]	0.25 μm CMOS	30% with -8 dBm	906 MHz
4	[26]	0.35 μm CMOS	15.76% with 12.7 dBm	900 MHz
5	[7]	SMS-7630	42.1% with -10 dBm	2450 MHz
6	[17]	HSMS-2852	10% with -10 dBm	915 MHz
7	[12]	130 nm CMOS	22.7% with -3 dBm	2400 MHz
8	[28]	HSMS-286B	55% with -30dBm	13.56 MHz
9	[16]	90 nm CMOS	40% with -17 dBm	868 MHz

followed by a resistive load to extract the DC power. The authors in [16] report a highly sensitive energy harvester using CMOS rectifier in 90 nm technology. They reported 1 volt output at minimum - 27 dBm input power.

A carbon nano tube (CNFET) based voltage multiplier or rectifier circuit for RF (radio frequency) energy harvesting applications is presented in [25]. The passive multi-stage RF to DC voltage booster circuit uses AC input signal of 60 mV to produce a DC output voltage of 389

mV, which is sufficient to drive circuits & systems in subthreshold region for ultralow power applications. Table I shows the various method used and their performance. Mostly designs are based on CMOS technology which requires minimum RF input power but maximum RF to DC conversion efficiency is lower as compared to HSMS technology.

IV. EFFECT OF MATCHING NETWORK

The output DC voltage and conversion efficiency of RF energy harvester badly affected due to diode's non linear behavior and value of matching network's element. Hence efficient design of matching network is essential to get optimum performance. The impedance of rectifier circuit varies with input signal frequency and load impedance due to non linear characteristics of rectifier diode, which limits the circuit efficiency. The matching network may effectively solve this problem can be realized either by using lumped element like resistor, inductor and capacitor or by using distributed elements such as microstrip lines. For L-matching network consisting of series inductor and shunt capacitor, the element value may be determined by using design equations [6]:

$$B_L = \pm\sqrt{R_L(Z_0 - R_L)} - X_L \qquad (1)$$

$$B_C = \pm \frac{\sqrt{(Z_0 - R_L)/R_L}}{Z_0} \qquad (2)$$

Where R_L and X_L represents real and imaginary part of the load impedance Z_L. Z_0 is the antenna impedance which is 50 Ω. The rectifier circuit consist of diode HSMS-2852 with impedance value $Z_L = (46.25 - J\,566.08)$ Ω at 0.9 GHz. In order to match the antenna impedance with diode, the value of series inductor and shunt

capacitor are 102.13 nH and 1 pF respectively calculated from eqn. 1 and 2. With these element values, L-matching network used in energy harvesting circuit is shown in fig. 2(a). Constructed prototype unit fabricated on GML make substrate with dielectric constant value $\varepsilon_r = 3.7$ is shown in fig. 2(c). It uses inductor and capacitor element supplied from Murata electronics to implement the matching network.

Fig. 2(b) represents the simulated and measured output voltage of harvester circuit in the presence and absence of matching network. It can be observe that harvesting circuit gives increased output voltage in the presence of matching network. It gives 0.5 volt output at -10
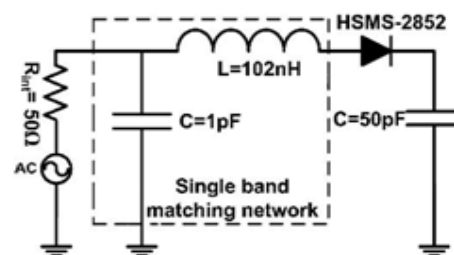

Fig. 2. (a) RF energy harvesting circuit with L-matching network

dBm input signal level with matching network, whereas without matching network it provides only 0.1 volt.

As input signal strength increase, output voltage of harvester circuit also increases. The rate of increase of output voltage is very low up to − 10 dBm input signal, but after it the slope of output voltage curve shows improvement.
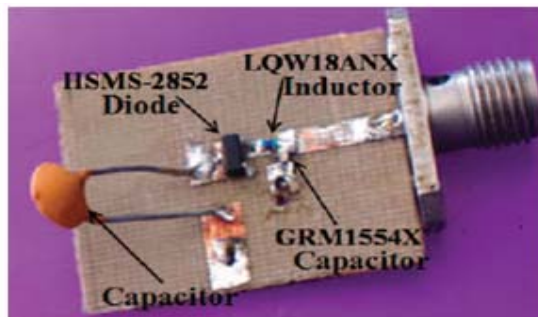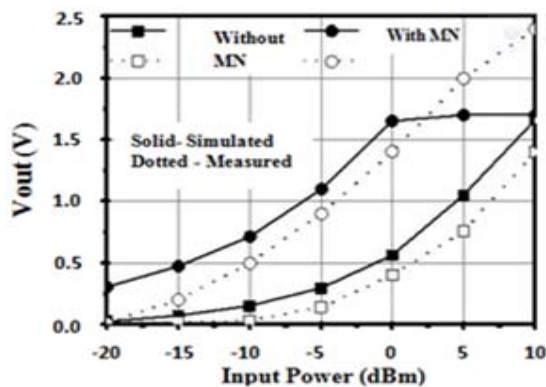

Fig. 2. (b) Simulated and measured output voltage of harvester circuit (c) Constructed harvester unit

V. CONCLUSION

In this paper the effect of diode's non linear characteristics and value of matching network elements on output voltage is presented. It has been observed that RF energy harvesting circuit achieves higher output voltage with High-Q matching network. It provides maximum power transfer from receiving antenna to rectifier circuit so that conversion efficiency of the circuit may increase, because this circuit has to work with very low input RF power level.

VI. REFERENCES

[1] A. P. Sample, A. N. Parks, S. Southwood, and J. R. Smith, "Wireless ambient radio power," *Wirelessly Powered Sensor Networks and Computational RFID(J. R. Smith, ed.)*, pp. 223-234, Springer New York, 2013.

[2] A. Meaamar, C. C. Boon, K. S. Yeo, and M. A. Do, "A wideband low power low-noise amplifier in CMOS technology,"*IEEE Trans. Circuits Syst.I,Reg.Papers*, vol. 57, no. 4, pp. 773-782, Apr. 2010.

[3] A. Shameli, A. Safarian, A. Rofougaran, M. Rofougaran, and F. D. Flaviis, "Power harvester design for passive UHF RFID tag using a voltage boosting technique", *IEEE Transactions on Microwave Theory and Techniques*, vol. 55, no. 6, pp. 1089-1097, June 2007.

[4] Bo Li, Xi Shao, Shahshahan, N., Goldsman, N., Salter, T., Metze, G.M., "An Antenna Co-Design Dual Band RF Energy Harvester*", IEEE Transactions on Circuits and Systems I, Regular Papers*, vol.60, no.12, pp.3256 - 3266, Dec. 2013.

[5] C. Sauer, M. Stanacevic, G. Cauwenberghs, N. Thakor, "Power Harvesting and Telemetry in CMOS for Implanted Devices", *IEEE Trans. On Circuits Syst.,* vol. 52, pp. 2605-2613, Dec. 2005.

[6] David M. Pozar. Microwave Engineering, *Wiley*, 3rd edition.

[7] G. Andia Vera, A. Georgiadis, A. Collado, and S. Via, "Design of a 2.45 GHz rectenna for electromagnetic (EM) energy scavenging", *Proc. Of IEEE Radio Wireless Symposium*, pp. 61-64. New Orleans, LA, Jan. 2010.

[8] Hucheng Sun; Yong-Xin Guo; Miao He; Zheng Zhong, "A Dual-Band Rectenna Using Broadband Yagi Antenna Array for Ambient RF Power Harvesting," *Antennas and Wireless Propagation Letters, IEEE* ,vol. 12, pp.918 - 921, 2013.

[9] H. Wang, L. Zhang, and Z. Yu, "A wideband inductorless LNA with local feedback and noise cancelling for low-power low-voltage applications", *IEEE Trans. Circuits Syst. I, Reg. Papers*, vol. 57, no. 8, pp.1993-2005, Aug. 2010.

[10] H. Yan, J. G. Macias Montero, A. Akhnoukh, L. C. N. de Vreede, J. N. Burghartz, "An Integration Scheme for RF Power Harvesting", *Proc. STW Annual Workshop on Semiconductor Advances for Future Electronics (SAFE 2005),* Nov. 2005, pp. 64-66.

[11] H. Hayami, M. Nakamura, and K. Yoshioka, "The Life Cycle CO2 Emission Performance of the DOE/NASA Solar Power Satellite System: A Comparison of Alternative Power Generation Systems in Japan", *IEEE Transactions on Systems, Man, and Cybernetics*, Vol. 35, NO. 3, August 2005 Page 34 – 40.

[12] J. Masuch, M. Delgado-Restituto, D. Milosevic, and P. Baltus, "An RF-to-DC energy harvester for co-integration in a low-power 2.4 GHz transceiver frontend", *IEEE International Symposium on Circuits and Systems (ISCAS)*, pp. 680-683, Seoul, South Korea, May 2012.

[13] J.A.Hagerty, F.B. Helmbrecht, W.H. McCalpin, R.Zane, and Z. B. Popovic, "Recycling ambient microwave energy with broad-band rectenna arrays," *IEEE Trans. Microw. Theory Tech.*, vol. 52, no. 3, pp. 1014-1024, Mar. 2004.

[14] K. Niotaki, S. Kim, S. Jeong, A. Collado, A. Georgiadis, and M. Tentzeris, "A compact dual-band rectenna using slot-loaded dual band folded dipole antenna", *Antennas and Wireless Propagation Letters, IEEE,* vol. 12, pp. 1634-1637, 2013.

[15] Li, B.; Shao, X.; Shahshahan, N.; Goldsman, N.; Salter, T.; Metze, G.M., "An Antenna Co-Design Dual Band RF Energy Harvester", *IEEE Transactions on Circuits and Systems I: Regular Papers,*vol. 99, pp.1 – 11, 2013.

[16] M. Stoopman, S. Keyrouz, H. J. Visser, K. Philips, and W. A. Serdijn, "Co-design of a CMOS rectifier and small loop antenna for highly sensitive RF energy harvesters", *IEEE Journal of Solid-State Circuits*, vol. 49, no. 3, pp. 622-634, March 2014.

[17] P. Nintanavongsa, U. Muncuk, D. R. Lewis, and K. R. Chowdhury, "Design optimization and implementation for RF energy harvesting circuits", *IEEE Journal on Emerging and*

Selected Topics in Circuits and Systems, vol. 2, no. 1, pp. 24-33, March 2012.

[18] R. M. Dickinson, "Evaluation of a microwave high-power reception-conversion array for wireless power transmission*", Jet Propulsion Laboratory, California Institute of Technology, Pasadena, CA, Tech. Memo* 33-741, Sept. 1975.

[19] RF HAMDESIGN Microwave equipments and parts [Online]. Available at: *http://www.rfhamdesign.com/products/paraboli cdishkit/1682909a390cc1b03/index.html.*

[20] S. P. Beeby, M. J. Tudor, and N. M. White, "Energy Harvesting Vibration Sources for Microsystems Applications", *Measurements Science and Technology*, Vol. 17, pp. 175-195, 2006.

[21] S. Keyrouz, H. Visser, and A. Tijhuis, "Multi-band simultaneous radio frequency energy harvesting", *7th European Conference on Antennas and Propagation (EuCAP), 2013*, pp. 3058-3061, 2013.

[22] S. Mandal, and R. Sarpeshkar, "Low-power CMOS rectifier design for RFID applications," *IEEE Transactions on Circuits and Systems I*, vol. 54, no. 6, pp. 1177-1188, June 2007.

[23] T. Le, K. Mayaram, and T. Fiez, "Efficient far-field radio frequency energy harvesting for passively powered sensor networks", *IEEE Journal of Solid-State Circuits*, vol. 43, no. 5, pp. 1287-1302, May 2008.

[24] T.W.R. East, "Self-steering, Self focusing phased array for SHARP", *International Symposium on Antennas and Propagation Society*, 1991, pp. 1732 – 1735, vol.3, June 1991.

[25] V. Kumar, A. Islam, "CNFET Based Voltage Multiplier Circuit for RF Energy Harvesting Applications", *Fifth International Conference on Communication Systems and Network Technologies, IEEE computer society,* pp. 789 – 791, 2015.

[26] Y. Yao, W. Jie, S. Yin, and F. F. Dai, "A fully integrated 900-MHz passive RFID transponder front end with novel zero-threshold

RFDC rectifier", *IEEE Transactions on Industrial Electronics*, vol. 56, no. 7, pp. 2317-2325, July 2009.

[27] M. Arrawatia, M. S. Baghini, and G. Kumar, "RF energy harvesting system from cell towers in 900MHz band," in *Proc. of IEEE National Conference on Communications (NCC)*, pp. 1-5, Bangalore, Jan. 2011.

[28] H. Sun, Y. Guo, Z. Zhong, "Design of a high-efficiency 2.45-GHz rectenna for low-input-power energy harvesting," *IEEE Antennas and Wireless Propagation Letters*, vol. 11, pp. 929-932, Aug. 2012.

[29] S. B. Alam, M. S. Ullah, and S. Moury, "Design of a low power 2.45 GHz RF energy harvesting circuit for rectenna," in *Proc. of IEEE International Conference on Informatics, Electronics & Vision (ICIEV)*, Dhaka, Bangladesh, May 2013.

[30] X. Shao, B. Li, N. Shahshahan, N. Goldman, T. S. Salter, and G. M. Metze, "A planner dual-band antenna design for RF energy harvesting applications," in *Proc. of IEEE International Semiconductor Device Research Symposium (ISDRS)*, College Park, MD, Dec. 2011.

[31] B. L. Pham, and A.-V. Pham, "Triple bands antenna and high efficiency rectifier design for RF energy harvesting at 900, 1900 and 2400 MHz,"in *Proc. of IEEE MTT-S International Microwave Symposium (IMS)*, Seattle, WA, June 2013.

[32] D. Masotti, A. Costanzo, and S. Adami, "Design and realization of a wearable multi-frequency RF energy harvesting system," in *IEEE Proc. Of European Conference on Antennas and Propagation (EUCAP)*, pp. 517-520, Rome, Italy, April 2011.

[33] S. Keyrouz, H. J. Visser, and A. G. Tijhuis, "Multi-band simultaneous radio frequency energy harvesting," in *IEEE Proc. of European Conference on Antennas and Propagation (EuCAP)*, pp. 3058-3061, Gothenburg, Sweden, April 2013.

DESIGN & ANALYSIS OF DISC FOR HYDRAULIC BRAKING SYSTEM OF A SOLAR CAR

Rahul Kumar Verma[1], Trapti Sharma[2], Vandana Jain[3]
[1]P.G Scholar, Automobile Engg, , RJIT BSF Academy Tekanpur
[2,3]Asst. Prof, Automobile Engg, , RJIT BSF Academy Tekanpur
Email: rkv_am@yahoo.in[1], traptisharmaster@gmail.com[2], vandana.iiitdm@gmail.com[3]

Abstract

The present research work aims to design of a disc for the braking system of the Solar Car. The disc of grey cast iron is modelled in Autodesk Inventor and Analysis of same was done in the FEA module of the Autodesk Inventor. Structural analysis of disc is carried out to study stress distribution, strain, deformation, etc for real world implementation. It is designed in a manner that the disc will support different loading condition without failure. Basic approach is to reduce the mass of disc which directly leads to reduce unsprang mass of the vehicle. As the friction between the disc pads and disc causes wheel to slow or stop where kinetic energy is converted to heat energy. In order to dissipate maximum heat, several vents are designed in the disc which may leads in reduction of mass of the disc. At the same time there should be enough strength to sustain under the dynamic conditions.

Introduction

A brake is a device which is used to retard or to stop the motion of vehicle. The purpose of the brakes is to stop the car safely and effectively without skidding in minimum possible time. In order to achieve maximum performance from the braking system, the brakes have been designed to lock up all four wheels. A disc brake is a wheel brake which slows rotation of the wheel by the friction caused by pushing brake pads against a brake disc with a set of calipers. To stop the wheel, friction material in the form of brake pads, mounted on a device called a brake caliper, on which the force is applied mechanically, hydraulically, pneumatically or electromagnetically against both sides of the disc.

Friction causes the disc and attached wheel to slow or stop. After the removal of force from disc pads, the pads retain its original position and the wheel can rotate freely again. Disc brakes have proven to be the most reliable and stable working, so they are widely used in modern automobiles. In a hydraulically actuated system, master cylinder and brake lines are used for transferring the motion of driver's pedal. The fluid filled in lines. The brake pedal linkage operates a piston in a master cylinder to pressurize the fluid inside the lines. Fluid pressure in each wheel cylinder or caliper forces the friction material against the drum or rotor. Hydraulic brakes work on the principle of pascal law.
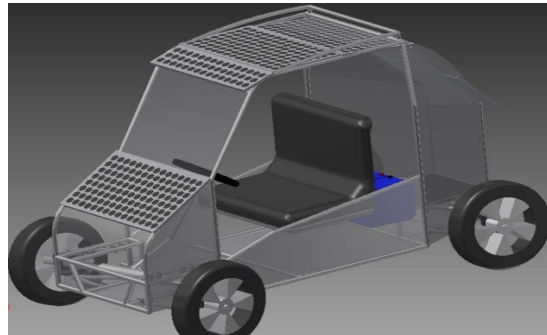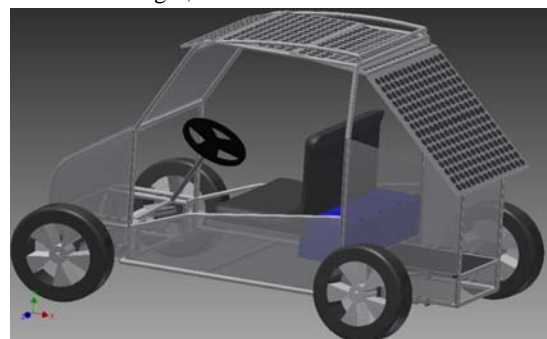

Fig.1, 3D model of Solar Car

Fig.2, 3D model of Solar Car

Design

Gross Weight of Vehicle, W = 3500 N

Weight on Front axle with no braking, W_1 = 1400 N

Weight on rear axle with no braking, W_2 = 2100 N

Height of cg, h= 547 mm

Wheel base, l= 1550 mm

Coefficient of friction b/w road & tyre, μ =0.6

Tire radius= 240 mm

Dynamic weight transfer

On front wheels =2254 N

On rear wheels = 1246 N

Brake force

Front wheel, f =1352.4 N

Rear wheels, f =747.6 N

Braking torque required

For front wheels = 162.288 Nm

For rear wheels = 89.712 Nm

Brake line pressure = 1.403 MPa

Clamping force = 971 N on each face

Brake Torque Actual =100 Nm

Stopping distance = 5.75 m

Braking efficiency = 80 %

Material

The material should have enough strength to withstand all the loads acting on it in dynamic conditions. The material selection also depends on number of factors such as material properties, availability and the most important parameter is the cost. Grey Cast Iron is selected for the material of disc. Properties of Grey Cast Iron are as under:

1.	Mass Density	7.15 g/cm^3
2.	Yield Strength	758 MPa
3.	Ultimate Tensile Strength	884 MPa
4.	Young's Modulus	120.5 GPa
5.	Poisson's Ratio	0.3 ul
6.	Shear Modulus	46.3462
7.	Coefficient of Thermal Expansion (m/°C)	46 W/m-K

Table.1, Properties of material for the Disc

Modelling

The design of a disc for a solar car is modelled in Autodesk Inventor software. It involves creating of sketch in the two dimensional sketch module and then transferring it to three dimensional sketch module and by using extrude command, the two dimensional sketch is converted to solid model or part. Disc for a braking system of the solar car is modelled. The assumptions which are made while modeling the process are given below.

- The disc material is considered as homogenous and isotropic.
- The problem domain is considered as axis- symmetric.
- Inertia & body force effects are negligible during the analysis.
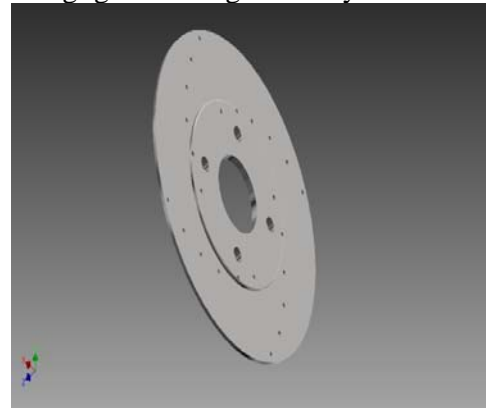
Fig.3, 3D model of Disc

Meshing

Meshing involves division of the entire of model into small pieces called elements. It is convenient to select the free mesh because the disc is circular in shape, so that shape of the object will not alter. To mesh the disc element type must be decided first. The numbers of elements after mesh are 5692 and the total numbers of nodes are 11285. Here, the description of element type is follows as:

1.	Avg. Element Size (fraction of model diameter)	0.1
2.	Min. Element Size (fraction of avg. size)	0.2
3.	Grading Factor	1.5
4.	Max. Turn Angle	60 deg
5.	Create Curved Mesh Elements	Yes

Table.2, Mesh Properties for the Disc

Fig.4, Meshed view of Disc
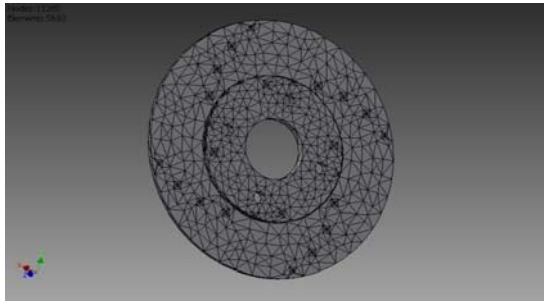
ANALYSIS

A structural analysis is performed over the disc when the loads & boundary conditions remain stationary & do not change over with the time. It is assumed that the load or field conditions are applied gradually, not suddenly. The system under analysis can be linear or nonlinear. Inertia and damping effects are ignored in structural analysis. Static analysis is used to determine displacements, stresses, etc. In structural analysis following matrices are solved [K][X]= [F],Where K is stiffness matrix, X is displacement matrix, & F is the force matrix.

Pressure Applied

A pressure is applied to the both faces the disc. Area of disc on which pressure is applied is shown by shaded region. Pressure of magnitude 1.5mpa is applied on the both side of disc.
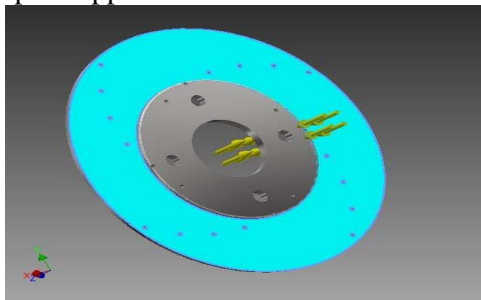

Fig.5, Pressure applied to the Disc

Von Mises Stress

The equivalent Von Mises Stress induced in the disc under the action of applied force. The maximum stress induced in the disc is 498.6 mpa.
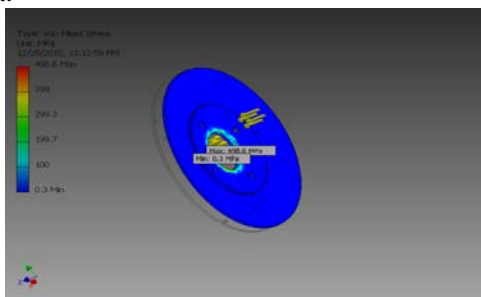
Fig.6 Von Mises Stress in the Disc

1st Principal Stress

The Principal Stress induced in the disc under the action of applied force. The maximum stress induced in the disc is 292.9 mpa.
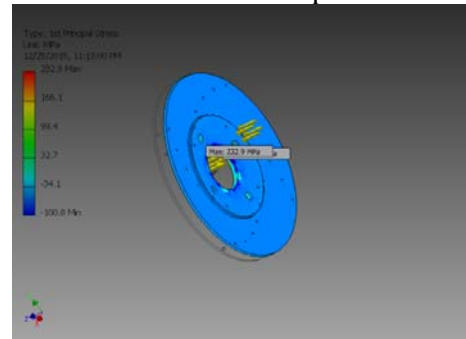
Fig.7 Principal Stress in the Disc

Displacement

The Deformation induced in the disc under the action of applied force. The maximum deformation induced in the disc is 0.308 mm.
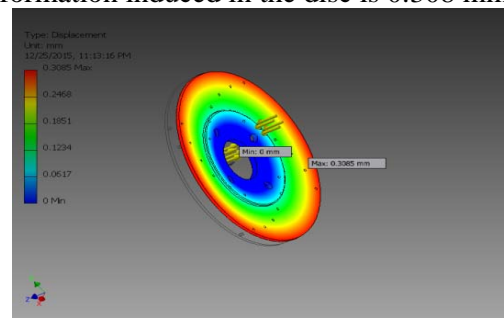
Fig.8 Deformation in the Disc

Safety Factor

The Factor of Safety in the disc under the action of applied force. The maximum Factor of Safety is 15 and the minimum Factor of safety recorded in the disc is 1.5 at orange zone.

Fig.9 FOS in the Disc

Equivalent Strain

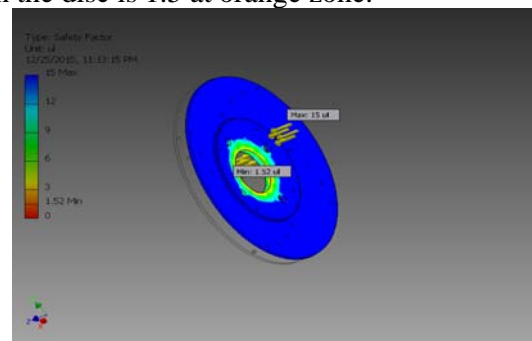The Equivalent Strain in the disc under the action of applied force. The maximum Equivalent Strain is 0.0037 and the minimum Equivalent Strain recorded in the disc is 0.000004.
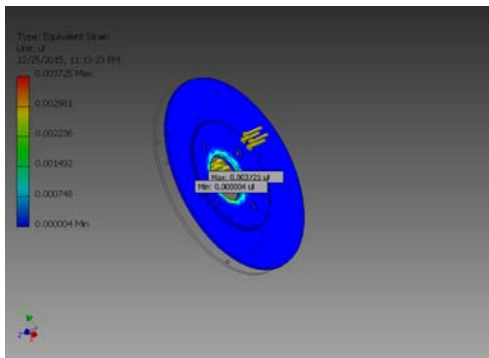
Fig.10 Strain in the Disc

Conclusion

The Disc is designed for the solar car in which brakes are applied by hydraulic mechanism. It is made up of Grey Cast Iron which has enough strength to sustain under variable loading condition. The thickness of designed disc is 3 mm which is validated by the results of Von mises stress, Principal stress, Strain, Deformation and FOS (Factor of Safety). Hence the designed disc is safe and would be suitable for implementation.

References

1. T Nakatsuji, K Okubo, T Fujii, M Sasada, Y Noguchi (2002) Study on Crack Initiation at Small Holes of Onepiece Brake Discs. Society of Automotive Engineers, Inc 2002-01-0926.

2. Akin, J.E. (1982) Application & Implementation of Finite Element Methods, Academic Press, Ornaldo, FL Page,318-323

3. Grieve D. G., Barton D. C., Crolla D. A. Buckingham J. T. (1998), Design of a lightweight automotive brake disc using finite element andtaguchi techniques, Proc. Instn. Mech. Engrs., Vol. 212, No 4, 245-254.

4. FLOQUET, A. AND DUBOURG, M.-C (1994) Non axis symmetric effects for three dimensional Analyses of a Brake, ASME J. Tribology, vol. 116, page 401-407.

5. V. M. M. Thilak, R. Krishnaraj, Dr. M. Sakthivel, K. Kanthavel, Deepan Marudachalam M.G, R.Palan, Transient Thermal and Structural Analysis of the Rotor Disc of Disc Brake.International Journal of Scientific & Engineering Research Volume 2, Issue 8, August-2011 1 ISSN 2229-5518

6. Autodesk Inventor helpbook 2015

E-WASTE MANAGEMENT AND ITS CONCERNS: A THEMATIC APPROACH

Swati Verma[1], Athar Hussain[2], V K Gupta[3], Shyam Lal[4]
[1]P G Scholar, Civil Engineering, Gautam Buddha University
[2,3]Associate Professor, Civil Engineering, Gautam Buddha University
[4]Professor, Civil Engineering, Gautam Buddha University
Email: slvswati@gmail.com[1], athariitr@gmail.com[2], vimalgupta_gupta@yahoo.com[3],
shyamlal561@gmail.com[4]

ABSTRACT

This paper reviews about the management of Electrical and Electronic waste (E-waste), its concerns and impact on the environment. The paper categorizes the E-waste management in three categories for effectively managing it. The author also discuss about the policies and recommendations regarding E-waste in the current scenario of E-waste in India and makes the recommendations about it.

Index Terms*: Concern, electrical and electronic waste, recommendations, scenario.

INTRODUCTION

In this silicon age, the continuous and constant betterment of technology has made life much easier as compared to previous times. Electronic gadgets like smartphones etc. have become a rage, all thanks to technological advances made by mankind. But this privilege has its own cons, one of them being the material waste generated by the consumption and disposal of these gadgets. This E-waste is the fastest stream of solid waste. Recycling and dumping of E-waste is more complicated and costly in comparison to general municipal solid waste.

What is E- Waste?

Electrical and Electronic waste is called E-waste. Any appliance using an electric power supply that has reached its end of life is known as E-waste[1]. (Each year 50 million tons of E-waste is produced. E-waste includes a wide and developing range of appliances ranging, such as refrigerators, air-conditioners, cell phones, stereo systems and consumable electronic items to computers discarded by users[2].

Why E-waste is Hazardous?

E-waste is hazardous because it contains number of toxic elements such as lead, mercury, cadmium etc. which are hazardous to humans and natural environment. E-waste shouldn't be directly dumped into landfills because it produces more harmful and toxic leachates than municipal solid waste. Also do not burn E-wastes such as net cables, circuits boards etc. in open air because it highly emits toxic fumes and gases which is very dangerous for our environment.
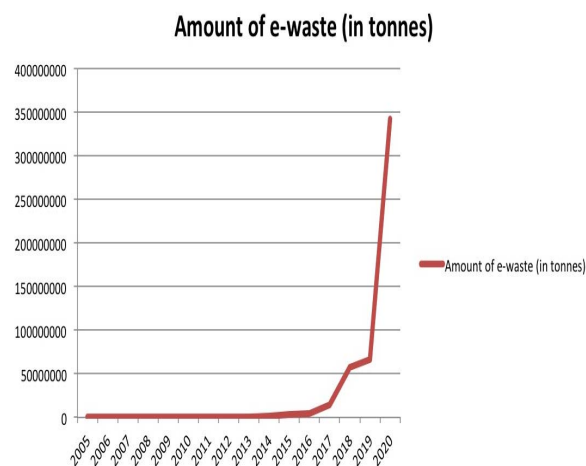

Fig 1. Graph illustrating projection of E-waste generation in India[3]
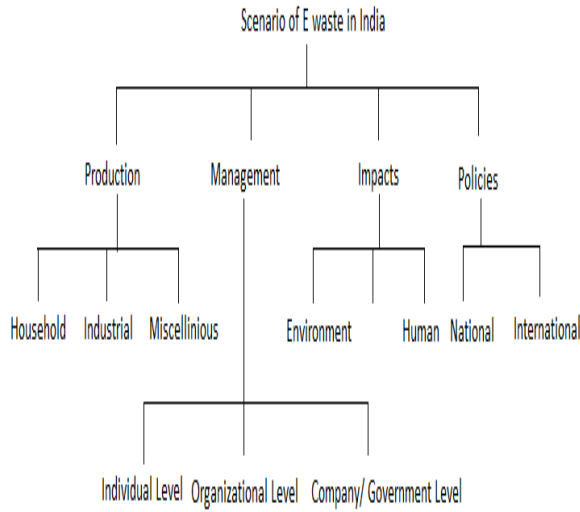
SCENARIO OF E-WSATE IN INDIA: HEIARCHY

Fig. Hierarchy of E watse in India

PRODUCTION:

E-waste is produced by household appliances, industrial machinery and other miscellaneous equipment. House hold appliances includes refrigerator, juicer, mixer, grinder, induction, batteries, exhaust fans, television (cathode ray tubes), computer, laptop, mobile phones etc.

Industrial machinery includes, CNC milling machines, CNC drilling machines, CNC lathe etc. Whereas machines like Gun Artillery, Tanks, X-ray machines, Medicinal Equipment's etc. falls under miscellaneous category. The figure1 shows the E-waste generated in India and its projection in future. This shows a huge requirement of E-waste management in near future. The above figure shows E-waste management scenario in India.

MANAGEMENT:

Management of E-waste is much difficult in handling, collection and storage rather than municipal solid waste. It should be managed effectively at various levels. These levels can be broadly classified into three types viz,

    1. Individual/Personal Level.
    2. Company & Government level.
    3. Organization and NGO's

Failure at any level may lead to collapsing of whole management structure.

INDIVIDUAL/PERSONAL LEVEL:

This is the most basic and fundamental level of E-waste management. Awareness should be created among people about E-waste. Consumers should be informed about the toxic substances present in the E-waste as well as safe handling and disposal of E-waste after use. Proper collection centers should be there to collect the E-waste. Various means of communications like Radio, Media, internet etc. can be used for effective and efficient awareness drives.

COMPANY AND GOVERNMENT:

Producers/manufacturers should be held responsible for the discarded E-waste and managing it in safe manner. The companies should start policies like take back service, etc. so that after using the Electrical and Electronics products, the consumer wouldn't discard them inappropriately. E-waste is made up of two components namely, valuable and non-valuable components. Components such as aluminum, copper, gold, palladium, silver etc. are valuable components and components like plastic, rubber, ceramics etc. are non-value components. Research suggest that the recycler would prefer to collect the obsolete batteries directly from the consumer rather than from the manufacture, only if, the incentive return to the consumer is less than 33.92%, the recycling fee is less than 6.46%, and the price of the recycled material is more than 31.08% of the price of the battery[4].

They also have to maintain records of E-waste generated by them and make such records available with state pollution control boards or the pollution of controlled comitteess[5]. Government should provide the recycling centers so that no one can dump the E-waste in open area and cause environment pollution. Toll free telephone number is provided to get E-waste picked up from home and recycled[6].

Various initiatives are taken for E-waste management by government, the ministry of environment and forest (MOEF) has notified the E-waste management rules.

"The Central Pollution Control Board (CPCB) with the help of IRG-Systems South Asia Private

Limited (IRGSSA) prepared a status report on "Management, Handling, and practices of E-waste Recycling in Delhi" during the year 2004-2005. Based on these studies it was realized that guidelines for Environmentally Sound Management (ESM) of E-waste is very much essential. As a first step towards ESM, guidelines have been published. The hazardous waste (Management and Handling) Rules, 1989 was amended in 2000 and 2003. The rules have been notified under environment (Protection) act, 1986 which talk about E-waste also. The hazardous waste (Management, Handling and Trans boundary Movement) Rules, 2008 also has been notified under environment (Protection) Act, 1986, which deals with E-waste[7].

ORGANIZATION AND NGO'S:
Due to uncontrolled disposal and burning of electrical and electronic waste, the involvement of Non-Governmental Organizations (NGOs) play a vital role in it. Saahas, the NGO involved in this pioneering effort, plans to hold campaigns in government offices to create awareness about E-waste and the need to dispose it safely[8].

IMPACTS:
Direct disposing, burning and recycling of E-waste in open areas affect both humans and environment badly. As compare to municipal solid waste, E-waste is much more hazardous to humans and environment because it contain thousands of components made of deadly chemicals like lead, cadmium, chromium, mercury, PVC (polyvinyl chlorides) and antimony etc.
Long term exposure of these toxic substances damage the nervous system, kidney, bones, reproductive and endocrine systems and some of them are carcinogenic and neurotoxic. Directly disposing of E-waste into the landfills contaminates the soil and ground water because it produces toxic leachate (liquid form) which is much more harmful than municipal solid waste. About 25000 workers are employed to scrap-yards in Delhi alone, where 10,000 to 20,000 tons of E- waste is handled every year, with computers accounting for 25 % of it[9].

Psychologically it is not preferred by any person to have waste of any kind including E-waste loitering around him or her. We all like to live in clean and green society.
Scientists who have experimentally determined in Guiyu, China (one of the popular E-waste recycling destination) have observed that because of recycling of E-waste, high lead content is found in the blood of workers. Children aged between 1-6 years living in Guiyu are found to be suffering from various types of anomalies in their brain due to high blood lead levels (BLLs) as compare to their neighboring town of Chendian, where there is no E-waste processing.
Guiyu had high incidence of skin damage, headaches, vertigo, nausea, chronic gastritis and gastric, duodenal ulcers, all of which may be caused by the primitive recycling processing of E-waste[10]. Children are particularly vulnerable to lead poisoning more so than adults because they absorb more lead from their environments[11,12,13,14,15,16,17].

POLICIES:
It can be classified into two groups i.e. national and international.
At the national level the MOEF, India had notified the E-waste management rules for the first time. Since then several policies and initiatives have been launched by Indian government. The E-waste (management and handling) Rules, 2011 recognized the producers liability for recycling and reducing e-waste in the country. This rule came into effect in May 1, 2012. This rule come under Environment Protection Act(EPA).
Internationally: Switzerland was the first country in the world where an official e-waste management system was established and operated. Two different recycling systems are active in the country. One is run by SWICO Recycling Guarantee (The Swiss Association for Information, Communications and Organizational Technology) and manages the "brown" electronic equipment (e.g. computers, televisions, radios, etc.), while the other is run by S.EN.S (Stiftung Entsorgung Schweiz System) and manages the "white" electrical equipment

(e.g. washing machines, refrigerators, ovens, etc.)[18].

RECOMMENDATIONS:

- Public should be made aware of the hazardous substances present in E-waste.
- They should not discard, dump and burn it openly in the air because it directly affects humans, animals and the environment.
- Awareness in the public should be there through various means of communications like newspaper, posters and booklets etc.
- The government should provide the suitable recycling yards/centers to facilitate recyclers and prevent them from toxic and harmful side effects of their profession.
- Government should ban those companies or manufactures which are using lead-acid batteries in their products.

REFERENCES:

[1]. OECD, OECD Environmental Outlook to 2030.Organization for Economic Cooperation and
http://213.253.134.43/oecd/pdfs/browseit/9708011E.PDF,(2008)

[2]. Basel Action Network, www. ban.org

[3].https://povertyversuspoison.wordpress.com/category/e-waste.

[4]. Rajendra Kumar Kaushal, Arvind K Nema and Jyoti Chaudhary, "Strategic Exploration of Battery Waste Management: A game-theoretic approach". Original article (SAGE Publications) in 2015. (DOI: 10. 1177/0734242X15587932)

[5]. India gets first E-waste management rules Piyali Mandal/ New Delhi June 09, 2011. Available from: http:/ /www.business-standard.com.

[6]. Dastidar AG.E-waste disposal is just a phone call away now. Avishek Dastidar. October 2009. Available from: http://www.hindustantimes.com.

[7]. Dr. Kousar Jahan Ara Begum, "Electronic Waste (E-Waste) Management in India: A Review". IOSR journal of humanities and social science. Vol 10, Issue 4 (May-Jun 2013),PP 46-57.

[8]. WEEE Recyle India .Available from: http://www.weeerecycle.in/city_background_e_waste_bangalore.htm

[9]. Ajeet Saoji, "E-Waste Management: An Emerging Environmental And Health Issue In India". National journal of medical research.

[10]. Qiu B, peng L, Xu X, lin X, Hong J, Huo X. 2004. Medical investigation of e-waste demanufacturing industry in Guiyu town. In: Proceedings of the International Conference on Electronic Waste and Extended Producer Responsibility, April 21-22, 2004, Beijing, Chhina:Greenpeace and Chinese Society for Environmental Sciences, 79-83.

[11]. Baghrust PA, McMichael AJ, Wigg NR, Vimpani GV, Robertson EF, Roberts RJ, et al. 1992. Environmental exposure to lead and children's intelligence at the age of seven years: the Port Pirie Cohort Study. N Engl J Med 327:1279-1284.

[12]. Grigg J.2004. Environmental toxins: their impact on children's health. Arch Dis Child 89:224-250.

[13]. Guilarte TR. Toscano CD, McGlothan JL, Weaver SA. 2003. Environmental enrichment reverses cognitive and molecular deficits induced by developmental lead exposure. Ann Neurol 53:50-56.

[14]. Jain NB, Hu H.2006. Childhood correlates of blood lead levels in Mumbai and Delhi. Environ Health Perspect 114:466-470.

[15]. Needleman H. 2004. Lead poisoning. Annu Rev Med 55:209-222.

[16]. Safi J, Fischbein A, EI Haj S, Sansour R, Jaghabir M, Hashish MA, et al. 2006. Chilhood lead exposure in the Palestinian Authority, Israel, and Jordan: results from the Middle Eastern regional cooperation project, 1996-2000. Environ Health Perspect 114:917-922.

[17]. Wasserman GA, Staghezza-Jaramillo B, Shortcut P, Popovac D, Graziano J .1998. The effect of lead exposure on behavior problems in preschool children. Am J Public Health 88:481-486.

[18]. D. Sinha-Khetriwal, P. Kraeuchi and M. Schwaninger, A comparison of electronic waste recycling in Switzerland and in India, Environ Impact Assess Rev. 25, pp. 492-504(2004).

NEW ID BASED FAIR BLIND SIGNATURES

Girraj Kumar Verma[1], B. B. Singh[2]
[1]P.G. Scholar, Department of Mathematics, SMS Govt. Model Science College, Gwalior, India
[2]Prof., Department of Mathematics, Govt. K.R.G. (PG) College, Gwalior, India
Email: girrajv@gmail.com[1], bbsinghkrg@gmail.com[2]

Abstract— A blind signature scheme is cryptographic primitive in which an user can obtain a valid signature from the signer, without revealing any information about message signature pair. Blind signatures are used in electronic payment systems, electronic voting machines, DRM systems etc. But, the anonymity of these signature schemes can be misused by criminals by money laundering or by dubious money. To prevent these crimes, the idea of fair blind signature was given by Stadler et al. In a fair blind signature scheme, there is a trusted third party judge who can provide a linking protocol to the signer to link his view to the resulting message signature pair. In this paper, we propose two identity based fair blind signature schemes one based on cut and choose method and another based on oblivious transfer protocol. The proposed schemes can be a good alternative for removing misuse of cryptographic protocols and key management problem in public key cryptographic protocols.

Index Terms— ID-Based Signature, Blind Signature, Fair Blind Signature, Oblivious Transfer.

I. INTRODUCTION

The idea given by Diffey and Hillman [14] in their seminal paper "New Directions in Cryptography", in 1976 has played a critical role in Cryptography. This article developed the notion of public key cryptography (PKC) and this new development inspired the generation of digital signature schemes for authenticity of source and the sender. In 1978, Rivest et al. [29] designed a first fully functional public key cryptography system based on factorization problem. In this article, they have designed a public key encryption as well as a digital signature scheme. Later, these signatures were used widely in several modified versions [2], [4], [6], [7].

In 1983 [8] D. Chaum gave the idea of blind signature schemes for electronic payment systems. A blind signature scheme is cryptographic primitive in which an user can obtain a valid signature from the signer, without revealing any information about message signature pair. The blind signatures are used in electronic payment systems, electronic voting machines, DRM systems etc [9]-[13], [16], [17], [27]. But, the anonymity of these signature schemes can be misused by criminals [31], [32] by money laundering or by dubious money. In 1993[26] Micali introduced the concept of fair cryptosystems to prevent the misuse of strong cryptographic protocols by criminals. In 1995[31] Stadler et al., designed two fair blind signature schemes, using cut and choose and oblivious transfer protocol [5]. In these schemes a trusted third party (known as judge) was also involved and who provides a linking of signer's view to the resulting message signature pair to remove anonymity. Later in 2004, Lin et al. [25], presented new development of fair cryptosystems and in recent years, some more applications of fair cryptosystems [19], [20], [22]-[25], [33] have been reported by cryptographers.

The applications of public key cryptography, created a new problem of key management of public keys. In 1984[30] Shamir introduced the idea of identity based cryptosystems for

removing the key management problem in public key cryptography. The first fully functional identity based cryptosystem was proposed in 2003[3] by Boneh and Franklin using bilinear pairing. In 2002[1], Barreto et al., designed some algorithms for pairing based cryptography and this development enhanced the interest of cryptographer community to design new identity based primitives [15], [21], [28]. In identity based cryptosystems, the public keys are derived from the identity of the user, such as their email, phone numbers etc.

In this article, we propose two identity based fair blind signature schemes, which are actually the identity based version of Stadler et al.'s [31] schemes.

The rest of the paper is organized as follows:

In section II, we have defined the identity based fair blind signatures and bilinear pairings which are creating a base for our signatures. In section III, we are considering fair blind signature by Stadler et al. and then we describe our proposed schemes and their analysis. Finally in section IV, we have concluded our discussion.

II. IDENTITY BASED FAIR BLIND SIGNATURES AND BILINEAR PAIRING

In this section, we are giving some brief discussion about fair blind signature and bilinear pairing.

A. Defining Identity Based Fair Blind Signature

An identity based fair blind signature scheme consist of several users, one signer and one trusted party known as judge and the following polynomial time algorithms:

(a)-Setup: This algorithm takes as input the security parameter k and outputs the key generation center KGC's master key, global public key and system parameter $params$.

(b)-Extract: An algorithm, which takes as input an identity $ID_U \in \{0, 1\}^*$ of any user U and master key of KGC and then outputs the public key and private key pair of the user U.

(c)-Signing: This algorithm is executed between user and signer and by executing the signing protocol, the user obtains a valid blind signature on a message of its choice such that the signer cannot link his view of the protocol to the resulting message signature pair.

(d)-Verification: By running this algorithm, the verifier defines the accept or reject the signature.

(e)-Correctness: This algorithm shows the correctness of the signature verification proof.

(f)- Blindness and Link Recovery: By running the link recovery or linking algorithm, the signer obtains the information from the judge that enables him to recognize the corresponding protocol view and the message signature pair.

There are two types of fair blind signatures, depending on the information provided by the judge during link recovery protocol.

Type-1: Given signer's view of the protocol, the judge delivers information that enables the signer (or to every body) to efficiently recognize the corresponding message signature pair(e.g. judge can also extract the message signature pair).

Type-2: Given the message signature pair, the judge delivers information that enables the signer to efficiently identify the sender of the message or to find the corresponding view of the signing protocol.

B. Bilinear Pairing

Let G_1, G_2 be two groups of same order q. We view G_1 as additive group (group of pints on elliptic curves) and G_2 as multiplicative group. Let P be an arbitrary generator of G_1. Assume that discrete log problem (DLP) is hard, in both G_1 and G_2. A mapping $e : G_1 \times G_1 \to G_2$, satisfying the following properties is called bilinear pairing:

Bilinearity:
$e(aP, bQ) = e(P, Q)^{ab} \quad \forall P, Q \in G_1, \forall a, b \in Z_n^*$
Or it can also be represented as follows:
$\forall P, Q, R \in G_1, e(P + Q, R) = e(P, R)e(Q, R)$ and
$e(P, Q + R) = e(P, Q)e(P, R)$

Non-degeneracy: There exist $P, Q \in G_1$, such that $e(P, Q) \neq 1$.

Computability: There is an efficient algorithm to compute $e(P, Q)$ for all $P, Q \in G_1$.

III. PROPOSED IDENTITY BASED FAIR BLIND SIGNATURES

In this section first we discuss fair blind signature scheme by Stadler et al [31] and then we propose our two identity based fair blind signature schemes one using cut and choose and another using oblivious transfer protocol.

A. Fair Blind Signature by Stadler et al.[31]

These signatures are based on Chaum's blind [8] signatures and on cut and choose method. The system parameters are as follows:

- (n, e), the signer's public key and (p, q, d) is master key as used in RSA signature.

- $E_j(.)$, the enciphering function of a judge's public key cryptosystems.

- $H : \{0, 1\}^* \to Z_n^*$ is a one way cryptographic hash function.

- k is a security parameter.

The Protocol:

Signature Generation:

(a) User first chooses $r_i \in_R Z_n$ For $i = 1, 2, 3, ...2k$, and strings $\alpha_i, \beta_i \in_R \{0, 1\}^*$ and computes

$u_i = E_j(m \| \alpha_i), v_i = E_j(ID \| \beta_i), m_i = r_i^e H(u_i \| v_i) \bmod n$

and sends m_i to the signer.

(b) Signer, chooses a subset $S \subset \{1, 2, 3, ...2k\}$ randomly of size k and sends to the sender.

(c) User then sends $r_i, u_i, \beta_i \quad \forall i \in S$ to the signer.

(d) Signer then checks

$m_i = r_i^e H(u_i \| E_j(ID \| \beta_i)) \bmod n$ for every $i \in S$ and hence computes $b = \left(\prod_{i \notin S} m_i \right)^d \bmod n$ and sends it to sender.

(e) The User computes $s = \dfrac{b}{\left(\prod_{i \notin S} r_i \right) \bmod n}$ and display $\{s, T\}$ as signature, where $T = \{(\alpha_i, v_i) \mid i \notin S\}$.

Signature Verification: The signatures can be verified by $s^e = \prod_{(\alpha_i, v_i) \in T} H\left(E_j(m \| \alpha_i) \| v_i \right) \bmod n$.

At the end of the execution of signing protocol, the signer is convinced that with overwhelming probability, each v_i has been formed correctly.

Since every v_i depends on ID, it is impossible for a dishonest signer to use information received during different sessions to generate a signature following the signing protocol.

B. Proposed Fair Blind Signatures using Cut and Choose

In this subsection, we are introducing our identity based fair blind signature scheme using cut and choose method used in [31]. This scheme is based on ID based signature scheme by K. G. Peterson [28].

(a)Setup: Let G_1 be an additive group of prime order q and G_2 be a multiplicative group of same order q. We assume the existence of a bilinear map $e : G_1 \times G_1 \to G_2$ with the property that discrete logarithm problem in both G_1 and G_2 is hard. Typically G_1, will be a subgroup of the group of points on elliptic curve over a finite field and G_2 will be a subgroup of associated finite field and map e may be derived from the Weil or Tate pairing over elliptic curves. We also assume that an element $P \in G_2$ satisfying $e(P, P) \neq 1_{G_2}$ is known. Let ID_s, be a string denoting the identity of the signer and ID is the string denoting session identifies of a user with signer. We consider, $H_1 : \{0, 1\}^* \to G_1$, $H_2 : \{0, 1\}^* \to Z_q$ and $H_3 : G_1 \to Z_q$ as three cryptographic hash functions. Hence system parameters are $param = (G_1, G_2, e, H_1, H_2, H_3, P, P_{pub}, q, k)$

(b)Extract: In our scheme a signer's public key is derived from his identity and is defined as $Q_{ID} = H_1(ID_s)$ and secret key as $D_{ID} = sQ_{ID}$, where $s \in_R Z_n^*$ is chosen by TA as his master key. We also assume $P_{pub} = sP$ is known to all.

(c)Signing: This algorithm is executed between user and the signer and at the end of this, a valid blind signature is generated. The user and the signer do the following steps:

1. Let the user wants to obtain a signature from the signer on the message $m \in \{0, 1\}^*$. For doing so, both of them agreed upon $ID \in \{0, 1\}^*$ as session identifier and user chooses

$\alpha_i, \beta_i \in_R \{0,1\}^{|I|}$ for $i = 1, 2, \ldots 2k$ where k is a security parameter.

2. Then user computes

$u_i = E_j(\alpha_i \| m), v_i = E_j(\beta_i \| ID), m_i = H(u_i \| v_i) \bmod n$ and sends m_i to the signer.

3. Signer, chooses a subset

$S \subset \{1, 2, 3, \ldots \ldots 2k\}$ randomly of size k and sends to the user.

4. User then sends $u_i, \beta_i \quad \forall i \in S$ to the signer.

5. Signer then computes and checks

$m_i = H(u_i \| E_j(\beta_i \| ID)) \bmod n \; \forall i \in S$ and then

computes $R = rP, b = \prod_{i \notin s} m_i$

and

$S_1 = r^{-1}(bP + H_3(R)D_{ID})$ where $r \in_R Z_n^*$ and sends (R, S_1) to the user.

6. User display (R, S_1, T) as signature,

where $T = \{(\alpha_i, v_i) \mid i \notin S\}$.

(d)Verification: Verifier runs the following algorithm for checking validity of the signature:

1. Verifier computes

$Q_{ID} = H_1(ID_s)$ and $b = \prod_{i \notin s} H_2(E_j(\alpha_i \| m) \| v_i)$ and

$H_3(R)$.

2. Accepts the signature iff

$e(P, P)^b e(P_{pub}, Q_{ID})^{H_3(R)} = e(R, S_1)$.

(e)Correctness: :

$e(R, S_1) = e(rP, r^{-1}(bP + H_3(R)D_{ID})) = e(P, bP + H_3(R)D_{ID})$

$\qquad = e(P, bP)e(P, H_3(R)D_{ID}) \quad = e(P, P)^b e(P, D_{ID})^{H_3(R)}$

$\qquad = e(P, P)^b e(P, sQ_{ID})^{H_3(R)} \quad = e(P, P)^b e(sP, Q_{ID})^{H_3(R)}$

$\qquad = e(P, P)^b e(P_{pub}, Q_{ID})^{H_3(R)}$

(f)Blindness and Link Recovery by Judge: Since user sends the value of $u_i = E_j(\alpha_i \| m)$ and β_i to the signer, so signer cannot link his view of the protocol to the resulting message signature pair. Since signer can verify the m_i,s randomly, so user cannot obtain signature on a wrong message.

When the signer wants to check m or ID (session identifier), he requests to the judge. The judge takes $u_i = E_j(\alpha_i \| m)$ and $v_i = E_j(\beta_i \| ID)$, and after decryption of these he does the following steps:

*Given the values $u_i, i \in S$, the judge can disclose the message m as in [31]. Therefore, the scheme is of type-I

*Given the signature (R, S_1, T), the judge can easily compute the identification string ID as in [31]. Therefore, the scheme is of type-II.

C. Fair Blind Signature Using Oblivious transfer

In this subsection, we are giving a new identity based fair blind signature scheme using oblivious transfer [5],[31]. We are developing this scheme on a variation of Fiat-Shamir signature scheme as described in [31]. In [31] Stadler et al. have explained the variation but they have not discussed the identity based version of this variation. We are first giving the identity based version of this variation and then use this variation to design our new protocol.

Fiat-Shamir Signature[18]:

Extraction: Signer generates his keys using RSA [30] and selects a cryptographic hash function $H : Z_n^* \times \{0,1\}^* \to \{0,1\}^k$ and defines $param = (n, e, H)$ and (p, q, d) as is master key.

Signing: Let ID be the user's identity such that $g = ID^d \bmod n$, signer then executes the following steps:

1. Chooses $r \in_R Z_n^*$ and computes $t = r^e \bmod n$ and $s = gr^{H(t,m)}$.

2. Display (s, t) as a signature on message m.

Verification: Verifier accepts the signature iff $s^e = ID t^{H(t,m)} \bmod n$.

ID-Based Variation of Fiat-Shamir Signature:

Extraction: Signer generates his keys using RSA [29] and selects two cryptographic hash function $\quad H_1 : Z_n^* \to Z_n^*, H_2 : Z_n^* \times \{0,1\}^* \to \{0,1\}^k$ and defines $param = (n, e, H_1, H_2)$ and (p, q, d) as is master key.

Signing: Let $ID \in Z_n^*$ be the user's identity such that $g = ID^d \bmod n$. For a security parameter k $(k > 80)$, we define $y_i = H_1(ID + i) \bmod n$ and $x_i = y_i^d \bmod n$ for $i = 1, 2 \ldots \ldots k$. Then signer performs the following algorithm:

1. Chooses $r \in_R Z_n^*$ and computes $t = r^e \bmod n$.

2. Computes $C = H(t, m)$ and let c_i be the i th bit of C.

3. Computes $s = g \prod_{i=1}^{k} x_i^{c_i} \bmod n$ and display (s,t) as a signature.

Verification: Verifier computes $C = H_2(t, m)$ and let c_i be the i th bit of C and accepts the signature iff

$$s^e = ID \prod_{i=1}^{k} H_1(ID + i)^{c_i} \bmod n.$$

Correctness:

$$s^e = g^e \prod_{i=1}^{k} (x_i^{c_i})^e \bmod n = ID \prod_{i=1}^{k} (H_1(ID + i))^{c_i} \bmod n$$

Proposed Fair Blind Signature using oblivious transfer:

The *params* and secret keys are same as described in variation of Fiat-Shamir signature and let message to be signed is *m*. Then the user and signer participate in the following way:

Signing:
1. Signer Chooses $r_1, r_2, \ldots \ldots r_k \in_R Z_n^*$ and computes $t = \prod_{i=1}^{k} r_i^e \bmod n$ and sends t to the user.

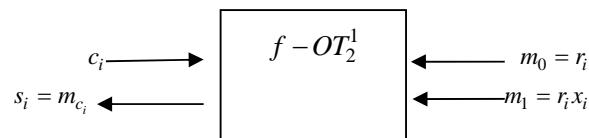**2.** User chooses $\alpha \in_R Z_n^*$ and computes
$\tilde{t} = t\alpha^e \bmod n$ and $C = H_2(\tilde{t}, m)$ and let c_i be the ith bit of C.

Then they use the following oblivious transfer protocol:

User   **Signer**

For $i = 1, 2, \ldots \ldots k$

$c_i \longrightarrow$ $\boxed{f - OT_2^1}$ $\longleftarrow m_0 = r_i$

$s_i = m_{c_i} \longleftarrow$ $\longleftarrow m_1 = r_i x_i$

*User then computes $\tilde{s} = \alpha \prod_{i=1}^{k} s_i \bmod n$ and display

$n(\tilde{s}, \tilde{t})$ as a valid signature.

Verification: Verifier accepts the signature iff

$$\tilde{s}^e = \tilde{t} \prod_{i=1}^{k} (H_1(ID + i))^{c_i} \bmod n.$$

Correctness:

$$\tilde{s}^e = \alpha^e \prod_{i=1}^{k} s_i^e = \alpha^e \prod_{i=1}^{k} r_i^e (x_i^e)^{c_i} = \tilde{t} \prod_{i=1}^{k} (x_i^e)^{c_i} = \tilde{t} \prod_{i=1}^{k} (H_1(ID + i))^{c_i}$$

Blindness and link recovery by Judge: Now, let us analyze the blindness of our scheme. We assume that the signer cannot determine the selection bit c_i (because of the $f - OT_2^1$). Therefore, *t* is the only value known to signer to use for linking his view to the resulting message signature pair. But for each valid signature $(\tilde{s}, \tilde{t})$ of a message *m* there is exactly one α with

$\tilde{t} = t\alpha^e \bmod n$ and therefore, $\tilde{s} = \alpha \prod_{i=1}^{k} r_i x_i^{c_i} \bmod n$,

where c_i be the ith bit of $C = H_2(\tilde{t}, m)$. So, the resulting signature is independent of the signing protocol and the signature scheme is perfectly blind signature scheme.

On the other hand considering the fairness of the scheme, if the signer sends the view of the protocol to the judge, the selection bit c_i can be determined and therefore the challenge *C* is known. This value could then be put onto a black list, so that everybody can recognize the message signature pair later.

Applications: There are several applications of fair blind signatures. One is to provide a tool to prevent money laundering in anonymous payment systems. In a payment system based on type-2 fair blind signature scheme the authorities can determine the origin of dubious money, while in typre-1 they can find out the destination of suspicious withdrawals.

Another application is the perfect crime scenario described in [32]: a customer is black mailed and forced to anonymously withdraw digital money from his account, acting as an intermediary between the blackmailer and the bank. In a perfectly anonymous payment system, the ransom could not be recognized later, but if a (type-1) fair blind signature scheme had been used, the judge, when the bank's view of the withdrawal protocol, can trace the blackmailed coin.

IV. CONCLUSION

In this research article, we have proposed two new identity based fair blind signatures for removing key management problem in public key cryptographic protocols. These signature schemes can be used for controlling the misuse of anonymity of cryptographic protocols. Although, these signature schemes are not much efficient non the less, they provides a practical solution for removing misuse of anonymity.

V. ACKNOWLEDGEMENT

The authors would like to thank Prof. Sunder Lal, Ex. Vice-Chancellor, Poorvanchal University, Jaunpur, India for their valuable co operation and motivation.

REFERENCES

[1] P.S.L. M. Barreto, H. Y. Kim and M. Scott, Efficient algorithms for pairing based cryptosystems, in proc. Of   CRYPTO-2002, LNCS-2442, Springer Verlag, pp. 354-369, 2002.

[2] M. Ben-Or, O. Goldreich,, S. Micali and R. L. Rivest, A fair protocol for signing contracts, Transaction on Information theory, IEEE, 36(1), pp. 40-46, 1990.

[3] D. Boneh and M. Franklin, Identity based encryption from   Weil pairing, SIAM J. of computing, pp.585-615,   extended abstract in Crypto-2001.

[4]   S. Brands, Untraceable off-line cash in wallet with observers, In proc. Of CRYPTO-93, LNCS-773, Springer Verlag, pp. 302-318, 1993.

[5]   G. Brassard, C. Crepeau and M. Santha, Oblivious   transfer   and   interesting   codes, Transaction on Information   Theory, IEEE, 42(6), pp. 1769-1780, 1996.

[6] J. Camenisch, J. M. Piveteau and M. Stadler, Blind Signature based on discrete logarithm problem, in proc. of   EUROCRYPT-94, LNCS-950, Springer Verlag, pp. 428-432, 1994.

[7] J. Camenisch, J. M. Piveteau and M. Stadler, An efficient payment system protecting privacy, in Proc. Of ESORICS-94, LNCS-875, Springer Verlag, pp. 207-215, 1994.

[8] D. Chaum, Blind Signature systems, in proc. Of CRYPTO-83,   LNCS-, Springer Verlag, pp.153-158, 1983.

[9]   D. Chaum, Blind signatures for untraceable payments, in: Advances in cryptology, pp. 199-203. Springer US (1983).   [10] D. Chaum, A. Fiat and M. Naor, Untraceable electronic cash, in proc. Of CRYPTO-88, LNCS-403, Springer Verlag, pp. 319-327, 1988.

[11] D. Chaum, Privacy protected systems, in proc. Of SMART   CARDS-2000, Elseveir Science, B. V. North Holland, pp.69-93.

[12] D. Chaum, B. DenBoer, E. Van Heyst, S. Mj Flnse and A. Steenbeek, Efficient offline electronic   checks,   in   proc.   Of EUROCRYPT-89, LNCS-434, Springer Verlag, pp.294-301, 1989.

[13] D. Chaum and T. Pedersen, Wallet database with Observers, in proc. Of CRYPTO-92, LNCS-740, Springer Verlag, pp.89-105, 1992.

[14] W. Diffey and M. E. Hillman, New directions in cryptography,   Transaction of Information Theory, IEEE, 22(6), pp.74-84, 1977.

[15] R. Dutta, R. Barua and P. Sarkar, Pairing based cryptographic   protocols: A Survey, available at http://eprint.iacr.org/2004/064.

[16] S. Even, O. Goldreich and A. Lempel, A randomized protocol   for signing contracts, Communications of ACM, 28, p.637-647, 1985.

[17] N. Ferguson, Single term offline coins, in proc. Of   EUROCRYPT-93, LNCS-765, Springer Verlag, pp.318-328, 1993.

[18] A. Fiat and A. Shamir, How to prove yourself: Practical solution to identification and signature problems, in proc. Of CRYPTO-86, LNCS-263, Springer Verlag, pp.186-194, 1986.

[19] G. Fucshbaurer and D. Vergaurd, Fair blind signatures without   random oracles, in proc. Of AFRICACRYPT- 2010, Springer Verlag, pp. 16-33, 2010.

[20] S. Han, E. Chang, X. Deng, L. Gao and W. Yeung, Practical fair anonymous undeniable signatures, Int. J. of Signal processing, 1(4), pp. 291-296, 2004.

[21] F. Hess, Efficient identity based signature schemes, in proc. Of SAC-2003, LNCS-2595, Springer Verlag, pp.310-324, 2003.

[22] X. Hou and C. H. tan, On fair traceable electronic cash, in proc. Of CNSR-05, IEEE, pp. 2005.

[23] E. Hufschmitt and J. Traore, Fair blind signatures   revisited,   in   proc.   Of PAIRING-2007, LNCS-4575, Springer Verlag, pp.   268-292, 2007.

[24] M. Jacobson, Blackmailing using undeniable signatures, in proc. Of EUROCRYPT-94, LNCS-950, Springer Verlag, pp. 425-427, 1994.

[25] M. H. Lin, C. C. Chang and Y. R. Yen, A fair and secure mobile agent environment based on a blind signature and proxy host, Computers and Security, 23, pp.199-212, 2004.

[26] S. Micali, Fair Cryptosystems, Technical Report MIT/ LCS/ TR -579, 1993.

[27] T. Okamoto and K. Otha, Universal electronic cash, in proc. Of CRYPTO-91, LNCS-576, Springer Verlag, pp. 324-337, 1991.

[28] K. G. Peterson, Identity based signatures from pairing on elliptic curves, available at http://eprint.iacr.org/2002/004.

[29] R. L. Rivest, A. Shamir and L. Adleman, A method for obtaining digital signatures and public key cryptosystems, Communica- tion of the ACM 21, pp.120-126, 1978.

[30] A. Shamir, Identity based cryptosystems and signature schemes, in proc. Of CRYPTO-84, LNCS-196, Springer Verlag, pp.47-53, 1984.

[31] M. stadler, M. Piveteau and J. Camenisch, Fair blind signatures, in proc. Of EUROCRYPT-95, LNCS-921,Springer Verlag, pp.209-219, 1995.

[32] S. Von, Solms and D. Naccache, On blind signatures and perfect crimes, Computers and Security-11, pp.581-583, 1992.

[33] W. T. Yin and W. Q. Yan, Fair quantum blind signatures, Chinese Physics B, 19(6), pp…, 2010.

EFFECTS OF ARTIFICIAL NEURAL NETWORK PARAMETERS ON ROLLING ELEMENT BEARING FAULT DIAGNOSIS

Deepak Kumar Gaud[1], Pratesh Jayaswal[2]

[1]Research Scholar, Department of Mechanical Engineering, MITS Gwalior, RGPV University, Madhya Pradesh, India,

[2]Asso. Prof., Department of Mechanical Engineering, MITS Gwalior, Madhya Pradesh, India

Email: dg.rscholar.mits@gmail.com[1], pratesh_jayaswal@yahoo.co.in[2]

Abstract— To ensure asset reliability the industries have been focused on the condition based maintenance (CBM). Fault detection and diagnosis are two of three condition based maintenance mainstays. Rolling Element is one of the major and essential components of rotating machinery. Thus researchers have been shown their interest in rolling element bearing fault detection and diagnosis for few decades. They used mostly the bearing vibration as fault characteristics for fault detection and used Artificial Neural Networks (ANNs) for bearing fault classification as well. The process of fault classification involves some Neural Network (NN) geometry and parameters, thus is not quits simple. There is no any predefined formula to select the optimal values for these network parameters. These parameters affect the reliability of fault diagnosis system. This paper investigates the effects of NN geometry and parameters on rolling element bearing fault diagnosis. The vibration signals are recorded for normal bearings, bearing with inner race fault, outer race fault and rolling ball fault from an appropriate experimental setup. The RMS vibration features are calculated then using Fast Fourier Transform (FFT). Rolling element bearing faults are classified as same using Back-Propagation Neural Network (BPNN) and the results are simulated.

Keywords—Artificial Neural Network, back-propagation algorithm, Condition Based Maintenance (CBM), Fast Fourier Transform (FFT).

I. INTRODUCTION

In a production system 60 to 75 % product cost accounts for maintenance and support activities which make the systems reliability a major issue. System's reliability depends upon Condition Based Maintenance (CBM) strategy. For many production systems the old maintenance strategies like break-down and preventive hold not good any time. These days the predictive maintenance strategy has been arisen in the form of an effective mainstay of CBM. Predictive maintenance offers online as well as offline condition monitoring of the machine or part and insures the condition of machine prior to any incipient part failure or major break-down which causes the unplanned shutdown. It also provides sufficient time to repair in comparison with other.

Rolling element bearing is one of the essential components in the vast majority of rotating machines. Rolling element bearing failure may affects the quality of product line working and create wastes in many ways. Thus rolling element bearing failure results in decrease product quality and increase product cost to the customer. Rolling element bearing may get defect due to any misalignment, looseness, improper installation, assess of load, poor lubrication, contamination, electric passage, insertion of foreign matter and progressive wear as listed in [1]. Rolling element bearing defects are classified as firstly on the basis of fault location and secondly on the basis of their fault type, It may be single point defect or it may be multi point defect as in [2]. Numbers of researchers are interested in finding the location of fault.

The main purpose of installing the rolling the rolling element bearing in machinery is to hold or support an element and transmit the moment of the load to the another element. When a machine rotates by drive, the shaft bearing response to the vibrations of the drive is main cause of vibration. All drives have nature to vibrate (*Vibrations cannot be eliminate*) and itself is not a fault. However excess of vibration can be a symptom of a developing fault and an early warning of machine failure. Many methods for rotating machinery fault diagnosis are presented in the literature on the basis of their different fault characteristics listed in [3]. In the present industrial scenario 70% bearing vibration, 20% wear particles are used as fault characteristics & remaining 10% covers all the other non-destructive testing including eddy current measurement as in [4]. By taking the vibration signals as characteristics fault features the fault detection and diagnosis of gear transmission system has been performed in [5]. When the signal is analyzed as a function of time then analysis is called time domain analysis. Time domain analysis has been performed to monitor the bearing health condition in [6]. This technique has been further subdivided as time waveform analysis and waveform indices as in [5]. How to set up, acquire and manipulate time waveform data is detailed in [7]. Time indices are listed as standard deviation, Root Mean Square (RMS) value, peak value, crest factor, shape factor, impulse factor, clearance factor, skewness and kurtosis etc. and calculated in [8]. In analyzing the signal in time domain one cannot find at what frequency an event occurred. Hence researchers have been focused on en effective technique (frequency domain analysis) for many decades. Frequency domain analysis employs Fast Fourier Transform (FFT) to transforms the time domain signal in frequency domain. FFT is used in this paper to extract features from row vibration signals. Rest of the paper is organized as follows: section 2 discusses the data acquisition. Section 3 describes the back-propagation algorithm. Section 4 discusses the Artificial Neural Network. Section 5 discusses NN geometry. Section 6 discusses NN parameters. Section 7 discusses results and analysis. Section 8 contains general discussion. Section 9 concludes the paper.

II. DATA ACQUISITION

The experimental setup consists of a Machine Fault Simulator (MFS) having an induction motor coupled with a rotating shaft supported with Rolling Element Bearings (REBs), CSI accelerometer, CSI 2400 dynamic signal analyzer with cable and PC interface, vibscanner to measure shaft speed in RPM and MATLAB R2009a software. The details of specimen (Self alignment rolling element bearing) are as follows:

Inner race dia (d) =25 mm
Outer race dia (D) =52 mm
Contact angle (β) =Zero degree
Number of balls (N_b) =13 per row
Ball diameter (d_b) =7.5 mm
Pitch diameter(d_p) =38.5 mm

The defects are produced artificially as follows:

TABLE I
Bearing defect geometry parameters

S. No.	Defect type	Location and number of defects	Defect size
1	Ball Defect	2 balls in one row, one by one	1*1mm, 0.1 mm deep
2	Inner Race Defect	3 defects at each row at pitch a pitch of 3 mm, both rows with defects	1*1mm, 0.2 mm deep
3	Outer Race Defect	3 defects at each row at pitch a pitch of 3 mm, both rows with defects	1*1mm, 0.2 mm deep

These listed faults cause their certain fault frequency to appear in the bearing vibrations hence there is one characteristic fault frequency associated with each of the four parts of the bearing. The fault frequencies are calculated, using the equations as in [9]

$$F_i = [N_b F_r \{1 + (d_b \cos(\beta)) / d_c\}] / 2$$
(1)

$$F_o = [N_b F_r \{1 - (d_b \cos(\beta)) / d_c\}] / 2$$
(2)

$$F_b = (d_c / d_b) F_r \{1 - (d_b \cos(\beta) / d_c)^2\}$$
(3)

where d_i is inner diameter, d_c is pitch circle diameter, d_b is diameter of ball, N_b is number of

balls, β is contact angle of ball, and F_r is the rotor frequency in Hz and F_i=Inner race fault frequency, F_o=Outer race fault frequency and F_b=Ball fault frequency.

Using the formulae (1), (2), and (3) and bearing geometry parameters listed in TABLE I, characteristics fault frequencies corresponding to each fault type are calculated. Time domain vibration signals (figure 1) are acquired at a sampling rate of 7680 Hz from the experimental setup for normal bearings, bearing with inner race fault, outer race fault and rolling ball fault by replacing one by one.
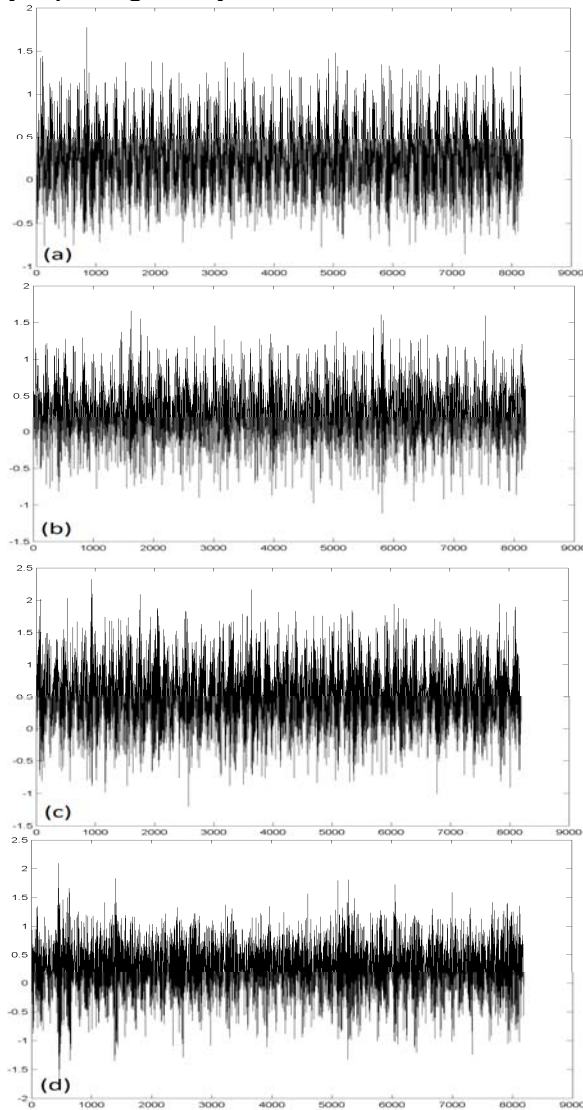

Figure 1. Vibration signals of healthy bearing (a), inner race defect (b), outer race defect (c), rolling ball defect (d).

III. BACK PROPAGATION ALGORITHM

The back-propagation algorithm is used to train the neural network in this paper follows the steps as in page 53 [10]

STEP 1: Normalize the input and output with respect to their maximum values. Neural network perform better if input and output lie between .1 and .9

STEP 2: Assume the number of neurons in the hidden neurons in the hidden layer to lie between $1 < m < 21$

STEP 3: $[V]$ represents the weights of synapses connecting input neurons and hidden neurons and $[W]$ represents weights of synapses connecting hidden and output neurons. Initialize the weight to small random values usually between -1 to 1 for our problem λ is taken as 1 and the threshold value θ is taken as zero.

$[V]^0$ =[random weights]
$[W]^0$ =[random weights]
$[V]^0 = [W]^0 = [0]$

STEP 4: For the training data, present one set of inputs and outputs. Present the pattern to the layer $\{I\}_I$ as input to the input layer. By using linear activation function, the output of the input layer may be evaluated as

$$\{O\}_I = \{I\}_I$$

1 x 1   1 x 1

STEP 5: Compute the inputs to the hidden layer by multiplying corresponding weights of synapsed as

$$\{I\}_H = [V]^T \{O\}_I$$

m x 1   m x 1 1 x 1

STEP 6: Let the hidden layer units evaluate the output using the sigmoidal function as

$$\{O\}_H = \begin{bmatrix} . \\ 1/(1+\exp(-I_{Hi})) \\ . \end{bmatrix}$$

m x 1

STEP 7: Computes the inputs to the output layer by multiplying corresponding weight of synapses as

$$\{I\}_o = [W]^T \{O\}_H$$

n x 1   n x m m x 1

STEP 8: Let the output layer units evaluate the output using sigmoidal function as

$$\{O\}_o = \begin{bmatrix} . \\ 1/(1+\exp(-I_{oj})) \\ . \end{bmatrix}$$

The above is the network output.

STEP 9: Calculate the error and the difference between the network output and desired output as for the ith training set as

$$E^P = \{\sqrt{\sum(T_j - O_{oj})^2}\} / n$$

STEP 10: Fond $\{d\}$ as

$$\{d\} = \begin{bmatrix} \cdot \\ (T_k - O_{ok})O_{ok}(1 - O_{ok}) \\ \cdot \end{bmatrix}$$

$n \times 1$

STEP 11: Find $[Y]$ matrix as

$$[Y] = \{O\}_H \langle d \rangle$$

$m \times n \quad m \times 1 \quad 1 \times n$

STEP 12: Find $[\Delta W]^{t+1} = \alpha[\Delta W]^t + \eta[Y]$

$m \times n \qquad m \times n \qquad m \times n$

$$\{e\} = [W]\langle d \rangle$$

$m \times 1 \quad m \times n \quad n \times 1$

$$\{d^*\} = \begin{bmatrix} \cdot \\ e_i(O_{Hi})(1 - O_{Hi}) \\ \cdot \end{bmatrix}$$

$m \times 1 \qquad m \times 1$

STEP 13: Find [X] matrix as

$$[X] = \{O\}_I \langle d^* \rangle = \{OI\}_I \langle d^* \rangle$$

$1 \times m \quad 1 \times 1 \quad 1 \times m \quad 1 \times 1 \quad 1 \times m$

STEP 14: Find $[\Delta V]^{t+1} = \alpha[\Delta V]^t + \eta[X]$

$1 \times m \qquad 1 \times m \quad 1 \times m$

STEP 15: Fin $\quad [V]^{t+1} = [V]^t + [\Delta V]^{t+1}$

$$[W]^{t+1} = [W]^t + [\Delta W]^{t+1}$$

STEP 16: Find error rate as

Error rate $= \sum E_P / (nset)$

STEP 17: Repeat step 4-16 until the convergence in the error rate is less than the tolerance value Once the process converges the final weights should be stored in a file.

IV. ARTIFICIAL NEURAL NETWORK

In a biological brain billions of neurons are responsible for the taken decision from the information provided by sense organs. Means the neurons are the main unit of a biological brain and convert input into output by forming a complex network between themselves and updating the weights. This idea of forming artificial neurons and updating the weights are implemented by the researchers in the field of technology to make decisions. Thus, the Artificial Neural Network (ANN) is the prototype of biological brain. Neural networks are formed by an input layer of neurons, an output layer of neurons and definite number of hidden layers of hidden neurons as shown in figure 2. ANNs have learning and generalization abilities. Numerous variations of ANNs have been proposed by the researchers in the literature on the basis of their learning algorithms, ANN structure, Transfer Function (TF) and training parameters etc. To classify the bearing faults on the basis of their location Back-Propagation Neural Network (BPNN) with single hidden layer is used in this present work.
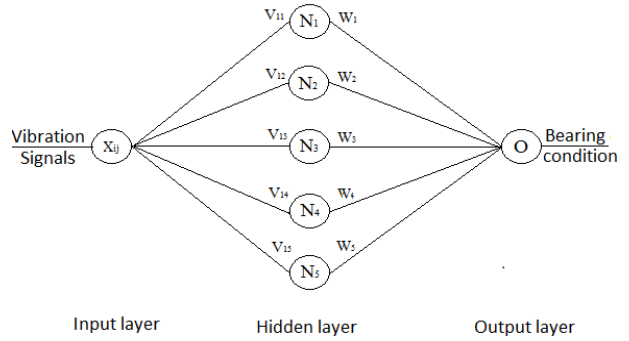

Figure 2 ANN structure

V. NEURAL NETWORK GEOMETRY

Neural networks (NN) have been used universally in function approximation. Hidden layer completes the neural network structure (Shown in figure 2) and constitutes the numbers of hidden neurons. There is no any criterion to select the optimal number of hidden neurons. Thus optimizing the number of hidden neurons for greater accuracy is one of the major & challenging tasks, hence a problem in hand. Usages of excessive hidden neurons may cause over fitting. Means the neural networks over-estimate the complexity of the given problem, which decreases the generalization capability, hence leads to significant changes in the prediction performance.

VI. NEURAL NETWORK PARAMETERS

A. Learning coefficient

Learning coefficient determines the size of the weight adjustment and influence the convergence rate. Negative value of learning coefficient causes the change of weight vector from the ideal weight vector. It cannot be zero; if

learning coefficient is zero then no any learning takes place. If its value is greater than 1, the weight vector will oscillate about its ideal position. The choice of smaller learning coefficient may increase convergence time and choice of smaller value may slow the convergence process as in page 51 [10]. Hence we must keep learning coefficient constant through all the iterations.

B. Momentum coefficient

Momentum term is also used to reduce the training time and enhance the training process. The effects of momentum coefficient on weight change are given by the equation page 52 [10]

$$[\Delta W]^{t+1} = -\eta(\partial E / \partial W) + \alpha[\Delta W]^t$$

(4)

Where $[\Delta W]^{t+1}$ is new weight, $[\Delta W]^t$ is the previous weight, $\partial E / \partial W$ is change in error with change in weight, η is learning coefficient and α is momentum coefficient

The momentum coefficient produces damping effect on searching procedure and may be considered as approximation to second order method. Thus the momentum term generally improves convergence of the back-propagation algorithm by using information from the previous iteration.

VII. RESULTS AND ANALYSIS

76 RMS features (19 for healthy bearing and 19 for each type of faulty bearing) are extracted by employing FFT and then using an IIR band pass filter to extract frequencies of interest at three nodes as (725-745), (381-387), (773-793). Trained the Back-Propagation Neural Network (BPNN) for different values of number of neurons in hidden layer, learning coefficient and momentum coefficient then results are simulated and plotted as error rate versus number of hidden neurons (Figure 3), error rate versus learning rate (Figure 4), error rate versus momentum rate (Figure 5). Bearing conditions are simulated as Healthy bearing, bearings with inner race fault, outer race fault and rolling ball fault (Figure 6).
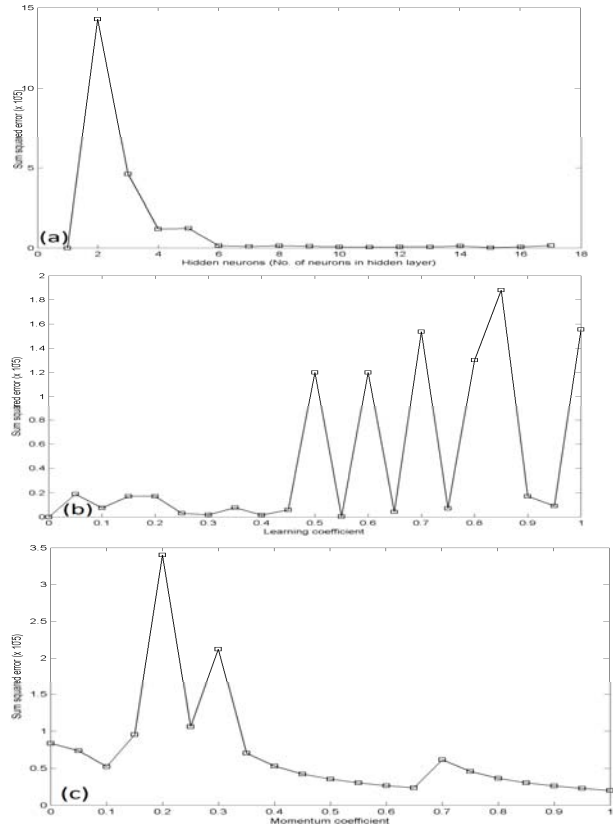

Figure 3 Error verses hidden neurons (a), error verses learning coefficient (b), error verses momentum coefficient (c)
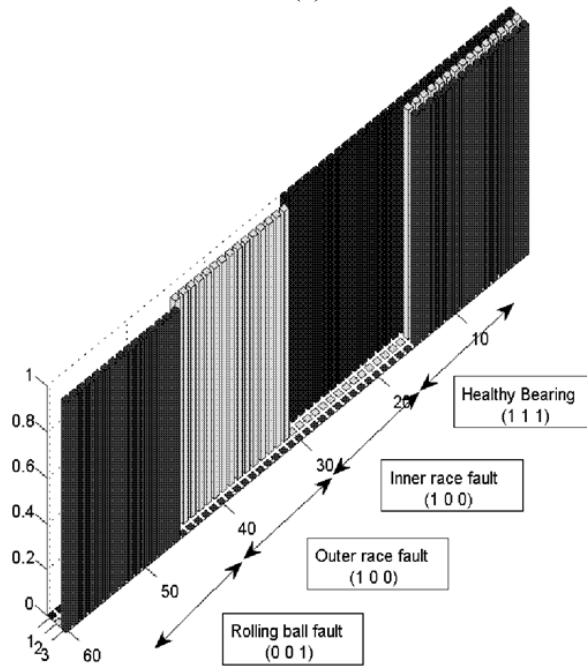

Figure 4 Bar graph showing bearing fault classification

VIII. DISCUSSION

Figure 3(a) shows very poor performance for two hidden neurons and abrupt improvement

sequentially for 3, 4, 5, and 6 neurons. Whereas the best performance shown for 10 neurons. Figure 3(b) shows the small increments and decrements in the performance for the value of learning coefficient from 0 to 0.45 and large ups and downs thereafter up to 1. The best performance has shown for 0.55. Figure 3(c) shows yielding poor performance for the value of momentum coefficient at 0.2. Two performance increasing gradients for 0.36-0.65 and 0.70-1.00 also have been shown. The best performance has met for 1.00. Figure 4 shows the bearing fault classification at optimal values of hidden neuron, learning coefficient and momentum coefficient as healthy bearing, inner race fault, outer race fault, and rolling ball fault.

IX. CONCLUSIONS

Time domain vibration signals are recorded from experimental setup, transformed to frequency domain using FFT and RMS features are extracted using an elliptic IIR band pass filter. This paper generally concludes as follows:

1) Features are trained using BPNN and results are simulated.
2) Bearing faults are successfully classified as Inner Race Fault (IRF), Outer Race Fault (ORF), and Rolling Ball Fault (RBF).
3) Investigated the effects of (NN) geometry and parameters on bearing fault diagnosis.

REFERENCES

[1] Ciprian Radu, "The Most Common Causes of Bearing Failure and the Importance of Bearing Lubrication," RKB Technical Review - February 2010.

[2] Jason R. Stack, Thomas G. Habetler, and Ronald G. Harley, "Fault Classification and Fault Signature Production for Rolling Element Bearings in Electric Machines," IEEE Trans. on Industry Applications, vol. 40, no. 3, May-June 2004.

[3] Pratesh Jayaswal, A. K. Wadhwani, and K. B. Mulchandani, "Machine Fault Signature Analysis," International Journal of Rotating Machinery Vol. 2008, Article ID 583982, 10 pages.

[4] A. R. Mohanty, "Video Lectures on Machine Fault Diagnosis and Signal Processing," National Program on Technology Enhancement and Learning, Indian Institute of Technology Kharagpur India.

[5] Pratesh Jayaswal, and Amit Aherwar, "Fault Detection and Diagnosis of Gear Transmission System via Vibration Analysis," The IUP Journal of Mechanical Engineering, Vol. 4, No. 3, 201142.

[6] Lakshmi Pratyusha, Shanmukha Priya, and VPS Naidu, "Bearing Health Condition Monitoring: Time Domain Analysis," International Journal of Advanced Research in Electrical, Electronics and Instrumentation Engineering, Vol. 3, Special Issue 5, December 2014.

[7] Timothy A. Dunton, "An Introduction to Time Waveform Analysis," Universal Technologies, Inc.

[8] Amit Shrivastava, and Dr. S. Wadhwani, "Development of Fault Detection System for Ball Bearing of Induction Motor Using Vibration Signal," International Journal of Scientific Research, Vol. 2, Issue 5, May 2013.

[9] Jason R. Stack, Thomas G. Habetler, and Ronald G. Harley, "Fault Classification and Fault Signature Production for Rolling Element Bearings in Electric Machines," IEEE Trans. on Industry Applications, Vol. 40, No. 3, May-June 2004.

[10] S. Rajasekaran, and G. A. Vijayalakshmi Pai, "Neural Networks, Fuzzy Logic, and Genetic Algorithms Synthesis and Applications," Prentice Hall India, Seventh Printing, February 2007.

A CRITICAL REVIEW ON FIRE RESISTANCE STRUCTURES

Darshan[1], Sanjith J[2], Ranjith A[3], Chethan G[4]

[1]P G Scholar, Department of Civil Engineering, Adhichunchanagiri Institute of Technology Chikkamagaluru, Karnataka, India

[2,3,4]Assistant Professor,Department of Civil Engineering, Adhichunchanagiri Institute of Technology, Chikkamagaluru, Karnataka, India

Email:sanjugou@gmail.com[1]

ABSTRACT

Basic concepts of risk-informed decision making for mitigating fire risk, and a general framework for assessing fire risk to building construction and for developing structural design requirements for fire conditions are described. Current best knowledge in thermal and mechanical properties and behaviors of normal strength concrete, high strength concrete, structural steel, and several major groups of common fire protection materials at elevated temperatures, which are necessary for performance-based engineering calculation, are presented. Modern fire-resistant design methodologies for concrete and steel structures are discussed, including methods based on standard fire tests as well as performance-based engineering analysis methods that involve heat transfer and structural analysis at elevated temperatures.

Keywords: **Building codes; concrete structures; design fire scenarios; fire-resistant design; fire risk mitigation.**

INTRODUCTION

One of the main reasons why Portland cement concrete is so widely used in building construction is that it can help satisfy the cardinal need for public safety in the face of the hazards of fire better than most alternative materials. Concrete is non-combustible and a reasonable insulator against the transmission of heat. In many applications, the main role of concrete in a fire is to protect any embedded steel for as long as possible against a rise in temperature to the point where its physical properties are reduced significantly, causing excessive structural deflections that might lead ultimately to collapse.

A new approach to high rise safety began emerging that required buildings to be constructed of columns, floors, walls and other elements that were fire resistive, defined as the ability of an element to withstand the effects of fire for a specified period of time without loss of its fire separating or load bearing function.

Various temperature-time curves are used today, depending upon the country and application. Figure 1.1 compares the ISO 834 test, the hydrocarbon fire
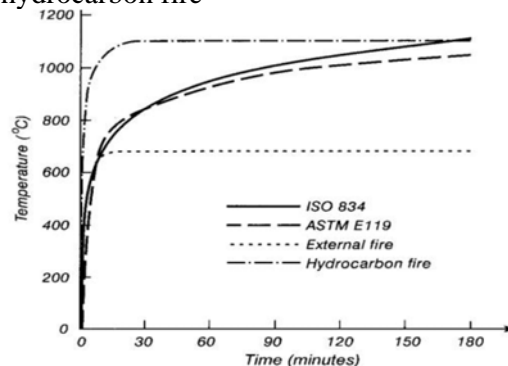

Figure 1:Temperaturevs. Time

A. *CONCRETE PROVIDES COMPREHENSIVE FIRE PROTECTION:*

Reducing deaths in fire and the impact of fire damage requires a comprehensive approach to

fire safety. The aim is to ensure that buildings and structures are capable of protecting both people and property against the hazards of fires. But private owners, insurance companies and national authorities may also have interests in fire safety for other reasons, such as **economic survival, data storage, environmental protection and upkeep of critical infrastructure**.

Structural fire protection measures must fulfil three aims:

i. **Personal protection** to preserve life and health;
ii. **Protection of property** to preserve goods and other belongings both in residential or commercial units that have caught fire, and in neighbouring properties. To this must be added substantial preservation of the building structures;
iii. **Environmental protection** to minimise the adverse effects on the environment through smoke and toxic gases as well as from contaminated water used for extinguishing fire.

Using concrete in buildings and structures offers exceptional levels of protection and safety in fire:

i. Concrete does not burn, and does not add to the fire load.
ii. Concrete has high resistance to fire, and stops fire spreading.
iii. Concrete does not drip molten particles, which can spread the fire
iv. Concrete is easy to repair after a fire, and so helps businesses recover sooner.
v. Concrete does not produce any smoke or toxic gases, so helps reduce the risk to occupants.

B. *PROTECTING PEOPLE:*

Very often fire threatens human life. This fact drives improvements in fire safety and compels us to design buildings that are capable of protecting people and their property against the hazards of fires. Concrete buildings and structures give personal protection against fire to preserve both life and health. Concrete behaves in fire, and how its material properties function effectively in terms of fire resistance .Life protection relies on concrete's inherent robustness, its non-combustibility and heat shielding properties to ensure that buildings remain stable during fire. This enables people to survive and escape, it allows fire-fighters to work safely and, what's more, it reduces the environmental impact caused by combustion products – this section explains how.

Risks of using combustible construction materials

1. An increase in fire load.
2. An increase in smoke and pyrolysis products.
3. Higher amounts of carbon monoxide.
4. Fire ignition of structural elements.
5. Fire ignition inside construction cavities.
6. Danger of smouldering combustion and imperceptible glowing
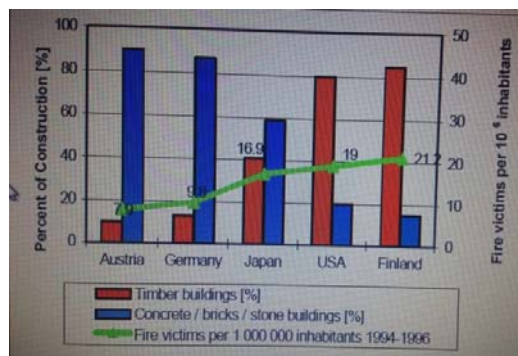7. Increasing occurrence of flashover

Figure 1.2: Fire deaths compared with construction type in five major countries

C. *Cementitious spray-fire proofing:*

Fireproofing's rendering something (structures, materials, etc.) proof against fire, or incombustible; or material for use in making anything fire-proof. It is a passive fire protection measure.

Figure 1.3: Construction worker applying spray resistive material

How can the surface appearance of the spray-fireproofing be improved?

i. **Hand troweling** may be applied to some spray applied fireproofing products to improve the surface appearance of the products.

ii. Surface decorative paint may be used as an Overspray on spray-applied fireproofing products for sealing, surface colouring or to increase light reflection.

FIGURE 1.4: Steel member with Hand troweling cementious spray fire proofing

Alternative fireproofing methods:

Among the conventional materials, purpose-designed spray fireproofing plasters have become abundantly available the world over. The inorganic methods include:

i. <u>Gypsum</u> plasters
ii. Cementitious plasters
iii. Fibrous plasters

Gypsum plasters have been lightened by using chemical additives to create bubbles that displace solids, thus reducing the bulk density. Also, lightweight <u>polystyrene</u> beads have been mixed into the plasters at the factory in an effort to reduce the density, which generally results in a more effective insulation at a lower cost. Fibrous plasters, containing either mineral wool, or ceramic fibres tend to simply entrain more air, thus displacing the heavy fibres.

FIGURE 1.5: Spray gypsum based plaster fireproofing being installed.

D. *List of fire-retardant materials:*

Fire retardant materials should not be confused with fire resistant materials. Whilst a fire resistant material is one that is designed to resist burning and withstand heat, fire retardant materials are designed to burn slowly.
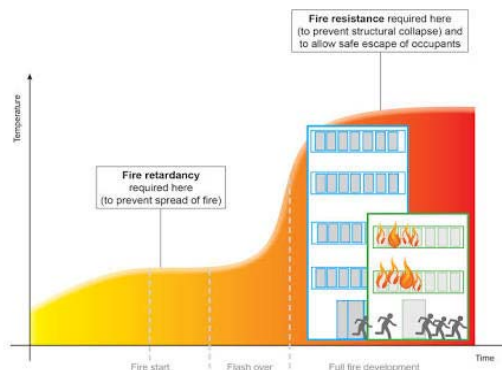

Figure 1.6: Showing the difference.

Fire-retardant materials used in buildings:

i. Rock wool
ii. Gypsum boards
iii. Asbestos cement
iv. Perlite boards
v. Proplex Sheets
vi. Calcium silicate boards
vii. Treated lumber plywood

Concrete prevents fire spread following earthquakes

The seismic design considerations that apply in some countries require designers to pay attention to thespecific problem of fires following earthquakes. This has been given due consideration in countries such as New Zealand, where concrete structures have been identified as having a low level of vulnerability to the spread of fire following earthquakes.

E. *FIRE RESISTANT BUILDINGS REQUIREMENTS:*

A building may be made more fire resistant by:

1. Using suitable materials.
2. Taking precautions in building construction
3. By providing fire alarm systems and fire extinguishers.

Using Suitable Materials:

The fire resisting material is having the following characters:

(a) It should not disintegrate under the effect of heat

(b) It should not expand under heat so as to introduce unnecessary stresses in the building
(c) The material should not catch fire easily
(d) It should not lose its strength when subjected to fire.

Fire resisting characteristics of some of the commonly used building materials are:

Stone: It is a bad conductor of heat. Sand stones with fire grains can resist fire moderately.

Granitedisintegrate under fire.

Lime stone: crumbles easily. Most of the stones disintegrate cooling period after heated by fire.
Brick: Bricks can resist heat up to 1200°C. At the time of construction, if good quality mortar is used, fire resistance is extremely good.
Timber: Any structure made of timbers is rapidly destroyed in fire. Timber enhances the intensity of fire. Use of heavy sections of timber in buildings is not desirable. To make timber more fire resistant the surface of timber is coated with chemicals such as ammonium phosphate and sulphate, boric acid and borax. Sometimes fire resistant paint is applied to timber used in the building.
Concrete: Concrete has got very good fire resistance. The actual behaviour of concrete in case of fire depends upon the quality of cement and aggregates used. In case of reinforced concrete and prestressed concrete, it also depends upon the position of steel. Larger the concrete cover, better is the fire resistance of the member.

There is no loss in strength in concrete when it is heated up to 250°C. The reduction in strength starts if the temperature goes beyond 250°C. Normally reinforced concrete structures can resist fire for about one hour at a temperature of 1000°C. Hence cement concrete is ideally used fire resistant material.
Steel: It is a good conductor of heat. Steel bars lose tensile strength. Steel yields at 600°C. They melt at 1400°C. Steel columns become unsafe during fire. Steel reinforcement weaken the reinforced concrete structures. Hence steel columns are usually protected with brick works or by encasing in concrete. Steel grills and beams are applied with fire resistant paints.
Glass: It is a poor conductor of heat. It expands little during heating. After heating when it cools,

cracks are formed in glass.
Aluminium: It is good conductor of heat. It has got higher resistance to fire.
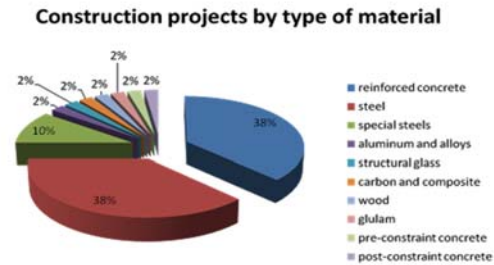**Asbestos Cement:** It is non-combustible material. It possesses high fire resistance.

Construction projects by type of material

- reinforced concrete
- steel
- special steels
- aluminum and alloys
- structural glass
- carbon and composite
- wood
- glulam
- pre-constraint concrete
- post-constraint concrete

Figure1.7:Percentage of materials used.

F. *FIRE RESISTANCE DESIGN CONSIDERATIONS.*

Fire safety is provided in a building by a combination of active fire suppression and passive fire protection. Active fire suppression includes fire fighting and automatic devices, such as sprinklers, to control the spread of fire. Passive fire protection includes measures, such as fire barriers, that control the spread of fire or insulations, such as concrete cover and spray-applied fire protection that delay the effects of fire on the structurecollapse in fire.

The following approaches can enhance fire resistance in buildings:
i.   Control fuel quantity and locations.
ii. Control fire spread.
iii. Control ventilation characteristics.
iv. Protect construction materials.

Loads for Structural Fire Design:-

The most likely loads at the time of a fire are much lower than the maximum design loads specified for normal temperature conditions. Most codes refer to an "arbitrary point-in-time load" to be used for the fire design condition. As an example, the ASCE document (ASCE 2005) gives the design load combination for fire Uf as

Uf = 1.2Dn + 0.5 Ln

Where, Dn and Ln are the design levels of dead and live load respectively

Design Equation:-The fundamental step in designing structures for fire safety is ,

Fire resistance ≥Fire severity

Where:

i.   *Fire resistance* = A measure of the ability of the structure to resist collapse, fire spread.

ii. *Fire severity* = A measure of the destructive impact of a fire

CONCLUSION

Concrete's excellent fire resistance has been proven by many tests performed for over 60 years. The American Concrete Institute and various building codes have developed prescriptive and analytical methods based on the fire tests on concrete components of structures. These methods provide architects and engineer a relatively easy way to select member proportions and reinforcement requirements for all but the very unusual structures. For the very unusual structures, alternate methods are available to adequately model or to test the complex behaviour of reinforced concrete components subject to fire. Despite potential deficiencies in performance at elevated temperatures arising from dehydration and thermal incompatibilities, concrete has a long-standing and justified reputation as a fire-resistant material, notwithstanding a long-recognized need for better means of testing and specifying endurance.

Development of temperature regime-structural behaviour models and greater understanding of thermal and mechanical properties are leading to significant improvements in specification and design against the extremes of fire and for moderately high temperature applications such as nuclear reactors. While striking advances have been made, full physical-chemical, thermodynamic explanations that tie together all the aspects of the very complex viscos-elastic, moisture-dependent behaviour pattern of concrete at elevated temperatures are still awaited.

REFERENCES

1. Collins Street Test (circa 1994) ByThe William Street.
2. French Car Park Fire Tests (1998-2001) A series of fire tests was conducted by the European Coal and Steel Council
3. NECK U (2002). Comprehensive fire protection with precast concrete elements – the future situation in Europe, Proceedings of BIBM 17th International Congress of the Precast Concrete Industry. Session 5,8 pp. Ankara, Turkish Precast Concrete Association. (CD only).
4. AMERICAN SOCIETY OF CIVIL ENGINEERS (2003) The Pentagon building performance report, ASCE, Washington, USA. 64 pp.
5. NARYANAN, N, and GOODCHILD, C H (2006) Concise Euro code 2, The Concrete Centre, Camberley, UK.107 pp.
6. ISO/CD 23932. Fire safety engineering – General principles. (under development).
7. DENOËL J–F (2006). Fire safety and concrete structures,
8. Association for Specialist Fire Protection, UK http://www.asfp.org.uk/index.html
9. Nanyang Technological University Fire Engineering Research Group http://www.ntu.edu.sg/cee/research/research_groups/fireresearch/research.htm
10. University of Manchester One-Stop Shop in Structural Fire Engineering http://www.mace.manchester.ac.uk/project/research/structures/strucfire/
11. University of Sheffield Fire Engineering Group http://www.fire-research.group.shef.ac.uk/
12. Wikipedia (Downloaded on dated 27/11/15)

EXTRACTION AND STUDIES ON SAPONIFICATION VALUES OF SOME NON EDIBLE SEED OILS FROM ARID ZONE OF RAJASTHAN

Akleshwar Mathur
Senior Assistant Professor, Department of Applied Sciences, JIET, Jodhpur
Email: akleshwar.mathur@jietjodhpur.ac.in

Abstract— The seed oils are a kind of secondary metabolites. A number of plants and trees supply good amount of oil seeds. Some of them are edible while others are non edible.

The non edible oils could be applied in industrial fields. These fields are soap manufacturing, paint and varnish, lubrication, animal food, fuel blending etc. The selection of oil for soap manufacturing can be done by saponification value. It is the number of milligrams of potassium hydroxide required to saponify 1g of fat under the conditions specified. It is affected by chain length of all the fatty acids present. The present paper deals with the extraction and determination of physicochemical properties of five seed oils with special reference to saponification values. The oils were extracted from seeds using petroleum ether as solvent and the acid values were determined by AOAC and ASTM methods. The acid values were found from the range of 162 to 292. It was concluded that the oils with high Saponification Value have good cleansing action than the lower ones.

Index Terms— Arid zone, cleansing action, potassium hydroxide, Saponification Value, seed oils.

I. INTRODUCTION

Fats and oils are the forms of energy stored in many organisms. These are triglycerides or derivatives of fatty acids (carboxylic acids with hydrocarbon chains of 4 to 36 carbons) may be saturated or unsaturated. Triacylglycerols are non polar, hydrophobic and insoluble in water because the polar hydroxyls of glycerol and the polar carboxylates of the fatty acids are bound in ester linkages.

When fats or oils are hydrolyzed under basic conditions, glycerol and salt of the corresponding fatty acid are obtained. This process is termed as Saponification means "soap making". Soap industry is one of the important commercial agencies. An industrial user should know the amount of free fatty acid present in the oil. The amount of free fatty acid is estimated by weight of alkali required for neutralization. For this purpose a known amount of oil/fat is warmed with strong aqueous caustic soda solution. By this the free fatty acids are converted into soap. This soap is removed and the amount of remaining fat is determined. This amount is subtracted from the initial amount of fat taken for the test.

The number of milligrams of potassium hydroxide required neutralizing the fatty acids present in one gram of oil or fat resulting from the complete hydrolysis is termed as saponification value. The information about the carbon chain and the average molecular weight of all the fatty acids present are obtained by this value. For example the long chain fatty acids have low saponification value as a fewer number of carboxylic functional groups are present per unit mass of the fat and have high molecular weight also, while the small fatty acids has high saponification value due to more number of carboxylic functional groups in per unit mass of

the fat.

Fats (triglycerides) upon alkaline hydrolysis (either with KOH or NaOH) yield glycerol and potassium or sodium salts of fatty acids (soap). [10]

Triacylglycerol   Glycerol   Soap
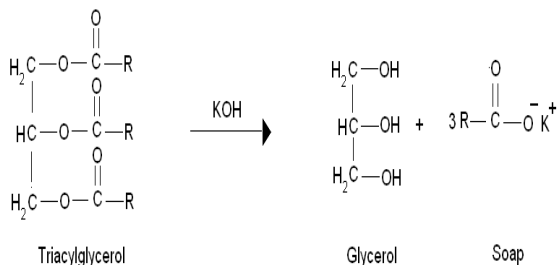
The Arid zone of Rajasthan is a good reservoir of desert plants which are adapted in dry climatic conditions. These plant species produce tones of seeds per year containing seed oil as a main constitute.[1-5] Some of them are suitable for human consumption called edible seeds/oils while others are non edible. Soap manufacturing is the most common application of these non-edible oils.

II. MATERIAL AND METHODS

A. Plant Species

The details of all the plant species were selected for analysis are given in Table .1[6-8]

Sp No	Botanical name	Common name	Family
1	*Nigella sativa*	Kalonji	Rannunculaceae
2	*Citrullus colycanthus*	Watermelon	Cucurbetaceae
3	*Terminaria catappa*	Wild almond	Combretaceae
4	*Leptadenia pyrotechnic*	Khimp	Asclepiadeceae
5	*Pergularia daemia*	Gadaria ke bel	Asclepiadeceae

B. Raw Material

The seeds for analysis were collected from wild regions of Jodhpur and adjoining areas. The seeds were dried in shade to remove excess of moisture. These were grinded to fine powder and subjected for analysis.

Nigella sativa

Citrullus collycanthus

Terminaria catappa

Leptadenia pyrotechnica

Pergularia damea

Plants and seeds of selected species

C. Moisture content

The moisture content in the seeds were kept 1-2% during analysis.

D. Extraction of oil

The known weight of grounded seeds were filled in a thimble and subjected in the Soxhelet Apparatus. Petroleum ether of boiling range 60-80⁰C is used for extraction. The solvent after extraction was recovered by distillation. The oil was filtered through sodium sulphite bed to remove moisture and stored in air tight viols.

E. Determination of Saponification Value

1 gm. of oil was taken into the round bottomed flask and 20 ml of 0.5 N alcoholic KOH solution

was added to it. The same procedure was followed without taking oil for blank titration .Both round bottomed flasks were refluxed for 1 hour .After reflux, both the round bottomed flasks were allowed to cool[8-9].

Both the samples were titrated using 0.5 N HCl with phenolphthalein indicator. The disappearance of pink color was recorded as the end point. Calculation was done by following formula-

Saponification Value= (Titre value of blank in ml – Titre value of sample in ml) x NKOH x Equivalent wt. of KOH.

III. RESULTS AND DISCUSSION

The saponification values obtained in this study has been shown in the Table.2.The lowest value was found for the seed oil of *Termenaria catappa* as 162 mg of KOH. The highest value was found for the seed oil of *Pergularia daemia* as 292.

The low value indicates the soft nature of soap with good cleansing action while the high value produces hard soap with fair cleansing action. It is clear from the above study that these oils could be applied for soap manufacturing with studies of other seed oil values.[11-12]

Table .2. Saponification values of seed oils

SR.NO.	PLANT SPECIES	SAP.VALUE	CATEGORY
1	*N.sativa*	200	Normal
2	*C.lanatus*	190	Normal
3	*T.catappa*	162	Low
4	*L.pyrotechnica*	196	Normal
5	*P.daemia*	292	High

IV.CONCLUSION AND FUTURE SCOPE

The saponification values obtained provide an idea about the molecular weight, structure of fatty acids and amount of lye for soap manufacturing. Although the accurate composition with percentage of fatty acids is obtained from Gas Chromatography of methyl esters yet the basic clue is obtained from sap values. The high value in case of species no.5 indicates presence of low fatty acids in abundance. The low value in species no.3 indicates good amount of higher fatty acids. The values for species 1, 2 and 4 resembles the normal values for vegetable oils.

The saponification values analyzed in the present study would be correlated to the chemical composition. Since the selected plants belong to Arid/semiarid climate, hence the commercial production of plants would provide better products. The soap obtained from these oils would be improved by addition of other oils/fats. The hard/soft nature, cleansing action, fluffy nature of foam and most important the skin care would be controlled by these values.

IV. REFERENCES

[1] M. M. Bhandari , Flora of Indian Desert", MPS Reports,Jodhpur,1990

[2] K. M. Nadkarni , Indian Materia Medica,volume2.

[3] J.F.Caius,The Medicinal and Poisinous Composites of India,FLS Journal,Bombay,Natural Historical Society,Volume –XLI.

[4] The Wealth of India-Raw Materials,volume-X CSIR-449

[5] Flora of Rajasthan-BSI volume-I,1991

[6] M.A.Deora ,P.Jaiswal,A.Mathur,M.R.K.Sherwani.JICS, 80,141,2003.

[7] P. Jaiswal , A. Mathur and M.R.K.Sherwani Oriental Journal of Chemistry,15(2),295(1999).

[8] AOAC,1997,Sec.C:Commercial Fats and Oils

[9] AOCS official methods Cd-3-25 for saponification value, AOAC Washington, D.C.

[10]Saponification value-Wikipedia, the free encyclopedia.

[11]Cynthia Nkolika Ibeto, Chukwuma Obiajulu Benedict Okoye, and Akuzuo Uwaoma Ofoefule,Comparative Study of the Physicochemical Characterization of Some Oils as Potential Feedstock for Biodiesel Production ,ISRN Renewable Energy, Volume 2012 (2012), Article ID 621518, 5 pages.

[12]Kailas M. Talkit , D. T. Mahajan and V. H. Masand Study on physicochemical properties of vegetable oils and their blends use as possible ecological lubricant , Journal of Chemical and Pharmaceutical Research, 2012, 4(12):5139-5144 .

APPLICATION OF TAGUCHI METHOD FOR OPTIMIZATION OF PROCESS PARAMETERS FOR MINIMUM SURFACE ROUGHNESS IN TURNING OF 45C8

Omvir Singh Bhaduria[1], Sanjay Goyal[2], Premanand S. Chauhan[3],
[1]PG Scholar, Mechanical Engineering, M.P.C.T Gwalior,
[2]Asst Prof., Mechanical Engineering, M.P.C.T Gwalior,
[3]Professor, Mechanical Engineering, IPS-CTM
Email: mihir22102@gmail.com[1], sanjaygoyal700@gmail.com[2], prempunit@gmail.com[3]

Abstract— Industries across the world are struggling to overcome the problem of rejection rate. In order to meet the customer's satisfaction, it is important to maintain the better quality of the product which can only be afforded by reducing the rejection rate. Surface roughness is one the important parameter in reducing the rejection rate. In this study, the Taguchi Method is used in order to find out the optimal cutting parameters to get the better surface roughness of 45C8 steel. Various cutting parameters viz: cutting speed, fed and depth of cut were taken and Taguchi method is used to find out the optimal combination so as to get the better surface roughness. Orthogonal arrays of Taguchi, the signal-to noise ratio (S/N) ratio, the analysis of variance (ANOVA) are employed to find the optimal levels and to analyze the cutting parameters on surface roughness. Finally confirmation tests with the optimal levels of cutting parameters are carried out in order to demonstrate the effectiveness of Taguchi optimization method.

Key words— ANOVA, 45C8 (EN8), Surface roughness, S/N Ratio, Taguchi Method.

I. INTRODUCTION

Metal cutting is one of the most important processes and broadly used manufacturing processes in mechanical industries (Yang et al., 1998) (Aggarwal .A et al, 2008). Highly competitive market requires high quality products at minimum cost. Products are manufactured by the transformation of raw materials (Davis, R et al, 2013). Industries in which the cost of raw material is a big share of the cost of finished goods, higher productivity can be achieved through proper selection and use of the materials. Surface finish is an important factor in manufacturing engineering and it can control the performance of mechanical parts and the production costs (Harsh Y Valeraa et al, 2014). Surface roughness is one of the important parameter in conventional machining. Optimizing this parameter is most challenging task in turning process. Industries are working more on reducing the rejection rate and improving the surface roughness. Better quality of the product can afford finest customer satisfaction. Highly competitive market requires high quality products at minimum cost. Products are manufactured by the transformation of raw materials in to finished goods. Surface roughness says about the quality of machining and also about the quality of product. The materials which have good surface finish posses better property as compared to lower surface finish of that material.

Surface roughness says about the quality of machining and also about the quality of product. The materials which have good surface finish posses better property as compared to lower surface finish of that material. Such surface roughness plays a very important role as one of the parameter in machining process. Industries across the world are struggling to overcome the problem of rejection rate. By reducing rejection rate and optimally utilization of machines and

their working conditions, we can not only be able to produce good products but can also reduce the cost significantly. Industries are more dependent on the working skills of the machine tool operators in selection of best cutting conditions. This helps not only in producing the product with less rejection rate, but also help in reducing the cost of the product.

The various literature reviews has revealed that several researchers attempted to analyze the optimal cutting conditions in turning operations. Armarego and Brown used the concept of maxima / minima of differential calculus to optimize machining variable in turning operation (E.J.A Armarego et al , 1969) . Brewer and Rueda have developed different monograms which assist in the selection of optimum conditions (R.C Brewer and R. Rueda). Few of the other techniques that have been used to optimize the machining parameters include goal programming (R.M Sundaram, 1978) and geometrical programming (P.G Petropoulos, 1973). Accuracy and surface roughness of the product are the matter of more attention in the industries now days. Surface roughness is the most significant criterion in determining the metal removal rate of the material. Surface roughness and dimensional accuracy are the key factors needed to forecast the machining performances of any machining operation (A.Mital, et al. 1988).

The main aim of this study is to obtain the significant factor those affect the surface roughness during the turning operation on EN 8 steel material on CNC turning center.

II. EXPERIMENTAL DETAILS

A. Material

The specimen used in the study is EN8 steel (40C8) in the form of round bar with 20 mm diameter and 60 mm cutting length. This steel is generally used for the manufacturing of shafts, studs, general purpose axles, keys, cam shafts etc. EN8 is a very popular grade of through-hardening medium carbon steel, which is readily machineable in any condition. 45C8 (EN8) in its heat treated forms possesses good homogenous metallurgical structures, giving consistent machining properties.

Fig 1: Sample of EN 8 steel

Fig 2: EN8 rods after machining operations

B. Experimental Setup

The experimental setup is carried out on CNC turning center. Computer Numerical Control (CNC) is a machine in which the functions and motions of a machine tool are controlled by means of a set of program based on G and M code. Experimental setup was carried out on CNC Lathe MCL12. This machine works on two X and Z direction along with spindle encoder feedback. Various programmes are designed by CAD/CAM on PC. Programme input and DNC online is executed from PC through RS232C interface. It has 4 station automatic tool turrets on which four tools can be mounted and used during the program. Other specification of the CNC Lathe MCL12 is given below.

Capacity of the Machine

Longitudinal Travel (Z axis)	300m
Cross Slide Travel (X axis)	150mm
Chuck size	5 inches
(127mm)	
Spindle Drive	3 H.P ac motor with VFD
Max Spindle Speed rpm	2000 – 2800
Max Machining Diameter	50mm
Type of Drive	AC Servo
Circulating Coolant	Available
Number of Axis	Two
Transmission	Ball Screw
Automatic Lubrication	Provided

CNC System of Machine
3 +1 Axis CNC System
Individual Industrial Controller
Define G, M, F, S, T, I, J, R Codes
DNC functions
Interface with PC through RS232
CAD/CAM/FSM compatibility

Fig 3: CNC Lathe – MCL 12

C. Design Layout

Experiment is carried out under dry condition using CNC Lathe MCL12 which has maximum spindle speed of 2800 rpm. During the process three things were kept constant viz: cutting tool, machining condition i.e. dry and diameter of rod (EN8 steel). Experiment was carried out with three different parameters viz: cutting speed (rpm), feed (mm/rev) and depth of cut with their three different levels as given in the table below. Most of these range of various parameters used were selected in view of data available in the literature, machine technical data. Optimal value of surface roughness was measured to get the result, which was measured by SURFCOM FLEX machine with a sampling length of 30 mm.

Fig 4: Surfcom Flex Machine

Table 1: Cutting Parameters

Factor	Cutting parameters	Level 1	Level 2	Level 3
N	Speed (rpm)	650	800	950
f	Feed (mm/rev)	0.1	0.2	0.3
d	Depth of Cut (mm)	0.2	0.4	0.6

III. DESIGN OF EXPERIMENT

A. Taguchi Method

In order to find out the optimal value of various combinations of our parameters taken to get the best surface finish, we have taken Taguchi method for analysis of parameters. Any research involves investigation of various parameters taken with different level. Doing an experiment with all the considered parameters factors is the most complicated and tough and also time consuming as well. Manually it is not easy to perform or study many experiments. Here the factor represents the any variables that impact the result of our experiment. Level is defined as the different setting in the variable can be set. There by priority some are considered factors and others are left behind. In CNC machining only two factors can be varied at one time while keeping the third one as fixed parameters, to understand the change in the surface roughness.

The Taguchi method is a well-known technique that provides a systematic and efficient methodology for process optimization and this is a powerful tool for the design of high quality systems. Taguchi approach to design of experiments is easy to adopt and apply for users with limited knowledge of statistics, hence gained wide popularity in the engineering and scientific community. This is an engineering methodology for obtaining product and process condition, which are minimally sensitive to the various causes of variation, and which produce high-quality products with low development and manufacturing costs.

This technique helps to study effect of many factors (variables) on the desired quality characteristic most economically. By studying the effect of individual factors on the results, the best factor combination can be determined (Roy, R.K., 2001). Taguchi is one of the solutions to such a problem. It allows us to vary the entire factor at time and still allow us to evaluate effect of each individual factor. It also allows us to experiment in limited number and predict the remaining combinations of the factors. Taguchi method provides a simple, competent and methodical approach to optimize the designs for performance, quality, and cost. The greatest advantages of the Taguchi method are to reduce the cost and to find out significant factors in a shorter time period (M.Sanylmaz, 2006).

In order to introduce the Taguchi's approach and his experimental design as well which may be used as under (Ross PJ, 1988):

- Processes as well as designing products which may be sounds to environmental conditions;
- Both designing and developing products/processes which may be sounds to component variation;
- Reducing deviation around a target value.

Taguchi has addressed Design, Engineering (offline) as well as Manufacturing (online) quality. This concept differentiates Taguchi technique from Statistical Process Control (SPC) which is entirely an online quality control technique (Ryan Thomas P, 1988), (Benton W C, 1991) .Taguchi ideas can be reduced into two fundamental concepts i). Quality losses should be defined as deviation from target, not conformance to arbitrary specifications. (Benton W C, 1991) ii). In order to achieve high system quality levels which may also be frugal which needs quality to be designed into product? It does not manufacture in to the product but only designs the quality (Daetz D, 1987) (Taguchi G).

It was proposed by Taguchi that engineering optimization of a process or product may be carried out in three steps viz; (i) system design, (ii) parameter design, and (ii) tolerance design. These three steps may be explained in bird's eye view as under

i. System Design: In this design, an engineer applies scientific and engineering Knowledge, which produce a basic functional prototype design. This design including the product design stage and the process design stage and further the process design stage as well.

ii. Product Design: It involves the selection of materials, components, tentative product parameter values, etc. In process design stage apart from tentative process parameter values it also includes the analysis of processing sequences and selections of production equipments.

System Design: System design may define as an initial functional design. It may be far from optimum in terms of quality and cost. The aim of the parameter design (Montgomery DC, 1997) may be defined, to optimize the settings of the process parameter values. It improves the

performance characteristics as well to identify the product parameter values. In this regard it is expected that the optimal process parameter values which have been obtained from the parameter design are not sensitive to the variation of environmental conditions and other concern noise factors. In this way it may be seen that the parameter design is the key step in the Taguchi method which achieves high quality without increasing cost.

B. Orthogonal Array L9

Taguchi's L9 Orthogonal Array was used in the design of experiment. There is powerful tool for design of high quality systems, i.e. Taguchi technique which has been used by many researchers tacitly. It also provides simple, efficient and systematic approach to optimize quality, cost and designs for performance. Taguchi technique is efficient tool for designing process that operates consistently and optimally over a variety of conditions. Taguchi technique is an experimental design technique, which is useful in reducing the number of experiments by using orthogonal arrays. Taguchi's approach to design of experiments is easy to adopt and apply for users with limited knowledge of statistics; hence it has gained a wide popularity in the engineering and scientific community (D.C.Montgomery, 1997). The main objective of Taguchi method is to ensure quality in the design phase. Taguchi technique also allows controlling the variations caused by the uncontrollable factors which are not taken into consideration at traditional design of experiment.

Table 2: L9 Orthogonal Array (a)

Experiment No	Variable 1	Variable 2	Variable 3	Variable 4
1	1	1	1	-
2	1	2	2	-
3	1	3	3	-
4	2	1	2	-
5	2	2	3	-
6	2	3	1	-
7	3	1	3	-
8	3	2	1	-
9	3	3	2	-

Table 2: L9 Orthogonal Array (b)

Experiment No	Variable 1	Variable 2	Variable 3	Variable 4
1	650	0.1	0.2	-
2	650	0.2	0.4	-
3	650	0.3	0.6	-
4	800	0.1	0.4	-
5	800	0.2	0.6	-
6	800	0.3	0.2	-
7	950	0.1	0.6	-
8	950	0.2	0.2	-
9	950	0.3	0.4	-

C. Signal to Noise ratio (S/N)

The signal to noise ratio (S/N ratio) is used to measure the proneness of the quality characteristic which was being investigated in a controlled manner. Well known Taguchi method reveals that the term 'signal' represents the desirable effect (mean) for the output attribute whereas the term 'noise' represents the undesirable effect (signal disturbance, S.D) for the output attribute which has got influence of outcome because of external factors viz; noise factors. The S/N ratio can be computed as

Nominal is the best $S/N_T = 10 \log\left(\frac{\bar{y}}{s_{\bar{y}}^2}\right)$

Larger-is-the better (maximize) $S/N_L =$

$$10 \log\left(\frac{1}{n}\sum_{i=1}^{n}\frac{1}{y_i^2}\right)$$

Smaller-is-the better (minimize) $S/N_S =$

$$-10 \log\left(\frac{1}{n}\sum_{i=1}^{n}y_i^2\right)$$

Where y is the average of observed data, s^2y is the variance of y, n is the number of observations and y is the observed data.

It is notable that these S/N ratios are explicit on a decibel scale. In this regard S/N_T is used if the aim is to reduce variability around a specific target, S/N_L in case the system is optimized when the response is as large as possible, and S/N_S in case the system is optimized when the response is as small as possible. Its factor level maximizes the appropriate S/N ratio are known as optimal. The object of this research was to create minimum surface roughness (Ra) in a turning operation. By virtue of this research smaller Ra values signify better or improved surface roughness. Therefore, a smaller-the-better

quality attribute was implemented and introduced in this study (Montgomery DC, 1997).

Table 3: S/N Ratio

Experiment	SR (1)	S/N Ratio
1	5.009	-13.99
2	7.031	-16.94
3	10.16	-20.13
4	4.664	-13.37
5	2.96	-9.42
6	8.468	-18.55
7	2.148	-06.64
8	2.187	-06.79
9	6.403	-16.12

D. Analysis of Variance (ANOVA):

The purport of the analysis of variance (ANOVA) was to gain those parameters which are significantly affecting the quality attribute. The total sum of square deviation, SS_T can be calculated using (Roy, R.K., 1990).

$SS_T = \sum_{i=1}^{y} y_i^2 - C.F$

where, *n* represents the number of experiments in the orthogonal array, y_i is the total surface roughness of *i*th experiment and *C.F.* is the correction factor. *C.F* may be computed as (Roy, R.K., 1990).

$$C.F = \frac{T^2}{N}$$

where, *T* is the sum of all total surface roughness.

The total sum of square deviations i.e. SS_T was segregated into two ways: the sum of squared deviation, SS_d *owing* to each process parameter and the sum of square error, SS_e. The percentage contribution which is denoted by *P,* in which each process parameter is the total sum of square deviation, SS_T that is a ratio of the sum of square deviation, SS_d because of each process parameter to the total sum of square deviation, SS_T.

To the point of view of statistical study, there is a test called *F*-ratios (variance ratio) to study which parameters have significant effects. For performing the *F* test, the mean of square deviation, SS_m *due* to each process parameter requires due calculation. The mean of square variations, SS_m *is* equal to the sum of square deviation, SS_d *divided* by the number of degree of freedom linked with the process parameters. As a result of it, the *F* value for each process parameter is merely the ratio of the mean of

square deviation, SS_m to the mean of square error, SS_e.

Table 4 shows the results of pooled ANOVA for the surface roughness test. In experiment, the F-ratios were obtained for 90% level of confidence. In addition to this, percentage contribution of each parameter was also calculated. The most significant factors were feed that contributed maximum to the total surface roughness. The contributions from these parameters were cutting speed (38.62%), feed (50.27%), depth of cut (8.70%) & other factor/error (2.39%). The optimal combination of parameters and their levels for achieving minimum surface roughness which are based on the S/N ratio and ANOVA analyses is A3B2C3 i.e. Cutting speed at level 3, feed at level 2, and depth of cut at level 3.

Table 4: ANNOVA

Parameters	DOF	Sum of Squares (S)	Variance Ratio F Ratio	% Contribution = S' /SS Total
		SS due to each Design	V treatment /V error	
Cutting Speed	2	77.33	65.57	**38.62**
Feed	2	100.31	85.05	**50.27**
Depth of Cut	2	18.33	15.54	**8.70**
All Others/ Error	2	1.179	0.58	2.39
Total	8	**197.17**		

Table 5: Mean S/N response table

Parameters	DOF	Levels		
		1	2	3
Cutting Speed	2	-17.02	-13.78	-9.85
Feed	2	-11.33	-11.05	-18.27
Depth of Cut	2	-13.11	-15.48	-12.06

E. Confirmation test

In order to verify the estimated results with the experimental results as well, the confirmation tests are performed. The confirmatory test is only required when the optimal permutation of parameters and their levels coincidently do not match with one of the experiments in the OA. The calculation of estimated value of the total surface roughness at optimum condition is done by adding the average performance to the contribution of each parameter at the optimum level using the following equations

$$Yopt = m + (mAopt – m) + (mBopt – m) + (mCopt - m) \quad m = \frac{T}{n}$$

where m is the average performance, T is the grand total of average total surface roughness for each experiment, n is the total number of experiments and *mAopt* is the average total surface roughness for parameter A at its optimum level, *mBopt* is the average total surface roughness for parameter B at its optimum level, *mCopt* is the average total surface roughness for parameter C at its optimum level.

When optimum combination of parameters and their levels did not correspond to any experiment of the orthogonal array then the necessity of confirmation test arises in this study. Since optimum combination of parameters i.e.A3B2C3 is not available in experiment list, hence experiment has been performed with this combination and found following result.

Table 6: Orthogonal Array (a)

Experiment No	Variable 1	Variable 2	Variable 3	Variable 4
10	3	2	3	-

Table 7: Orthogonal Array (a)

Experiment No	Variable 1	Variable 2	Variable 3	Result
10	950	0.2	0.3	2.015 μm

IV. RESULT

On the basis of various experiments and analysis carried out, following are the results that we obtained.

The graph to show the effect of cutting speed has been plotted (fig 5.).
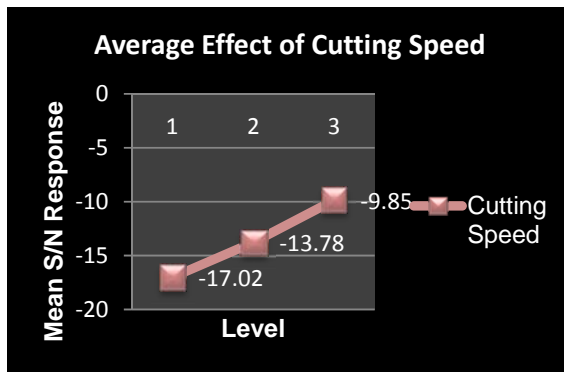
Fig 5: Effect of Cutting speed

The graph to show the effect of feed has been plotted (fig 6)
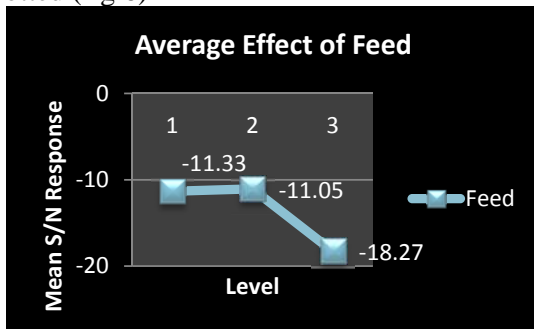

Fig 6: Effect of feed

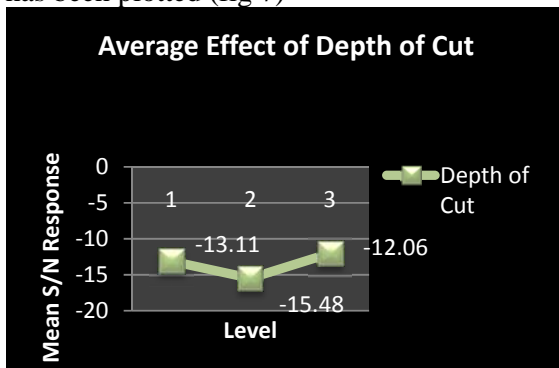The graph to show the effect of depth of cut has been plotted (fig 7)

Fig 7: Effect of depth of cut

The combined effect has been shown in the graph (fig 8)

Fig 8: Effect of cutting parameters

Pie diagram and bar chart to show the contribution of various process parameters has been drawn (fig 9 & fig 10)
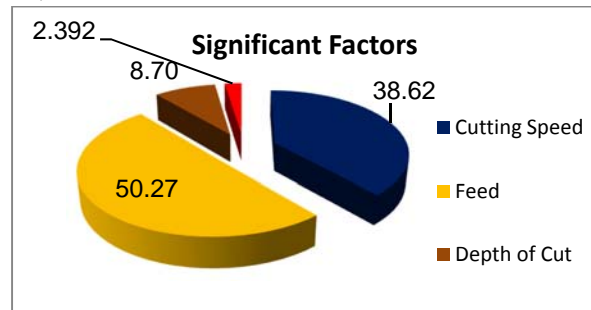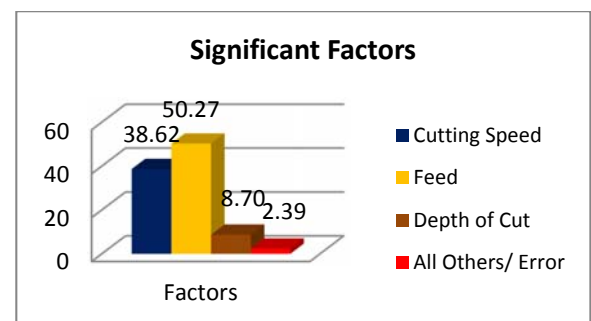

Fig 9: Contribution of Significant Factors (a)

Fig 10: Contribution of Significant Factors (b)

V. CONCLUSION AND SCOPE FOR FUTURE WORK

A. Conclusion

From the analysis of the results, the following can be concluded from the present study:

1. The optimum conditions are A3B2C3 i.e. Cutting speed at level 3, feed at level 2, and depth of cut at level 3.
2. The optimum surface roughness is 2.015 µm
3. The most significant factors was feed that contributed maximum to the total surface roughness
4. The contribution of parameters is cutting speed (38.62%), feed (50.27%), depth of cut (8.70%) & other factors/ error (2.39%).

B. Scope for future work

The present work has been carried out without considering interaction effect. In future work can be done after considering interaction effect. Work can also be done to find out the optimum combination of process parameters for different steels as well other alloys. The application of this

work can also be done in any industry to reduce rejection rate.

REFERENCES

[1] 1] Yang, W. H., & Tarng, Y. S. (1998). Design optimization of cutting parameters for turning operations based on the Taguchi method. Journal of Materials Processing Technology, 84(1), 122-129.

[2] [2] Aggarwal, A., Singh, H., Kumar, P., & Singh, M. (2008). Optimizing power consumption for CNC turned parts using response surface methodology and Taguchi's technique—a comparative analysis. Journal of materials processing technology, 200(1), 373-384.

[3] Davis, R., John, V., Lomga, V. K., & Horo, R. P. (2013). The Application of Taguchi's Optimization Method in Wet Turning Operation of EN 19 Steel. International Journal of Mechanical & Production Engineering Research & Development (IJMPERD), 3(2).

[4] Harsh Y Valeraa, Sanket N Bhavsara (2014). Experimental Investigation of Surface Roughness and Power Consumption in Turning Operation of EN 31 Alloy Steel - 2nd International Conference on Innovations in Automation and Mechatronics Engineering, ICIAME 2014

[5] E.J.A Armarego and R.H Brown, The machining of metals prentice Hall, 1969

[6] R.C Brewer and R. Rueda , "A Simplified Approch to the optimum selection of machining parameters ", Engines Digest vol.24,NO.9,PP 133-150

[7] R.M Sundaram, "An application of Goal programming technique in metal cutting", Int.j.prod, Res. Vol 16 NO5,1978, PP375-382.

[8] P.G Petropoulos, "optimum selection of machining rate variable by Geometric programming ",Int .J .prod .Res,vol.11,NO,4,1973 PP 305-314

[9] A.Mital, M.Mehta, "surface roughness Prediction models for fine turning", International journal of production research 26 (1988) 1861-1876

[10] Roy, R.K., 2001, "Design of Experiments using The Taguchi Approach: 16 Steps to Product and Process Improvement". John Wiley & Sons, Inc.

[11] M.Sanylmaz, Design of experiment and an application for Taguchi method in quality improving activity,M.S. Thesis, Dumlupmar university,Turkey,(2006).

[12] Ross PJ. Taguchi techniques for quality engineering. New York: McGraw-Hill; 1988.

[13] Ryan Thomas P, Qual prog , (1988) 34-36.

[14] Benton W C, Int J Prod Res , 29(1991) 1761-1770.

[15] Daetz D ,Qual Progr ,20(1987) 54-61.

[16] Taguchi G,Quality engineering in production.

[17] Montgomery DC. Design and analysis of experiments. 4th ed. New York: Wiley; 1997.

[18] D.C.Montgomery, (1997), Design and analysis of experiments, 4th edition, John Wiley & sons.

[19] Montgomery DC. Design and analysis of experiments. 4th ed. New York: Wiley; 1997.

[20] Roy, R.K., 1990, "*A Primer on the Taguchi method*". Competitive Manufacturing Series, Van Nostrand Reinhold, New York.

A REVIEW ON CLOUD SECURITY ISSUES

Mahendra Badnora[1], Jitendra Sharma[2]
[1]Research Scholar, Dept of CSE, RIT, Indore
[2]Asst Professor, Dept of CSE, RIT, Indore
Email:badnora@gmail.com[1]

Abstract

The Cloud computing is the way of using a network of remote servers hosted on the Internet to store, process and manage data, rather than on to the local server. Security is the most important concern in the cloud computing because the user data is transferring through the insecure medium i.e. Internet. In this paper, we present an overview of existing issues related to the cloud security and algorithms for fine-grained access control and data security in the cloud environment. All these algorithms are described more or less on their own. Cloud security is a very popular task. We also explain the fundamentals of sequential rule mining. We describe today's approaches for cloud security. From the broad variety of efficient algorithms that have been developed we will compare the most important ones. We will systematize the algorithms and analyze their performance based on both their run time performance and theoretical considerations. Their strengths and weaknesses are also investigated. It turns out that the behavior of the algorithms is much more similar as to be expected.

Introduction

More recently, Lots of schemes have been already proposed to achieve flexible and fine-grained access control. Unfortunately, these schemes are only applicable to systems in which data owners and the service providers are within the same trusted domain. In cloud computing, the data owner and Service providers are usually in different domain, a new access control scheme utilizing attributed-based encryption is proposed, which adopts the so-called key-policy attribute-based encryption (KP-ABE) to enforce fine-grained access control. This scheme has some drawbacks such as flexibility in attribute management and lacks scalability in dealing with multiple-levels of attribute authorities.

Over the last few years, cloud computing has evolved as one of the most effective domain in the IT Industry and has lulled and grabbed attention from both academic and professional world. Cloud computing holds the promise of providing computing as the fifth utility [1] after the other four utilities (water, gas, electricity, and telephone). The cloud computing provide scalability, flexibility, cut down the cost and capital investment and increased operational efficiency, and so on as its benefits. Different service-oriented cloud computing models have been proposed, including Infrastructure as a Service (IaaS), Platform as a Service (PaaS), and Software as a Service (SaaS). Numerous commercial cloud computing systems have been built at different levels, e.g., Amazon's EC2 [2], Amazon's S3 [3], and IBM's Blue Cloud [4] are IaaS systems, while Google App Engine [5] and Yahoo Pig are representative PaaS systems, and Google's Apps [6] and Salesforce's Customer Relation Management (CRM) System [7] belong to SaaS systems. These different cloud computing systems provides benefits to enterprise users by cut down the cost of hardware/software or no need to hire IT professionals to maintain this systems, on the other hand, utilities supplied by cloud computing are being offered at a comparatively low price in a pay-as-per-use style.

The benefits bring by cloud computing paradigm are exciting for IT companies, academic researchers, and potential cloud users, security becomes the serious problem in cloud

computing, will prevent cloud computing extensive applications and usage in the future. One of the most important security issues is data security and privacy in cloud computing due to its Internet- based data storage and management. Cloud users have to give their data to CSP's (cloud service provider) for storage and business uses, while the CSP's are commercial enterprise which cannot be trustworthy. For any organization, data is very important. If the confidentiality of the data is disclosed to their competitors or to the public, the enterprise will face a big problem. Thus the cloud user need the assurance that the confidentiality of their data is not going to be reveal in front of outsiders, including cloud providers and their competitors. This is the basic data security which is required. Other than that, flexible and fine-grained access is also desired in cloud computing environment.

Literature Review

The literature review is divided into two sections. In first section we describe the cloud securities general overview and in second section we describe and compare the different algorithms for Attribute Based Encryption.

In paper [1] the authors define the cloud computing and provide the architecture for creating cloud by using technologies such as Virtual Machines (VMs). It also explains the market strategy for resource management including both customer-driven service management and computational risk management to sustain Service Level Agreement (SLA)-oriented resource allocation. Moreover, it highlights the difference between High Performance Computing (HPC) workload and Internet-based services workload.

The state-of-the-art Cloud technologies have limited support for market-oriented resource management and they need to be extended to support: negotiation of QoS between users and providers to establish SLAs; mechanisms and algorithms for allocation of VM resources to meet SLAs; and manage risks associated with the violation of SLAs. Moreover, interaction protocols needs to be extended to support interoperability between different Cloud service providers. In addition, we need programming environments and tools that allow rapid creation of Cloud applications.

In this paper [8], the authors shows the security policies and with different methods and their limitation. This model defines policy as the collection of interdependent statements of provisioning and authorization. Each statement identifies context-sensitive session requirements. A reconciliation algorithm attempts to identify a policy instance compliant with the stated requirements. We define and prove the correctness of an efficient two-policy reconciliation algorithm, and show by reduction that three or more policy reconciliation is unmanageable. It also identifies several heuristics for detecting and combating intractable provisioning policy reconciliation, and shows that reconciliation of (many) reasonable authorization policies can be efficient.

Policy in our model defines interdependent statements of provisioning (session configuration) and authorization. We show that the general problem of provisioning policy reconciliation is unmanageable. By restricting the language, we show that reconciliation of two policies becomes manageable. However, reconciliation of three or more policies under this restriction remains unmanageable. The design and implementation of the Ismene policy language is based on the Policy Model. The Ismene language and supporting infrastructure is built on top of previously designed algorithms.

In paper [9], the authors described the different security issues and challenges in accepting cloud computing model. Usually the data services provided by the cloud are delivered by the third party provider who owns the infrastructure. The challenges related to cloud computing are based on the users authenticity. IDC conducted a survey in 2008 for knowing the challenges due to which the organizations feared to adopt cloud computing.

The challenges are as follows: Security, Costing Model, Charging Model, Cloud Interoperability Issue and Service Level Agreement [SLA].

In this paper [10], the authors discussed issues related to security with Cloud Based Computing and Cloud Operating Systems. In recent time,

the Cloud computing experienced a remarkable increase in popularity as major companies such as Google and Microsoft have started to release cloud based products, denote the use of the cloud, and even release an open source Cloud OS. As the popularity of cloud computing increases the demand for security will increase. In this the authors try to figure out specific security concerns for cloud computing as well as shared security issues between cloud and other computing. It also propose a method for allowing the user to select specific security levels of security for items and make a list of security items that all users should be aware of before opting to use cloud based services.

There are lots of security issues related to cloud computing. Few of them are as follows.XML signature [11], Flooding [11], Browser Security [11], Reputation fate Sharing [12], Loose Control over Data, dependence of Internet and many more.

This section shows the algorithms based on Attribute based Encryption.
Attribute Based Encryption (ABE) is one of the encryption schemes, which is a novel domain where such policies are magnified and glorified in the encryption algorithm itself. The existing ABE schemes are of two types. They are Key-Policy ABE (KP-ABE) scheme and Ciphertext-Policy ABE (CP-ABE) scheme. In KP-ABE scheme, attribute are associated with keys and data is associated with attributes. The can be decrypted only when the keys associated with the policy that is satisfied by the attributes associating with data. In CP-ABE schemes, attribute policies are associated with data and attributes are associated with keys and only those keys that the associated attributes satisfy the policy associated with the data are able to decrypt the data. The scheme proposed in the paper [13] is based on the KP-ABE, tries to provide the fine grained access control. But this current work not provides the fine grained access, data confidentiality and scalability simultaneously. The different algorithms are as follows:

   A. Key-policy Based Attribute Based Encryption

Key-policy Attribute Based Encryption scheme is public key cryptography that is for one-to-many communication. In this data are

associated with attributes for which a public key is defined. The encryptor associates the set of attributes to data by encrypting it with public key. Access structure is defined as access tree over the data with attributes which is assigned to users. The secret key is defined to show the access structure. The user is able to decrypt the data or message, if and only if the ciphertext satisfy the access structure.

KP-ABE [13] is access control mechanism, which works with re-encryption techniques for efficient user revocation in cloud computing. This scheme permits a data owner to reduce most of the computational overhead to cloud servers. The KP-ABE encryption scheme is used to provide fine-grained access control. Each file or message is encrypted with a symmetric data encryption key (DEK), which is again encrypted by a public key corresponding to a set of attributes in KPABE, which is generated corresponding to an access structure. The data file that is encrypted is stored with the corresponding attributes and the encrypted DEK. Only if the corresponding attributes of a file or message stored in the cloud satisfy the access structure of a users key, then the user is able to decrypt the encrypted DEK, to decrypt the file or message.

The problem with this scheme is that the encryptor is not able to decide who can decrypt the encrypted data except choosing descriptive attributes for the data, and has no choice but to trust the key issuer.

   B. Expressive Key Policy Attribute Based Encryption

Among the encryption methods in clouds Attribute-based Encryption (ABE), allows fine-grained access control on encrypted data. In the Key Policy Attribute Based Encryption, Each file or message is encrypted with a symmetric data encryption key (DEK), which is again encrypted by a public key corresponding to a set of attributes in KPABE, which is generated corresponding to an access structure. This expressive key-policy attribute based encryption (KP-ABE) schemes allowing for non-monotonic access structures (i.e., that may contain negated attributes) and with constant cipher- text size. Towards achieving this goal, show that a certain class of identity-based

broadcast encryption schemes generically yields monotonic KP-ABE systems in the selective set model. A new efficient identity-based revocation mechanism, when combined with a specific instantiation of our general monotonic construction, provides rise to the first truly expressive KP-ABE realization with constant size ciphertext. The drawback of these new constructions is that private keys have quadratic size in the number of attributes. On the opposite side, they reduce the number of pairing evaluations to a constant that seems to be a novel feature among expressive KP-ABE schemes.

C. Ciphertext-policy Attribute Based Encryption

In lots of decentralized systems users should only able to access the data if a user own certain set of attribute. The only way to apply such policies is to employ a trusted server to store the data and mediate access control. If server compromises the stored data, then the secrecy of the data is also compromised. For complex access structure, a new system is designed on encrypted data that known as CP- ABE [14]. Data secure by using this encrypted techniques even if the storage server is untrusted. Previously defined Attribute- Based Encryption systems based on key attributes to describe the encrypted data. Data encrypted by user private key which are specified by a set of attributes and decrypt by a specific policy over these attributes specifying which users are able. In this system, decryption keys only support user attributes that are organized logically as a single set, so users can only use all possible combinations of attributes in a single set issued in their keys to satisfy policies. This policy conceptually near to former access control method such as Role-Based Access Control (RBAC).

This system is based on how attributes and policy are associated to ciphertext and users' decryption key. In CP-ABE scheme, a monotonic structure is associated with the ciphertext, and set of attributes associated with users' decryption key. Unlike KP-ABE, the roles of ciphertext and decryption key are switched in CP-ABE. The encryptor chooses the tree access policy to encrypt the data, and set of attributes are used to create decryption key. If the set of attributes associated with decryption key satisfy the tree access policy associated with the ciphertext, and then the key can be used to decrypt the ciphertext.

The CP-ABE scheme is not good enough to support access control in modern enterprise environment. Because it requires flexibility and efficiency in specifying policies and user attributes. In this scheme, the key used for decryption supports only user attributes organized as a single set, so user can use all possible sets of attributes in a single set issued with keys to satisfy policies.

D. Cipher Text Policy Attribute Set Based Encryption(CP-ASBE)

Cipher Text Policy Attribute Set Based Encryption is a new variant of CP-ABE, unlike existing CP-ABE schemes that represent user attributes as a single set of keys, organizes the user attributes into a recursive set based structure and allows user to impose dynamic constraints on how those attributes may be combined to satisfy the policy.
In CP-ASBE, uses recursive set structure is denied to maintain users' attributes unlike CP-ABE which uses single set of attributes to satisfy the policies.

In CP-ABE Scheme, user attributes are organized as the single set for decryption key, the user can use all possible set of attributes in a single set issued in their key to satisfy policies. To solve this problem, new scheme introduced known as Cipher text Policy Attribute Set Based Encryption. It is extended form of CP-ABE which manages user attributes into a recursive structure.

CP-ASBE allows, the user attributes to allow in recursive set and policies that can selectively restrict decryption user to use attributes from within a single set or allow them to combine attributes from multiple sets. CP-ASBE can support compound set of attributes without scarifies with the flexibility to easily specify the policies involved in singleton attributes. It also supports multiple numerical assignments for a given attribute by placing each assignment in separate set.

Conclusion

Cloud computing offers different advantages for organizations and individuals. There are certain issues related to the security and privacy of the user data. Cloud security is the major issue in cloud computing. We studied different security issues and different type of algorithms of encryption for fine grained access control and security of user data. We will try to improve the mechanism of single set of attributes present in the previous work by using hierarchical attributes set of users.

References

[1] R. Buyya, C. ShinYeo, J. Broberg, and I. Brandic, "Cloud computing and emerging it platforms: Vision, hype, and reality for delivering computing as the 5th utility," Future Generation Comput. Syst., vol. 25, pp. 599–616, 2009.

[2] Amazon Elastic Compute Cloud (Amazon EC2) [Online]. Available: http://aws.amazon.com/ec2/

[3] Amazon Web Services (AWS) [Online]. Available: https://s3.amazonaws. com/

[4] R. Martin, "IBM brings cloud computing to earth with massive new data centers," InformationWeek Aug. 2008 [Online].Available:http://www.informationwee k.com/news/hardware/data_centers/209901523

[5]Google App Engine [Online]. Available: http://code.google.com/appengine/

[6] K. Barlow and J. Lane, "Like technology from an advanced alien culture: Google apps for education at ASU," in Proc. ACM SIGUCCSUser Services Conf., Orlando, FL, 2007.

[7] B. Barbara, "Salesforce.com: Raising the level of networking," InfoToday, vol. 27, pp. 45–45, 2010.

[8] P. McDaniel and A. Prakash, "Methods and limitations of security policy reconciliation," in Proc. IEEE Symp. Security and Privacy, Berkeley, CA, 2002.

[9] Kuyoro S. O., Ibikunle F. & Awodele O. ,"Cloud Computing Security Issues and Challenges", International Journal of Computer Networks (IJCN), Volume (3) : Issue (5) : 2011

[10] J. C. Robert II, W. Al- Hamdani "Who Can You Trust in the Cloud? A Review of Security Issues Within Cloud Computing", Information Security Curriculum Development Conference 2011, October 7-9, 2011, Kennesaw, GA, USA.

[11] Jensen, M., Schwenk, J., Gruschka, N., and Iacono, L. 2009.On technical Security Issues in Cloud Computing. IEEE International Conference on Cloud Computing.

[12] Y. Chen, V. Paxson, and R. Katz.What's New About Cloud Computing Security? Technical Report UCB/EECS-2010-5, Berkeley, 2010

[13] S. Yu, C. Wang, K. Ren, and W. Lou, "Achiving secure, scalable, and fine-grained data access control in cloud computing," in Proc. IEEE INFOCOM 2010, 2010, pp. 534–542.

[14] J. Bethencourt, A. Sahai, and B. Waters, "Ciphertext-policy attribute based encryption" in Proc. IEEE Symp. Security and Privacy, Oakland, CA, 2007.

SIMULATION OF PHOTOVOLTAIC ARRAY USING MATLAB / SIMULINK: ANALYSIS, COMPARISON & RESULTS

Anwarul M Haque[1], Swati Sharma[2], Devendra Nagal[3]
[1]Asst. Prof.,Power Electronics Department, VGEC Chandkheda, Ahmedabad, Gujarat, India,
[2,3]Asst. Prof, Electrical Engineering Department, Jodhpur National University,
Jodhpur, Rajasthan, India,
Email: haqueanwarul@yahoo.co.in[1], er.swati.sharma15@gmail.com[2], devendranagal@gmail.com[3]

Abstract— solar energy maintains life on earth and it is an infinite source of clean energy. Since last five decades, numerous studies have been performed on different design aspects and performance characteristics of Photovoltaic (PV) cells with a common objective of producing fully integrated PV modules to compete with the traditional energy sources. There is an increasing trend for the use of solar cells in industry and domestic appliances because solar energy is expected to play substantial role in future smart grid as distributed renewable source. This reviews the generalized optimization of mathematical modelling and simulation of Solar Photovoltaic System. The location of the power point maximal is unknown, for that purpose we use PV model, PV module and PV array simulation to sustain the PV array functioning spot at the Maximum Power Point (MPP). Here single diode equivalent circuit is employed in order to explore I-V and P-V characteristics of a 170W, BP 3170 module made of 72 solar cells (silicon nitride multi-crystalline) in series, using MATLAB/Simulink.

Index Terms—PV array, Simulation, Solar cell working and characteristics, Standard Test Conditions.

I. INTRODUCTION

The need for a cleaner environment and the continuous increase in energy demand, makes decentralized renewable energy production more and more significant. Solar cells, come in many different shapes and sizes and are made of electricity - producing materials. When sunlight shines on a PV cell, the absorbed light generates electricity. The mono-crystalline and poly-crystalline silicon cells are the only found at commercial scale at present era. To model a solar cell, it is imperative to assess the effect of different factors on the solar panels and to consider the characteristics given by the manufacturers in the datasheet [10].

The datasheet which gives the electrical characteristics is calculated under standard test condition. The PV array is composed of several interconnected photovoltaic modules. To obtain the required power, voltage and current, the PV modules are associated in series and parallel. Thus, the mathematical models for PV array are attained while utilizing the basic description and equivalent circuit of the PV cells.

From the theory of the photovoltaic, a mathematic model of the PV is presented. The simulation of the photovoltaic array is realized with SIMULINK block. The temperature and the irradiance are specified. The Simulink model uses a current source, voltage source and the value of the resistance in series and parallel of the PV. The number of modules in series and parallel are set. The result is used for the Simulink block as a current source to obtain the voltage and current delivered from PV.

II. STANDARD TEST CONDITIONS (STC)

Uniform conditions are usually specified so that a performance comparison can be made between different PV units (cell, modules). The

parameters obtained from the testing are usually provided on the manufacturer's datasheet. Measurements are performed under standard test conditions and the electrical characteristics obtained characterize the module accurately under these conditions. The conditions are specified as follows [1].

- The reference vertical irradiance E_o with a typical value of 1000W/m^2
- Reference cell temperature for performance rating, T_o a typical value of 25°C with a tolerance of ±2 °C.
- AM =1.5 (A specified light spectral distribution with an air mass). It provide a relative measure of the path of sun must travel through the atmosphere.

In addition to supplying performance parameters at the Standard Test Conditions manufacturers also provide performance data under the Nominal Operating Cell Temperature (NOCT).This is defined as the temperature reached by the open circuited cells in a module under the following conditions:

- Irradiance on cell surface is 800W / m^2
- The ambient temperature is 20°C (293 K)

To account for other ambient conditions the approximate expression below may be used:

$$T_{cell} = T_{amb} + (N_{oct} - 20)* S / 0.8 \quad (1)$$

Where

T_{cell} is cell temperature (°C);
T_{amb} is the ambient temperature;
N_{oct} is the Nominal Operating Cell Temp &
S is the solar irradiance (kW/m^2).

III. PHOTOVOLTAIC CONSTRUCTION AND WORKING

In most of solar cells, the absorption of photons takes place in semiconductor materials, resulting in the generation of the charge carriers and the subsequent separation of the photo-generated charge carries. Therefore, semiconductor layers are the most important parts of a solar cell.

A. Silicon Solar Cell

A solar cell is a device that converts the energy of sunlight directly into electricity by the photovoltaic effect [3]. Although there are many kinds of solar cells developed by using different semiconductor materials, the operating principle is identical. The most commonly known solar

cell is configured as a large-area p-n junction made from silicon. When a piece of p-type silicon is placed in intimate contact with a piece of n-type silicon, a diffusion of electrons occurs from the region of high electron concentration (the n-type side) into the region of low electron concentration (p-type side). Similarly, holes flow in the opposite direction by diffusion [3].
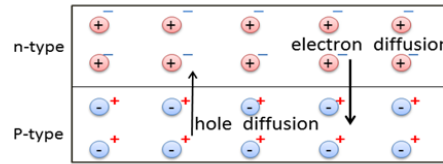
(a) Diffusion current I_D from the p side to the n side
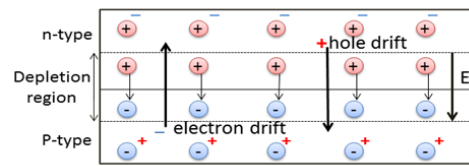
(b) Drift current I_S from n side to the p side and the depletion zone

Fig. 1 I_D, I_S, and depletion zone of a p-n junction

This forms a diffusion current I_D from the p side to the n side Fig. 1 (a). When the electrons diffuse across the p-n junction, they recombine with holes on the p-type side. The diffusion of carriers does not happen indefinitely because of an electric field which is created by the imbalance of charge immediately on either side of the junction which this diffusion creates. The electric field established across the p-n junction generates a diode that promotes charge flow, known as drift current I_S, that opposes and eventually balances out the diffusion current I_D. The region where electrons and holes have diffused across the junction is called the depletion zone Fig. 1 (b).

B. Photo-generated Current and Voltage

When a visible light photon with energy above the band-gap energy strikes a solar cell and is absorbed by the solar cell, it excites an electron from the valence band. With this newfound energy transferred from the photon, the electron escapes from its normal position associated with its atom, leaving a localized "hole" behind [3]. When those mobile charge carriers reach the vicinity of the depletion zone, the electric field sweeps the holes into the p-side and pushes the electrons into the n-side, creating a

photo-generated drift current. Thus, the p-side accumulates holes and the n-side accumulates electrons Fig. 2 which creates a voltage that can be used to deliver the photo-generated current to a load. At the same time, the voltage built up through the photovoltaic effect shrinks the size of the depletion region of the p-n junction diode resulting in an increased diffusion current through the depletion zone.
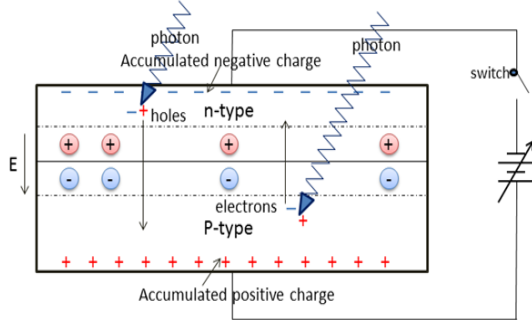

Fig. 2 Illustration of drift current as well as photo-generated current and voltage

Hence, if the solar cell is not connected to an external circuit (switch in the open position in Fig. 2), the rise of the photo-generated voltage eventually causes the diffusion current ID balancing out the drift current IS until a new equilibrium state is reached inside a solar cell [3].

C. P V Cell Constructions
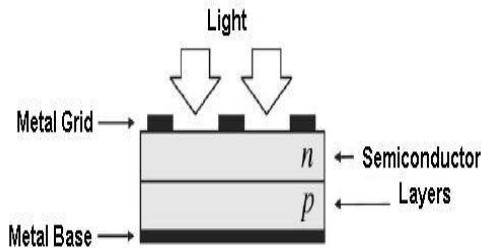
Fig. 3 Photovoltaic Cell Constructions

A photovoltaic cell is basically a semiconductor diode whose p-n junction is exposed to light [1]. Photovoltaic cells is made of several types of semiconductors using different Manufacturing processes. The mono-crystalline and polycrystalline silicon cells are the only found at commercial scale at present era.

Silicon PV cells are composed of a thin layer of bulk Si or a thin Si film connected to electric terminals. One of the sides of the Si layer is doped to form the P–n junction. A thin metallic grid is placed on the Sun-facing surface of the semiconductor. Fig. 3 illustrates the physical structure of PV cell [1], [2].

D. P V Cell Working

Photons of light with energy higher than the band-gap energy of PV material can make electrons in the material break free from atoms that hold them and create hole- electron pairs, as shown in Fig. 2.
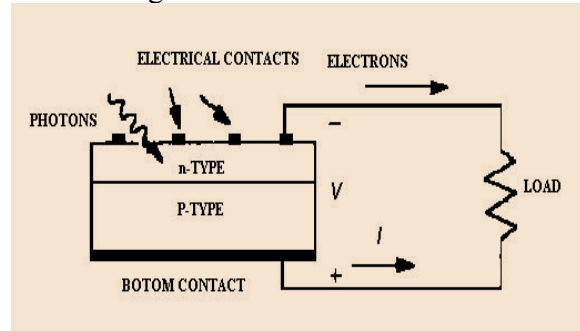
Fig. 4 Working Principle of PV Cell

These electrons, however, will soon fall back into holes causing charge carriers to disappear. If a nearby electric field is provided, those in the conduction band can be continuously swept away from holes toward a metallic contact where they will emerge as an electric current. The PV cell has electrical contacts on its top and bottom to capture the electrons, as shown in Fig. 4. When the PV cell delivers power to the load, the electrons flow out of the n- side into the connecting wire, through the load, and back to the p-side where they recombine with holes [1]. Note that conventional current flows in the opposite direction from electrons [15].

IV. PHOTOVOLTAIC PERFORMANCE

A. Photovoltaic Characteristics

Three classic parameters that are very important on the PV characteristics are:

1. **Short circuit point**, the voltage over the module is zero and the current is at its maximum (short circuit current I_{sc}).

2. **Maximum power point** (**MPP**), where the product of current and voltage has its maximum (defined by I_{mpp} V_{mpp}).

3. **Open circuit point**, where the current is zero and the voltage has its maximum (open circuit voltage V_{oc}).

The power delivered by a PV cell attains a maximum value at the points (I_{mp}, V_{mp}). The classical points are shown in Fig. 5 and are

usually given as part of a manufacturer's data sheet for a PV module.

Another important parameter of the PV characteristics is called the **Fill Factor (FF)** Fig. 6. It is a term that describes how the curve fills the rectangle that is defined by (V_{oc}) and (I_{sc}). It gives an indication of the quality of a cell's semiconductor junction and measures of how well a solar cell is able to collect the carriers generated by light. It is defined as: [4]
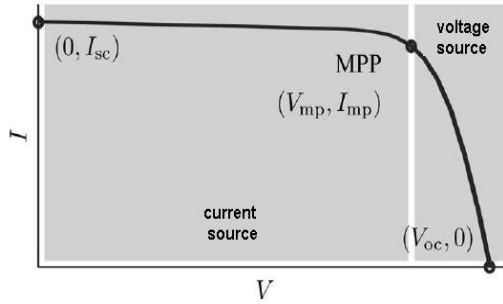

Fig. 5 IV Characteristics of PV

$$FF = V_{mpp}I_{mpp} / V_{oc}I_{oc} \qquad (2)$$

After a simple manipulation the following equation is attained.

$$V_{oc}I_{oc} \, FF = V_{mpp}I_{mpp} = P_{max} \qquad (3)$$
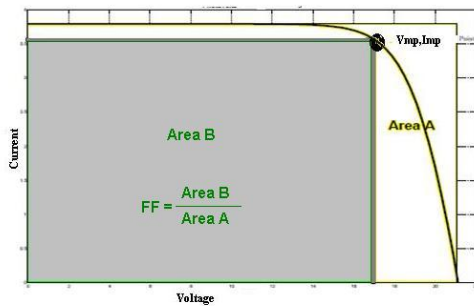
Fig. 6 Photovoltaic module characteristics showing the Fill factor

It can be easily observed that FF is always < 1 and ranges from material to material. The closer the value of the Fill Factor is to unity, the better the operation of the PV cell. *For high quality cells, Fill Factors over 0.85 can be achieved. For typical commercial devices the value lies around 0.68.*

B. Effect of Change in irradiation on I-V Characteristics of the PV Array

In Fig. 7 when the irradiation increases, the current increases more than the voltage and the power at maximum power point P_{mpp} increases as well.
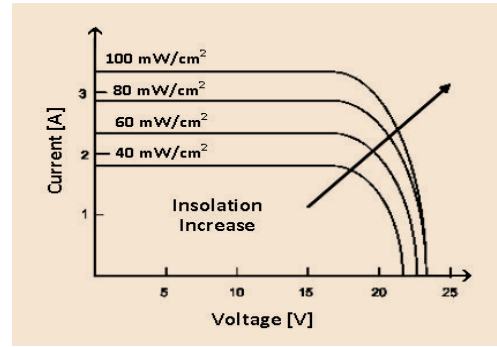
Fig. 7 I-V Characteristics of the PV as functions of irradiation

C. Effect of Change in Temperature on I-V Characteristics of the PV Array

Fig. 8 shows the variation of the current with the temperature, the current changes less than the voltage. Thus, a dynamic point exists on the I-V curve at MPP. The entire PV system has to execute at its maximum output power as shown in Fig. 9 [13]. *The location of the power point maximal is unknown, for that reason we use calculation models and search algorithms methods to sustain the PV array functioning spot at the MPP.*
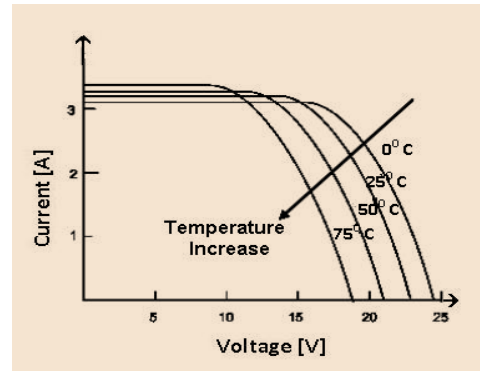
Fig. 8 I-V Characteristics of the PV as function of Temperature
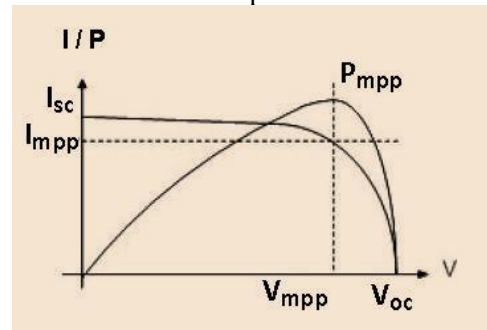
Fig. 9 I-V Curves, P-V Curve with the MPP

V. PV CELL MODEL

PV cell is a semiconductor p-n intersection that transforms sunlight to electrical power. To

model a solar cell, it is imperative that we assess the effect of different factors on the solar panels and to consider the characteristics given by the manufacturers in the datasheet. It is to be noted that to form a PV module, a set of cells are connected in series or in parallel. Thus, the mathematical models for PV array are attained while utilizing the basic description equivalent circuit of the PV cells [4], [9].

A PV cell is usually embodied by an electrical equivalent of one-diode; series resistance (R_s) and parallel resistance (R_p) is shown in Fig. 10. The different parameters characteristics of the PV cells are:

I_{ph} : currents generated by the solar cells (A)
R_s : resistance in series (Ω)
R_p : resistance in parallel (Ω)
G_a : irradiance from the sunlight (W/m^2)
T_c : cell temperature (K)
I_d : diode current (A)
I : output current of the PV (A)
V : output voltage of the PV (V)

Manufacturer of the solar module gives other parameters needed to model the solar cells. The datasheet which gives the electrical characteristics is calculated under standard test condition STC when the temperature T is 25°C and the irradiance G is 1000 W/m^2.
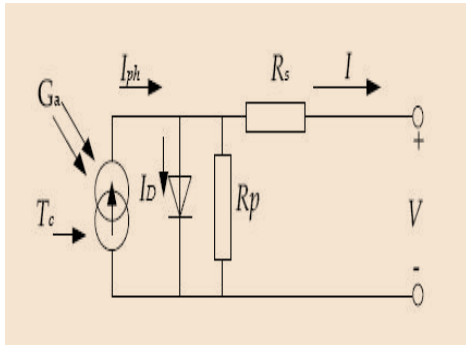
Fig. 10 Equivalent circuit of solar cell with one diode

The parameters that can be found inside the datasheet are

V_{oc} : open circuit voltage (V)
I_{sc} : short-circuit current (A)
P_{mp} : power at maximum power point
V_{mp} : voltage at maximum power point
I_{mp} : current at maximum power point

The solar cell is model first, then extends the model to a PV module, and finally models the

PV array. From fig. 10, the output current of the PV cell is [11], [15].

$$I = I_{ph} - I_d \tag{4}$$

Where

I_{ph} : photon produced by the cell
I_d : diode current

By Shockley equation, the diode current Id is given by

$$I_d = I_0\left(e^{qV_d/kT} - 1\right) \tag{5}$$

Where

I_o : reverse saturation current of diode
q : elementary electron charge (1.602x10^{-19}C)
V_d : diode voltage
k : Boltzmann constant 1.381x10^{-23} (J/K)
T : temperature in Kelvin (K)

The relation between voltage and current result by replacing the diode current

$$I = I_{ph} - I_d \tag{6}$$

Current equal to zero calculating at temperature T_1. [4] Where V_d is the output voltage of the PV cell. The reverse saturation I_o is found by using the above equation. By setting the current

$$I_0(T_1) = \frac{I_{ph}(T_1)}{(e^{qV_{oc}/kT} - 1)} \tag{7}$$

The current generated by the solar cells I_{ph} can be approximated with the short circuit current I_{sc} in [4]. The current generated can be calculated for other irradiance. The standard current, temperature and irradiance from the datasheet are used to determine the current at different condition [11].

$$I_{sc} \approx I_{ph} \tag{8}$$

$$I_{sc}(T_1) = \left(\frac{G}{G_{nom}}\right) I_{sc}(T_{1,nom}) \tag{9}$$

Where

$I_{sc}(T_1)$: current at temperature T_1
$T_{1\ nom}$: the temp. of cell from datasheet at STC
G_{nom} : irradiance from datasheet at STC

After calculation [5], gives the equation of the PV

$$I = I_{ph} - I_0 \left[e^{q\left(\frac{V+I.R_s}{akT}\right)} \right] - \left(\frac{V+I.R_s}{R_p} \right) \qquad (10)$$

Where a, is the diode quality factor between 0 and 1 and must be estimated. The value of "a" is equal to 1 for ideal diode. V is the cell voltage. For a PV module, the cell voltage is multiplied by the total amount of the cells found within the series. The reverse saturation current I_0 depends on the temperature T. It is calculated by the following equation [1].

$$I_0 = I_0(T_1) \left(\frac{T}{T_1} \right)^{\frac{3}{n}} . e^{\frac{qV_q(T_1)}{ak\left(\frac{1}{T} - \frac{1}{T_1}\right)}} \qquad (11)$$

The value of resistance in series R_s is quantified from the slope dv/di of the I- V curve at the point open circuit voltage [7]. The equation R_s is given by

$$R_s = -\frac{dV}{dI} - \frac{akT/q}{I_0 . e^{\left(\frac{qV_{oc}}{akT}\right)}} \qquad (12)$$

The model is completed by using the following recursive equations to find the currents [4]. The recursive equation is used to calculate the current for a PV cell. It is more convenient to solve numerically. The equation introduces a simplified method to calculate resistance in series and neglect the resistance in parallel [15].

$$I_{n+1} = I_n - \frac{I_{ph} - I_n - I_0 \left[e^{q\left(\frac{V+I_n.R_s}{akT}\right)} - 1 \right]}{-1 - I_0 \left(\frac{q.R_s}{akT} \right) e^{q\left(\frac{V+I_n.R_s}{akT}\right)}} \qquad (13)$$

VI. MODEL OF PV MODULE

The following model uses different method to calculate the resistance series and resistance parallel. For example, the BP 3170 is made of 72 solar cells (silicon nitride multi-crystalline) in series and provides 170W of nominal maximum power. The maximum power point's voltage is 35.8V and current delivered at maximum power point is 4.75 A. The parameters of the BP 3170 are given in Table - 1, which is essential to model the PV array.

TABLE I PV MODULE BP 3170
DATASHEET AT STC

Short circuit current I_{sc}	5.2A
Open circuit voltage V_{oc}	44.2
Current at maximum power point I_{MPP}	4.75
Voltage at maximum power point V_{MPP}	35.8
Number of cells in series N_s	72
Temperature coefficient of I_{sc}	$(0.065\pm0.015)\%/^oc$
Temperature coefficient of V_{oc}	$- (160\pm20)mV/^oc$

Different models of the photovoltaic are developed in so many literatures. The following equation developed in [6] will be used mainly in this report. The model consists of finding the curve characteristic of the PV module from the datasheet.

The goal is to find the values of R_s and R_p that makes the mathematical P-V curve coincide with the experimental peak power at the (V_{mp}, I_{mp}) point. The value of R_s and R_p are reached when the iteration stopped for P_{max} calculated is equal to P_{max} estimated.

The circuit model of the PV module is shown in Fig. 11. It is a controlled current source with the equivalent resistors and the equation of the model above. The variation of the power being taken by the load varies the PV voltage.
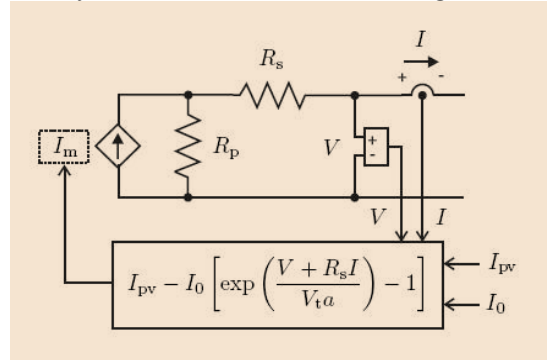

Fig. 11 Circuit model of the photovoltaic module

VII. PHOTOVOLTAIC ARRAY

The PV array is composed of several interconnected photovoltaic modules. The modelling process is the same as the PV module from the PV cells. The same parameters from the datasheet are used. To obtain the required power, voltage and current, the PV modules are associated in series and parallel [14]. The number of modules connected in series and

connected in parallel must be calculated. Fig. 12 shows a photovoltaic array, which consists of multiple modules, linked in parallel and series. N_{ser} is the total quantity of modules within the series and N_{par} is amount of modules in parallel. The number of modules modifies the value of resistance in parallel and resistance in series. The value of equivalent resistance in series and resistance in parallel of the PV array are: [1], [2], [14].

$$R_{s,array} = \frac{R_{s,module} \cdot N_{ser}}{N_{par}}$$

$$R_{p,array} = \frac{R_{p,module} \cdot N_{ser}}{N_{par}} \qquad (14)$$

After extending the relation current voltage of the PV modules to a PV array, the new relation of current voltage of the PV array is calculated in [6] by

$$I = I_{pv}N_{par} - I_0N_{par}\left[\exp\left(\frac{V + R_s\left(\frac{N_{ser}}{N_{par}}\right)I}{V_t a N_{ser}}\right) - 1\right] - \frac{V + R_s\left(\frac{N_{ser}}{N_{par}}\right)I}{R_p\left(\frac{N_{ser}}{N_{par}}\right)} \qquad (15)$$

Where I_o, I_{pv}, V_t are the same parameters used for a PV modules.
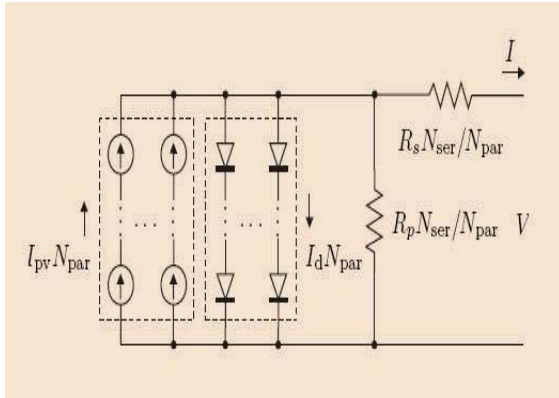
Fig. 12. PV Array composed of N_{ser} x N_{par} modules

This equation is valid for any given array formed with identical modules. The photovoltaic array will be simulated with this equation. The simulation circuit must include the number modules series and parallel. Fig. 13 shows the circuit model of the PV array [15].
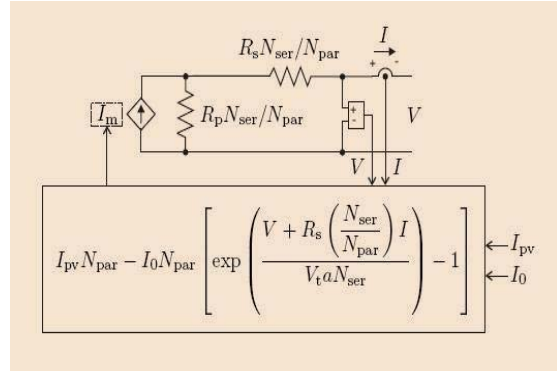
Fig. 13 Model structure of the Photovoltaic array

It constitute from the single- diode photovoltaic I-V model which provides the all necessary information to effortlessly develop a single-diode photovoltaic array model for analyzing and simulating a photovoltaic array.

VIII. SIMULATION OF PHOTOVOLTAIC ARRAY

The simulation of the photovoltaic array is realized with Simulink block. The MATLAB model of the photovoltaic array is based from [2], [16]. The input parameters required for the models are:

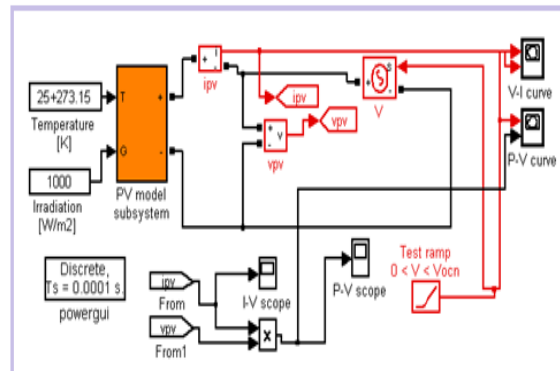|		
N_s	:	number of cells in series
N_{pp}	:	number modules in parallel
N_{ss}	:	number of modules in series
A	:	1.3977, diode constant
K	:	$1.38e^{-23}$, Boltzmann constant
I_{scn}	:	nominal short-circuit voltage
K_p	:	voltage temperature constant
K_i	:	current temperature coefficient
V_{mp}	:	voltage at maximum power
I_{mp}	:	current at maximum power

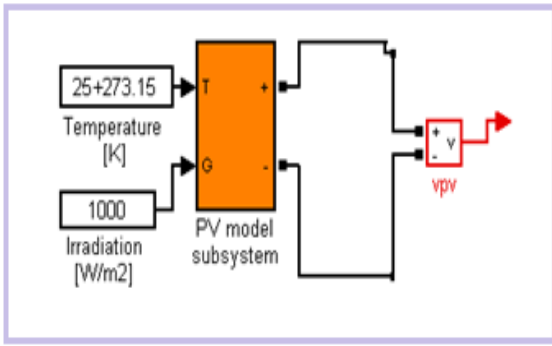Fig. 14 Simulink diagram for the model of the photovoltaic array

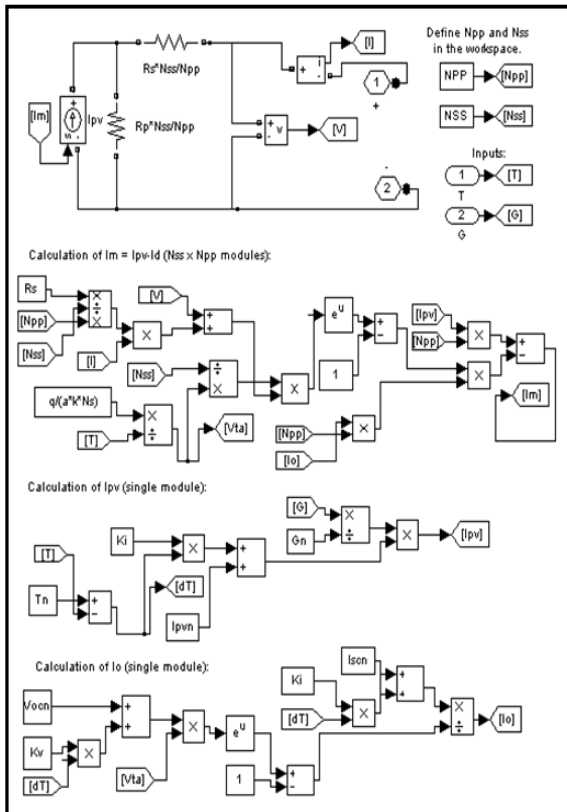Fig. 15 Simulink block of the photovoltaic array / module

Fig. 16 Simulink subsystem model of the photovoltaic array / module

The model of the photovoltaic array has been implemented in Simulink as shown in Fig. 14. The temperature and the irradiance are specified. This simulation allows having the curve I-V and P-V characteristics. The Simulink model uses a current source, voltage source and the value of the resistance in series and parallel of the PV. The number of modules in series and parallel are set with N_{ss} and N_{pp}. The I_m result is used for the Simulink block as a current source to obtain the voltage and current delivered from PV [8], [16].

Fig. 15 is the representation block of the PV that can be used with different power circuits in Simulink. It can be noted that the inputs of the PV are the irradiation & temperature, the outputs are the voltage and the current. Fig. 16 shows the mask interface of this PV model. The input parameter for this model is the photovoltaic current. The variation of the current from the photovoltaic, varies the photovoltaic output voltage. The Simulink model is derived from the model described in [2], [16].

IX. PHOTOVOLTAIC ARRAY CHARACTERISTICS

In this simulation I-V and P-V characteristics of the PV are simulated only for one module. It means here value of N_{ss} and N_{pp} are taken 1. Fig 17 displays the Simulation results. In Fig. 17(a), the current-voltage characteristics of the PV module BP 3170 is exposed. It can be noted that the maximum current output is 4.75A and the maximum voltage is 35.8 V. These are the same value as given from the manufacturer in Table 1. Fig. 17(b) is the power versus voltage curve. It can be noted that the maximum power of the single module is 170 W [8], [12].
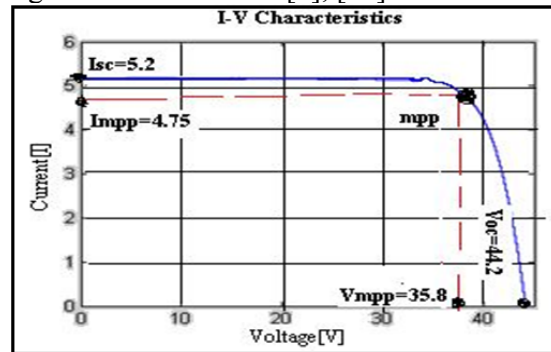

Fig. 17 (a) I-V curve of the BP 3170 module at T=25°C and G=1000 W/m^2

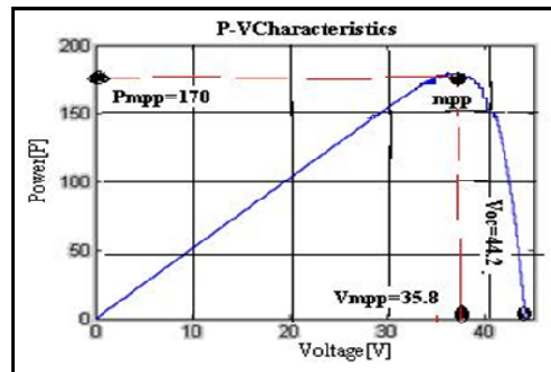Fig. 17 (b) P-V curve of the BP 3170 module at T=25°C and G=1000 W/m^2

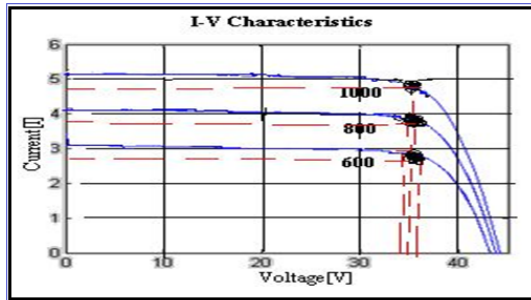## X. SIMULATION OF PHOTOVOLTAIC WITH VARIATION IN IRRADIATION

Fig. 18 (a) I-V curve of the BP 3170 module with variation in irradiation

In this case, the irradiance varies from 600, 800 and 1000 and the temperature is constant. The Simulink model in Figure 14 was used. The result in The Fig. 18 (a) is the current- voltage curve, which shows the current decreases significantly when the irradiance decreases [6].
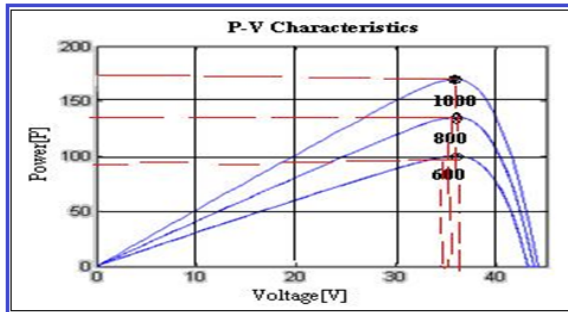

Fig. 18 (b) P-V curve of the BP 3170 module with variation in irradiation

Fig. 18 (b) is the power-voltage curve which shows that the maximum power of the PV decrease when the irradiance decreases.

XI. CONCLUSION

PV array constitutes from Single- diode PV model provides the all necessary information to develop effortlessly a single - diode photovoltaic array model for analysis and simulation [Fig.13].

From the simulation result maximum output current is 4.75A & the maximum voltage is 35.8 V. These are the same value as specified in the datasheet of manufacturer (Table 1). Simulation result [Fig. 17(b)] maximum power delivered by the single module is 170 W is again matches with datasheet.

We observed that the current & the maximum power of the PV decrease significantly, when the irradiance decreases at secured temperature [Fig 18(a) & (b)].

REFERENCES

[1] Gwinyai Dzimano, B.S, "Modeling of photovoltaic systems" The Ohio State University, 2008.

[2] Marcelo Gradella Villalva, Jonas Rafael Gazoli, and Ernesto Ruppert Filho, "Comprehensive Approach to Modeling and Simulation of Photovoltaic Arrays", IEEE Transactions on Power Electronics, Vol. 24, No. 5, Pp 1198-1208, May 2009.

[3] Huiying Zheng, "Solar Photovoltaic Energy Generation and Conversion —From Devices to Grid Integration" Dissertation for Doctor of Philosophy, Department Of Electrical & Computer Engineering, University Of Alabama, Tuscaloosa, Alabama, pp 6-8, 2013.

[4] M. G. Villalva, J. R. Gazoli, E. Ruppert F. "Modeling and Circuit-Based Simulation of Photovoltaic Arrays", Brazilian Journal of Power Electronics, Vol 14, No.1, February 2009.

[5] Akihiro Oi. "Design and Simulation of Photovoltaic Water Pumping System", California Polytechnic State University, an Luis Obispo, September 2005.

[6] Lawrence Dunn, Michael Gostein, Keith Emery, "Comparison of Pyranometers vs. PV Reference Cells for Evaluation of PV Array Performance", Proceedings of the 38th IEEE Photovoltaic Specialists Conference (PVSC), Austin, pp 1-6, June 3-8, 2012.

[7] Sushen Narkhede, Rajpritam, "Modeling of photovoltaic array" National Institute of Technology, Rourkela.

[8] Anwarul M Haque, Devendra Nagal, Dr Swati Sharma "usage of power electronics for maximum power point tracking in photovoltaic (pv) systems", selected for publication in International Conference-Research Design & Development in Enginnering-Engineering Management & Sciences, January 2016.

[9] Smita Pareek, Ratna Dahiya, "Simulation and Performance Analysis of Individual Module to Address Partial Shading cum Parameter Variation in Large Photovoltaic Fields", Journal of Energy And Power Sources, Vol. 2, No. 3, 2015, pp. 99-104, March 30, 2015

[10] Hanne Kauko," A MATLAB program for PV module performance analysis based on

real outdoor data stored in a PostgreSQL database", Thesis for Master's Degree Programme in Renewable Energy University of Jyv¨askyl¨a, Department of Physics, Joint Research Centre, Jussi Maunuksela, University of Jyv¨askyl¨a, 2.12.2008

[11]Basim Alsayid, "Modeling and Simulation of Photovoltaic Cell/Module/Array with Two-Diode Model", International Journal of Computer Technology and Electronics Engineering (IJCTEE) Volume 1, Issue 3, ISSN 2249-6343, pp-6-11, June 2012.

[12]L Siva Chaitanya Kumar, K Padma, "Matlab/Simulink Based Modelling and Simulation of Residential Grid Connected Solar Photovoltaic System" International Journal of Engineering Research & Technology (IJERT), Vol. 3 Issue 3, ISSN: 2278-0181, pp 1577-1586, March – 2014.

[13]Venkatesh Busa, Kiran Kumar Narsingoju , G.Vijay Kumar, "Simulation Analyis of Maximum Power Control of Photo Voltaic Power System", International Journal on Advanced Electrical and Electronics Engineering, (IJAEEE), ISSN (Print): 2278-8948, Volume-1, Issue-1, pp 9-14, 2012.

[14]Jangwoo Park, Hong-geun Kim, Yongyun Cho, Changsun Shin, "Simple Modeling and Simulation of Photovoltaic Panels Using Matlab/Simulink", Advanced Science and Technology Letters Vol.73 (FGCN 2014), ISSN: 2287-1233 ,pp.147-155, 2014.

[15]Anwarul M Haque, Devendra Nagal, Dr. Swati Sharma "Photovoltaic system: A source to Harness Solar Energy" proceedings of 'International Conference on Emerging Trends in Scientific Research (ICETSR-2015)', published by Institute of Research and Development (IRD-India) ISBN 978-2-642-24819-9, pp 73-78, 17-18 December 2015.

[16]Anwarul M Haque, Dr. Swati Sharma, Devendra Nagal, "Simulation of Traditional and Proposed Switched Inductor Buck Boost Converter Connected with Photovoltaic Module by Simulink / Matlab for Analysis, Comparison and Results" International Journal of Scientific & Engineering Research (IJSER), Volume 6, Issue 11, ISSN 2229-5518, pp 1115-1120, November-2015.

CEMENT CONCRETE PAVER BLOCKS FOR RURAL ROADS

Poonam Sharma[1], Ramesh Kumar Batra[2]
[1]P.G Scholar, Civil Engg., IPS-C.T.M
[2]Prof. Civil Engg, IPS-C.T.M
Email: poonam.ce1020@gmail.com[1], headce.ips@gmail.com[2]

Abstract

Solid unreinforced pre-cast cement blocks concrete paver is a versatile, aesthetically attractive, functional, cost effective and requires little or no maintenance if correctly manufactured and placed. Paver blocks can be used for different traffic categories i.e. Non-traffic, Light-traffic, Medium-traffic, Heavy-traffic and Very heavy traffic. Most concrete block paving constructed in South Africa has performed satisfactorily but there are two main areas of concern: occasional failure due to excessive surface wear, and variability in the strength of blocks. Paving block is a very common and popular method of hard landscaping that is suitable for various applications including: driveways, paths, public utility areas, garage, forecourts and roads etc. After the useful life of paver blocks, demolished ones can be used as recycle aggregate conveniently.

This project strictly follows IS 15658:2006 for Paver Blocks. Aggregate which passes from 20 mm sieve and retain on 4.75 mm sieve is going to be used. The removal of contaminants such as reinforcement, paper, wood, plastics and gypsum should be done. Concrete produced with such recycled concrete aggregate is called recycled aggregate concrete (RAC)

In rural area the road construction is under progress, flexible & rigid roads are constructed in combination according to need. Generally flexible payments are constructed outside the village boundary. However the rigid payments are laid inside the village portion. It is seen that the cost of rigid payment is quite high as compare to flexible payment. In this study the work is carried out to replace the rigid payments by concrete bock pavers.

Key words: Cement Concrete Paver Block

Literature Review on Paver Blocks

Segmented concrete paving is a system of individual shaped blocks arranged to form a continuous hardwearing surface overlay. Over the past two decades, paving composed of segmental blocks has become a feature of our towns and cities. It is to be found in commercial industrial and residential areas, in the paving malls, plazas, parking areas and bus stops. It has been successfully used for embankment walls, slope protection and erosion control. During this period, extensive research has been carried out on the engineering characteristics and structural performance of segmental block paving. Existing pavements subjected to heavy bus traffic and industrial loads have been monitored and their service life shown to be satisfactory. The South African Bureau of Standards has published specifications relating to the quality of concrete paving blocks and required standards of construction. The Committee of Urban Transport Authorities has published a catalogue of designs for segmental block pavements. The engineering and specification aspects have been satisfactorily solved, and this type of paving has a proven performance and service record. But the aesthetic use of segmented paving and the contribution it can make to improve our urban landscape is only now being appreciated.

History Paver Blocks

Although pavers made out of concrete may be a new product, the use of paving blocks as a surfacing material is anything but new. Flagstones were being used to pave village streets. Cobblestones were the traditional

method of stone paving, being uncut and often water-worn stones or large pebbles about 150mm in size. Later hand-cut stone blocks were introduced. Road-making using brick were also common depended on the availability of clay bricks in India. Concrete paving blocks were first manufactured in the Netherlands in 1924. It was probably World War II that led to the growth of concrete blocks as a paving material. Large areas of the Netherlands were destroyed during the War and, because clay bricks were in short supply, concrete blocks were introduced as an alternative. Subsequently, concrete block paving (cbp) became recognized as a paving material in its own right. The research carried out by Shackel in the late '70s and early '80s remains the most comprehensive yet conducted into the performance of concrete block paving. A hierarchy of block shapes was developed, the existing design curves were examined, the role of the bedding and jointing sands was investigated in earnest, and various base and sub-base materials were tested. Most of the research by Shackel was carried out in South Africa. This has resulted in South Africa being recognized as a world leader in concrete block paving.

Concrete pavers are a versatile paving material, which due to the availability of many shapes, sizes and colors, has endless streetscape design possibilities. The use of concrete block paving can be divided into sub heads like Roads, Commercial Projects, Industrial Areas, Domestic paving and Specialized Applications as Cladding vertical surfaces, Storm water channels, Embankment protection under freeways and Roof decks

Concrete block paving is not limited to flat, level surfaces, but can be laid on near-vertical surfaces to create interesting architectural features. The crocodile farm near Brits used concrete block paving extensively to pave the entire area. Concrete block paving was chosen because it provided a non-destructible, non-slip surface. Embankment protection alongside freeways. The use of concrete block paving is a very effective and quick method of slope protection. Concrete block paving using specially developed blocks has been used successfully in lining storm water channels. Century City roof deck with a good detail across the expansion joint.

Physical requirement for un-reinforced precast cement concrete paver blocks are categorized under three categories according to IS 15658: 2006 and they are given below:

General Requirements

1. All paver blocks shall be sound and free from cracks or other visual defects which will interfere with the proper paving of the unit or impair the strength or the performance of the pavement constructed with the paver blocks.

2. When two layer paver blocks are manufactured there shall be proper bonding between the layers. Delaminating between the layers shall not be permitted. The compressive strength of the two layer blocks shall meet specified requirements.

3. When paver blocks with false joints, surface reliefs or projections are supplied, the same shall be specified. Also, the surface features shall be well formed and be devoid of any defects.

Obligatory Requirements

1. Visual requirements

Visual inspection of quality of paver blocks shall be carried out in natural daylight, prior to the test for other properties. The inspection shall be conducted by the purchaser and the manufacturer jointly at a location, agreed to between them, normally at the site or factory.

2. Dimensions and Tolerances

The recommended dimensions and tolerances for paver blocks are measured by steel calipers and steel ruler. Specified tolerance as IS 15658: 2006 is given below in table.

S.No.	Dimensions	Recommended values	Tolerance limit	
			Thickness <100mm	Thickness >100mm
1.	Width, W	To be specified by manufacturer	± 2mm	± 3mm
2.	Length, L	To be specified by manufacturer	± 2mm	± 3mm
3.	Thickness, T	50 to 120 mm	± 3mm	± 4mm
4.	Aspect ratio (L/T)	Maximum 4.0	+ 0.2	+ 0.2
5.	Arris/Chamfer	Minimum: 5mm Maximum: 7mm	± 1mm	± 1mm
6.	Thickness of wearing layer	Minimum: 6mm	+2mm	+ 2mm
7.	Plan area, Ast	Maximum: $0.03m^2$	$+ 0.001m^2$	$+ 0.001m^2$
8.	Wearing face area,	Minimum 75% of plan area	- 1%	- 1%
9.	Squareness	Nil	± 2mm	± 3mm

Table 1: Recommended Dimension and tolerance for paver blocks

3. Water Absorption

The water absorption, being the average of the three units, and water absorption of paver block shall not be more than 6% by mass and in individual samples, the water absorption should restricted to 7 percent.

4. Compressive Strength

Compressive strength of paver blocks shall be specified in terms of 28 days compressive strength. The average 28 days compressive strength of paver blocks shall meet the specific requirement. Individual paver block strength shall not be less than 85% of the specified strength.

5. Abrasion Resistance

Abrasion resistance is a property which allows a material to resist wear. Materials which are abrasion resistant are useful for situations in which mechanical wearing and damage can occur, including delicate applications such as the construction of space shuttle components. Numerous companies manufacture abrasion resistant products for a variety of applications, including products which can be custom fabricated to meet the needs of specific users.

The Abrasion resistance of paver blocks may be specified in the to the test results, which should be complied with by the manufacturer

6. Optional Requirements

A. Tensile Splitting Strength

The tensile strength is one of the basic and important properties of the concrete. The concrete is not usually expected to resist the direct tension because of its low tensile strength and brittle nature. However, the determination of tensile strength of concrete is necessary to determine the load at which the concrete members may crack. The cracking is a form of tension failure. Apart from the flexure test the other methods to determine the tensile strength of concrete can be broadly classified as (a) direct methods, and (b) indirect methods. The direct method suffers from a number of difficulties related to holding the specimen properly in the testing machine without introducing stress concentration, and to the application of uniaxial tensile load. Which is free from eccentricity to the specimen? As the concrete is weak in tension even a small eccentricity of load will induce combined bending and axial force condition and the concrete fails at the apparent tensile stress other than the tensile strength. As there are many difficulties associated with the direct tension test, a number of indirect methods have been developed to determine the tensile strength. In these tests in general a compressive force is applied to a concrete specimen in such a way that the specimen fails due to tensile stresses developed in the specimen. The tensile stress at which the failure occurs is termed the tensile strength of concrete.

The splitting tests are well known indirect tests used for determining the tensile strength of concrete sometimes referred to as split tensile strength of concrete. The test consists of applying a compressive line load along the opposite generators of a concrete cylinder placed with its axis horizontal between the compressive platens. Due to the compression loading a fairly uniform tensile stress is developed over nearly 2/3 of the loaded diameter as obtained from an elastic analysis. The magnitude of this tensile stress f (acting in a direction perpendicular to the line of action of applied loading) is given by the formula (IS: 5816-1999):

$$f = \frac{2P}{\pi l d},$$ Where P= Maximum load applied in Newton,

l=length of specimen in mm, d=Cross sectional dimension of specimen in mm

B. Flexural Strength/Breaking Load

Maximum fiber stress developed in a specimen just before it cracks or breaks in a flexure test. Flexural yield strength is reported instead of flexural strength for materials that do not crack in the flexure test. An alternate term is modulus of rupture. The Flexural strength/ Breaking Load of paver blocks are done when it is required by purchaser and its test value should be specified by the purchaser.

C. Freeze-Thaw Durability

When water freezes, it expands about 9 percent. As the water in moist concrete freezes it produces pressure in the pores of the concrete. If the pressure developed exceeds the tensile strength of the concrete, the cavity will dilate and rupture. The accumulative effect of successive freeze-thaw cycles and disruption of paste and aggregate can eventually cause expansion and cracking, scaling, and crumbling of the concrete. When required for application in freeze and thaw environment, the purchaser may specify limits to the test results, which should be completed with bt the manufacturer.

D. Color and Texture

Color and texture is given to paver block to make it visible and also for skid resistance or to provide friction. When required, the color and texture of paver blocks should be manually agreed to between the purchaser and the manufacturer.

E. Grade Destination of Paver and Design of Concrete Block Pavement

Recommended grades of paver blocks to be used for construction of pavements having different traffic categories are given in table below. Since minimum value slump concrete is used in production of paver blocks, the quality of blocks produced will depend upon various parameters like the capacity of compaction and vibration of machine, grade of cement used, water content, quality of aggregate used, their gradation and mix design adopted, additives used, handling equipment employed, curing methods adopted, level of supervision, workmanship and quality control achieved etc

S. No.	Grade Design ation of Paver Blocks	Specified Compressive Strength of Paver Blocks at 28 Days N/mm^2	Traffic Category	Recommended Minimum Paver Block Thickness in mm	Traffic Examples of Application
1.	M-30	30	Non-Traffic	50	Building premises, monuments premises, landscapes, public garden/parks, domestic drivers, paths and patios, embankment slopes, sand stabilization area etc
2.	M-35	35	Light-Traffic	60	Pedestrian plazas, shopping complex ramps, car parks, office driveways, housing colonies, office complexes, rural roads with low volume traffic, farm houses, beach sites, tourist resorts local authority footways, residential roads etc.
3.	M-40	40	Medium-Traffic	80	City Streets, small and medium market roads, low volume roads, utility cuts on arterial roads etc
4.	M-50	50	Heavy-Traffic	100	Bus terminal, industrial complexes, mandi houses, roads on expansive solis, factory

					floor, service stations, industrial pavements etc
5.	M-55	55	Very Heavy-Traffic	120	Container terminal, ports, docks yards, mine access roads, bulk cargo handling areas, airport pavement etc.

NOTE

1. Non-traffic areas are defined as areas where no vehicular traffic occurs.

2. Light-Traffic is defined as a daily traffic up to 150 commercial vehicles exceeding 30 KN laden weight, or an equivalent up to 0.5 million standard axels (MSA) for a design life of 20 years (A standard axel is defined as a single axle load of 81.6 KN)

3. Medium traffic is defined as a daily traffic of 150 – 450 commercial vehicles exceeding 30 KN laden weight, or an equivalent up to 0.5 – 2.0 MSA for a design life of 20 years.

4. Heavy traffic is defined as a daily traffic of 450 – 1500 commercial vehicles exceeding 30 KN laden weights, or an equivalent of 2.0 to 5.0 MSA for design life of 20 years.

5. Very heavy traffic is defined as a daily traffic of more than 1500 commercial vehicles exceeding 30 KN laden weight, or an equivalent of more than 5.0 MSA for design life of 20 years.

Table 2: Grades of paver blocks for traffic categories.

Outcome of Review

It is observed from the review that paver blocks can be used for different categories of traffic such as Non-Traffic, Light-Traffic, Medium-Traffic, Heavy-Traffic & Very Heavy-Traffic with the confirmation of specifications of Table 2 as shown. In nearby areas of Gwalior the Concrete paver blocks are used in non-traffic area but not in traffic roads. These can be used on roads for different types of traffic roads.

The object of this paper is to draw attention of Road Developing Authorities to use these blocks in habitation area where the speed of vehicles is restricted. These blocks are precast blocks so their quality can be monitored at construction shed & not at road site. At road site the well compacted base will be essential to lie. The well compacted base is also essential in case of concrete roads. The different types & shades of concrete paver blocks, their patterns & jointing arrangement are shown below

Different types & shades of concrete paver blocks

Concrete Paver Blocks Laying patterns
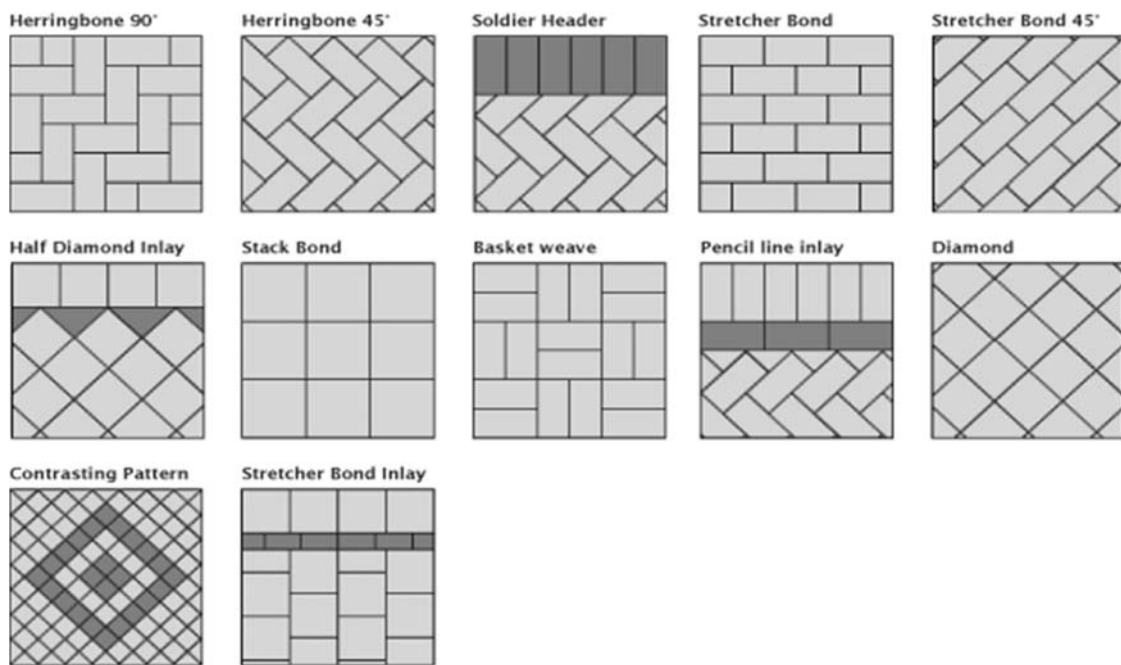
Different Jointing Arrangements

Typical Arrangement used for Drive Way

Conclusion

As per above review, these concrete paver blocks can be used at habitation areas on rural roads. It will give a good aesthetic view as compare to cast in situ concrete roads. As regard of maintenance point is concern the damaged blocks can be easily replaced where as in case of concrete roads the replacement of damaged concrete is difficult. The further analysis & monitoring can be categories under scope for future work.

Scope for Future work

If these blocks are used at habitation areas of rural roads then their construction cost, maintenance cost & other easiness, difficulties can be visualized for future use in different situations.

As these are precast blocks, the research activities can be easily done at work sheds even at the time when the construction work is under progress.

References

1. IS 15658:2006 on "Precast Concrete Blocks for Paving – Specification," Bureau of Indian Standards.
2. IS 5816:1999 (Reaffirmed 2004) Splitting Tensile Strength of Concrete- Method of Testing (First Revision).
3. IRC SP: 63-2004 "Guidelines for Use of Interlocking Concrete Block Pavement" Indian Roads Congress.
4. IRC: SP: 49 – 1998: "Guidelines for Use of Dry Lean Concrete as Sub-base for Rigid Pavement," Indian Roads Congress.
5. IRC SP-11-1988: "Handbook of Quality Control for Construction of Roads and Runways," Indian Roads Congress, (Second Revision).
6. IRC: 19-1977, "Standard Specifications and Code of Practice for Water Bound Macadam."
7. IRC: 63-1976, "Tentative Guidelines for the Use of Low Grade Aggregates and Soil Aggregate Mixtures in Road Construction."
8. IRC: 50-1973, "Recommended Design Criteria for Use of Cement Modified Soil in Road Construction."

ANALYSIS AND DESIGN OF STEERING AND SUSPENSION SYSTEM BY MATHEMATICAL AND COMPUTATIONAL METHODOLOGY

Akash Sood[1], Abhishek Pandey[2], Savita Vyas[3], Avadesh K. Sharma[4]

[1,2]P.G Scholar, Mechanical Engg.,Rajiv Gandhi Proudyogiki Vishwavidyalaya, Bhopal, India

[3]Asst. Prof., Mechanical Engg., Rajiv Gandhi Proudyogiki Vishwavidyalaya, Bhopal, India

[4]Asst. Prof., Mechanical Engg.,Madhav Institute of Technology & Science, Gwalior, India

Email:akku.sood@live.com[1], savita_vyas@hotmail.com[3], sharma.avadesh@gmail.com[4]

ABSTRACT

This paper introduces a design and analysis of suspension and steering system of Formula SAE vehicle by both mathematical and computational methodology for optimum performance. The design is according to the Formula SAE rulebook. The deep understanding is established between logics and parameters of vehicle. The design parameters are decided either from logics or from worst condition of track and the simulation of parameters are conducted.

Key words: Formula SAE, Suspension Design, Steering Design, ADAMS, Iteration Charts.

INTRODUCTION

In Formula SAE International the design is very important due to its regress condition of track the stability and effective handling of vehicles depends upon of designers selection of optimum steering and suspension geometry which particularly includes the wheel camber, caster and king pin inclination.[1] For light vehicles, advances in modeling techniques are making the analysis of handling behavior a much more realistic process is possible then classical quasi-static techniques.[2] The dependent and independent parameters are decided by mathematical model further the simulation has been done in ADAMS the mass of vehicle, damping coefficient of damper, scrub radius and frequency are independent parameters[3]. Dependent parameters are optimized and calculated by a new and iterative method proposed by this paper, flow charts on vehicle parameter design selection are drafted and tabulated iteration are done. For steering system same methodology is used for calculating the dependent and independent parameter further the test are performed to verify the mathematical model on ADAMS.

TERMINOLOGY AND DEFINITIONS

S.No.	Terminology	Symbol	Unit
1	Mass of vehicle	m	kg
2	Damping coefficient	C_C	Dimensionless
3	Society of Automotive Engineers	SAE	-
4	Formula SAE	F-SAE	-
5	Kilo metre per hour	kmph	Km/h
6	Wheel centre stiffness coefficient	K	N/m
7	Motion Ratio	M	Dimensionless
8	Damper damping coefficient	C_D	Ns/m

9	Spring travel	X	mm
10	Longitudinal load transfer	L_X	N
11	Longitudinal force according to acceleration	F_X	N
12	Height of C.G.	H	mm
13	Wheel base	W	mm
14	Stiffness of spring	K_S	N/m
15	Ride frequency	f	Hz
16	Roll gradient	θ/a	deg-s^2/m
17	Lateral load transfer	L_Y	N
18	Distance between roll centre and C.G.	X'	mm
19	Acceleration	a	m/s^2
20	Torsional rigidity of chassis	K_t	Nm/deg
21	Track width	T	mm
22	Lateral Force	F_Y	N
23	Rack travel	t	mm
24	Steering arm length	l	mm
25	Caster angle	α	deg
26	King pin angle	γ	deg
27	Steering ratio	S_R	Dimensionless
28	Steering angle	θ	deg
29	Scrub radius	R_S	mm

PROBLEM DESCRIPTION
Independent Parameters
Mass

The mass of vehicle is decided by taking care of all the components of vehicle and driver. Special attention is also given to the forces which are generated by the mass, because of this forces condition rise to failure. The decision of mass of vehicle is according to the above constraint.

Damper coefficient

Theoretically we have to keep critical damping but due to some losses in the mass-spring damper system; the designer must keep it tending to critical damping but on under damping side. The damping coefficient is taken to die out frequency of system.

Scrub radius

It is the distance between centre point of contact patch and point where the steering axis cut the ground, the fundamental reason to take scrub radius is to feel the ride on steering wheel, but it has a problem regarding the large scrub radius will tends to increase the wear of tyre, hence tyre life get decrease drastically for high scrub radius. Formula type car the ground contact should be strong, the requirement of lateral force at cornering are high thus the optimized scrub radius us needed. One more additional benefit of scrub radius is that at cornering when the wheel base has tendency of change then it will provide more rectangular shape so the stability is maintained. **Frequency**

The selection of frequency of the system should be such that it should not resonate with any part of human body, otherwise it will result in nervous breakdown of driver. Also the frequency should not match with frequency of the vehicle component also including the air drag experienced by the car.[4]

Dependent Parameters

The rest parameters are of dependent type thus table optimization technique is used to decide the parameters

Iteration of Frequency by taking constant motion ratio.

Frequency	$f_1 = 4.7$	$f_2= 4.8$	$f_3= 4.9$	$f_4= 5.0$	$f_5= 4.6$	$f_6= 4.5$	$f_7= 4.45$
K	52.26×10^3	54.50×10^3	59.15×10^3	59.15×10^3	50.06×10^3	47.90×10^3	46.85×10^3
C	37.18×10^2	37.97×10^2	38.76×10^2	39.55×10^2	40.34×10^2	41.13×10^2	23.46×10^2
M	0.8	0.8	0.8	0.8	0.8	0.8	0.8
K_s	81.6×10^3	85.26×10^3	92.42×10^3	96.46×10^3	78.21×10^3	74.84×10^3	73.2×10^3
C_d	58.09×10^2	61.18×10^2	67.8×10^2	70.37×10^2	34.85×10^2	34.19×10^2	33.51×10^2
X	11.022	10.65	9.531	9.14	11.50	12.02	12.5
C_g	25	23.4	22	21.3	26	28	29

Iteration Chart: 1

Iteration of motion ratio by taking frequency constant.

Motion Ratio	$M_1 = 0.8$	$M_1= 0.85$	$M_1= 0.75$	$M_4= 0.87$
K	46.85×10^3	46.85×10^3	46.85×10^3	46.85×10^3
C	23.46×10^2	23.46×10^2	23.46×10^2	23.46×10^2
f	4.45	4.45	4.45	4.45
K_s	73.2×10^3	64.84×10^3	78.42×10^3	61.89×10^3
C_d	33.51×10^2	29.8×10^2	34.7×10^2	26.9×10^2
X	12.5	13.88	11.15	14.54
C_g	29	30	30.8	32

Iteration Chart: 2

$$Lx = \frac{Fx*H}{W} \longrightarrow X = \frac{Lx}{Ks} \longrightarrow Ks = \frac{Lx}{x}$$

$$F = \frac{1}{2Pi}\sqrt{\frac{K}{m}} \longleftarrow K = Ks * M^2$$

Flow Chart: 1

Iteration of C.G. by considering the optimum value of motion ratio as constant.

C.G. height mm	$h_1=180$	$h_2=220$	$h_3=300$	$h_4=362$
W	1550	1550	1600	1562.02
L_x	139.35	170.32	225	278.1
X	14.54	14.54	5	5
K_s	9.58×10^3	11.71×10^3	15.47×10^3	61.89×10^3
F	1.63	1.57	3.78	4.45
M	0.87	0.87	0.87	0.87

Iteration Chart: 3

$$\frac{\theta}{a} = \frac{m*X}{Kt} \longrightarrow X' = \frac{\theta*Kt}{a*m} \longrightarrow Ks = \frac{2*Kt}{T^2} \longrightarrow X = \frac{F}{Ks} \longrightarrow K = Ks * M^2 \longrightarrow F = \frac{1}{2\pi}\sqrt{\frac{K}{m}}$$

Flow Chart: 2

Iterating other parameters by taking the previously determined values as constant.

Track width	$T_1 = 1200$	$T_2 = 1220$	$T_3 = 1250$	$T_4 = 1270$
h	362	362	362	362
X'	116	195.4	232.76	231.032
K_s	61.89×10^3	61.89×10^3	61.89×10^3	61.89×10^3
K_t	44.56×10^3	46.9×10^3	48.34×10^3	49.9×10^3
θ/a	0.5	0.8	1.3	1.25
f	0.45	4.45	4.45	4.45
M	0.87	0.87	0.87	0.87

Iteration Chart: 4

All the basic dependent and independent parameters are known and approximating the values up to some acceptable previous design consideration to get the next step optimal limit of design parameter.

Steering system component design

1 .Open loop control   2. Close loop control

Switch action only   ECU

The steering is closed feedback system in which the driver gives input and the steering system or the control system generates output in the form of steer angle and then the road reacts back on system and gives feedback to the driver.

Input ⟶ control ⟶ output

Feedback
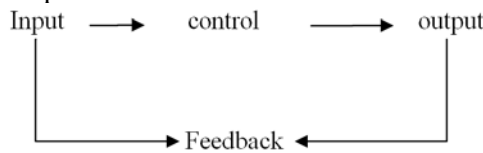
Loop Diagram: 1

The design of steering system is done in two steps the first is steering kinematics and then the dynamics of steering is designed as per the kinematic design.

1 .Steering kinematics → steering ratio
2. Steering dynamics → steering moment
Mathematic modeling of steering system

Rack travel is described as the amount by which rack will travel for one complete rotation of pinion.
Let's name this parameter as "t".
t will be a function of pinion pitch to rack pitch ratio.
Wheel travel is defined as angle by which wheel will get steered.
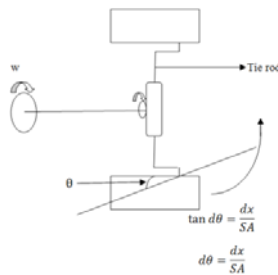
Figure 1: Steering diagram
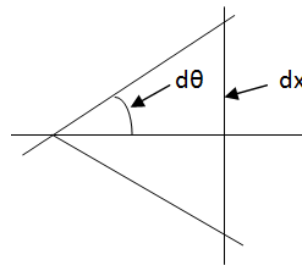
Figure 2: Zoomed view of tyre displacement

Now,
If rack travels t, steering wheel rotates by 360 degrees.
Thus, if rack travels x steering wheel rotates by $\frac{(360x)}{t}$ degrees.

So, if tire rotate by $\frac{x}{SA}$ rad. or $\frac{180x}{\pi \cdot SA}$ deg. then steering wheel rotates by $\frac{(360x)}{t}$ deg.

So, this is our steering ratio.

Now, let's calculate values: As the older calculations have some acceptable values,
Wheel base = 1562 mm, and the minimum radius we will cover = 7 m (7000 mm)
So, $\frac{1562}{7000} = 12.7 ≈ 13 \deg$ (approx.)
We will assume steering ratio = 18:1,
We have maximum rack travel = 40 mm,
So, 360 → 40 mm rack travel

13*18 = 234 deg (steering wheel angle)

$$\frac{6.28 \cdot 94}{?} = \frac{234 \, deg}{18}$$

SA = 114.6 ≈ 115 mm,

If a man applies 100 N of force on the steering wheels,
And if radius of steering wheel is say R = 10 cm then torque (T) = 10 N-m.
If radius of pinion is say 1 cm then force on tie rod = 1000N.
If arm is 32 mm then steering torque (T') = 1000 N*115 mm = 315 mm.
Now, if we want 20% of it as align torque then caster trail = 24.190 mm

So, the caster angle tanθ = caster trail/radius of wheel = 24.190/256
θ = 5.455 deg.

Now, Fluctuation in longitudinal force is = 600 N
Then, required torque is of 6.5 N-m to feel on steering,
Then scrub radius R_S = 10.7 mm.
In front view joint axis provide kingpin angle & in the side view joint axis provide caster angle
For calculation of kingpin angle:

$$tan\gamma = \frac{half \, of \, contact \, patch - scrub \, radius}{radius \, of \, wheel}$$
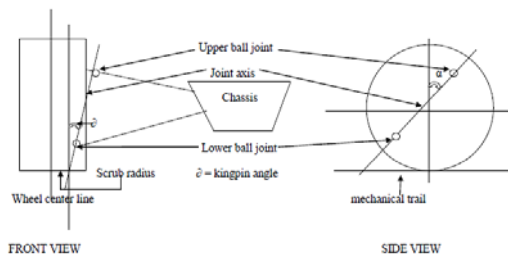
Figure 3: Front view and side view
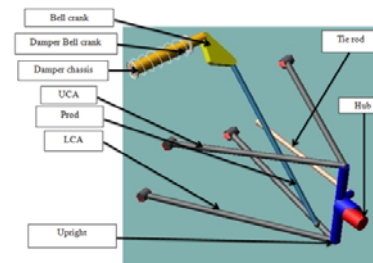
Figure 4: Descriptive view of front wishbone assembly
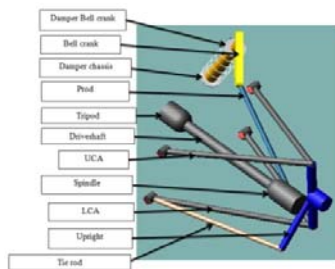
Figure 5: Descriptive view of rear wishbone assembly
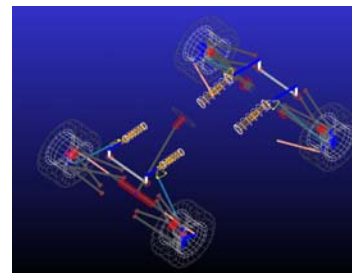
Figure 6: Rendered wireframe ISO view
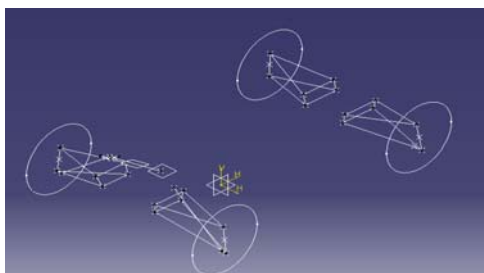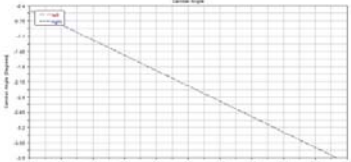

Figure 7: Wireframe ISO view
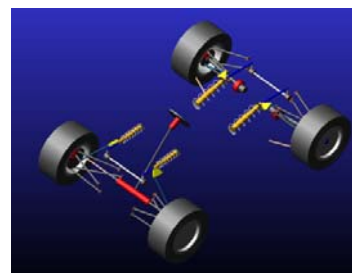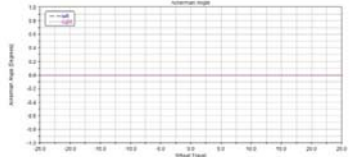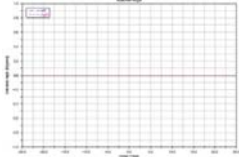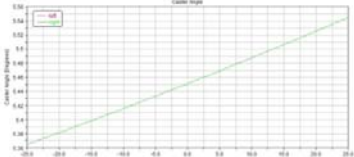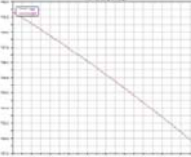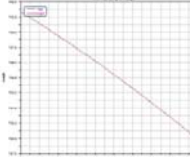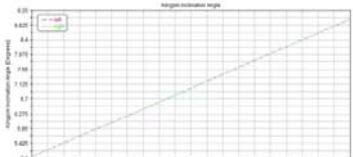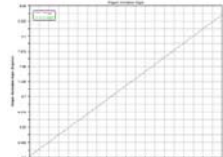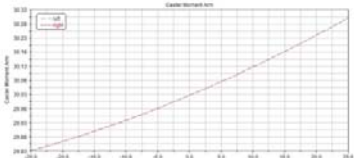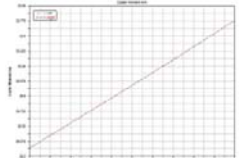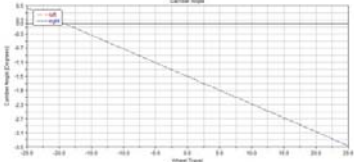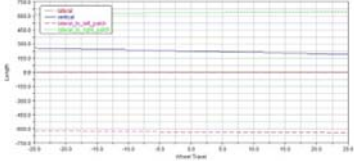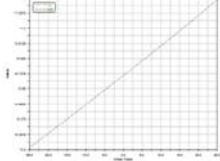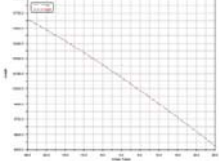
Figure 8: Rendered ISO view

Parallel wheel travel	Opposite wheel travel	Remarks
Figure 9: Ackerman Angle v/s Wheel Travel	**Figure 10:Ackerman Angle v/s Wheel Travel**	Ackerann angle stability is maintained for both type of wheel travel.
Figure 11: Caster Angle v/s Wheel Travel	**Figure 12: Caster Angle v/s Wheel Travel**	The maximum casterr angle is 5.48° for parallel wheel travel and 5.714° for opposite wheel travel both values are in considerable limit.
Figure 13: Front View Swing Arm Length v/s Wheel Travel	**Figure 14: Front View Swing Arm Length v/s Wheel Travel**	Change in swing arm length is directly proportional to the change in camber, kingpin and position of roll center; hence the considerable amount of change is seen for both parallel and opposite wheel travel of 25 mm bump and rebound.
Figure 15: Kingpin Inclination Angle v/s Wheel Travel	**Figure 16: Kingpin Inclination Angle v/s Wheel Travel**	The change of kingpin angle is measured and a linear curve is formed which shows the stability of the kingpin angle having 5.0625° at bump and 8.920° at rebound.
Figure 17: Caster Moment Arm v/s Wheel Travel	**Figure 18: Caster Moment Arm v/s Wheel Travel**	The overall caster moment at arm is 30.30 N-m, at parallel wheel travel and 30.775 N-m for opposite wheel travel, 25-30% of steering torque was balanced by the aligning torque to help driver by giving self returning moment for steering, so by the caster line inclination of 24.2 mm and wheel offset of 5.8 mm generates 26% self returning moment of overall caster moment.

Figure 19: Camber Angle v/s Wheel Travel	**Figure 20: Camber Angle v/s Wheel Travel**	The reference value of camber angel is -1.5˚ and the change in camber angle is linear ranging from 0.487˚ of positive and -3.498˚ of negative camber at parallel wheel travel and for opposite wheel travel value ranges from -0.4875˚ to -3.9˚.
Figure 21: Roll Center Location v/s Wheel Travel	Figure 22: Scrub Radius v/s Wheel Travel	Figure 23: Side View Swing Arm Length v/s Wheel Travel

OBSERVATIONS

1. The ride frequency of vehicle is between 4 Hz to 6 Hz which is said to be ideal frequency for a performance vehicle.
2. As spring travel is 14.54 mm it shows ground clearance value will be less. And the work succeeds in minimizing the ground clearance, which is project objective.
3. Center of gravity height is 362 mm which is also again a result of good designing. And as a consequence the roll propensity will be low. Also it will minimize the effect of longitudinal load transfer.
4. Motion ratio value comes out to be 0.87 which means more load will be transfer through the wishbones than usual design. As a result, spring will bear less load transfer that's why the spring travel get reduce.

RESULTS

Overall ride frequency (f)	4.45 Hz	Distance between R.C. and C.G. (X')	232.76 mm
Ride rate constant (K)	46848 N/m	Torsion stiffness of chassis (K_t)	48343 N-m/deg.
Overall vehicle damping constant (C)	2346 N-sec/m	Roll of chassis (θ)	1.3˚
Motion ratio (M)	0.87	Contact patch of tire	220 mm
Stiffness of spring (K_S)	61897 N/m	Steering angle	13˚
Damper damping coefficient (C_D)	2696 N-sec/m	Steering ratio (S_R)	5:1
Spring travel (X)	14.54mm	Rack travel	40 mm
Height of C.G. (H)	362mm	Steering arm (SA)	32 mm
Wheel base (W)	1562.02mm	Caster angle (α)	1.2˚
Track width (T)	1250mm	Kingpin angle (θ)	16.98˚

CONCLUSION

The designing process for static conditions is completed. The numerically solved values are near approximate the simulated values hence our design procedure is correct for such kind of vehicle design. This paper includes static and dynamic parameters according to the objectives. The work successfully achieved the objective. Result implies that car designing using ADAMS has very good scope of improving vehicle geometry, behavior and performance. The overall analysis satisfies the constraints and of Formula SAE International rulebook, so the vehicle modeling under the dynamic analysis is considerable.

REFERENCES

[1] H. Heisler, Advanced Vehicle Technology, Second. Butterworth-Heinemann, 2002.

[2] J. Fenton, Advances in Vehicle Design, First. Professional Engineering Publishing Limited London, 1999.

[3] "Tune To Win - Carroll Smith.pdf." .

[4] A. Sood and P. Singh, "ANALYSIS OF SPACE FRAME OF FORMULA SAE AT HIGH SPEED WITH ERGONOMIC AND VIBRATIONAL," Int. J. Mech. Eng. Technol., vol. 6, no. 11, pp. 202–212, 2015.

[5] "Fundamentals Of Vehicle Dynamics - Thomas D. Gillespie.pdf." .

[6] "Race Car Vehicle Dynamics - Milliken & Milliken.pdf." .

[7] E. F. G. Iii and A. R. Salinas, "Introduction to Formula SAE ® Suspension and Frame Design."

[8] L. Hamilton, P. Joyce, C. Forero, and M. McDonald, "Production of a Composite Monocoque Frame for a Formula SAE Racecar," SAE Tech. Pap., vol. 2, 2013.

[9] B. A. Jawad and J. Baumann, "Design of Formula SAE Suspension," no. 724, 2002.

[10] M. Huang and N. Jones, Vehicle Crash Mechanics, vol. 56, no. 5. 2002.

[11] R. Stone and J. K. Ball, "Automotive Engineering Fundamentals," 2004, p. 636.

[12] "Automotive Technology Principles, Diagnosis, and Service.pdf." .

[13] W. Karwowski and B. Peacock, Automotive Ergonomics. Taylor & Francis, 1993.

[14] R. G. J. Flay, A. R. Hammond, N. Zealand, and F. M. Student, "Aerodynamic design of a formula sae race car," BBAA VI Int. Colloq. Bluff Bodies Aerodyn. Appl., pp. 1–4, 2008.

[15] J. C. Dixon, The Shock Absorber Handbook. 2007.

[16] "Performance Tuning in Theory & Practice.pdf." .

[17] A. W. M. Bonnick, Automotive: Computer Controlled Systems Diagnostic Tools and Techniques. Butterworth-Heinemann, 2006.

[18] S. Nawani, "International Journal of Aerospace and Mechanical Engineering FEM Analysis of BAJA Chassis International Journal of Aerospace and Mechanical Engineering," vol. 1, no. 1, pp. 40–44, 2014.

[19] N. D. Smith, "Understanding Parameters Influencing Tire Modeling," 2004.

[20] S. Barbat, X. Li, P. Prasad, A. Engineering, F. M. Company, and U. States, "Vehicle-to-vehicle front-to-side crash analysis using a CAE based methodology," pp. 1–8.

[21] B. a Jawad and B. D. Polega, "Design of Formula SAE Suspension Components," Engineering, vol. 1, no. 724, pp. 1–10, 2002.

[22] S. Description, "Intelligent Testing to Advance Vehicle Performance," no. June, 2010.

[23] F. R. Committee, "2013 Formula SAE ® Rules Table of Contents," p. 176, 2015.

THERMODYNAMIC ANALYSIS OF NEWTONIAN AND LAMINAR FLOW ALONG AN INCLINED HEATED PLATE WITH EFFECTS OF HYDROMAGNETIC IN POROUS AND NON POROUS REGIONS

Rajiv Dwivedi[1], Alka Pradhan[2] , Anand Bhatanagar[3]
[1]Associate Prof., Dept. of Applied Science and Humanities,IPS-C.T.M
[2,3]Asst. Prof., Dept. of Applied Science and Humanities,IPS-C.T.M
Email: rajivdwivedi81@gmail.com[1], dralka.ips@gmail.com[2],anandbhatanagar.ips@gmail.com[3]

ABSTRACT - **The purpose of this work is to thermodynamic analysis of Newtonian and laminar flow along an inclined heated plate with effects of hydromagnetic and porous media in two regions. The upper surface of the liquid film is considered free and adiabatic. The effect of heat generation by viscous dissipation is included in the analysis. The influence of the viscous dissipation on velocity, temperature and entropy generation is examined.**

Index Terms: Inclined plate, Thermodynamic analysis, viscous dissipation

I. INTRODUCTION

The study of flow through porous medium is important, because of its interesting application in diverse field of science, engineering and technology. The practical application are in the percolation of water through soil, extraction and filtration of oil from wells, the drainage of water, irrigation and sanitary engineering and also in the inter disciplinary field, such as Biomedical engineering etc. The lung alveolar is an example that finds application in an animal body. The classical Darcy's law Musakat (1937) states that the pressure gradient pushes the fluid against the body forces exer1ted by the medium which can be expressed as,

$$\vec{V} = -\left(\frac{K}{\mu}\right)\nabla P \qquad (1)$$

The law gives good results in the situations when the flow is unidirectional or the flow is at low speed. In general the specific discharge in the medium need not be always low. As the specific discharge increase, the convective force developed and the internal stress generates in the fluid due to viscous nature as fiber glass, papers of dandelion the flow occurs even in the absence of the pressure gradient. Modification for the classical Darcy's law was considered by the Beverse & Jaseph (1967), Saffman (1971) and others. A generalized Darcy's law proposed by Brinkman (1947) is given by

$$\mu\nabla^2\vec{V} - \left(\frac{K}{\mu}\right)\nabla\vec{V} - \nabla P = 0 \qquad (2)$$

where μ and K are coefficient of viscosity of the fluid and permeability of the porous medium.
The generalized equation of momentum for the flow through the porous medium is

$$\mu\nabla^2\vec{V} - \left(\frac{K}{\mu}\right)\nabla\vec{V} - \nabla P = \rho\left[\frac{\partial\vec{V}}{\partial t} + (\vec{V}.\nabla)\vec{V}\right] \qquad (3)$$

The classical Darcy's law helps in studying flows through porous medium. In the case of highly porous medium such as papers of dandelion etc., the Darcy's law fails to explain the flow near the surface in the absence of pressure gradient. The Non-Darcian approach is employed to study the problem of flow through highly porous medium

by several investigators. Charyalu & Ramacharyulu (1978), Charyulu (1997) and Singh (2002) etc. studied the flow employing Brinkman Law (1947) for the flow through highly porous medium.

I1n the present problem, we are considering the effect of magnetic field on flow of a Newtonian fluid between parallel plates with porous lining. The flow becomes two layered flow one in the porous region and other in the clear region such type of a flows find application in the inter-disciplinary fields such as Biomedical engineering etc. The flow of the blood is one such application. The blood may be represented as a Newtonian fluid and the flow of blood is two layered Lightfoot (1974) and Shukla et al. (1980). The effect of magnetic field and the coefficient of porous medium and the effect of the thickness of the porous lining on the physical quantities of the fluid flow are discussed.

II. MATHEMATICAL FORMULATION

The Newtonian in compressible fluid flow is considered between two infinite parallel plates y=±h. The two parallel plates having lining of porous medium of thickness δ. The length of the plates lies parallel to the x-axis and y-axis is perpendicular to the length of the plates. The velocity of the fluid is given as (Up, 0, 0) in the porous region and (Uc, 0, 0) in the non-porous 1region. The equation of continuity is satisfied with the choice of the velocity. The equation of motion in the two regions is given by,
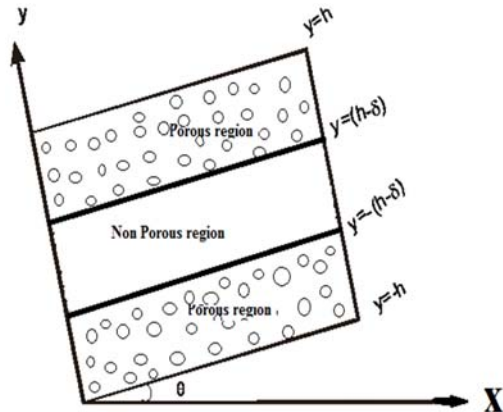

Figure : 1 Modal of the problem

The Brinkman momentum equation:

$$\mu \frac{d^2 u_p}{dy^2} - \sigma B_0^2 u_p - \frac{\mu}{K} u_p + \rho g \sin\theta = 0;$$

$$-h \le y \le -(h-\delta) \, and \, (h-\delta) \le y \le h \qquad (4)$$

$$\mu \frac{d^2 u_c}{dy^2} + \rho g \sin\theta = 0;$$

$$-(h-\delta) \le y \le (h-\delta) \qquad (5)$$

Introducing the following dimensionless variables for the velocity and transverse distance;

$$U_p = \frac{\mu u_p}{\rho g h^2 \sin\theta}, U_c = \frac{\mu u_c}{\rho g h^2 \sin\theta}, Y = \frac{y}{h},$$

$$X = \frac{x}{P_e h}, P_e = \frac{\rho C_p h^3 g \sin\theta}{\mu k}, M = \frac{\sigma B_0^2}{\mu} \qquad (6)$$

Where M is the magnetic parameter, P_e is the Peclet number, k is the thermal conductivity and ρ be the fluid density.

The dimensionless equation (4) becomes

$$\frac{d^2 U_p}{dY^2} - r^2 U_p + 1 = 0 \qquad (7)$$

Where $r^2 = h^2 \left(M + \frac{1}{K} \right)$

With $-1 \le Y \le -(1-\frac{\delta}{h}) \, and \, (1-\frac{\delta}{h}) \le Y \le 1$ (8)

The dimensionless equation (5) becomes

$$\frac{d^2 U_c}{dY^2} + 1 = 0 \qquad (9)$$

$$with \quad -(1-\frac{\delta}{h}) \le Y \le (1-\frac{\delta}{h}) \qquad (10)$$

The Boundary conditions:

$$U_c = U_p = 0 \quad at \quad Y = \pm(1-\frac{\delta}{h})$$

$$U_p = 0 \qquad at \qquad Y = \pm 1 \qquad (11)$$

The velocity profiles are obtained by integrating equation (7) and (9) with using boundary conditions (11), we get the solutions;

$$U_p = \frac{1}{r^2} \left[1 - \frac{\cosh(rY)}{\cosh(r)} \right] \qquad (12)$$

$$U_c = \frac{-1}{r^2}\left[\frac{r^2}{2}\left\{Y^2 - \left(1-\frac{\delta}{h}\right)^2\right\} + \frac{\cosh\left\{r\left(1-\frac{\delta}{h}\right)\right\}}{\cosh(r)} - 1\right] \quad (13)$$

where U_p is the velocity for porous region and U_c is the velocity for non porous region.

III. THE STEADY-STATE THERMAL ENERGY EQUATION

$$\rho C_p u \frac{\partial T}{\partial x} = k\frac{\partial^2 T}{\partial y^2} \quad (14)$$

With inlet condition

$$T(0,y) = T_0 \quad (15)$$

Constant heat flux at the lower wall:

$$\frac{\partial T(x,0)}{\partial y} = -\frac{q}{k} \quad (16)$$

Adiabatic wall:

$$\frac{\partial T(x,h)}{\partial y} = 0 \quad (17)$$

Where T is the absolute temperature and T_0 is the temperature at the inlet.

Using the following dimensionless variables for temperature $\theta = \frac{k(T - T_0)}{qh}$ then the energy equation can be written in the following becomes dimensionless form

$$U\frac{\partial \theta}{\partial X} = \frac{\partial^2 \theta}{\partial Y^2} \quad (18)$$

Subject to the following conditions:

$$\theta(0,1) = 0; \frac{\partial \theta(x,0)}{\partial y} = -1; \frac{\partial \theta(x,1)}{\partial y} = 0 \quad (19)$$

To get a solution of (18), applying the method of separation of variables and we get the solutions as

Case (i): The dimensionless temperature (θ_p) for Porous region:

$$\theta_P = \lambda_1 X + \frac{\lambda_1}{r^2}\left[\frac{Y^2}{2} - \frac{\cosh(rY)}{r^2\cosh(r)} - \frac{1}{2} + \frac{1}{r^2}\right] - Y + 1 \quad (20)$$

where $\lambda_1 = \dfrac{r^2}{\left[1 - \dfrac{\tanh(r)}{r}\right]}$

Case (ii): The dimensionless temperature (θ_c) for Non Porous region:

$$\theta_C = \lambda_2 X + \frac{\lambda_2(1-Y^2)}{24r^2}\left[\begin{array}{c}(1+Y^2) - 6\left(1-\frac{\delta}{h}\right)^2 \\ + \frac{12}{r^2}\left\{\frac{\cosh\left\{r\left(1-\frac{\delta}{h}\right)\right\}}{\cosh(r)} - 1\right\}\end{array}\right] - Y + 1 \quad (21)$$

where $\lambda_2 = \dfrac{r^2}{\left[1 - \dfrac{r^2}{6}\left\{1 - 3\left(1-\frac{\delta}{h}\right)^2\right\} - \dfrac{\cosh\left\{r\left(1-\frac{\delta}{h}\right)\right\}}{\cosh(r)}\right]}$

IV. ENTROPY GENERATION RATE

According to Mahmud and Fraser [6], the entropy generation rate is define as

$$E_G = \frac{k}{T_0^2}\left[\left(\frac{\partial T}{\partial \bar{x}}\right)^2 + \left(\frac{\partial T}{\partial \bar{y}}\right)^2\right] + \frac{\mu}{T_0}\left(\frac{\partial \bar{u}}{\partial \bar{y}}\right)^2 \quad (22)$$

The dimensionless entropy generation number may be defined by the following relationship:

$$N_s = \frac{kT_0^2}{q^2}E_G \quad (23)$$

In terms of the dimensionless velocity and temperature, the entropy generation number becomes

$$N_s = \frac{1}{P_e^2}\left(\frac{\partial \theta(x,y)}{\partial x}\right)^2 + \left(\frac{\partial \theta(x,y)}{\partial y}\right)^2 + \frac{Br}{\Omega}\left(\frac{\partial u(y)}{\partial y}\right)^2$$
$$= N_x + N_y + N_f \quad (24)$$

Where the dimensionless parameters $Br = (\rho^2 g^2 \sin^2\theta h^3)/q\mu$ is the Brinkman number, $\Omega = (qh/kT_0)$ the dimensionless temperature difference. The viscous dissipation parameter ($B = Br\,\Omega^{-1}$) is defined as the product of the Brinkman number and the inverse of dimensionless temperature difference .The viscous dissipation parameter is an important dimensionless number for the irreversibility analysis. It determines the relative importance of the viscous effects for the entropy generation. N_x and N_y are the entropy generation by heat transfer due to both axial and transverse heat conduction respectively and N_f is the entropy generation due to fluid friction.

Case (i): Entropy generation rate (N_{Sp}) for Porous region:

$$Ns_p = \frac{1}{P_e^2}\left(\frac{\partial \theta_p(X,Y)}{\partial X}\right)^2 + \left(\frac{\partial \theta_p(X,Y)}{\partial Y}\right)^2 + \frac{Br}{\Omega}\left(\frac{\partial U_p(Y)}{\partial Y}\right)^2$$

$$= N_{xp} + N_{yp} + N_{fp} \qquad (25)$$

Where Ns_p is the entropy generation rate per unit volume for porous region, N_{Xp} is the entropy generated due to heat transfer in the axial direction for porous region, N_{Yp} is the entropy generated due to heat transfer in the transfer direction for porous region and N_{Fp} is the entropy generated due to the fluid friction for porous region.

Case (ii): Entropy generation rate (N_{Snp}) for Non Porous region:

$$Ns_{np} = \frac{1}{P_e^2}\left(\frac{\partial \theta_{np}(X,Y)}{\partial X}\right)^2 + \left(\frac{\partial \theta_{np}(X,Y)}{\partial Y}\right)^2 + \frac{Br}{\Omega}\left(\frac{\partial U_{np}(Y)}{\partial Y}\right)^2$$

$$= N_{xnp} + N_{ynp} + N_{fnp} \qquad (26)$$

Where Ns_{np} is the entropy generation rate per unit volume for non porous region, N_{Xnp} is the entropy generated due to heat transfer in the axial direction for non porous region and N_{Ynp} is the entropy generated due to heat transfer in the transfer direction for non porous region, NF np is the entropy generated due to the fluid friction for non porous region.

V. RESULT AND DISCUSSIONS

It is clear from the Figure 2 that velocity of porous region (U_p) decrease in convergent manner on increasing magnetic parameter (M).if permeability parameter is taken constant (K=1). In Figure 3 that velocity of porous region (U_p) increase in convergent manner on increasing permeability parameter (K), for constant magnetic parameter (M=1).

The velocity of non porous region (U_C) profile for different values of magnetic parameter (M) is examine in Figure 4 and for different values of permeability parameter (K) it is clear that in Figure 4 if the values of magnetic parameter (M) is increase then velocity of non porous region decrease, for constant permeability parameter

(K=1) and in Figure 5, the velocity of non porous region increase on increasing permeability parameter (K).for constant magnetic parameter (M=1).

Figure 6 shows the divergent variation of temperature of porous region opposed to Y axis for different values of group parameter (r).it clear that in figure if the value of group parameter (r) is increase then the temperature of porous region is decreases with constant value of X=1. In figure 7 the temperature of porous region rises along with the increment in the different values of X for constant value of group parameter ($r = 0.2$). More over lines are showing variation of temperature along with X is almost parallel to each other.

In Figure 8 the temperature of non porous region rises along with the increment in the different values of X for constant value of group parameter ($r = 0.2$) and $\delta/h = 0.2$. More over lines are showing variation of temperature along with X is almost parallel to each other. In Figure 9, rise of the temperature of nonporous region is noticed if value of group parameter (r) increases for constant value of X=0.2 and the height of non porous region to the height of medium bears a thickness of porous region ($\delta/h = 1$). In Figure 10 the temperature of non porous region increases if the value of δ/h is increases for constant values of $X = 0.2$ and $r = 0.2$.

In Figure 11, the entropy generation rate of porous region (N_{Sp}) increases on increasing group parameter ($Br\Omega^{-1}=B$) in a very narrow region. Also initial variation of entropy generation rate of porous region (N_{Sp}) is almost coinciding with each other. For constant value of $Pe =100$ $X = 0.2$, $r = 0.2$. In Figure 12, the entropy generation rate of porous region (N_{Sp}) increases on increases group parameter (r) with the constant values of Pe=100 and group parameter ($Br\Omega^{-1}= 0.2$). As well as initial variations are closer and latter variations are wider.In Figure 13, the entropy generation rate of non porous region (Ns_{np}) increases on increasing the value of group parameter ($Br\Omega^{-1}=B$).

Also initial variation of entropy generation rate of non porous region (Ns_{np}) is coinciding with each other. For constant value of Pe=100, δ/h=1, r =1. The spartial distribution of the entropy generation rate of non porous region (Ns_{np}) for different values of group parameter (r) is plotted in Figure 14. It is interesting to note that entropy generation rate decreases in transverse direction and decreases with an increase in group parameter (r).it is clear in figure that the entropy generation rate of non porous region (Ns_{np}) almost same at both the terminal points of the channel. It shows that the negligible effects of magnetic field and porous permeability at terminal points of the channel. Figure 15 shows the spartial distribution of entropy generation rate of non porous region (Ns_{np}) for different values of the thickness of porous region (δ/h).for all the values of δ/h the entropy generation rate decreases in the transverse direction and increase with an increase in the values of δ/h . Figure shows the entropy generation rate of non porous region (Ns_{np}) almost same at both the terminal points of the channel. It is clear that the negligible effects of different values of δ/h at terminal points of the channel.

VI. CONCLUSION:

This paper presents the application of the second law of thermodynamics analysis of Newtonian flow along an inclined heated plate with effects of hydromagnetic and porous media in two regions. The velocity and temperature profiles are obtained and used to evaluate the entropy generation numbers for porous and non porous region. For different values of the group parameters, the entropy generation rate is function of Brinkman number as shown by the graph which gradually increases symmetrically about the centerline in the transverse direction from the lower wall towards the upper wall. This clearly implies that viscous dissipation has negligible effect on both regions i.e. Porous and Non porous region the entropy generation rate at the initial part of a channel.
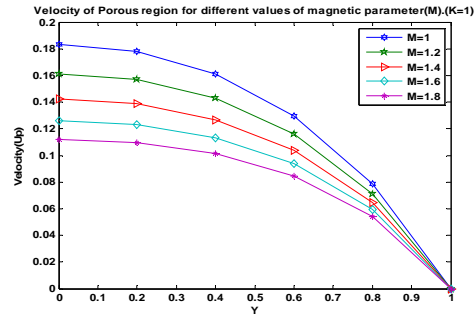

Figure 2: Velocity profile of Porous region for different values of magnetic field (M).
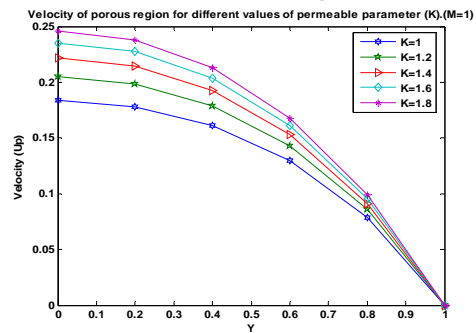

Figure 3: Velocity profile of Porous region for different values of permeable parameter (K).
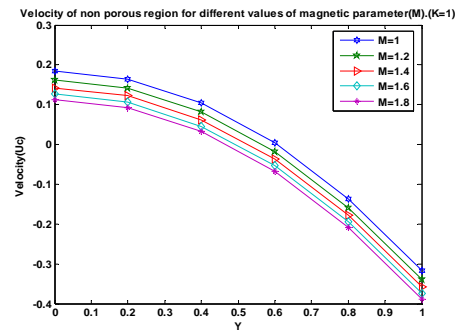

Figure 4: Velocity profile of Non Porous region for different values of magnetic field (M).
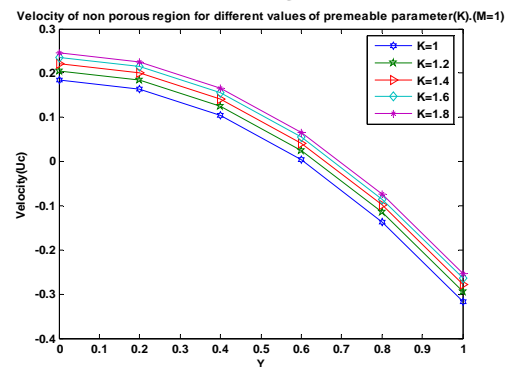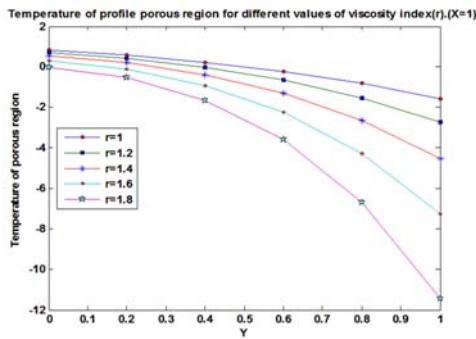

Figure 5: Velocity profile of Non Porous region for different values of permeable parameter (K).

Figure 6: Temperature profile of Porous region for different values of viscosity index (r).
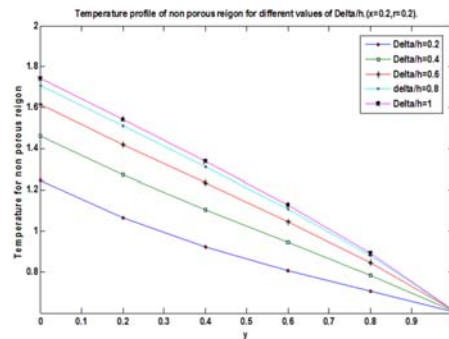

Figure: 7: Temperature profile of Porous region for different values of axial distance (X).

Figure: 8: Temperature profile of Non Porous region for different values of axial distance (X).

Figure: 9: Temperature profile of Non Porous region for different values of viscosity index *r*.

Figure: 10: Temperature profile of Non Porous region for different values of porous region thickness *δ/h*.
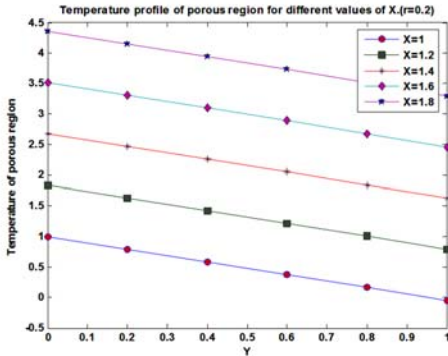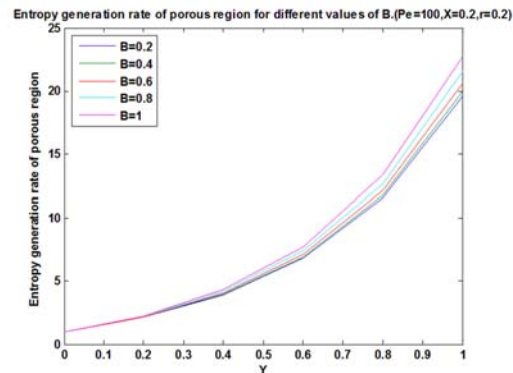

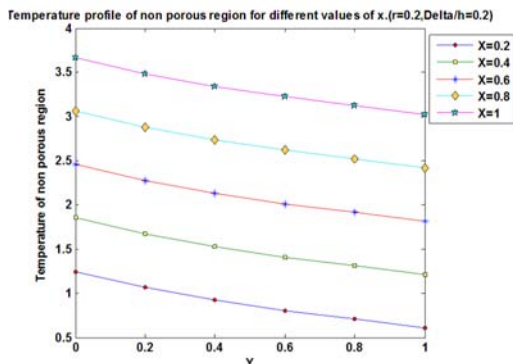**Figure: 11: Entropy generation rate profile of Porous region for different values of group parameter *B*.**
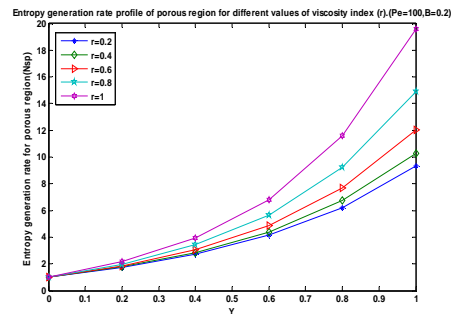
Figure: 12: Entropy generation rate profile of Porous region for different values of viscosityindex *r*.

Figure: 13: Entropy generation rate profile of Non Porous region for different values of group parameter *B*.

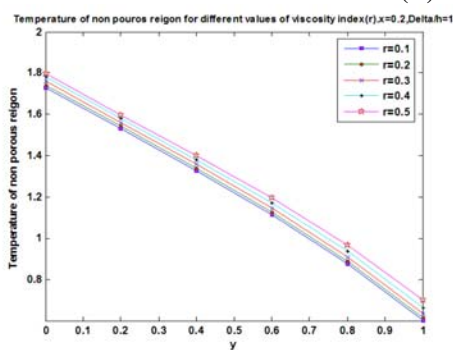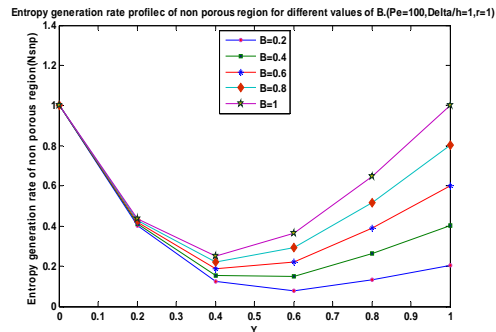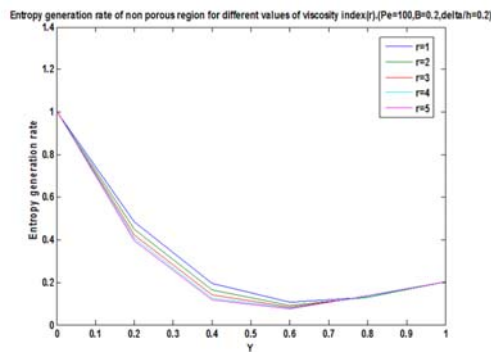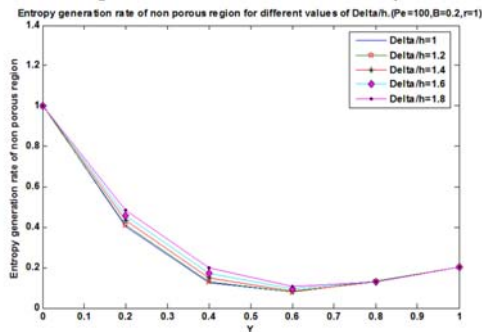**Figure: 14: Entropy generation rate profile of Non Porous region for different of viscosity index *r*.**

Figure: 15: Entropy generation rate profile of Non Porous region for different values of porous region thickness *δ/h*.

VII. REFERENCES

[1]. Bejan, A., Second law analysis in heat transfer. *Energy. 1980, 5, 721 732.*

[2]. Bejan, A. Entropy Generation through Heat and Fluid Flow. *John Wiley & Sons. Inc.: Canada 1994, Chapter 5, p 98.*

[3]. Bejan, A.. Entropy Generation Minimization, CRC Press Flow. *John Wiley & Sons. Inc.: Canada 1996, Chapter 5, p 98.*

[4]. Bejan, A. Entropy Generation Minimization, *C RC Press: USA* 1996.

[6]. Mahmud, S. and Fraser, R. A., The second law analysis in fundamental convective heat transfer problems. *Int. J. of Thermal Sciences 2002, 42 (2), 177-186.*

[7]. Makinde, O. D., Exothermic explosions in a s lab: A case study of series summation technique. *Int. Comm. Heat and Mass Transfer 2004, 31,8 , 1227-1231.*

[8]. Rama Subba, Reddy Gorla , David M. Pratt, Second Law Analysis of a non-Newtonian Laminar Falling Liquid Film along an Inclined Heated Plate. *Entropy, 2007, 9, 30-41.*

[9] . Sahin, A.Z. Entropy generation and pumping power in a turbulent fluid flow through a smooth pipe subjected to constant heat flux. *Exergy, an International Journal 2002, 2, 314-321.*

[10]. Woods, L.C. Thermodynamics of fluid systems, *Oxford University Press*, Oxford, 1975.

TEACHING VOCABULARY FOR THE ENHANCEMENT OF

ENGLISH LANGUAGE

Yogita Verma

Asst. Prof.,Department of Humanities, RJIT, BSF Academy, Tekanpur, Gwalior

Email-dollyogita@yahoo.co.in

Abstract : Teaching English language to regional language students has always been very challenging for teachers and for that they have been engaging in experiments and finding the different- different ways to teach English language. As we know that students are always active and curious to know new things .This paper is an attempt to highlight the hidden curiosity in students and how they are curious to know whatever come in front of them so for that as we enter in the class we should give them some different words and start with asking questions like:

Q-What does it mean?

Q-What is the antonym of this word?

Q-What is the synonym of this word?

Q-What are the differences between so and so words?

Q-Do you know the words having same sounds with different spellings and different meaning?

  Q-Do you know a particular word with many uses?

  Q-Give one word substitution for this word?

Like this if we start the class then we find that to ask something new we have to learn something new .These questions are just like a tool for the enhancement of knowledge for the teachers as well as for the students.

Introduction

This paper shows how to make the language comprehensible to know the meanings , differences synonyms , antonyms , homonyms and one word substitutions . The teachers of 21st century must be innovative, imaginative, and resourceful and adopt new techniques to teach vocabulary. There are several methods to teach vocabulary which I have experimented in my lectures. As I enter in my class I write some words on the black / white board to ask first of all what does it mean or whether they know the synonyms or antonyms of particular word or they know the difference between these two. It is always a pre lesson plan. It always makes the lesson interesting which we are going to teach in the next class.

Methods

Synonyms and antonyms are very interesting. For that either we can give direct words or some fill in the blanks exercise. For example, Give the synonyms of given words.

Synonyms

Apposite : suitable

Dissipate : waste

Incessant : continues

Melancholy : gloomy

Prodigal : extravagant

Now give the antonyms of given words.

Antonyms

Boisterous × calm

Gaity × mourning

Ominous × auspicious

Savage × civilized

Tranquil × agitated

In English language there are hundreds of words with the same sounds and different meanings and spellings thus it is very essential to know the difference between them to comprehend language. In speaking the result may not lead to any disaster but in writing it definitely causes disastrous .A very small spelling also makes a great difference. To make the students aware of difference between fill in the blanks technique is very effective. For instance,

Fill in the blanks with the proper words .
A-
1 - The bird will _____ in no time . (soar , sore)
2 - Can you _____ any example . (cite , site)
3 - I would _____ the job . (except , accept)
4 - At last he achieved his _____ (goal , gaol)
5 - She was the _____ worker in the field . (loan , lone)

B- Distinguish between the following pairs of words :
1 - course, coarse
2 - draught, drought
3 - stationary, stationery
4 - veil, vale
5 - weather, whether

Asking some different words is a small task given just in the beginning of the class to develop interest in students. It normally takes 5 to 10 minutes. It is just like simple game or we can say it is warm up activity. Here is a simple game for word building or we can call it vocabulary brainstorm where we have to write some letters on the black/white board and each student is asked to write down on one paper all the letters then they have to make as many words as they can provided the middle letter. Now we can ask how many words of four or more word can you make from the letters shown? And every word must contain the central letter. It is a timed game. The student with maximum

words wins. Here is an example:

		V		R
			A	
		B		E

Example: Brave, Rave, Aver, Beaver, Bereave

One word substitution as the phrase indicates itself are the words that replace group of words or a full sentence effectively without creating any kind of ambiguity in the meaning of the sentences. Like the word "Autobiography" can be used in the place of sentence "The life story of a man written by himself ". It is very important to write precisely and speak in a single word. Generally, we speak or write in a garrulous way. But it is seen that precise words are always understood easily by all. At the time we become verbose which is not required and we are required to talk or speak precisely. This not only makes the language easily comprehendible but also makes it beautiful. The other way, we can say that these words are used to bring an effect of compression in any kind of writing , when we have to write a lot with in limitation of time and space , there these kind of words can prove quite handy. In English language there are a lots of single words for a group of words that can be used effectively to make the writing to the point that to without losing the meaning of the context for example,

Give one Word Substitution
1- One who is able to both the hands together in writing and playing
Ambidextrous
2 - One who compiles dictionary
Lexicographer
3- One who is not sure of the existence of God
Agnostic
4 - A fictitious name used by an author
Pseudonym
5 - A person with a long experience of any occupation
Veteran

Conclusion:-
Teaching vocabulary through the question answer technique can lead to proficiency in the use of English language. It has been always a

creating meaningful situation in the classroom. The class can be involved in an interaction session where there is an exchange of questions and answer. Vocabulary is indeed one of the most important elements of any language. Teaching vocabulary is normally done at the pre reading stage of a lesson therefore it is very essential to teach vocabulary in the beginning only because the learners are then ready to comprehend the lesson which the teacher is going to teach the next and like this paper several methods are here to give students more opportunity to communicate and practice more English .

References:

1 - A handbook of teaching English , Sharda Kaushik, Published Orient Blackswan 2009,

2 - Innovation in English language teaching , Z. N. Patil Published by Orient blackswan 2012.

3 - Teaching of English , Mohammad Aslam Published by Cambridge University , New Delhi 2003,

4 - WWW. target study .com

REVIEW PAPER ON DESIGN AND FATIGUE ANALYSIS OF LEAF SPRING FOR AUTOMOBILE SUSPENSION SYSTEM

Dev Dutt Dwivedi[1], V. K. Jain[2]

[1]P. G Scholar, Mechanical Engineering, IPS College of Technology Management

[2] HOD, Mechanical Engineering, IPS College of Technology Management, Gwalior MP India

Email: Dev.dwivedi182@gmail.com[1], profvkjain@gmail.com[2]

ABSTRACT

This paper reviews the general study on the configuration and investigation of leaf spring. A vehicle suspension system fundamentally influences the vehicle behaviour, i.e. vibration attributes stability and comfort. Leaf springs are generally utilized in the suspension system of a vehicle and are subjected to a fluctuating cycles resulting to failure by fatigue. A great amount of exploration has been conducted to enhance leaf spring performance. Presently in vehicle industry steel spring has replaced the composite leaf spring. Fiberglass material has better strength and is lighter in weight as contrast with steel for leaf spring. A wide amount of study has been conducted in this paper to investigate the design and analysis of leaf spring and leaf spring fatigue life. A leaf spring has also been designed on ANSYS Workbench

Introduction

A spring is an elastic body, whose expand in size when load applied and regain its original shape when removed. Leaf spring is the simplest form of spring used in the suspension system of vehicle.It absorbs automobile vibrations, shocks and loads by springing action and to some extend by damping functions.It absorbs energy in the form of potential energy. Springs capacity to absorb and store more strain energy makes the suspension system more comfortable. Most widely used leaf spring type is semi-elliptic inheavyand light automobile vehicles. The multi leaf spring comprises of various steps called blades while mono leaf spring is of only one step. Number of steps increases the spring absorbing capability.For heavy vehicles multi leaf spring are used while light vehicle mono leaf spring can be used.
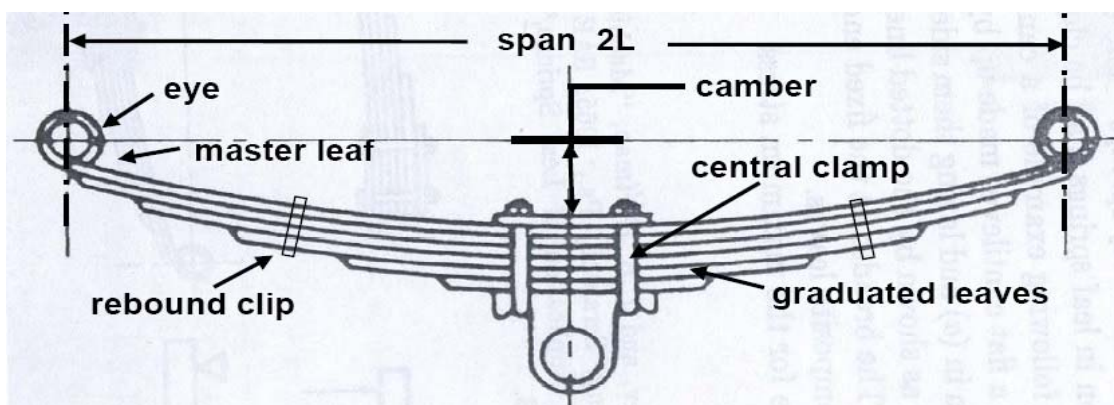

Fig. 1 Schematic of Laminated semi-elliptic leaf spring

Springs initially given a camberso they will have a tendency to bend under loading condition. The leaf spring works under two hypothesis uniform strength and uniform width.
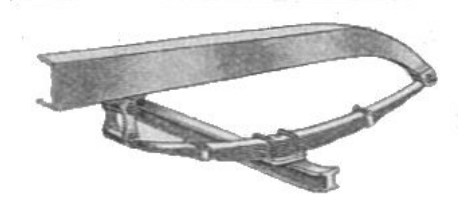
The master leaf spring is the longest and has eyes at its end while remaining steps of spring are called graduated leaves.Types of different leaf springs are shown in figure 2.
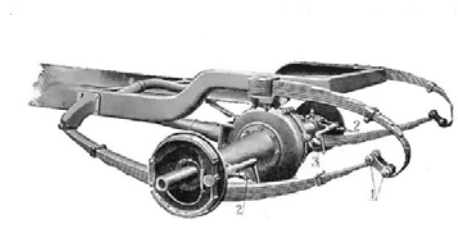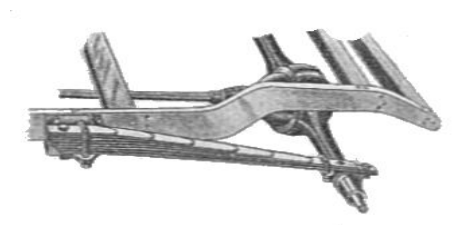
Elliptic

Semi elliptic

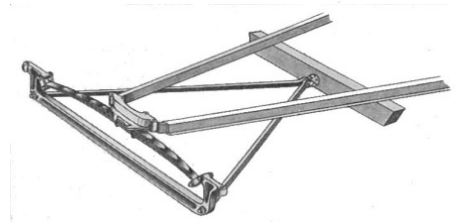Three quarter elliptic

Quarter elliptic

Transverse leaf spring

Figure 2 Types of leaf spring

Literature review

Mahmood M. shokrieh and DavoodRezaei[1] studied design, analysis and optimization of leaf spring. In their study they have replaced a steel leaf spring by a composite one. Primary target of their study was to design a spring that possess least weight and is capable of bearing a given static externalforce without any failure. They conducted work on a four-leaf steel spring which used in back suspension system of light and heavy vehicles. They used ANSYS V5.4 to study the four-leaf steel spring. Theyobtained the deflection and stress results and compared their results with analytical and experimental results available. Utilizing the results obtained for steel leaf spring they designed a composite leaf spring considering spring geometry optimization made of fiberglass with epoxy resin with stress and displacement as design constraints. They analysed this spring utilizing ANSYS and verified their results with experimental results and of finite element solution of same dimensions. They found that composite leaf spring weigh 80% less and stress developed is also less compared to steel leaf spring. The composite leaf spring natural frequency is found to be higher that of steel leaf spring and can avoid the resonance at the road.

AjitabhPateriya, Mudassir Khan[2] studied dynamic characteristics of spring loadedusing ANSYS. Fluid-solid interaction mesh

deformation between the valvedisc and surrounding fluid has been used to study the motion of the valve disc for differentmaterials. Differentmaterials have been used consideringsimilar boundary condition for finding the best suitable material. FEM analysis result shows that La2Zr2O7 is best suitable material. Maximum shear stress considered is 0.20395 MPa which is greaterfor Aluminium alloy. For weight and cost comparison the Aluminiumalloy material should be preferred.

Pozhilarasu V. and T ParameshwaranPillai [3] studied analysis of steel and composite leaf spring. They compared the conventional leaf spring and composite (Glass fibre reinforced plastic – GFRP) leaf spring. They used ANSYS software for studying conventional steel leaf spring and composite leaf spring for similar conditions. They fabricated a glass/epoxy composite leaf spring using hand layup method. The universal testing machine has been used to test the results of conventional steel and composite leaf spring. Under the same static loading condition deflection and stress of conventional steel and composite leaf spring has been obtained and results shows a wide difference between the results.

Aishwarya A.L., A. Eswarakumar, V.Balakrishna Murthy [4] conducted free vibration analysis of composite leaf springs. They generated a three dimensional leaf spring on ANSYS. They studied the effect of variation of width, relative movements of the leaves, friction between the spring leaves. They noticed that friction coefficient does not affect the results. They noticed that leaf width improves the natural frequency.

T.N.V.Ashok Kumar, E. VenkateswaraRao, S. V. Gopal Krishna [5] conducted design and material optimization of heavy vehicle leaf spring. They conducted their study to find out the effect on displacement, deflection, weight and frequencies. They used ANSYS to conduct their study and compared their results between steel leaf spring and composite leaf spring made of glass/epoxy and Kevlar/epoxy. They used layer stacking method by changing the reinforcement angled for 3 layers, 5 layers and 11 layers. They compared the weight of conventional steel leaf spring with that of composite leaf spring and found a weight reduction of 27.5%.

K.A. SaiAnuraagand BitraguntaVenkataSivaram[6] studied the comparison of static, dynamic & shock analysis for two & five layered composite leaf spring. They modelled their leaf spring using Unigraphics software NX7.5. They sued ANSYS to analyse their study. They have done static, dynamic and shock analysis. For analysing the results they have used five layered and two layered composite leaf spring. They noticed maximum displacement in the two layered leaf spring compared to five layered 101.5mm to 83.23mm. They noticed that Von-mises stress for five layered leaf spring is more compared to two-layered. For shock analysis as time increases, the displacement initially increases, reaches a maximum and then decreases for a two layer mode, for five layered the deflection v/s time for five layer mode where the displacement initially decreases, reaches a minimum and then increases as the time progresses.

E. Mahdi a, O.M.S. Alkoles[7] conducted study on light composite elliptic springs for vehicle suspension. They numerically and experimentally studied the impact of ellipticityratio on woven roving wrapped composite elliptical springperformance.They conducted different experiments by changing the ellipticity ratio (a/b) from one to two for composite leaf springs. They found that spring rate and failure loads get influenced by ellipticity ratio and get highest spring rate for ellipticity ratio (a/b) 2.0. They represented a failure mechanics and found that with wall thickness, spring rate and failure increases. They concluded that composites leaf spring can be utilized for light and heavy trucks.

Y. N. V. Santhosh Kumar, M. VimalTeja[8] studieddesign and analysis of composite leafspring. In addition to they talked about the advantages of composite material like higher specific stiffness and strength, higher strength to weight proportion. In their study they have used composite leaf spring utilizing E-Glass/Epoxy instead of steel leaf spring.They targeted their study towards the reducing the weight of it. They used Pro-E to design the spring and ANSYS Metaphysics to analyses it. They found that composite leaf spring with epoxy weighs 60.48 less compared to conventional steel leaf spring and stresses developed were within limits with

factor of safety.They also concluded that good strength has been found if fibres in the laminate oriented longitudinally.

PankajSaini, AshishGoel, Dushyant Kumar[9] conducted study on light vehicles design and analysis. They aimed their study at reducing weight and compare the stress developed in the composite leaf spring compared to steel leaf spring. They selected three materials glass fibrereinforced polymer(E-glass/epoxy),carbon epoxy and graphite epoxy is utilized against ordinary steel. They found that composite leaf spring weigh 92% less and developed less stresses compared to steel leaf spring. From the static examination results it is found that there is a most extreme relocation of in the steel leaf spring. After conducting experiments they found that only graphite/epoxy composite leaf spring has higherstresses compared to steel leaf spring. E-Glass/Epoxy reduces the weight by 81.22%, Graphite/Epoxy by 91.95% and 90.51 % for Carbon/Epoxy over steel leaf spring. Thus they concluded that E-glass/epoxy composite leaf spring can be utilized in place of steel leaf spring.

ManasPatnaik, NarendraYadav,[10] conducted finite element and experimental study on parabolic leaf spring. Eye Distance & Depth of camber have been selected as input parameter for DOE. They focused this study on mini loader truck parabolic leaf spring, with loading capacity of 1 Tonne. CATIA V5 R20 has been used to model the leaf spring.Eye Distance and Depth of camber have beenvaried to see their effect on von-misses and displacement andresults have been plotted.They concluded with camber,average amount of displacement decreases and average amount of von misses stress increases,with eye distance,average amount ofdisplacementand von misses stress increases.They concluded that the optimum dimensions pertaining to parabolic leaf spring can be achievedby various plots obtained from design ofexperiments.

Ashish V.Amrute, Edward Nikhil karlus[11] studied design and evaluation of leaf spring. They targeted their study towards the comparison of composite leaf spring and steel leaf spring. Different comparison parameters were stress developed, weighing capacity and load carrying capacity.Tata ace ex vehicle leaf spring has been considered in the present study.

In their study they have tried to replace the steel leaf spring by composite leaf spring. Bending stress has been found to be decreased by 25.05% i.e. for the same load carrying capacity less stresses developed in the composite leaf spring. The steel leaf spring weighs around 10.27kg while composite leaf spring with E-glass/Epoxy weighs just 3.26 kg. They concluded that the weight get reduced by 67.88%.

H.A.AI-Qureshi [12] conducted study on composite material leaf spring.They considered a composite car and focused their study on design, analysis and fabrication of its leaf spring. Design, fabrication and testing on amono composite leaf spring with variable thickness with same mechanical and geometrical properties to multileaf steel spring wereconducted. They did field test preceded by laboratory experiments to check ride qualities on various GFRP spring which were mounted insteadof steel spring on jeep. They found GFRP springsto be more adaptable and produces less noise and harshness compared to steel leaf spring. They also noticed 80% less weight and higher natural frequency.

Rupesh N. Kalwaghe, K. R. Sontakke[13] conducted study on Design and Analysis of Composite Leaf Spring by Using FEA and ANSYS. They substituted a steel leaf spring by a composite leaf spring.Because for same load carrying capacity composite leaf spring possess high strength to weight proportion for same dimensions. A semi-elliptical composite multi leaf spring made of E-glass/epoxy is designed. Less stresses and deflection has been found for same load carrying capacity. Results compared well with the theoretical results.They had done a comparative study and found that composite leaf spring with E-Glass/Epoxy weighs 67.88% less compared to steel leaf spring. In their study they suggest to use E-glass/epoxy composite leaf spring from stiffness and stress perspective.

C.Madan Mohan Reddy, D.RavindraNaik, Dr M.Lakshmi Kantha[14] Reddy conducted study on analysisand testing of two wheeler suspension helical compression spring.They focused their study on suspension system springs modelling, analysis and testing. They try to replace the steel helical spring in automobiles. They carried a comparative study. They calculate the stress and deflection of helical spring. They compared their

FEA results with experimental values.The found chrome vanadium steel spring has 13-17% less maximum stress and 10% less specific weight compared to steel spring. They validate their

Figure 3 shows the sketch of the leaf spring designed in ANSYS. Effect of load applied by the vehicle will be studied on this spring. Stress

FEA results with the experimental values and found excellent similarity of 95% in deflection and of 97% in shear stress pattern.

and strain analysis will also be done on the designed leaf spring. Table 1 shows the dimensions of the leaf spring designed in ANSYS.
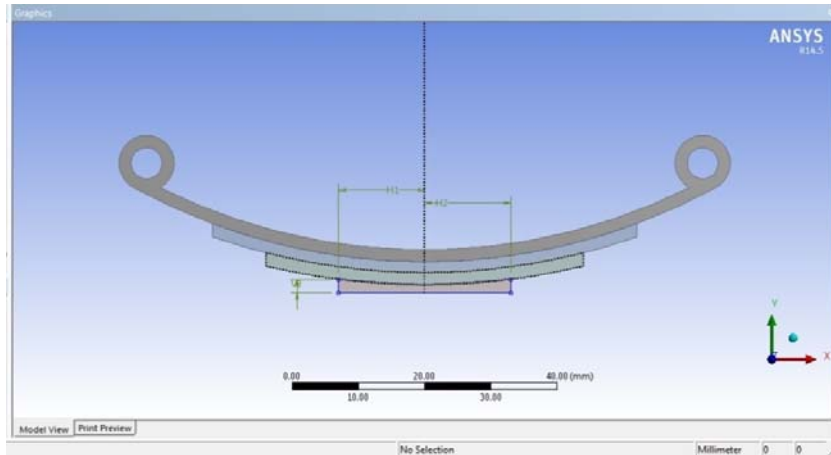

Figure 3 Model of leaf spring designed in ANSYS

Table 1 Details about the leaf spring

Leaf Spring Part	Top part	Bottom part	Radius	Vertical Distance
Eye outer part			4.2mm	
Eye inner part			2.3mm	
Master leaf	40mm	45mm		
Graduated leaf 1	32mm	32mm		2mm
Graduated leaf 2	24mm	24mm		2mm
Bottom leaf	17mm	17mm		2mm
Load applied	40N			
Span (Eye centre to centre)	85mm			
No of graduated leafs	3			
Width of leafs	6mm			

Conclusion

From the writing survey it is seen that the goal was to get a spring with least weight that is prepared to do conveying given static outside powers by limitations restricting burdens and removals. For that the steel leaf spring is supplanted by composite leaf spring. Composite leaf spring is superior to steel leaf spring. Composite materials have more flexible strain and high quality to weight ratio to steel.It is reasoned that composite leaf spring is a successful trade for the current steel leaf spring in car. The burdens in the composite leaf spring are much lower than that of the steel spring.

References

1. Mahmood M. Shokrieh , DavoodRezaei, *Analysis and optimization of a composite leaf spring*, Composite Structures, 60 (2003) 317–325.
2. AjitabhPateriya, Mudassir Khan, *Structural and thermal analysis of spring loaded safety valve using FEM*, International journal of mechanical engineering and robotics research, 4(1), 430-434.
3. Pozhilarasu V. and T ParameshwaranPillai, *Performance analysis of steel leaf spring with composite leaf spring and fabrication of composite leaf spring*, International journal

of engineering research and Science & Technology, 2(3), 102-109.

4. Aishwarya A.L., A. Eswarakumar, V.Balakrishna Murthy, *Free vibration analysis of composite leaf springs*, International journal of research in mechanical engineering &technology, 4(1), 95-97.

5. T. N. V. Ashok Kumar, E. VenkateswaraRao, S. V. Gopal Krishna, *Design and Material Optimization of Heavy Vehicle Leaf Spring*, International Journal of Research in Mechanical Engineering & Technology, 4(1), 80-88.

6. K.A. SaiAnuraag and BitraguntaVenkataSivaram, *Comparison of Static, Dynamic & Shock Analysis for Two & Five Layered Composite Leaf Spring*, Journal of Engineering Research and Applications, 2(5), 692-697.

7. E. Mahdi a, O.M.S. Alkoles a, A.M.S. Hamouda b, B.B. Sahari b, R. Yonus c, G. Goudah, *Light composite elliptic springs for vehicle suspension*, Composite Structures, 75, 24–28.

8. Y. N. V. Santhosh Kumar, M. VimalTeja, *Design and Analysis of Composite Leaf Spring,*Dept. of Mechanical Engineering, Nimra College of Engineering & Technology, Ibrahimpatnam, Vijayawada. (2012)

9. PankajSaini, AshishGoel, Dushyant Kumar, *Design and analysis of composite leaf spring for light vehicles*, International Journal of Innovative Research in Science, Engineering and Technology 2(5), May 2013.

10. ManasPatnaik, NarendraYadav, RiteshDewangan, *Study of a Parabolic Leaf Spring by Finite Element Method & Design of Experiments*, International Journal of Modern Engineering Research, 2(4), 1920-1922 .

11. H.A.AI-Qureshi, *Automobile leaf spring from composite materials,*Journal of materials processing technology, 118(2001).

12. Ashish V. Amrute, Edward Nikhil karlus, R.K.Rathore, *Design and assessment of multi leaf spring,'* International journal of research in aeronautical and mechanical engineering.

13. Rupesh N Kalwaghe, K. R. Sontakke, *Design and Anslysis of composite leaf spring by using FEA and ANSYS,* International journal of scientific engineering and research, 3(5), 74-77.

DESIGN AND ANALYSIS OF AOTOMOBILE LEAF SPRING USING ANSYS

Dev Dutt Dwivedi[1], V. K. Jain[2]

[1]P. G Scholar, Mechanical Engineering, IPS College of Technology Management

[2] HOD, Mechanical Engineering, IPS College of Technology Management, Gwalior MP India

Email: Dev.dwivedi182@gmail.com[1], profvkjain@gmail.com[2]

ABSTRACT

Design and analysis of composite leaf spring has been done in the present paper. ANSYS 14.5 has been used to conduct the analysis. Static structural tool has been used of ANSYS. A three layer composite leaf spring with full length leave. E-Glass/epoxy composite material has been used. Conventional steel leaf spring results have been compared with the present results obtained for composite leaf spring. E-glass/epoxymaterial is better in strength andlighter in weight as contrast with conventional steel leaf spring. A wide amount of study has been conducted in this paper to investigatethe design and analysis of leaf spring and leaf spring fatigue life.

Introduction

A spring is an elastic body, whose expand in size when load applied and regain its original shape when removed. Leaf spring is the simplest form of spring used in the suspension system of vehicle.It absorbs automobile vibrations, shocks and loads by springing action and to some extend by damping functions.It absorbs energy in the form of potential energy. Springs capacity to absorb and store more strain energy makes the suspension system more comfortable. Most widely used leaf spring type is semi-elliptic inheavyand light automobile vehicles. The multi leaf spring comprises of various steps called blades while mono leaf spring is of only one step. Number of steps increases the spring absorbing capability.For heavy vehicles multi leaf spring are used while light vehicle mono leaf spring can be used.

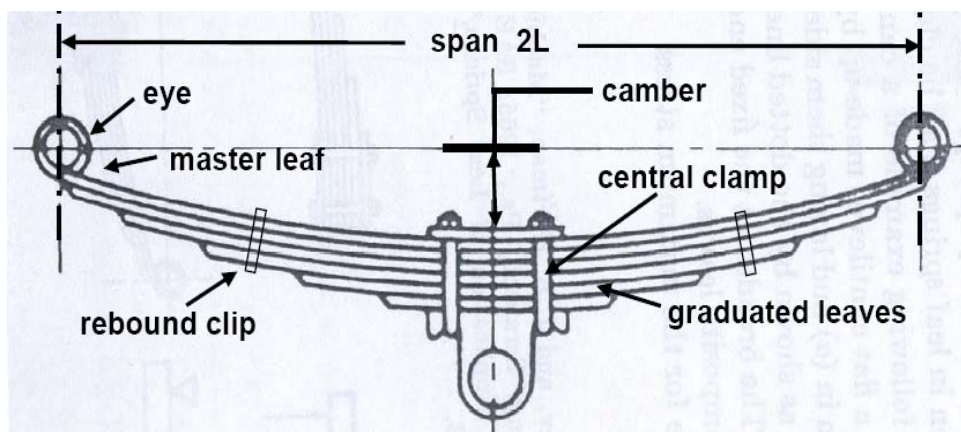Fig. 1 Schematic of Laminated semi-elliptic leaf spring

The master leaf spring is the longest and has eyes at its end while remaining steps of spring are called graduated leaves.Types of different leaf springs are shown in figure 2.

Springs initially given a camberso they will have a tendency to bend under loading condition. The leaf spring works under two hypothesis uniform strength and uniform width.
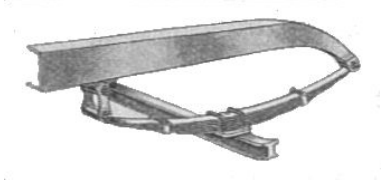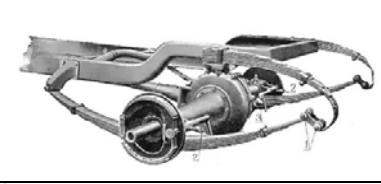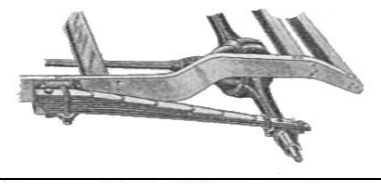
Elliptic	
Semi elliptic	
Three quarter elliptic	
Quarter elliptic	
Transverse leaf spring	

Figure 2 Types of leaf spring

Literature review

C.Madan Mohan Reddy,D.RavindraNaik, Dr M.LakshmiKantha Reddy[1] conducted study on analysis and testing of two wheeler suspension helical compression spring. They focused their study on suspension system springs modelling, analysis and testing. They try to replace the steel helical spring in automobiles. They carried a comparative study. They calculate the stress and deflection of helical spring. They compared their FEA results with experimental values.The found chrome vanadium steel spring has 13-17% less maximum stress and 10% less specific weight compared to steel spring. They validate their FEA results with the experimental values and found excellent similarity of 95% in deflection and of 97% in shear stress pattern. AjitabhPateriya, Mudassir Khan [2] studied dynamic characteristics of spring loaded using ANSYS. Fluid-solid interaction mesh deformation between the valve disc and surrounding fluid has been used to study the motion of the valve disc for different materials. Differentmaterials have been used considering

similar boundary condition for finding the best suitable material. FEM analysis result shows that La2Zr2O7 is best suitable material. Maximum shear stress considered is 0.20395 MPa which is greater for Aluminium alloy. For weight and cost comparison the Aluminiumalloy material should be preferred.

Pozhilarasu V. and T ParameshwaranPillai [3] studied analysis of steel and composite leaf spring. They compared the conventional leaf spring and composite (Glass fibre reinforced plastic – GFRP) leaf spring. They used ANSYS software for studying conventional steel leaf spring and composite leaf spring for similar conditions. They fabricated a glass/epoxy composite leaf spring using hand layup method. The universal testing machine has been used to test the results of conventional steel and composite leaf spring.

Composite material

A composite material is characterized as a material made out of two or more constituents joined on a naturally visible scale by mechanical

and chemical bonds. Composites are blends of two materials in which one of the materials is known as the "matrixphase" and is implanted in the other material called the "reinforcing stage". Numerous composite materials offer modulus that is either equivalent or superior to any metals. In light of their low specific gravities, the strength to weight-proportion and modulus to weight-proportions of these composite materials are better than those of metallic materials. The fatigue quality weight proportions and fatigue damage tolerance of numerous composite overlays are fantastic. Thus, fibre composite have risen as a noteworthy class of basic material, are either utilized or being considered as substitutions for metal in numerous weight-basic parts in aviation, car and different businesses. High internal damping limit is another advantage. This prompts better vibration energy and results in decreased noise to neighbouring structures. High damping limit of composite materials can be advantageous in numerous car applications in which noise, vibration, and hardness is a basic issue for travellercomfort.

Building geometry in Design Modular

Figure 3 shows the sketch of the leaf spring designed in ANSYS. Dimensions of the spring have been shown in table 1.

Fig. 3 Model of leaf spring designed in ANSYS

Table 1 Details about the leaf spring

Leaf Spring Part	Top part	Bottom part	Radius	Vertical Distance
Eye outer part			4.2mm	
Eye inner part			2.3mm	
Master leaf	40mm	45mm		
Graduated leaf 1	32mm	32mm		2mm
Graduated leaf 2	24mm	24mm		2mm
Bottom leaf	17mm	17mm		2mm
Load applied	40N			
Span (Eye centre to centre)	85mm			
No of graduated leafs	3			
Width of leafs	6mm			

Meshing of Leaf Spring

Fig.4 Meshing of leaf spring designed in ANSYS

Results

From the results it can be observed that the total deformation for E-Glass/Epoxy material is less compared to conventional steel leaf spring material. Equivalent stress generated in the composite E-Glass/Epoxy leaf spring is less compared to steel leaf spring. Less maximum shear stress and maximum principal stress have been found in E-Glass/Epoxy material compared to conventional steel leaf spring.
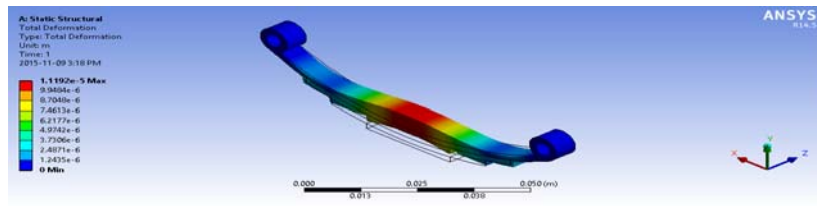
Fig.5 Total Deformation steel
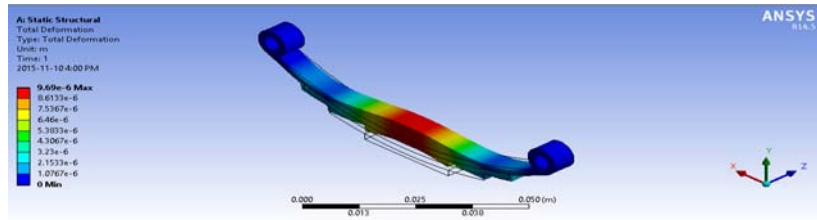
Fig.6 Total Deformation E-Glass/Epoxy
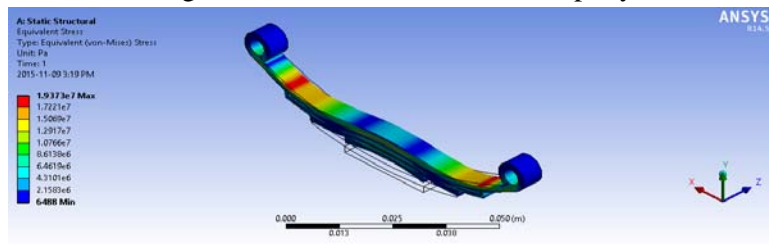
Fig.7 Equivalent stress of steel
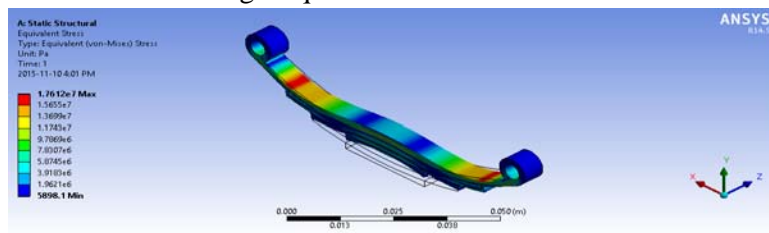
Fig.8 Equivalent stress of E-Glass/Epoxy
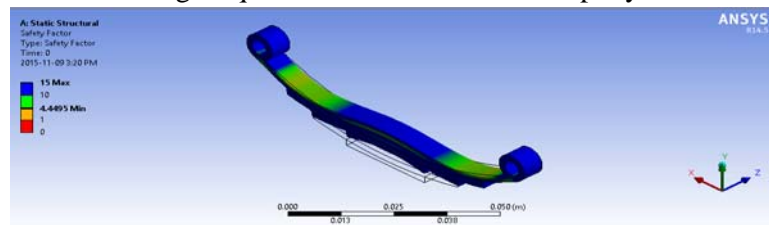
Fig.9 Safety factor of steel
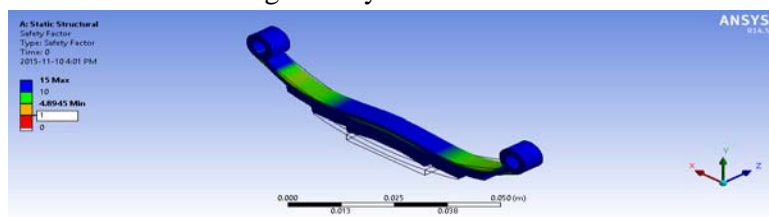
Fig. 10 Safety factor of E-Glass/Epoxy
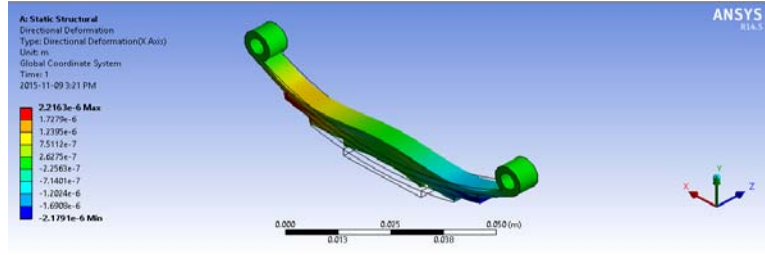
Fig. 11Directional deformation of steel
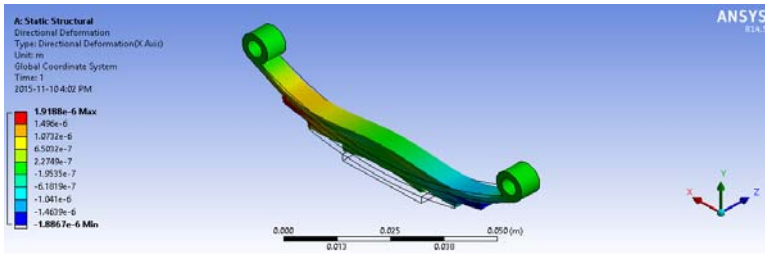
Fig. 12Directional deformation of E-Glass/Epoxy
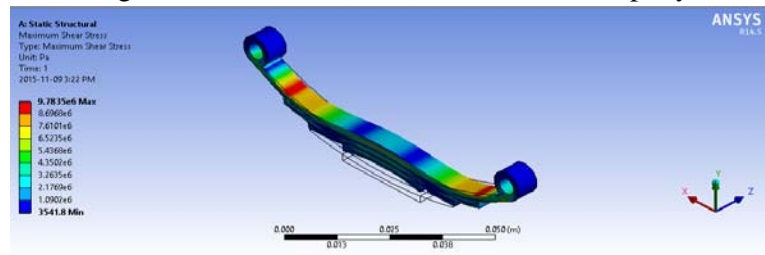
Fig. 13Maximum shear stress of steel
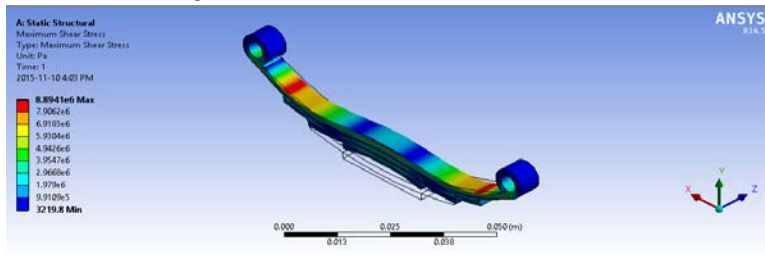
Fig. 14Maximum shear stressof E-Glass/Epoxy
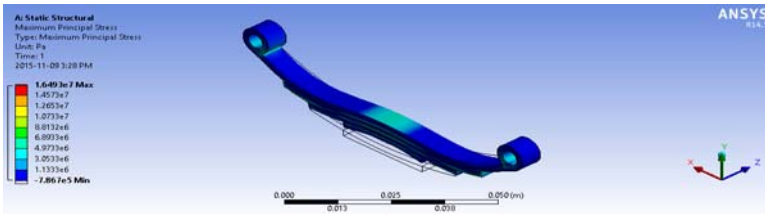
Fig. 15Maximum principal stress of steel
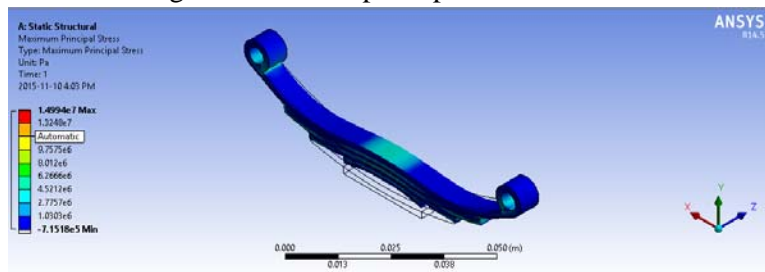
Fig. 16Maximum principal stress of E-Glass/Epoxy

Table 2 Comparison of steel and E-Glass/Epoxy results

Parameters	Conventional steel leaf spring	E-Glass/Epoxy composite leaf spring
Total Deformation (maximum)	$1.1192e^{-5}$	$9.69e^{-6}$
Equivalent stress (maximum)	$1.9373e^{7}$	$1.7612e^{7}$
Directional deformation (maximum)	$2.2163e^{-6}$	$1.9188e^{-6}$
Maximum shear stress (maximum)	$9.7835e^{6}$	$8.8941e^{6}$
Maximum principal stress (maximum)	$1.6493e^{7}$	$1.4994e^{7}$

Conclusion

1. Results demonstrate that composite leaf spring deflection for a particular load is less compared to conventional leaf spring.
2. Stress generated in the E-Glass/Epoxy leaf spring is lower than steel leaf spring.
3. Composite (E-Glass/Epoxy) leaf spring directional deformation is low compared to steel leaf spring.
4. Composite leaf spring is lighter in weight compared to conventional steel leaf spring.

References

1. C. Madan Mohan Reddy, D. RavindraNaik, Dr M. Lakshmi Kantha, *Study on analysis and testing of two wheeler suspension helical spring*,

2. AjitabhPateriya, Mudassir Khan, *Structural and thermal analysis of spring loaded safety valve using FEM*, International journal of mechanical engineering and robotics research, 4(1), 430-434.

3. Pozhilarasu V. and T ParameshwaranPillai, *Performance analysis of steel leaf spring with composite leaf spring and fabrication of composite leaf spring*, International journal of engineering research and Science & Technology, 2(3), 102-109.

4. Aishwarya A.L., A. Eswarakumar, V.Balakrishna Murthy, *Free vibration analysis of composite leaf springs*, International journal of research in mechanical engineering &technology, 4(1), 95-97.

5. T. N. V. Ashok Kumar, E. VenkateswaraRao, S. V. Gopal Krishna, *Design and Material Optimization of Heavy Vehicle Leaf Spring*, International Journal of Research in Mechanical Engineering & Technology, 4(1), 80-88.

6. K.A. SaiAnuraag and BitraguntaVenkataSivaram, *Comparison of Static, Dynamic & Shock Analysis for Two &* *Five Layered Composite Leaf Spring*, Journal of Engineering Research and Applications, 2(5), 692-697.

7. E. Mahdi a, O.M.S. Alkoles a, A.M.S. Hamouda b, B.B. Sahari b, R. Yonus c, G. Goudah, *Light composite elliptic springs for vehicle suspension*, Composite Structures, 75, 24–28.

8. Y. N. V. Santhosh Kumar, M. VimalTeja, *Design and Analysis of Composite Leaf Spring,*Dept. of Mechanical Engineering, Nimra College of Engineering & Technology, Ibrahimpatnam, Vijayawada. (2012)

9. PankajSaini, AshishGoel, Dushyant Kumar, *Design and analysis of composite leaf spring for light vehicles*, International Journal of Innovative Research in Science, Engineering and Technology 2(5), May 2013.

10. ManasPatnaik, NarendraYadav, RiteshDewangan, *Study of a Parabolic Leaf Spring by Finite Element Method & Design of Experiments*, International Journal of Modern Engineering Research, 2(4), 1920-1922 .

11. H.A.AI-Qureshi, *Automobile leaf spring from composite materials,*Journal of materials processing technology, 118(2001).

12. Ashish V. Amrute, Edward Nikhil karlus, R.K.Rathore, *Design and assessment of multi leaf spring,*' International journal of research in aeronautical and mechanical engineering.

13. Rupesh N Kalwaghe, K. R. Sontakke, *Design and Anslysis of composite leaf spring by using FEA and ANSYS,* International journal of scientific engineering and research, 3(5), 74-77.

14. Mahmood M. Shokrieh , DavoodRezaei, *Analysis and optimization of a composite leaf spring*, Composite Structures, 60 (2003) 317–325.

DIGITAL IMAGE WATERMARKING IN WAVELET DOMAIN USING CHAOTIC SEQUENCE

Sumit Pathak[1], Sumit Tiwari[2], Saurabh Agrawal[3]
[1]Asst. Prof.,Department of Computer Science, IPS-CTM Gwalior, India
[2,3]P.G. Scholar,CSE Dept..SRCEM Banmore, M.P. India
Email:sumitpathakcs@gmail.com[1], sumitgwalior23@gmail.com[2], toc.saurabh@gmail.com[3]

Abstract—This paper introduce a method for digital watermarking based on discrete wavelet transform (DWT) using chaotic sequence as a spreading signal. Chaotic sequences are generated through chaotic map, which is determined by initial condition and parameters. The underlying system use wavelet transform to convert original cover image from spatial domain to frequency domain and employs chaotic sequence to spread the watermark over wavelet coefficient. A large number of uncorrelated, random-like, yet deterministic chaotic sequences can be exploited to add the original watermark image to original image .In this type of watermarking the size of original watermark is less than the size of wavelet coefficient. Size of watermark image is made equal to size of wavelet coefficient by chaotic sequence mapping and embedded into the high frequency sub-band of original image. The coefficients whose energies were fewer than the others were selected to hide watermark.

Keywords—Digital watermarking, Wavelet transform, Chaotic sequence.

I. INTRODUCTION

Digital watermarking can be used to insert invisible data into an object helping to track down pirate copies and to prove rightful ownership in a dispute. In principle, watermarking technologies can be applied to any kind of multimedia object, however to achieve the best possible results schemes are normally optimized on a particular medium. The term Digital watermark was first used by Komatsu and Tominaga in 1988[1]. However it was in 1954, Emil Hembrooke of the Muzac Corporation filed a patent for watermarking music works [2]. Since that time, a number of watermarking technologies have been developed and deployed for a variety of applications. Interest in embedded signaling continued throughout the next 35 years. For example, systems were developed for advertisement verification and device control. However, digital watermarking did not receive substantial interest as a research topic until the 1990's. In the first half of that decade, interest in the topic expanded rapidly and today entire conference proceedings are devoted to the subject. In later half of the decade, there was an explosion of interest in digital systems for the watermarking of various content[3].The digital watermarking can be applied to many digital media objects like, image, audio, video, three – dimensional model, executable code, IC's etc. The proposed applications of these methods are many and varied, and include identification of the copyright owner, indication to recording equipment that the marked content should not be recorded, verification that content has not been modified since the mark was embedded, and the monitoring of broadcast channels looking for marked content.

II. THEORETICAL BACKGROUND

A) General model of watermarking

Water marking is processes for embedding the one information into other information. And digital image watermarking can be defined as processes of embedding the image into other image. The image in which image is embedded is known as cover image and the image which is used to embed, is known as watermark.

A Watermarking processes can be composed of the three parts.

- Watermark
- Encoding processes (insertion algorithm)
- Decoding processes (extraction algorithm)

Watermark can be different for different owner. In other word each user has a unique watermark or an owner can also add different watermark in different cover image. The verification algorithm authenticates the object determining both the owner and the integrity of the object.

1) Insertion Process(Encoding)

For the embedding process the inputs are the watermark, cover object and the secret or the public key. The watermark used can be text, numbers or an image. The resulting final data received is the watermarked data W. A block general diagram of this process is shown below.
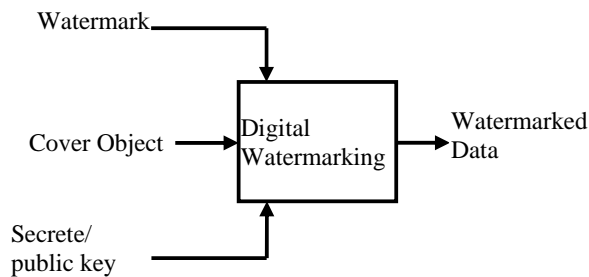
Fig 1 Digital watermarking – Imbedding

2) Extraction Process

Extraction employ watermarked image as a input, cover image used in encoding process and same secrete/public key. The output of this process is recoverd watermark. A block general diagram of this process is shown below.
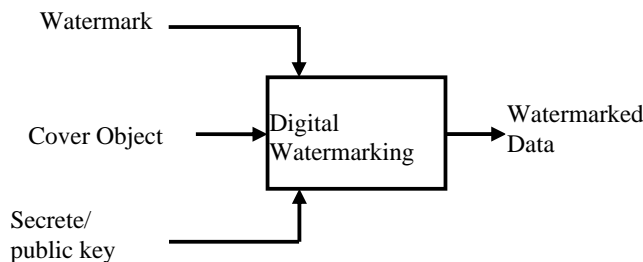
Fig 2 Digital watermarking – Extraction

B. Basic watermarking technique

Watermarks do not always need to be hidden. Watermarking can be broadly classified in two categories:
- Visible watermarking technique
- Invisible watermarking technique

1) Visble watermarking

Visible watermarking was the first and most primitive way of watermarking. In this method the cover object is taken and the watermark in added on it. This makes the watermark visible on the cover object. This was good for identification purposes.

Visible watermarks were created by using Lena's images as the cover images. These images were 8-bit gray scale images. The watermark was chosen as a monochrome image exactly of the same size as the cover object. The watermarked image was achieved by changing the pixel intensity values in the cover image corresponding to white pixels in the watermark. This type of watermarking could only be used for owner identification purposes. For all other applications invisible watermarking is used. An example of visible watermarking is shown in fig 3.

(a)   (b)   (c)

Fig 3 (a) Leena 256*256, (b) watermark image, (c) watermarked image

Most of the literature has focused on the invisible digital watermarking as it has more application in today's digital world. Visible digital watermarks are strongly linked to the original paper watermarks that have been traced back to the end of 13th century [2].

1) Invisble watermarking

In invisible digital watermarking, information is added as digital data to audio, picture, or video, but it cannot be perceived as such (although it may be possible to detect that some amount of information is hidden in the signal).

The watermark may be intended for widespread use and thus, is made easy to retrieve or, it may be a form of steganography, where a party communicates a secret message embedded in the digital signal. In either case, as in visible watermarking, the objective is to attach ownership or other descriptive information to the signal in a way that is difficult to remove. It also is possible to use hidden embedded information as a means of covert communication between individuals. Invisible watermarking can be classified on the basis of their working domain.

- Spatial working domain watermarking
- Frequency working domain watermarking
- Wavelet working domain watermarking

A) Spatial working domain watermarking

Watermarking techniques can be broadly classified into two categories. They are spatial domain watermarking and frequency domain watermarking. In spatial domain watermarking technique, watermark message is added in to spatial domain. In this type of watermarking we do not perform any image processing operation on host image. We directly perform watermarking operation between pixel of message image and pixel of cover object. Spatial domain watermarking technique are simple and computationally efficient, because they modify the color, luminance or brightness values of a digital image pixels, therefore their application is done very easily, and requires minimal computational power. Example of such type of method is Least Significant Bits watermarking (LSB).

The simplest technique used for hidden watermarking is to hide the message bits in the Least Significant Bits (LSB) of the cover object. The advantage with this method is that even if a part of the stego image is cropped the receiver can still get the required message, as the message is embedded a number of times. The message for this case is considered to be very small as compared to the cover object.

B) Frequency working domain watermarking

Watermarking can be applied in the frequency domain by first applying a transform like discrete cosine transforms (DCT). In a similar manner to spatial domain watermarking, the values of chosen frequencies can be altered from the original. Since high frequencies will be lost by compression or scaling, the watermark signal is applied to lower frequencies, or better yet, applied adaptively to frequencies that contain important information of the original picture. Since watermarks applied to the frequency domain will be dispersed over the entirety of the spatial image upon inverse transformation, this method is not as susceptible to defeat by cropping as the spatial technique. However, there is more a tradeoff here between invisibility and decodability, since the watermark is in effect applied indiscriminately across the spatial image. DCT based watermarking is example of this type of watermarking.

In DCT domain watermarking, we first perform discrete cosine transform on cover object and then we embed watermark in to transform image. Frequency domain watermarking involves computation of the DCT of the pixel matrix of both the image as well as the watermark to be embedded on it. Then DCT coefficients are scaled and added. Finally the resulting DCT coefficients are subjected to IDCT. Here we can observe that in frequency domain watermarking, lot of complex logic is involved.

III. PROPOSED METHOD FOR EMBEDDING DIGITAL WATERMARK

A) Wavelet transform

According to Rehmi Post in [4], a wavelet transform is a "tool for carving up functions, operators, or data into components of different frequency, allowing one to study each component separately." In more **practical terms** this means that a wavelet transform decomposes a signal into windows of different resolutions. For doing so, a wavelet transform applies a wavelet on the (one-dimensional) data of interest resulting in a multiresolution signal representation. This is done by separating the signal and details at a frequency determined by the wavelet and then keep repeating this on the low frequency output of this operation until some condition is met (e.g. the signal has become too small to be split again). Like other linear transforms on the space of real/complex valued functions, the wavelet transform is a

change of basis. This is similar to e.g. the Fourier series, only that instead of using the base functions sine and cosine functions wavelets are used. The signal to decompose can be continuous (e.g. functions) or discrete (e.g. images), and thus we distinguish between the continuous wavelet transform (CWT) and the discrete wavelet transform (DWT).

An Image can be represent on multiple resolutions, which are called multiresolution analysis (MRA). Wavelet transform decomposes an image into a set of band limited components which can be reassembled to reconstruct the original image without error. The fact that wavelet-based data structure has been adopted in the established image coding standard JPEG200 encouraged extensive watermarking study in wavelet transform. Wavelet transform separates an image into a lower resolution approximation image (LL) as well as horizontal (HL), vertical (LH) and diagonal (HH) detail comments.

(a)

(b)
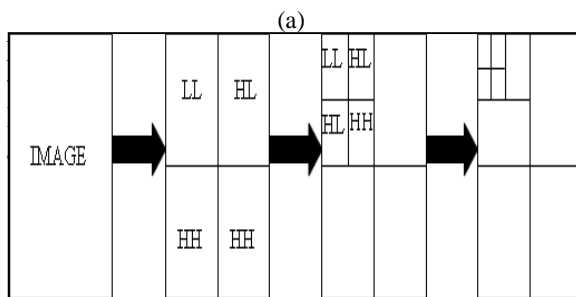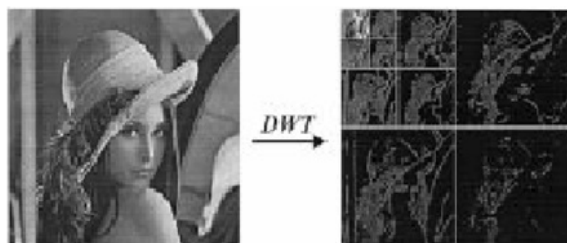
Fig 3 (a) Wavelet Transforms of Image (b) Multidimensional Wavelet Transforms

B) Properties of wavelet transform

Depending on the target application, a wavelet is characterized by a number of properties. Some of these considered relevant for image processing applications are:

Compact support means that a wavelet's values are zero outside a bounded interval. Wavelets with compact support are usually said to have good time or space localization properties.

Smoothness is responsible for good approximation at coarser detail levels; the lack of it usually leads to blocky and/or edgy artifacts.

Filter length determines over how many wavelet coefficients a single signal value is distributed in the transform domain. This is of interest for applications like image compression or watermarking where the signal is manipulated in the transform domain.

C) Application in Image watermarking

The DWT (Discrete Wavelet Transform) [8] separates an image into a lower resolution approximation image (LL) as well as horizontal (HL), vertical (LH) and diagonal (HH) detail components. The process can then be repeated to computes multiple "scale" wavelet decomposition, as in the 2 scale wavelet transform shown below in Fig. 6. One of the many advantages over the wavelet transform is that it is believed to more accurately model aspects of the HVS as compared to the FFT or DCT. This allows us to use higher energy watermarks in regions that the HVS is known to be less sensitive to, such as the high resolution detail bands {LH, HL, HH). Embedding watermarks in these regions allow us to increase the robustness of our watermark, at little to no additional impact on image qualitynot use hard tabs, and limit use of hard returns to only one return at the end of a paragraph. Do not add any kind of pagination anywhere in the paper. Do not number text heads-the template will do that for you?
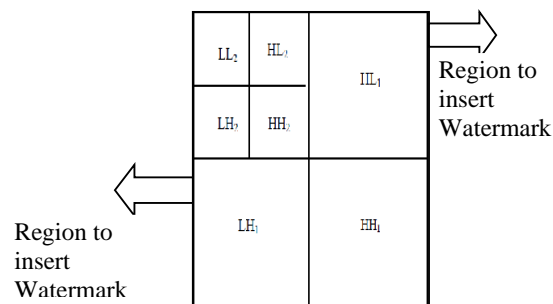
Fig4 Sub Band Theory of Wavelet Transforms

D) Chaotic sequence

A chaotic system is a deterministic dynamical system whose states change with iterations in a deterministic way *[U]*,i. e., a nonlinear

dynamical system model based on its N previous values can be described as

$$C_n = f(c_{n-1}, c_{n-2}, c_{n-3} \ldots \ldots c_{n-N}, a)$$

Where, A is the bifurcating parameter. A chaotic system generates a set of aperiodic signals with a "noise-like" and broad power spectrum. The system is very sensitive to initial conditions. A slight difference in initial conditions will produce totally different sequences, which possess good correlation properties [5].

These characteristics of a chaotic signal are very helpful in digital watermarking applications. The noise-like and wideband output of a chaotic system can be used as the spreading sequence to spread out copyright information. Because of the good correlation properties of chaotic signals, the inserted information can be retrieved properly when the correlation detector is applied. Furthermore, the correlation of certain chaotic spreading sequences is close to the optimal correlation performance for the application of image watermarking. Thus, it is reasonable to expect that using chaotic spreading sequences is superior to widely used classical spreading sequences, such as m-sequences and Gold sequences in terms of robustness and security.

A) Watermarking Using Chaotic Sequence
A large number of uncorrelated, random-like, yet deterministic signals can be generated in the interval of $(-1, 1)$ by executing the logistic map equation recursively. And quantization of these numbers also does not destroy the desirable properties of these kinds' sequences [7].

Encoding: To embed or to encode watermark in to cover object, first we transform the cover object from spatial domain to frequency using wavelet transform and calculate wavelet coefficient. Ann embedding process can be done according to equation.

$$I_w(x, y) = I(x, y) + k \times W(x, y)$$
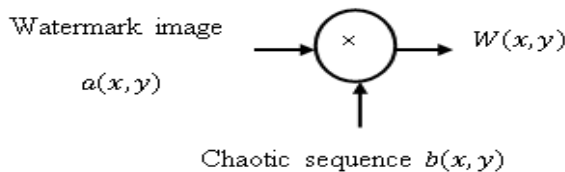
Fig Embedding Process

(a)   (b)   (c)
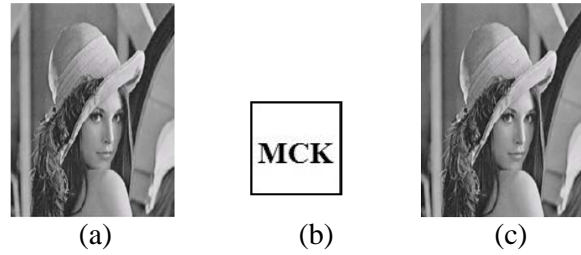
Fig (a) Cover Image, (b) Watermark Image, (c) Watermarked Image

Decoding: To recover the original watermark $a(x, y)$, the watermarked image $I_w(x, y)$ is multiplied at the receiver again with a pseudonoise sequence which is an exact replica of that used for embedding the data.
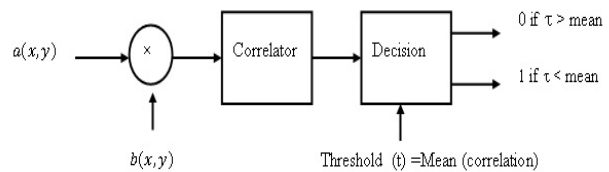
Fig Decoding Process

Fig describes the block diagram of watermark extraction process. Same chaotic sequences that have been used in embedding process, generated $a(x, y)$ by logistic map.

$$C = I_w(x, y) \times b(x, y)$$
$$= (a(x, y) \times b(x, y) + I(x, y) \times b(x, y)$$
$$= a(x, y) \times b^2(x, y) + I(x, y) \times b(x, y)$$

The above equation shows that the watermark image $a(x, y)$ is multiplied twice with the noise signal $b(x, y)$, whereas the unwanted or the cover image $I(x, y)$ is multiplied only once with the noise signal. So $b^2(x, y)$ becomes 1 and the product $I(x, y) \times b(x, y)$ is the unwanted noise signal that can be filtered out during the process of correlation by setting the threshold as mean of correlation. Hence, at the receiver we recover the watermark image $a(x, y)$ [6].

a)   (b)   (c)
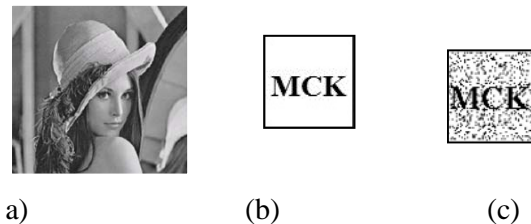
Fig (a) Watermarked Image, (b) original Watermark, (c) Recovered Watermark

IV. CONCLUSION AND FUTURE WORK

This paper presents the technique of image watermarking using chaotic sequence. The chaotic sequences are distinguished by their wideband, noise-like, nonlinear characteristics, simple generation and storage these sequence show zero cross correlation, and low auto correlation since these sequence is very sensitive with respect to their initial condition which could be useful in the recovery of watermarks by using spread spectrum techniques. The watermarked images and the PSNR obtained using the proposed method ensures robustness and quality of the watermarked image. It has proven that chaotic sequence provides improvement in the value of PSNR for watermarked image. Hence the method can serve as a suitable substitute for other algorithms available at present. Digital Watermarking has many objectives in image watermarking like authentication, owner identification, copy control, Fingerprinting, data authentication and many more. This thesis presents a watermarking technique for gray scale image. This work can be extended to embed watermark in to colour image and it can be further extended to imbed watermark in video film. Since video film is composed of multiple frames or multiple images so having embedded watermark in one image we could also embed watermark in to multiple images one after one or simultaneously. And we can serve the various objectives of image watermarking for video watermarking also.

References

[1] I.J. Cox, M.L. Miller, and J.A. Bloom, "digital Watermarking", Morgan Kaufmann Publishers 2002.

[2] S.Katzenbeisser, Petitcolas, F.A.P, "Information hiding techniques for steganography and digital watermarking", Artech House Publishers, 2000.

[3] M.Gnanaguruparan, "Recursive secret sharing in visual cryptography", MS thesis, Louisiana State University.

[4] http://cpk.auc.dk/dicom/Eo2/*CDMA*.htm

[5] Devaney R.L., "An Introduction to Chaotic Dynamical Systems", Wesley Publishing Company, Inc., California, 1989.

[6] Siyue Chen, "Chaotic Spread Spectrum with Application to Digital Image Watermarking", MS Thesis, University of Calgary.

[7] S.Haykin, "Communication Systems", *4th edition, John Wiley and Sons, Inc, 2001*.

[8] M.D.Swatson, B.Jhu, A.H.Tewfik, "Transparent robust image watermarking", Department of Electrical engineering,University of Minnesota.

A QUARTIC LEGENDRE SPLINE COLLOCATION METHOD TO SOLVE FREDHOLM INTEGRO DIFFERENTIAL EQUATION

B. M. Pandya[1], D. C. Joshi[2]

[1]Asst. Prof., Dept.of Applied Mathematics, Sardar Vallabhbhai Patel Institute of Technology, Vasad
[2]Asst. Prof., Dept.of Mathematics,Veer Narmad South Gujarat University, Surat, Gujarat, India.
E-mail: pandyabhavini@gmail.com[1], dilip_joshi2002@yahoo.co.in[2]

Abstract— In this paper, a new approach to solve Fredholm integro differential equation has been introduced. Quartic Legendre spline collocation technique is used to solve Fredholm integro differential equation. Using this novel approach we have tried to achieve more accuracy compare to other traditional methods. Using the prescribed method the solution of this problem is reduce to a linear system of equations. The results demonstrate the applicability and accuracy of the technique.

Index Terms— Quartic Legendre polynomial, spline collocation, Integro differential equation

I. INTRODUCTION

Integro differential equations appears in various physical problems in sciences and engineering. It can be find useful in a wide range of application fields such as Computer graphics, Image processing, Biological problems and financial problems. Therefore, their numerical solutions are very useful to analyse the problems related to various fields. But it is usually becomes difficult to solve Integro differential equations analytically so there is an always a need to find an approximate solution which may be efficient and accurate.

Many attempt has been done to solve integro differential equations before, like Homotopy perturbation methods [1], [2], New Homotopy Analysis method (NHAM) [3], Wavelet-Galerkin method [4], Differential transform method(DTM) [5], Adomain decomposition method [6], CAS wavelets method [7], Sine-Cosine wavelets [2].

Spline function is very useful function in getting smoother approximations of a various problems of engineering and higher mathematics. It has a good ability of approximation. Various authors has been used spline function since last decade for solving differential equation, integral equation, integro differential equation, partial differential equation and fractional differential equation.

There is not a well expressed orthogonal basis in spline space to date [8]. Here we have constructed an orthogonal basis for the nth degree spline space with the help of Legendre polynomial. Hence we have extended idea of using Legendre spline function instead of spline function for approximating solution of second order integro differential equations of the form:

$$y''(x) + y'(x) + f(x)y(x) +$$
$$\lambda \int_a^b k(x,s)y(s)ds = g(x), \quad y(a) = y_0 \qquad (1.1)$$

where the functions f(x), g(x) and k(x, s) are sufficiently smooth real valued functions.

The remainder of this paper is organized as follows: In Section 2, we describe the basic formulation of Quartic Legendre spline collocation method required for our subsequent development. In section 3 description of the method is given and Section 4 is devoted to the applicability and accuracy of propose method by considering numerical examples. Also a conclusion is given in the last Section.

II. QUARTIC LEGENDRE SPLINE POLYNOMIAL

Let u(x) be a function defined on an interval [a, b] and $\Delta: a = x_0 < x_1 < \cdots \ldots \ldots < x_N = b,$ be

a given partition of the interval [a, b]. Each point x_i (i = 0 (1) N) is also called a knot or node, for the space of spline functions.

A polynomial function $s(x) \in C^2[a, b]$, which interpolates u(x) at the mesh points x_i, $i = 0(1)N$ is called a Quartic Legendre spline, if it coincides with a Quartic Legendre polynomial $s_i(x)$ in each subinterval $[x_i, x_{i+1}]$. Let u_i be an approximation to $u(x_i)$ obtained by a segment $s_i(x)$ passing through points (x_i, u_i) and (x_{i+1}, u_{i+1})

For each segment $[x_i, x_{i+1}]$, $s_i(x)$ has the following form

$$s_i(x) = \frac{1}{8}a_i[35(x-x_i)^4 - 30(x-x_i)^2 + 3]$$
$$+ \frac{1}{2}b_i[5(x-x_i)^3 - 3(x-x_i)] + \frac{1}{2}c_i[3(x-x_i)^2 - 1]$$
$$+ d_i(x-x_i) + e_i$$

Where, $s_i(x_i) = y_i$, $s_i(x_{i+1}) = y_{i+1}$, $s_i''(x_i) = M_i$, $s_i''(x_{i+1}) = M_{i+1}$, $s_i'''(x_i) = F_i$, $s_i'''(x_{i+1}) = F_{i+1}$ and $s_i^{iv}(x_i) = \frac{F_i + F_{i+1}}{2}$

$$a_i = \frac{F_i + F_{i+1}}{210}$$

$$b_i = \frac{M_{i+1} - M_i}{15h} - \frac{h}{60}(F_{i+1} + F_i)$$

$$c_i = \frac{M_i}{3} + \frac{F_{i+1} + F_i}{84}$$

$$d_i = \frac{1}{h}(y_{i+1} - y_i) + \frac{h^3}{48}(F_{i+1} + F_i) - \frac{h}{6}M_{i+1}$$
$$- \frac{h}{3}M_i + \frac{M_{i+1}}{10h} + \frac{M_i}{10h} + \frac{h}{40}(F_{i+1} + F_i)$$

$$e_i = y_i + \frac{1}{6}M_i + \frac{1}{240}(F_{i+1} + F_i)$$

III. DESCRIPTION OF THE METHOD

To develop the Quartic Legendre spline collocation method for solving the integro-differential equation (1.1) the interval [a, b] is divided into n equal subintervals using the grids i = 0, 1, …… ,n where $h = \frac{b-a}{n}$, the Quartic Legendre Spline S(x) interpolating the functions y(x) at the grid points is given by the equation

$$s_i(x) = \frac{F_{i+1} + F_i}{48}(x-x_i)^4$$
$$+ \left(\frac{M_{i+1} - M_i}{6h} - \frac{h}{24}(F_{i+1} + F_i)\right)(x-x_i)^3$$
$$+ \frac{M_i}{2}(x-x_i)^2$$

$$+ \left[\frac{h^3}{48}(F_{i+1} + F_i) - \frac{h}{6}(M_{i+1} + 2M_i) + \frac{1}{h}(y_{i+1} - y_i)\right](x - x_i)$$
$$+ y_i \tag{3.1}$$

Where $M_i = s''(x_i)$ and $y_i = y(x_i)$. The unknown derivative M_i are related by enforcing the continuity condition on $s'(x)$. Differentiating (3.1), we obtain

$$s_i'(x) = \frac{F_{i+1} + F_i}{12}(x-x_i)^3$$
$$+ \left(\frac{M_{i+1} - M_i}{2h} - \frac{h}{8}(F_{i+1} + F_i)\right)(x-x_i)^2$$
$$+ M_i(x-x_i)$$
$$+ \left[\frac{h^3}{48}(F_{i+1} + F_i) - \frac{h}{6}(M_{i+1} + 2M_i) + \frac{1}{h}(y_{i+1} - y_i)\right] \tag{3.2}$$

$$s_i''(x) = \frac{F_{i+1} + F_i}{4}(x-x_i)^2$$
$$+ \left(\frac{M_{i+1} - M_i}{h} - \frac{h}{4}(F_{i+1} + F_i)\right)(x - x_i) + M_i \tag{3.3}$$

$$s_i'''(x) = \frac{F_{i+1} + F_i}{2}(x - x_i)$$
$$+ \left(\frac{M_{i+1} - M_i}{h} - \frac{h}{4}(F_{i+1} + F_i)\right) \tag{3.4}$$

We obtain one sided limits of the derivative from (3.2) as

$$s_i'(x_i^-) = \left[\begin{array}{c} -\frac{h^3}{48}(F_i + F_{i-1}) \\ + \frac{h}{6}(2M_i + M_{i-1}) \\ + \frac{1}{h}(y_i - y_{i-1}) \end{array}\right], i = 1,2,…,n \tag{3.5}$$

$$s_i'(x_i^+) = \frac{h^3}{48}(F_{i+1} + F_i) - \frac{h}{6}(M_{i+1} + 2M_i)$$
$$+ \frac{1}{h}(y_{i+1} - y_i), i = 0,1,2,……,n-1 \tag{3.6}$$

Similarly we obtain from equation (3.3) that
$$s_i''(x_i^-) = [M_i], \quad i = 1,2,……,n \tag{3.7}$$
And
$$s_i''(x_i^+) = [M_i], \quad i = 0,1,……,n-1 \tag{3.8}$$
Also from equation (3.4) we obtain
$$s_i'''(x_i^-) = \frac{M_i - M_{i-1}}{h} + \frac{h}{4}(F_i + F_{i-1}),$$

$$i = 1,2,……,n \tag{3.9}$$
and

$$s_i'''(x_i^+) = \left(\frac{M_{i+1}-M_i}{h} - \frac{h}{4}(F_{i+1}+F_i)\right),$$
$$i = 0,1,......,n-1 \qquad (3.10)$$

The continuity condition $s'(x_i^+) = s'(x_i^-)$ gives the consistency relation

$$M_{i+1} + 4M_i + M_{i-1} = \frac{6}{h^2}[y_{i+1} - 2y_i + y_{i-1}]$$
$$+ \frac{h^2}{6}[F_{i+1} + 2F_i + F_{i-1}],$$
$$i = 1(1)N-1 \qquad (3.11)$$

The continuity condition $s'''(x_i^+) = s'''(x_i^-)$ gives the consistency relation

$$M_{i+1} - 2M_i + M_{i-1} = \frac{h^2}{4}[F_{i+1} + 2F_i + F_{i-1}],$$
$$i = 1(1)N-1 \qquad (3.12)$$

Now we collocate equation (1.1) at the uniform grid points $x_i = x_0 + ih$, $i = 0,1,......,n$ with $x_0 = a$ and $x_n = b$

Thus (1.1) becomes

$$y''(x_i) + y'(x_i) + f(x_i)y(x_i)$$
$$+\lambda \sum_{j=0}^{n-1} \int_{s_j}^{s_{j+1}} k(x_i,s)y(s)ds = g(x_i), \quad i = 0,1,......,n$$

Using equation (3.1) it can be written as

$$y''(x_i) + y'(x_i) + f(x_i)y(x_i)$$
$$\lambda \sum_{j=0}^{n-1} \int_{s_j}^{s_{j+1}} k(x_i,s)\left\{ \begin{array}{l} \frac{F_{j+1}+F_j}{48}(s-s_j)^4 \\ +\left(\frac{M_{j+1}-M_j}{6h}\right)(s-s_j)^3 \\ \quad -\frac{h}{24}(F_{j+1}+F_j)\right) \\ +\frac{M_j}{2}(s-s_j)^2 \\ +\left[\frac{h^3}{48}(F_{j+1}+F_j)\right. \\ \left. +\frac{h}{6}(M_{j+1}+2M_j)\right](s-s_j) \\ +\frac{1}{h}(y_{j+1}-y_j) \\ +y_j \end{array} \right\} ds$$
$$= g(x_i), \quad i = 0,1,......,n$$

Now substituting $s = s_j + ph$ and simplifying

$$y''(x_i) + y'(x_i) + f(x_i)y(x_i)$$
$$+h\lambda \sum_{j=0}^{n-1} \int_0^1 k(x_i,s_j+ph)\left\{ \begin{array}{l} \left[\frac{F_{j+1}+F_j}{48}(h)^4\right. \\ \left. *(p^4-2p^3+p)\right] \\ +\frac{h^2}{6}(p^3-p)M_{j+1} \\ +\frac{h^2}{6}(-p^3+3p^2-2p)M_j \\ +py_{j+1}+(1-p)y_j \end{array} \right\} dp$$
$$= g(x_i), \quad i = 0,1,......,n$$

We now split above equation into two as

$$y''(x_0) + y'(x_0) + f(x_0)y(x_0)$$

$$+h\lambda \sum_{j=0}^{n-1} \int_0^1 k(x_0,s_j+ph)\left\{ \begin{array}{l} \left[\frac{F_{j+1}+F_j}{48}(h)^4\right. \\ \left. *(p^4-2p^3+p)\right] \\ +\frac{h^2}{6}(p^3-p)M_{j+1} \\ +\frac{h^2}{6}(-p^3+3p^2-2p)M_j \\ +py_{j+1}+(1-p)y_j \end{array} \right\} dp$$
$$= g(x_0) \qquad (3.13)$$

And

$$y''(x_i) + y'(x_i) + f(x_i)y(x_i)$$

$$+h\lambda \sum_{j=0}^{n-1} \int_0^1 k(x_i,s_j+ph)\left\{ \begin{array}{l} \left[\frac{F_{j+1}+F_j}{48}(h)^4\right. \\ \left. *(p^4-2p^3+p)\right] \\ +\frac{h^2}{6}(p^3-p)M_{j+1} \\ +\frac{h^2}{6}(-p^3+3p^2-2p)M_j \\ +py_{j+1}+(1-p)y_j \end{array} \right\} dp$$
$$= g(x_i), \quad i = 1,2,...,n \qquad (3.14)$$

Putting (3.6) and (3.8) for i = 0 in equation (3.13) we get

$$M_0 + \frac{h^3}{48}(F_1+F_0) - \frac{h}{6}(M_1+2M_0) + \frac{1}{h}(y_1-y_0) + f_0 y_0$$

$$+h\lambda \sum_{j=0}^{n-1} \int_0^1 k(x_0,s_j+ph)\left\{ \begin{array}{l} \left[\frac{F_{j+1}+F_j}{48}(h)^4\right. \\ \left. *(p^4-2p^3+p)\right] \\ +\frac{h^2}{6}(p^3-p)M_{j+1} \\ +\frac{h^2}{6}(-p^3+3p^2-2p)M_j \\ +py_{j+1}+(1-p)y_j \end{array} \right\} dp$$
$$= g(x_0) \qquad (3.15)$$

Similarly putting (3.5) and (3.7) in (3.15) we get

$$M_i - \frac{h^3}{48}(F_i+F_{i-1}) + \frac{h}{6}(M_i+2M_{i-1})$$
$$+\frac{1}{h}(y_i-y_{i-1}) + f_i y_i$$

$$+h\lambda \sum_{j=0}^{n-1} \int_0^1 k(x_i,s_j+ph)\left\{ \begin{array}{l} \left[\frac{F_{j+1}+F_j}{48}(h)^4\right. \\ \left. *(p^4-2p^3+p)\right] \\ +\frac{h^2}{6}(p^3-p)M_{j+1} \\ +\frac{h^2}{6}(-p^3+3p^2-2p)M_j \\ +py_{j+1}+(1-p)y_j \end{array} \right\} dp$$
$$= g(x_i), \quad i = 1,...,n \qquad (3.16)$$

Using equations (3.15) and (3.16) together with equation (3.11) and (3.12) consists of 2n+1 equations with 4(n) +1 unknowns

$$y_i, M_i, \text{ and } F_i \quad i = 0,1,......,n.$$

However, to determine the values of these unknowns, four more equations are required. These equations are obtained by using the initial condition of equation (1.1) and by imposing a free boundary conditions given below

$F_0 = 0$ And $F_2 = 0$ (3.17)

IV. NUMERICAL EXPERIMENT

In this section the propose method described in section 3 is applied to some examples of second order integro differential equations. All computations are carried out by using MATLAB.

Example 4.1: Consider the following IDE [N. Ebrahimi et al (2014)[11]], H.M.Jaradat et al (2009)[12], Ahmet Yildirim (2009)[13]]

$$y''(x) = e^x - x + \int_0^1 xty(t)dt; \; y(0) = 1, y'(0) = 1 \qquad (4.1)$$

Solution:

Using the Quartic LSC method and with the help of equations (3.11), (3.12) and $F_0 = 0$, $F_2 = 0$, equation (4.1) is reduce to system of equations and which are being solved using gauss elimination method gives the unknowns

$M_1 = 2.3415 \; M_2 = 2.1761$
$F_1 = -12.0556 \; y_1 = 1.6409 \; y_2 = 2.7156$

Repeat the same process for h = 1/3, we get the following values of unknowns
M1=1.4005; F1=3.0840; F2=-0.2314; M0=1.3382; M2=1.9575; M3=2.7329; u1=1.4080; u2=1.9793; u3=2.7715

Table (I a) presents the comparison of solution of our method with the exact solution and Table (I b) presents the comparison of absolute error of our method with the method implemented in [11].

I a: Quartic LSC solution of second order Fredholm IDE (4.1)

x:	Quartic LSC solution : h=1/2	Quartic LSC Solution : h=1/3	Exact Solution : y(x)=e^x
0	1	1	1
0.1	1.0942	1.1066	1.1052
0.2	1.2002	1.2265	1.2214
0.3	1.3193	1.3496	1.3499
0.4	1.4522	1.5079	1.4918
0.5	1.6409	1.6494	1.6487
0.6	1.8075	1.8251	1.8221
0.7	1.9986	2.0173	2.0138
0.8	2.2147	2.2244	2.2255
0.9	2.4557	2.4501	2.4596
1.0	2.7210	2.7187	2.7183

I b: Absolute errors of Quartic LSC solution of Fredholm IDE (4.1)

x:	Absolute Error Quartic SLC: h=1/2	Absolute error Quartic SLC: h=1/3	Absolute Error : [11] N=10	Absolute Error : [11] N=30
0	0	0	0	0
0.1	1.1×10^{-2}	1.4×10^{-3}	4.39×10^{-6}	4.82×10^{-7}
0.2	2.1×10^{-2}	5.1×10^{-3}	1.81×10^{-5}	2.0×10^{-6}
0.3	3.06×10^{-2}	3.0×10^{-4}	4.24×10^{-5}	4.69×10^{-6}
0.4	3.96×10^{-2}	1.61×10^{-2}	7.83×10^{-5}	8.67×10^{-6}
0.5	7.8×10^{-3}	7.0×10^{-4}	1.27×10^{-4}	1.41×10^{-5}
0.6	1.46×10^{-2}	3.0×10^{-3}	1.91×10^{-4}	2.11×10^{-5}
0.7	1.52×10^{-2}	3.5×10^{-3}	2.70×10^{-4}	2.99×10^{-5}
0.8	1.08×10^{-2}	1.1×10^{-3}	3.67×10^{-4}	4.07×10^{-5}
0.9	3.9×10^{-3}	9.5×10^{-3}	4.85×10^{-4}	5.37×10^{-5}
1.0	2.7×10^{-3}	4.0×10^{-4}	6.25×10^{-4}	6.91×10^{-5}
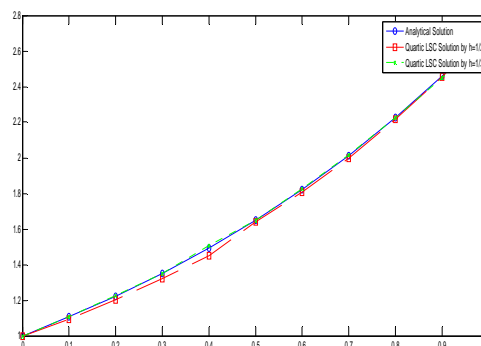
Fig. 4.1: A comparison of solutions of IDE (4.1)

Example 4.2: Consider the following IDE [A.A.Hemeda (2012)[14]]

$$y''(x) = 2 - \left(\frac{2x}{3}\right) + \int_0^1 xty'(t)dt; \; y(0) = 0, y'(0) = 0 \qquad (4.2)$$

Solution:
The collocation equations are

$$M_0 = 2$$

$$2F_1 - \frac{M_1}{12} - \frac{M_0}{6} = 0$$

$$\frac{755M_0}{1536} + \frac{F_1}{7680} + \frac{F_3}{15360} + \frac{F_6}{15360} + \frac{187M_1}{384} + \frac{17M_2}{1536} + \frac{y_1}{4} - \frac{3y_2}{8} = \frac{5}{3}$$

$$-\frac{13M_0}{768}+\frac{F_1}{3840}+\frac{F_3}{7680}+\frac{F_0}{7680}+\frac{91M_1}{192}+\frac{401M_2}{768}+\frac{y_1}{2}-\frac{3y_2}{4}=\frac{4}{3}$$

We get the unknowns as

$$M_1=2 \quad M_2=2 \quad F_1=0 \quad y_1=0.25 \quad y_2=1.0$$

And solutions are shown in the following table

II: Quartic LSC solution of second order Fredholm IDE (4.2)

x:	Quartic LSC Solution:	Exact Solution: x^2
0	0	0
0.1	0.01	0.01
0.2	0.04	0.04
0.3	0.09	0.09
0.4	0.16	0.16
0.5	0.25	0.25
0.6	0.36	0.36
0.7	0.49	0.49
0.8	0.64	0.64
0.9	0.81	0.81
1.0	1	1

REFERENCES

[1] Bush, A.W. 1992. Perturbation methods for engineers and scientists. Library of engineering Mathematics. CRC Press Boca Raton Florida.

[2] Tavassoli, M.K., Ghasemi. M. and Babolian, E., 2007, Comparison between Homotopy perturbation method and Sine-Cosine wavelets method for solving linear integro-differential equations. Int. J. Comput. Math. Appl., 54, 1162-1168

[3] Taiwo, O.A., Adewumi, A.O. and Raji, R.A., 2012, Application of new homotopy analysis method for first and second orders integro-differential equations. Int.J. Sci. Tech., 2(5), 328-332.

[4] Avudainayagam, A. and Vani, C., 2000, Wavelet-Galerkin method for integro-differential equations. Appl. Numer. Math., 32, 247–254.

[5] Darania, P. and Ebadian, A., 2007, A method for the numerical solution of the integro differential equations. Appl. Math. and Comput., 188, 657-668.

[6] El-Sayed, S.M. and Abdel-Aziz, M.R., 2003, A comparison of Adomian's decomposition method and Wavelet-Galerkin method for solving integro-differential equations. Appl. Math. Comput. 136, 151–159.

[7] Han, D.F. and Shang, X.F., 2007, Numerical solution of integro-differential equations by using CAS wavelet operational matrix of integration. Appl. Math. Comp. 194, 460 –466.

[8] Youngwei wei, Guozhao wang, ping yang, Legendre like Orthogonal basis for spline space, Science direct, Computer aided design 45(2013) 85-92.

[9] N.Parandin and S.Chenari and S.Heidari, (2013), A Numerical Method for Solving Linear Fredholm Integro – Differential Equations of the First Order, Journal of Basic and Applied Scientific Research 3(1s)192-195, ISSN 2090-4304

[10] H. H. Omran, (2009), Numerical methods for solving the first order linear Fredholm volterra integro differential equation, Journal of Al-Nahrain University Vol.12 (3), September, , pp.139-143, Science direct.

[11] N. Ebrahimia,∗ and J. Rashidiniaa, (2014), Spline Collocation for Fredholm and Volterra Integro-Differential Equations, International Journal of Mathematical Modelling & Computations Vol. 04, No. 03, 289- 298.

[12] H. M. Jaradat, Fadi Awawde, O. Alsayyed, (2009), Series solution to the high-order integro differential equations, Analele Universitˇaˏtii Oradea Fasc. Mathematica, Tom, 247–257.

[13] Ahmet Yildirim, (2010), Application of He's Variational Iteration Method to Nonlinear Integro-Differential Equations, Z. Nature for sch. 65a, 418–422.

[14] A. A. Hemeda, (2012), New Iterative Method: Application to nth-Order Integro-Differential Equations, International Mathematical Forum, Vol. 7, , no. 47, 2317 – 2332.

DESCRIBING AND VERIFYING WEB SERVICES COMPOSITION USING PI-CALCULUS

Saurabh Agrawal[1], Sumit Tiwari[2], Sumit Pathak[3]
[1,2]P. G. Scholar, CSE Dept., SRCEM Banmore,(M.P.) India
[3]Asst. Prof., Department of Computer Science,IPS-CTM Gwalior, India
Email: toc.saurabh@gmail.com[1], sumitgwalior23@gmail.com[2], sumitpathakcs@gmail.com[3]

ABSTRACT

This paper introduces a formal method for describing and verifying web services composition using Pi-Calculus. Web services are the basic unit of service oriented architecture (SOA). They are software applications that are implemented and published by web service providers and invoked by web service requesters over a network. The main purpose of web service technologies is to allow applications on different platforms to exchange business data. One of the ad-vantages of service oriented architecture is web services composition; we can compose existing web services to create new web services. In agent based web services composition, agent accepts request from web service consumers and searches Universal description and discovery (UDDI) registry against the requirements of the consumer to find appropriate web services. By using in-formation provided by UDDI, agent invokes those web services. So this composition frees the web service requester to search the UDDI registry for required web services and then manually invoke those services. Before implementing a web services composition, it should be verified for correctness to improve the reliability. Formal methods are mathematical based techniques used for specification and verification of software systems. Pi-Calculus is a kind of process algebra which is used to model concurrent systems with mobility. In this work, we have formally described web services composition using Pi-Calculus. For verification we have used mobility workbench (MWB) tool.

Key Words: Web Services Composition, Mobility Workbench, Universal description and discovery (UDDI).

1. INTRODUCTION

Web services are the programs that can be accessed over internet. Web services are platform and language independent, they can use any operating system and programming language. The main components of web service architecture are service provider, service requester and service registry. Service provider implements web services and publishes information required to access those services. Service registry (also called UDDI registry) is used to store this information, any service requester can find information to access a particular web service from this registry. Reusability is one of the advantages of web services. We can compose two or more web services which already exist; it reduces the efforts of implementing new web services. Sometimes it is necessary to compose two or more web services because a single service is not sufficient for some complex applications.

Every web services composition algorithm should be validated before implementation for its correctness. We have used Pi-Calculus [4] for describing and modeling web service composition; for verification process we have used MWB [6].

2. RELATED WORK

In recent years several methods have been used to model web service composition. CCS [7] is used to model concurrent systems, but it cannot be used for mobility. In [8], the method used is based on partial-order planning problems and

uses first-order logic. In this method predicates are used to define every process specification of WSCDL, then these predicates are written in Prolog tool for verification. In [9], a method based on temporal logic of actions (TLA) is proposed. Web services are modeled as automata and described using TLA, then verified using TCL (a model checker of TLA). In [10], FSM (finite state automata) is used to describe the web service composition and it is translated into programs described by Promela and finally verified using model checking tool SPIN. In [11], Colored petri-nets(CPN) is used, it is similar to Petri-nets with an extra advantage that has programmable elements.

We have used Pi-calculus, it is used to model concurrent systems with mobility. In pi-calculus communication links are transferred as names.

3. ONLINE MOVIE TICKET BOOKING EXAMPLE

a. Description of web services composition

We have taken an example of movie ticket booking service to describe the web services composition. The services used in this example are Client service, web service composition agent (WSCA), Registry service, Bank service and Multiplex service. Web service composition agent (WSCA) service accepts request from client service and searches the services which are required to fulfill the request in the Registry. If the required services found in registry then WSCA asks information from client, and with this information it invokes the multiplex service, otherwise it sends a refuse message to client. If required seats are available then Multiplex service invokes Bank service otherwise it sends a message to WSCA indicating that seats are not available, which is sent to client by WSCA. In case seats are available, Bank service sends a message to client for payment. When the amount is paid by client, Bank confirms by sending a message to multiplex service and Multiplex service sends this confirmation to WSCA, eventually which is sent to client.

The messages are described as follows:

Publish_Multiplex (Pub_M) : Multiplex service publishes itself into Registry.

Publish_Bank (Pub_B) : Bank service publishes itself into Request Registry.

(req) : Ticket booking request from Client.

Search : message from WSCA to Registry for searching the required services.

msg : message from registry to WSCA that the services are found or not.

Ask_Info (ask) : WSCA asks the requirement of client.

Provide_Info (pro) : Client provides the detailed information such as name of Movie, date and number of seats etc.

Invoke_Multiplex (Inv_M) : WSCA invokes multiplex service with information provided by client.

Invoke_Bank (Inv_B) : Multiplex service invokes Bank service.

Inform_pay (Inf_pay) : Bank service sends a message to client for paying the required amount.

Pay : Client pays the required amount.

Pay_succsess (pay_succ) : Bank service informs multiplex service that payment has received.

Confirmation_Multiplex (Conf_M) : Multiplex service sends   confirmation to WSCA.

Confirmation_WSCA (Conf_WSCA) : WSCA sends confirmation to Client.

Refuse (ref): WSCA sends this message to client when the required services to fulfill the request are not available in   -registry.

Not_Available (not_av): Multiplex service sends this message to WSCA when required seats are not available, which is sent to client.
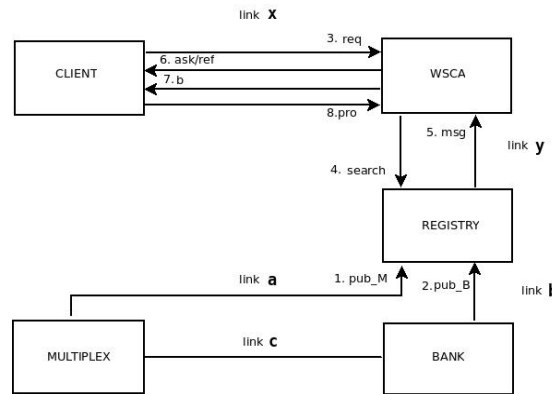
Figure 1: Web services composition model for online movie ticket booking system

The description of different agents in pi-calculus is Given as follows :

Bank(b,c)$\overline{b}$ pub_B.c   (inv_B).$\overline{b}$ inf_pay.b(pay). $\overline{c}$ pay_succ.Bank (b,c)

Multiplex(a,c)=$\overline{a}$ pub_M.a(msg).([msg=inv_M] $\overline{a}$ not_av.Multiplex(a,c)+[msg=inv_M]$\overline{c}$ inv_B.c(pay_succ).$\overline{a}$ conf_M.Multiplex(a,c))

Registry(a,b,y)=a(pub_M).b(pub_B).y(search).

$\bar{y}$ msg. $\bar{y}$ a. $\bar{y}$ b.Registry(a,b,y)

Client(x,a)= $\bar{x}$ req.x(msg1).([msg1=ask]x(b). $\bar{x}$ pro.x(msg2).([msg2=not_av]0+b(inf_pay). $\bar{b}$ pay.x(conf_WSCA).Client(x,a)) + [msg1=ref]0)

WSCA(x,y,a)=x(req). $\bar{y}$ search.y(msg1).([msg1=found]y(a).y(b). $\bar{x}$ ask. $\bar{x}$ b.x(pro). $\bar{a}$ inv.a(msg2).([msg2=not_av] $\bar{x}$ not_av.WSCA(x,y,a)+[msg2=conf_M] $\bar{x}$ conf_WSCA.WSCA(x,y,z))+[msg1=not_found] $\bar{x}$ ref.WSCA(x,y,a))

b. Verification of web services composition.
The MWB code for different agents is given as follows:
agent
Bank(b,pub_B,c,inv_B,inf_pay,pay,pay_succ)= 'b<pub_B>.c
(nv_B).'b(inf_pay).b(pay).'c<pay_succ>.Bank< b,pub_B,c,inv_B,inf_pay,pay,pay_succ>
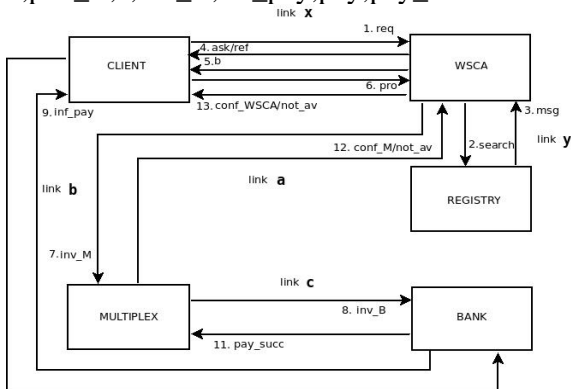
Figure 2: Web services composition model for online movie ticket booking system after transfer of link 'a' and 'b'.
agent
Multiplex(a,pub_M,msg,inv_M,not_av,c,inv_B, conf_M,pay_succ)='a<pub_M>.a(msg).([msg=i nv_M]'a<not_av>.Multiplex<a,pub_M,msg,inv _M,not_av,c,inv_B,conf_M,pay_succ>+[msg=i nv_M]'c<inv_B>.c(pay_succ).'a<conf_M>.Mul tiplex<a,pub_M,msg,inv_M,not_av,c,inv_B,con f_M,pay_succ>)

agent
Registry(a,pub_M,b,pub_B,y,search,msg)=a(pu b_M).b(pub_B)y(search).
'y<msg>.'y<a>.'y<b>.Registry<a,pub_M,b,pub _B,y,search,msg>

agent
Client(x,req,msg1,ask,b,pro,msg2,not_av,inf_pa

y,pay,conf_WSCA,ref)='x<req>.x(msg1).([msg 1=ask]x(b).'x<pro>.x(msg2).([msg2=not_av]0+ b(inf_pay).'b<pay>.x(conf_WSCA).Client<x,re q,msg1,ask,b,pro,msg2,not_av,inf_pay,pay,conf _WSCA,ref>)+[msg1=ref]0)
agent
WSCA(req,y,search,msg1,found,ask,b,pro,a,inv _M,msg2,not_av,
conf_WSCA,not_found,ref)=x(req).'y<search>. y(msg1).([msg1=found]y(a).y(b).'x<ask>.'x<b >.x(pro).'a<inv_M>.a(msg2).([msg2=not_av]'x <not_av>.WSCA<req,y,search,msg1,found,ask, b,pro,a,inv_M,msg2,not_av,conf_WSCA,not_fo und,ref>+[msg2=conf_M]'x<conf_WSCA>.W SCA<req,y,search,msg1,found,ask,b,pro,a,inv_ M,msg2,not_av,conf_WSCA,not_found,ref>)+[msg1=not_found]'x<ref>.WSCA<req,y,search, msg1,found,ask,b,pro,a,inv_M,msg2,not_av,con f_WSCA,not_found,ref>)

In verification process, we have checked deadlocks for different agents, it ensures the correctness of web services composition algorithm.

4. ONLINE BOOK PURCHASE SYSTEM
a. Description of web service composition
The services used by this system are client service, Book shop service, Database service and Delivery service (fig. 3). Here x and w are communication links of Client service with Book shop service and Delivery service, respectively. Similarly, y and z are communication links of Book shop service with Database service and delivery service respectively.

First, Client service sends a request to Book Shop service for purchasing a book by specifying required information such as name of book and authors name. Book shop service then sends a lookup message to database service whether the requested book is available or not. Database service sends a message to Book Shop service based on avail-ability of that book.
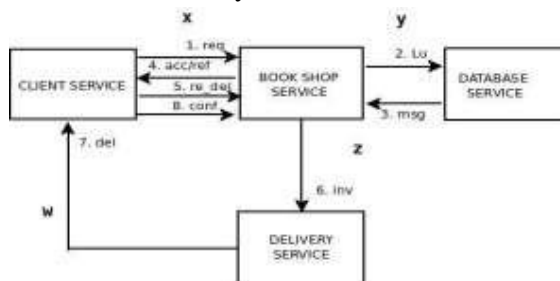
Now Book Shop service replies to Client service about the requested book by sending accept or refuse message. If book is available then it sends accept message otherwise sends refuse message. Now Client service confirms its request by sending a request de-livery message. This message contains information about client i.e. address and phone number etc. After receiving this message, Book Shop service invokes delivery service with appropriate information. Delivery service then delivers the book to client and client sends a confirmation message to Book Shop service. For simplicity, we assumed that amount for book is paid at the time of delivery i.e. in person.

The various messages used in this system are described as follows :

req : Client service requests for a book.

Lu : Book Shop service sends this message to Database service to check the avail-ability of that book.

msg : Database service sends availability information to Book Shop service.

acc : Book Shop service sends this message to client service if book is available.

ref : Book Shop service sends this message to client service if book is not available.

req del : Client confirms its request by sending its information such as address and phone number etc.

inv : Book Shop Service invokes delivery service.

del : Delivery service delivers the required book to client.

conf : Client service sends confirmation to Book Shop Service.

The description of different agents in pi-calculus is given as follows:

Client service : $CS(x,w) = xreq.x(msg)$.
([msg=acc] xdel
book. w(del).x conf.$CS(x,w)$ +
[msg=ref]0)$BSS(x,y,z)$ +
[msg=not found]zref.$BSS(x,y,z)$)

Delivery service : $DS(z,w) = z(inv):wdel.DS(z,w)$

Database service : $DBS(y) = y(lu):ymsg.DBS(y)$

Composite Web service = $(CSjBSSjDSjDBS)$

b. Verification of web service composition

The MWB code for different agents is given as follows :

agent $CS(x; req; msg; acc; del book; del; conf; ref) =^0 x < req > :x(msg):([msg = acc]^0 x < del book > :w(del):x < conf > :CS < x; req; msg; acc; Del book; del; conf; ref> +[msg = ref]0)$ agent $BSS(x; req; y; lu; msg; found; acc; req del; z; inv; conf; not found; ref) = x(req):^0 y < lu > :y(msg):([msg = found]x < acc > :x(req_ddel):^0 z < inv > :x(conf):BSS < x; req; y; lu; msg; found; acc; req del; z; inv; conf; not found; ref > +[msg = not found]^0 x < ref > :BSS < x; req; y; lu; msg; found; acc; req del; z; inv; conf; not found; ref >)$ agent $DS(z; inv; w; del) = z(inv):^0 w < del > :DS < z; inv; w; del >$ agent $DBS(y; lu; msg) = y(lu):^0 y < msg > :DBS < y; lu; msg >$

In verification process, we have checked deadlocks for different agents through MWB, it ensures the correctness of web services composition algorithm.

5. CONCLUSION

Formal description and verification is necessary before implementing a web service composition algorithm because it ensures the correct working of composition i.e. there is no deadlock. Online movie ticket booking example is used to show the modeling process. The Pi calculus is useful to describe formally this system and the concurrent actions of the processes. This paper describes the model using formal approach Pi calculus and checks correctness of model with the help of MWB.

REFERENCES

[1] Pat. P.W. Chan, Michael R. Lyu, Dynamic Web service composition : A new approach in building reliable web services, 22nd international conference on Advance information networking and applications, 2008.

[2] Snehit Prabhu, Towards distributed dynamic web service composition, eighth international symposium on autonomous decentralized systems(ISADS'07), 2007.

[3] R. Miler, The polyadic pi-calculus : a tutorial, research report ECS-LFCS-91-180. University of Edinburgh, October 1991.

[4] J. Parrow, An introduction to the pi-calculus, Dep. Teleinformaties, Royal institute of technology, Stockholm.

[5]   R. Milner, J. Parrow and D. Walker, A calculus of mobile process(part 1 and 2), Journal of information and computing, 100:1-77, September 1992.

[6]   Bjorn Victor and Faron Moller, The Mobility Workbench : A tool for the pi-calculus, Uppsala University and University of Edinburgh, February 1994.

[7]   Li Bao, Weishi Zhang, Xiuguo Zhang , Describing and verifying web services using CCS, proceedings of the seventh international conference on parallel and distributed computing, applications and technologies, 2006.

[8] Zahra Madani, Naser Nematbakhsh, A logical formal model for verification of web service choreography, Twelfth international conference on computer and information technology, December, 2009.

[9] Hongbing Wang, Chen Wang, Yan Liu, A logic based approach to web service composition and verification, Second world conference on services, 2009.

[10]   Zhao Wei, Rongsheng Dong, Xiangyu Luo, Fang Liu, Model checking Airline tickets reservation system based on BPEL, third international conference on genetic and evolutionary computing, 2009.

A REVIEW ON PREDICTING STUDENT PERFORMANCE USING DATA MINING METHOD

Karunendra Verma[1], Arjun Singh[2], Purushottam Verma[3]
[1]PhD-Scholor, CSE Dept., SPSU Udaipur(Raj.)
[2]Asst. Professor, CSE Dept., SPSU, Udaipur(Raj.)
[3]Asst. Professor, CSE Dept., IPS-CTM, Gwlalior (M.P.)
Email: k.verma2006@gmail.com[1], arjun.singh@spsu.ac.in[2], puruverma22@gmail.com[3]

Abstract:
"Data mining methods are often implemented for analyzing available data and extracting Information and knowledge to support decision-making. This review paper is aimed at revealing the high potential of data mining applications for university management benefits."

Introduction:

Now a days Universities are operating in a very complex and highly competitive environment. The main challenge for modern universities is to deeply analyze their performance, to identify their uniqueness and to build a strategy for further development and future actions.

University management should focus more on the profile of admitted students, getting aware of the different types and specific students' characteristics based on the received data. They should also consider if they have all the data needed to analyze the students at the entry point of the university or they need other data to help the managers support their decisions as how to organize the marketing campaign and approach the promising potential students.

This paper is focused on the implementation of data mining techniques and methods for acquiring new knowledge from data collected by universities. The main goal of the paper is to reveal the high potential of data mining applications for university management.

The specific objective of the proposed research work is to find out if there are any patterns in the available data that could be useful for predicting students' performance at the university based on their personal and pre-university characteristics.

The university management would like to know which features in the currently available data are the strongest predictors of university performance. They would also be interested in the data − is the collected data sufficient for making reliable predictions, is it necessary to make any changes in the data collection process and how to improve it, what other data to collect in order to increase the usability of the analysis results.

Review of literature:

The implementation of data mining methods and tools for analyzing data available at educational institutions, defined as Educational Data Mining (EDM) [15] is a relatively new stream in the data mining research. Extensive literature reviews of the EDM research field are provided by Romero and Ventura [15], covering the research efforts in the area between 1995 and 2005, and by Baker and Yacef [2], for the period after 2005.

The data mining project that is currently implemented at UNWE is focused on finding information in the existing data to support the university management in better knowing their students and performing more effective university marketing policy. The literature review reveals that these problems have been of interest for various researchers during the last few years. Luan discusses in [9] the potential applications of data mining in higher education and explains how data mining saves resources while maximizing efficiency in academics.

Understanding student types and targeted marketing based on data mining models are the research topics of several papers [1, 9, 10, 11].

The implementation of predictive modeling for maximizing student recruitment and retention is presented in the study of Noel-Levitz [13]. These problems are also discussed by DeLongetal [5]. The development of enrollment prediction models based on student admissions data by applying different data mining methods is the research focus of Nandeshwar and Chaudhari [12]. Dekkeretal. [6] focus on predicting students drop out.

Kovacicin [8] uses data mining techniques (feature selection and classification trees) to explore the socio-demographic variables (age, gender, ethnicity, education, work status, and disability) and study environment (course program and course block) that may influence persistence or dropout of students.

Ramaswami and Bhaskaran [14] focus on developing predictive data mining model to identify the slow learners and study the influence of the dominant factors on their academic performance, using the popular CHAID decision tree algorithm.

Yuetal[18] explore student retention by using classification trees, Multivariate Adaptive Regression Splines (MARS), and neural networks. Cortez and Silva [4] attempt to predict student failure by applying and comparing four data mining algorithms − Decision Tree, Random Forest, Neural Network and Support Vector Machine.

Kotsiantiset al. [7] apply five classification algorithms (Decision Tree, Perceptron-based Learning, Bayesian Net, Instance Based Learning and Rule-learning) to predict the performance of computer science students from distance learning.

Research Methodology:

In Data mining numbers of steps like Data Understanding, Data Preparation, Modeling, Evaluation and Deployment for finding consistent and reliable results.

The software tool that is used for the project implementation is the open source software WEKA, offering a wide range of classification methods for data mining [17].

During the "Data Preprocessing" Phase, student data from the two databases is extracted and organized in a new flat file. The preliminary research sample is provided by the university technical staff responsible for the data collection and maintenance, and includes data about 10330 students, described by 20 parameters, including gender, birth year, birth place, living place and country, type of previous education, profile and place of previous education, total score from previous education, university admittance year, admittance exam and achieved score, university specialty/direction, current semester, total university score, etc. The provided data is subjected to many transformations. Some of the parameters are removed, e.g., the birth place and the place of living fields containing data that is of no interest to the research.

The selected target variable in this case, or the concept to be learned by data mining algorithm, is the "student class". A categorical target variable is constructed based on the original numeric parameter university average score. It has five distinct values (categories) − "excellent", "very good", "good", "average" and "bad". The five categories (classes) of the target (class) variable are determined from the total university score achieved by the students.

During the "Modeling Phase", the methods for building a model that would classify the students into the five classes (categories), depending on their university performance and based on the student pre-university data, are considered and selected. Several different classification algorithms are applied during the performed research work, selected because they have potential to yield good results. Popular WEKA classifiers (with their default settings unless specified otherwise) are used in the experimental study, including a common decision tree algorithm C4.5 (J48), two Bayesian classifiers (NaiveBayes and BayesNet), a Nearest Neighbour algorithm (IBk) and two rule learners (OneR and JRip).

5. Achieved Results & Comparison:

Several different algorithms are applied for building the classification model, each of them using different classification techniques. The WEKA Explorer application is used at this stage

Class	NaiveBayes				BayesNet			
	10-fold Cross validation		Percentage split		10-fold Cross validation		Percentage split	
	TP Rate	Precision	TP Rate	Precision	TP Rate	Precision	TP Rate	Precision
Bad	0.821	0.791	0.835	0.804	0.817	0.813	0.835	0.819
Average	0.352	0.209	0.348	0.183	0.38	0.237	0.417	0.222
Good	0.521	0.644	0.545	0.649	0.598	0.626	0.597	0.633
V.Good	0.681	0.576	0.679	0.588	0.616	0.599	0.613	0.601
Excellent	0.184	0.277	0.14	0.268	0.237	0.312	0.199	0.264
Weighted Average	0.581	0.59	0.59	0.597	0.591	0.596	0.591	0.598

Table 1. Results for the Bayesian Classifiers

Class	J48 – 10-fold Cross validation		J48 – Percentage split	
	True Positive Rate	Precision	True Positive Rate	Precision
Bad	0.83	0.851	0.84	0.892
Average	0.081	0.384	0.096	0.344
Good	0.729	0.665	0.742	0.667
Very Good	0.69	0.639	0.687	0.646
Excellent	0.015	0.211	0.032	0.429
Weighted Average	0.659	0.631	0.666	0.648

Table 2. Results for the decision tree algorithm (J48)

Class	k-NN Classifier							
	k=100				k=250			
	10-fold Cross validation		Percentage split		10-fold Cross validation		Percentage split	
	TP Rate	Precision	TP Rate	Precision	TP Rate	Precision	TP Rate	Precision
Bad	0.358	0.944	0.335	0.972	0.154	1	0.078	1
Average	0	0	0	0	0	0	0	0
Good	0.662	0.614	0.69	0.617	0.626	0.602	0.651	0.598
Very Good	0.712	0.592	0.705	0.6	0.733	0.576	0.727	0.586
Excellent	0	0	0	0	0	0	0	0

| Weighted Average | 0.609 | 0.57 | 0.616 | 0.578 | 0.592 | 0.561 | 0.593 | 0.565 |

Table 3. Results for the k-NN Classifier

Class	OneR				JRip			
	10-fold Cross validation		Percentage split		10-fold Cross validation		Percentage split	
	TP Rate	Precision	TP Rate	Precision	TP Rate	Precision	TP Rate	Precision
Bad	0	0	0	0	0.823	0.845	0.738	0.776
Average	0	0	0	0	0.043	0.313	0	0
Good	0.688	0.545	0.689	0.542	0.731	0.618	0.744	0.615
Very Good	0.584	0.555	0.572	0.553	0.625	0.634	0.614	0.636
Excellent	0.006	0.15	0.032	0.214	0.082	0.506	0.081	0.375
Weighted Average	0.548	0.481	0.543	0.479	0.634	0.621	0.63	0.601

Table 4. Results for the rule learners

The results for the performance of the selected classification algorithms (TP rate percentage split test option) are summarized and presented on Fig. 1.
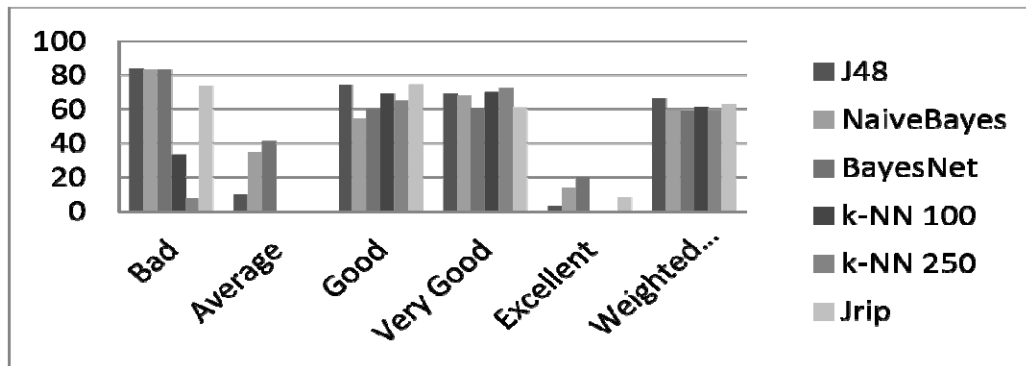
Fig. 1. Classification algorithms performance comparison

,

6. Conclusion:

The results achieved by applying selected data mining algorithms for classification on the university sample data reveal that the prediction rates are not remarkable (vary between 52-67 %). Moreover, the classifiers perform differently for the five classes. The data attributes related to the student's University Admission Score and Number of Failures at the first-year university exams are among the factors influencing most the classification process.

7. Future Work:

Using Association rule in mining we can find different relationship among the classes and predict the student performance and comparison can be done with the earlier results. To check whether accuracy is increased and prediction rate is up to the mark.

8. References:

1. Antons, C., E. Maltz. Expanding the Role of Institutional Research at Small Private Universities: A Case Study in Enrollment Management Using Data Mining. – New Directions for Institutional Research, Vol. 131, 2006, 69-81.
2. Baker, R., K. Yacef. The State of Educational Data Mining in 2009: A Review and Future Visions. – Journal of Educational Data Mining, Vol. 1, October 2009, Issue 1, 3-17.
3. Chapma n, P., et al. CRISP-DM 1.0: Step-by-Step Data Mining Guide 2000. SPSS Inc. CRISPWP-0800, 2000. http://www.spss.ch/upload/1107356429_Cri spDM1.0.pdf
4. Cortez, P., A. Silva. Using Data Mining to Predict Secondary School Student Performance.EUROSIS.A.Brito andJ.Teixeira,Eds.2008,5-12.
5. DeLong, C., P. Radclie, L. Gorny. Recruiting for Retention: Using Data Mining and Machine Learning to Leverage the Admissions Process for Improved Freshman Retention. – In: Proc. of the Nat. Symposium on Student Retention, 2007.
6. Dekker, G., M. Pechenizkiy, J. Vleeshouwer s. Predicting Students Drop Out: A Case Study. – In: Proceedings of 2nd International Conference on Educational Data Mining (EDM'09), 1-3 July 2009, Cordoba, Spain, 41-50.
7. Kotsiantis, S., C. Pierrakeas, P. Pintelas. Prediction of Student's Performance in Distance Learning Using Machine Learning Techniques. Applied Artificial Intelligence,Vol.18,2004,No5,411-426.
8. Kovaicic, Z. Early Prediction of Student Success: Mining Students Enrolment Data. – In: Proceedings of Informing Science & IT Education Conference (InSITE'2010), 2010, 647-665. Luan, J. Data Mining and Its Applications in Higher Education. – New Directions for Institutional Research, Special Issue Titled Knowledge Management: Building a Competitive Advantage in Higher Education, Vol. 2002, 2002, Issue 113, 17-36.
9. Luan, J. Data Mining and Its Applications in Higher Education. – New Directions for Institutional Research, Special Issue Titled Knowledge Management: Building a Competitive Advantage in Higher Education, Vol. 2002, 2002, Issue 113, 17-36.
10. Luan, J. Data Mining Applications in Higher Education. SPSS Executive Report. SPSS Inc., 2004. http://www.spss.ch/upload/1122641492_Dat a%20mining%20applications%20in%20hi gher%20education.pdf
11. Ma, Y., B. Liu, C. K. Wong, P. S. Yu, S. M. Lee. Targeting the Right Students Using Data Mining. – In: Proceedings of 6th ACM SIGKDD International Conference on Knowledge Discovery and Data Mining, Boston, 2000, 457-464. 12. Nandeshwar, A., S. Chaudhari. Enrollment Prediction Models Using Data Mining, 2009.
12. http://nandeshwar.info/wpcontent/uploa ds/2008/11/DMWVU_Project.pdf
13. Noel-Levitz. White Paper. Qualifying Enrollment Success: Maximizing Student Recruitment and Retention Through Predictive Modeling. Noel-Levitz, Inc., 2008. https://www.noellevitz.com/documents/shar ed/Papers_and_Research/2008/QualifyingE nrollmentSuccess08.pdf
14. Ramaswami, M., R. Bhaskaran. A CHAID Based Performance Prediction Model in Educational Data Mining. – IJCSI International Journal of Computer Science Issues, Vol. 7, January 2010, Issue 1, No 1, 10-18.
15. Romero, C., S. Ventura. Educational Data Mining: A Survey from 1995 to 2005. – Expert Systems with Applications, Vol. 33, 2007, 135-146.
16. Vandamme, J., N. Meskens, J. Superby. Predicting Academic Performance by Data Mining Methods. – Education Economics, Vol. 15, 2007, No 4, 405-419.
17. Witten, I., E. Frank. Data Mining: Practical Machine Learning Tools and

Techniques. Morgan Kaufmann Publishers, Elsevier Inc., 2005.

18. Yu, C., S. DiGangi, A. Jannasch-Pennell, C. Kaprolet. A Data Mining Approach for Identifying Predictors of Student Retention from Sophomore to Junior Year. – Journal of Data Science, Vol. 8, 2010, 307-325.

19. Kabakchieva, D., K. Stefanova, V. Kisimov. Analyzing University Data for Determining Student Profiles and Predicting Performance. – In: Proceedings of 4th International Conference on Educational Data Mining (EDM'2011), 6-8 July 2011, Eindhoven, The Netherlands, 347-348.

20. BULGARIAN ACADEMY OF SCIENCES CYBERNETICS AND INFORMATION TECHNOLOGIES • Volume 13, No 1 Sofia • 2013 Print ISSN: 1311-9702; Online ISSN: 1314-4081DOI: 10.2478/cait-2013-0006

FINITE ELEMENT ANALYSIS OF REINFORCED CONCRETE BEAM USING ANSYS

Pradeep singh[1], Abhishek Mishra[2], Arpit Kulshreshtha[3]

[1,2,3]PG Scholar, Dept. of Civil Engg., IPS College of Technology & Management, Gwalior –R.G.T.U, Bhopal

Email:pradeepkumar.imliya@gmail.com[1],abhimishra.mishra918@gmail.com[2], arpit@kulshreshtha.in[3]

ABSTRACT

Present paper here deals with simulation of concrete reinforced beams using ANSYS. Effect of different Fibre Reinforced Polymer will also be studied. The Fibre Reinforced Polymer (FRP) as an external reinforcement is used extensively to deal with the strength requirements related to flexure and shear in structural systems. Review of the published work has been conducted in the present paper. First the simple concrete beam will be modelled in ANSYS then the FRP material will be laminated over it. Effect of tension and various loading condition will be studied in the present paper.

Introduction

Upgrading of solid structures may be required for a wide range of reasons. The solid structures may have turned out to be fundamentally in sufficient for instance, because of material deterioration, poor configuration ordevelopment,maintenance absence, redesigning of outline burdens, for example, natural causes like earthquakes. ButGFRP and solid epoxy pastecan strengthenthe structures. Fundamentally the method includes giving extra layers of GFRP to concrete surfaces. These plates act compositely with the solid and increase the load carrying capacity. The utilization of GFRP to steel and solid structures has turned out to be progressively alluring because of the understood great mechanical properties of these materials. These properties aregood strength to density proportion, good corrosion resistance, less cost of maintenance and lessinstallation time with routine materials.

Failure criteria for FRP laminate

- Hashin Criteria for 2D developed in 1980
- Criteria for matrix failure under transverse compression
- Criteria for fibre failure under tension
- Criteria for fibre failure under compression
- Criterion for matrix damage in biaxial compression

Banu D. et al [1] studied the numerical modelling of two-way reinforced concrete slabs strengthen with carbon fibres reinforced polymer strips. They applied FRP as an external layer to the RC (Reinforced Concrete) beams. They have used ANSYS software to analysis the effect of FRP material as an external layer to see the effect of it on load carrying capacity. They have used SOLI65 element to model the 3D concrete beams while SOLID45 has been used to design the thick shells. They have conducted their results for load-deflection and ultimate carrying capacity.

Scordelis A.C. et al[2] studies finite element study of reinforced concrete beams with diagonal tension cracks.The most punctual production on the use of the limited component system to the investigation of RC structures was exhibited. In their study, basic shafts were examined with a model in which concrete and fortifying steel were spoken to by consistent strain triangular components, and an extraordinary bond join component was used to associate the steel to the solid and portray the bond slip impact. A direct flexible investigation was performed on shafts with predefined split examples to decide

essential hassles in solid, stresses in steel fortification and bon stresses.

Parandaman P. and Jayaram M.[3] studied the Finite element analysis of reinforced concrete beam retrofitted with different fibre composites.

- They have use Pro-E software for modelling and ANSYS for analysis the modelled geometry.
- The used carbon fibre reinforced polymer (CFRP) sheet for first layer of RC beam, glass fibre reinforcedpolymer (GFRP) sheet for second layer and Kevlar fibre reinforced polymer (KFRP) sheet for third layer.
- SOLID65 element for concrete beam and SOLID45 element for FRP has been used by them.
- They found that deflection has been minimized around 75% compared to the conventional RC beam when CFRP used.
- Deflection minimized around 65% when GFRP used and 60% when KFRP used.
- Load carrying capacity increases by using FRP laminates.
- Strength increases after using FRP laminates.

TaranuN. and Bejan L. [4] studied Mechanical modellingof composite ARMIDE cu fibre.From the assortment of strands used to make FRP materials the carbon filaments have been observed to be more suitable in understanding the composite strips utilized for the basic restoration of strengthened solid twisted components. The carbon filaments have high quality toweight what's more, solidness to-weight proportions, low warm dilatation coefficient, high weaknessresistance, substance inactivity, strength at high temperatures, high removal resistance, great warm conductivity, low thickness, and high strain quality. A few hindrances of this sort of fibre are low effect quality, high electric conductivity and high costs. Musmar M. A. et al [5] nonlinear finite element analysis of shallow reinforcedconcrete beams using solid65 element. They targeted their study towards the study of shallow reinforced concrete beam for transverse loading. SOLID65 eight node isotropic elements have been used to model the concrete beam. The analysis has been conducted using ANSYS. They concluded

- Cracking initially occurs in the vertical flexural from in the model.
- The cracking increases with increment in the load.

- The relationship between the load and deflection has been found to be linear elastic up to cracking moment strength then it inclines in horizontal plane.

Santhakumar R. and Chandrasekaran E. [6] analysed retrofitted reinforced concrete shearbeams using carbon fibre composites. They have studied the effect of CFRP on the concrete beam with fibre orientation of $45°$ and $90°$. A quarter part of the beam has been studied by them. They have compared their results with the experimental results available and found in good agreement. For un-cracked and pre-cracked beam at ultimate stage they found variation in the results but not large. They concluded that the numerical results help in tracking the formation and propagation of the crack which was not obtained by the experimental results because of the CFRP laminate sheets.

Ibrahim A. M. and Mahmood M. S. [7] finite element modelling of reinforced concrete beams strengthened with FRP laminates. They analysed the model for reinforced concrete beamsreinforced with fibre reinforced polymer (FRP) laminates using finite elementsmethod (FEM) adopted by ANSYS. The models have been establishedutilizing a smearedcracking method for concrete and 3D-layered elements for FRPcomposites. The results obtained have been matchedwith the experimental data for six beams with different conditions from researches. The results have been compared for load-deflectioncurves and failure load at mid length which are in good agreement. But the finite elements results found to be slightly stiffer than that from the experimental results. The maximum difference is 7.8% for all cases included in ultimate loads.

Robert R. S. and Prince A. G. [8] studied finite element modelling on behaviour of reinforced concrete beam-column joints retrofitted with carbon fibre reinforced polymer. The Finite element modelling (FEM) has turned to be recreating the physical conduct of complex building frameworks. The (FEA) programs have increased normal acknowledgment among architects in industry and analysts. The examination of retrofitted with carbon fibrereinforced polymer sheets (CFRP) utilizing ANSYS have been exhibited in this paper. Three different strengthened sheet of CPRF on solid shaft were displayed utilizing ANSYS. Both the

ends of the beam in investigation have been kept pivoted. Static load was connected at the free end of the cantilever bar. The analyses have been conducted for the retrofitted beam and the outcomes have been exhibited.

More R. U. and KulkarniD. B. [9] studied flexural behavioural study on RC beam with externally bonded aramid fibre reinforced polymer.They represent the flexural manner of Aramid fibre reinforced polymer (AFRP) with RC beams of M_{25} grade cement. Results have been conducted for beam (simply supported) of cross-section 100mm×150mm×1200mm with laminated by aramid fibre polymer sheets. The impacts of reinforcing on burden conveying limit and impact of harm degree are talked about in subtle element. The outcomes demonstrate that the heap conveying limit of bars was essentially expanded as the quantity of layer expanded. The acceptance of the trial results was finished by utilizing ANSYS programming. To concentrate on the flexural conduct of the pillar, the examples were just subjected to two point stacking system just. The bars were wrapped with AFRP sheets in single layer and twofold layers along the length at the base face of the bar. The present work incorporates Effect of harm

level of the pillar and impact of number of layers. In this manner it is an achievable technique for fortifying and retrofitting of RC pillars.

Jayajothi P. et al [10] studied finite element analysis of FRP strengthened RC beams using ANSYS. Remotely fortified FRP sheet can be utilized to increase flexural quality of strengthened solid pillars. Strengthened solid bars remotely fortified with fibre strengthened polymer sheets utilizing limited component strategy embraced by ANSYS. The precision of the limited component model is checked with help of correlation its outcomes with the trial results. The heap redirection bends acquired from the limited component investigation holds great with the trial results

Modelling of beam
A beam with dimensions shown in table 1 has been drawn in the present case. ANSYS 14.5 has been used to model the beam and the analysis part has also been conducted in the ANSYS. A load of 5KN has been adopted to see the effect of the load on the deflection. The total deflection and directional deflection results have been plotted.
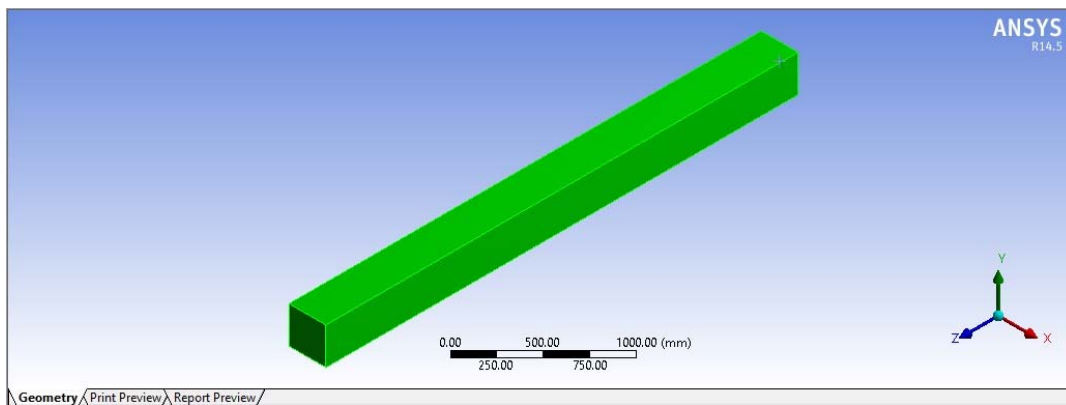
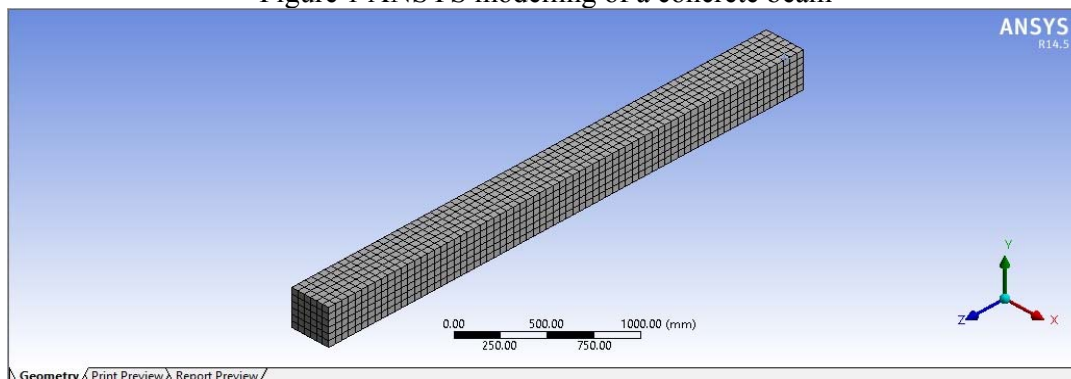
Figure 1 ANSYS modelling of a concrete beam

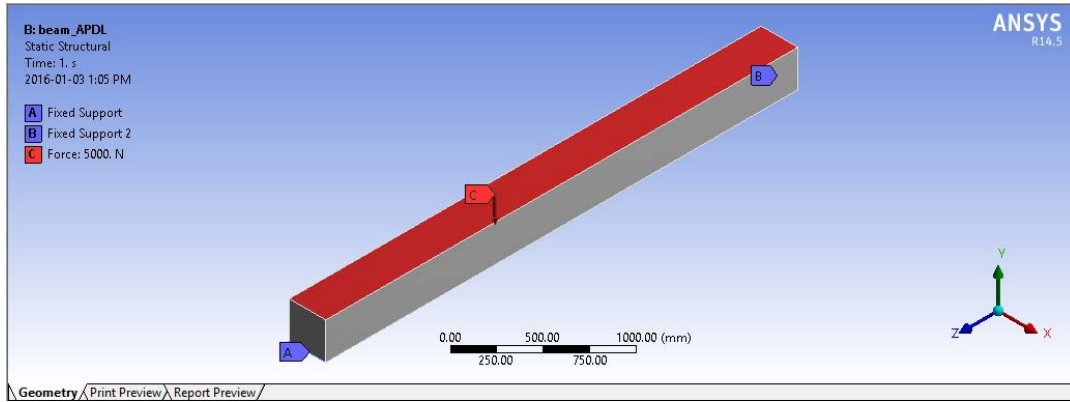Figure 2 Meshing of the concrete beam in ANSYS

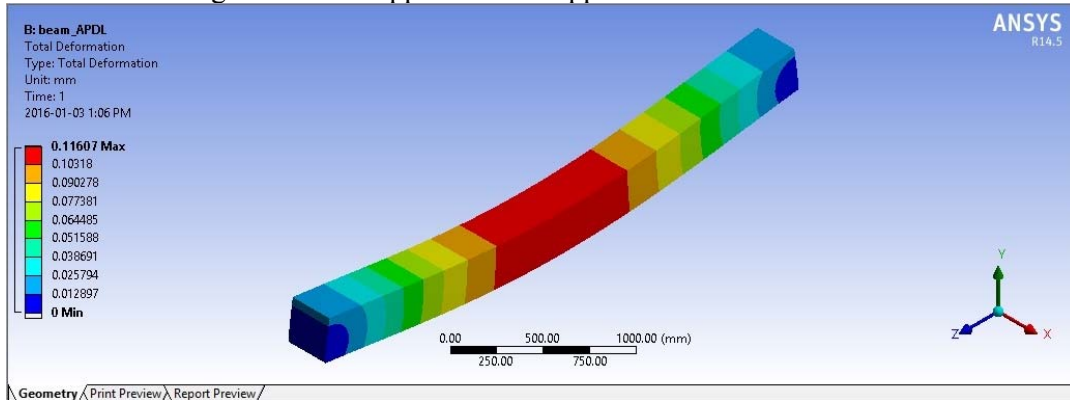Figure 3 Loads applied fixed support at the ends and a load
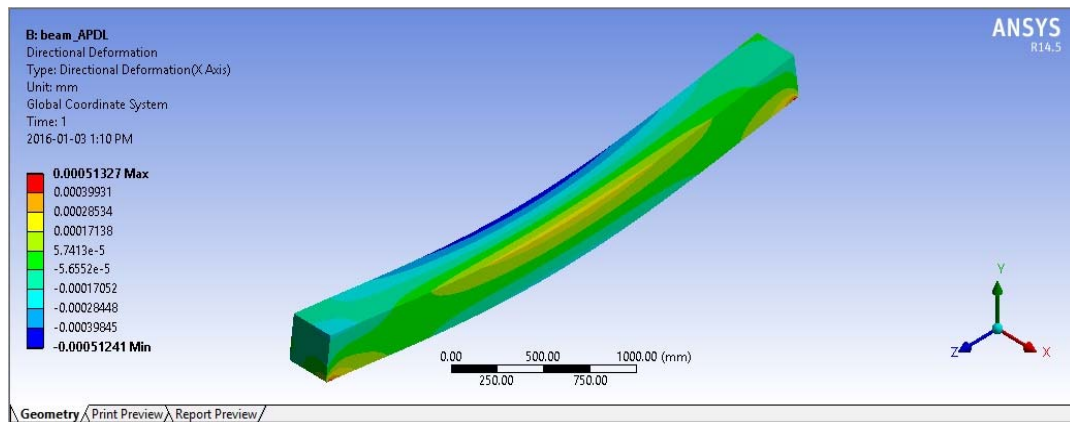

Figure 4 Total deflection of the beam

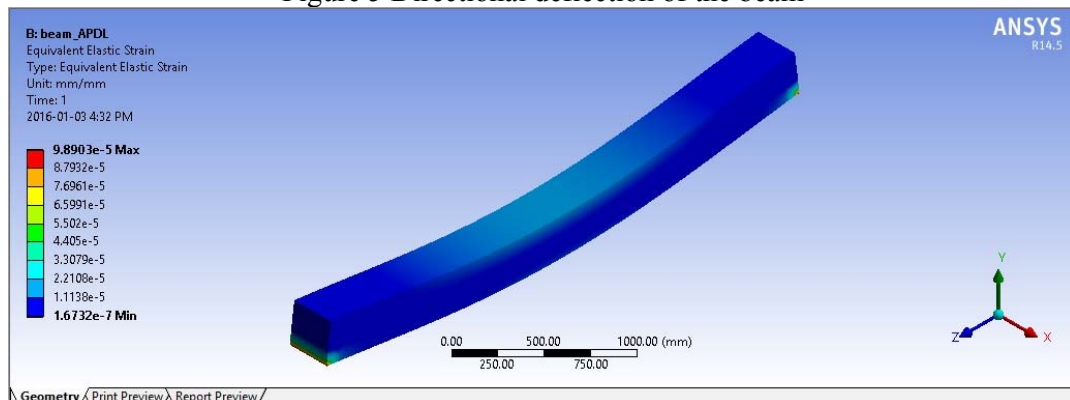Figure 5 Directional deflection of the beam

Figure 6 Equivalent elastic strain

Conclusion

1. A concrete beam has been solved in the present problem
2. FEM software help in solving the beam problem
3. Total deflection and directional deflection results have been plotted.
4. Equivalent elastic strain results have been plotted

References

1. Banu D., Barros R. C. D. and Taranu N., Numerical Modelling of Two-Way Reinforced Concrete Slabs Strengthened With Carbon Fibber Reinforced Polymers Strips, *International Conference on Experimental Mechanics*, 22-27. 2012.

2. Scordelis A.C., Ngo D and Franklin H.A., Finite Element Study of Reinforced Concrete Beams with Diagonal tension Cracks. *Proceedings of Symposium on Shear in Reinforced Concrete,* 42, 1972.

3. Parandaman P. and Jayaram M., Finite element analysis of reinforced concrete beam retrofitted with different fibre composites, *Middle-East Journal of Scientific Research* 22(7), 948-953, 2014.

4. Taranu N., Bejan L., Mecanicamediilor composite armate cu fibre, Editura CERMI, Iaşi, 2005.

5. Musmar M. A., RjoubM. I. and Hadi M. A.A.,Nonlinear Finite Element Analysis of Shallow Reinforced Concrete Beams Using Solid65 Element, *ARPN Journal of Engineering and Applied Sciences,* 9(2), 85-89, 2014.

6. Santhakumar R. and Chandrasekaran E.,Analysed Retrofitted Reinforced Concrete ShearBeams Using Carbon Fibre Composites, *Electronic Journal of Structural Engineering,* 4 66-74, 2004.

7. Ibrahim A. M. and Mahmood M. S., Finite Element Modelling of Reinforced Concrete Beams Strengthened With FRP Laminates, *European Journal of Scientific Research*, 30(4), 526-541, 2009.

8. Robert R. S. and Prince A. G., Finite Element Modelling on Behaviour of reinforced concrete beam-column joints retrofitted with carbon fibre reinforced polymer, *International Journal of Civil and Structural Engineering*, 1(3), 576-582, 2010.

9. More R. U. and KulkarniD. B. Flexural Behavioural Study on RC Beam with Externally Bonded Aramid Fibre Reinforced Polymer, *International Journal of Research in Engineering and Technology*, 3(7), 316-321, 2014.

10. Jayajothi P., Kumutha R. and Vijai K., Finite Element Analysis of FRP Strengthened RC Beams Using Ansys,*Asian Journal of Civil Engineering*, 14(4), .631-643, 2013.

ULTRASONIC STUDIES OF ORGANOMERCURY DITHIO COMPLEXES IN ACETONE AT VARIOUS TEMPERATURES

Sharmila Jain[1], S. K. Srivastava[2], Mukta Srivastava[3]
[1]Lect.,Govt. Polytechnic College, Morena
[2]H.O.D. School of Studies in Chemistry, Jiwaji University, Gwalior
[3]Asst. Prof., Dept. of Applied Sciences and Humanities,
IPS College of Technology & Management
Email: Jainsharmila23@gmail.com[1], muktaips@gmail.com[3]

ABSTRACT

Ultrasonic velocity and density measurements of various solutions of different concentrations of O, O' - Propylene dithio phosphate of mercury [phHgS(S)POGO]G=-CH$_2$C(H)-CH$_3$ in acetone have been carried out at 30, 35, 40° C . The experimental data were used to calculate other thermodynamic and acoustic parameters such as Isentropic compressibility, intermolecular free length, molar sound velocity, molar volume, apparent molar compressibility, specific acoustic impedance and salvation number. The significant information about intermolecular interactions between an organometallic moiety and acetone (non aqueous) have been obtained.

I.   INTRODUCTION

Ultrasonic velocity and its related properties have been extensively used to study physiochemical behaviour and molecular interactions in a variety of solution containing organic and inorganic molecules[1-5] however , little attention has been paid to organometallic solutes [6-7]which have attained considerable importance in recent years . In continuation to our earlier work on ph$_2$SnCl$_2$ in acetone and acetonitrile, Me$_2$TeI$_2$ in acetone system[8-10], the present study was undertaken to examine the intermolecular interaction of organomercury dithio complexes in acetone at various temperatures. Three organomercury dithio complexes were synthesized[11] and their reactivity with various soft Lewis acids and Lewis bases was reported[12-13]. The organomercury compounds are extensively used in biological fields as fungicides, insecticides and bactericides and in the industrial field as stabilisers, oil antioxidant and water repellent etc. Hg-C bonding in organomercury compounds is relatively weak. These compounds are insoluble in water, sufficiently stable and having no sharp melting point. These compounds show dissociation reaction in benzene when kept for at least 12 hours in solvent at room temprature. The final product of dissociation reaction is mercury.

2. EXPERIMENTAL

The experimental technique and instrumentation are similar to those reported earlier[8-10]. The ultrasonic velocity was measured by using a multi frequency interferometer working at 1MHz. The accuracy of the ultrasonic values was ± 0.2%. O ,O- Propylene dithio phosphate of mercury was synthesized[11]. The solution of different concentrations were prepared in acetone and kept for two hours in a thermostat at the desired temperature. Organomercury compounds are partially soluble in solvent. The densities of solvent and solutions at different temperatures were measured with a pyknometer and accuracy of the results was ± 0.1 gm/cm^3. Various acoustic parameters such as adiabatic(isentropic) compressibility β, intermolecular free length Lf , specific acoustic impedance Z, molar volume V, molar sound

velocity R, apparent molar compressibility ØK and salvation number Sn have been calculated as mentioned earlier[8-10].

3. RESULT AND DISCUSSION

From the measured ultrasonic velocity and density measurements, various parameters V, , Lf , Z , R, ØK and Sn are calculated for O ,O-Propylene dithio phosphate of mercury- acetone system and results are presented graphically in Fig. 1-5 with data table 1-5.

 The primary effect of dissolution of a solute in a solvent is a change in the compressibility of the solution because of various types of interactions[14] taking place between solute and solvent molecules. A higher interaction brings the interacting molecules closer , thus reducing the intermolecular free length and consequently making the solution harder to compress due to decrease of isentropic compressibility. Since the bonding in organomercury complex is predominantly covalent the compressibility is not that low as in the case of electrolyte where it can reach thousands of atmospheres. The ultrasonic velocity (V) of for O, O- Propylene dithio phosphate of mercury in acetone gradually decreases with rise in temperature. The behavior is due to corresponding changes in isentropic compressibility and density. The intermolecular free length (Lf) decreases linearly with the increasing molar concentration over the entire range of concentration under investigation. The decrease of Lf in the system is due to a closer approach of the interacting molecules as O ,O-Propylene dithio phosphate of mercury molecule is having large surface area which results in the decrease of compressibility also. The change in Lf, according to Eyring and Kincaid[15] also indicate that there is significant interaction between solute and solvent molecules. The molar volume, molar sound velocity, specific acoustic impedance and apparent molar compressibility increase with increasing concentration.

The ultrasonic velocity, density and specific acoustic impedance decrease with increasing temperature while isentropic compressibility, intermolecular free length, molar volume increase with the increasing temperature. The increase of isentropic compressibility and intermolecular free length is due to increase in the average kinetic energy of the interacting molecules as reported by Mednis[16].Although molar sound velocity increases with concentration. It is independent of temperature.

It is concluded from the present investigation that significant interaction takes place in the binary system of O, O- Propylene dithio phosphate of mercury in acetone which increases with concentration. The interaction increases linearly. The interaction is found to decrease with the increase of temperature as non aqueous solvent gets vaporized on increasing temperature.

 The above results indicate that the solutions in which solute are partially soluble can show considerable interactions in solution.

Table:-1 Conc. of solutions and their respective ultrasonic velocities (m/s)

conc.(moles/L)	Velocity at 30°C	Velocity at 35°C	Velocity at 40°C
0	1117	1100	1091.32
0.2384	1124	1114.6	1101
0.2981	1131	1120.3	1109.4
0.3726	1134	1125	1118.2
0.4657	1140	1132.1	1124.7
0.5118	1149	1137	1130.5
0.5445	1152	1142	1133.1
0.7127	1156	1145	1138

SERIES 1 at 30°C
SERIES 2 at 35°C
SERIES 3 at 40°C
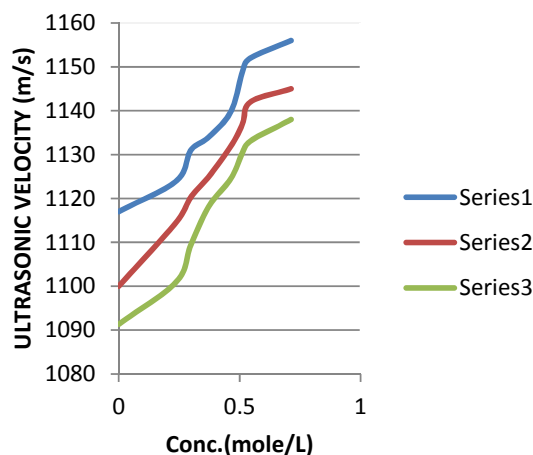
FIG.1

Table:- 2 Concentration of solutions and their respective isentropic compressibility)(cm²dyne⁻¹)

Conc.(mole/l)	β x10⁻¹² at 30°C	β x10⁻¹² at 35°C	β x10⁻¹² at 40°C
0	103.71	106.98	101.38
0.2384	92.12	94.47	97.21
0.2981	90.07	92.51	94.57
0.3726	89.16	90.83	92.97
0.4657	87.81	89.67	90.96
0.5118	85.66	87.84	89.31
0.5445	83.98	85.94	87.5
0.7127	77.71	81.05	83.71

SERIES 1 at 30°C
SERIES 2 at 35°C
SERIES 3 at 40°C

FIG.2

SERIES 3 at 40°C

FIG.3

Table:- 4 Conc. of solutions and their respective specific acoustic Impedance(Z x 10⁻⁵)

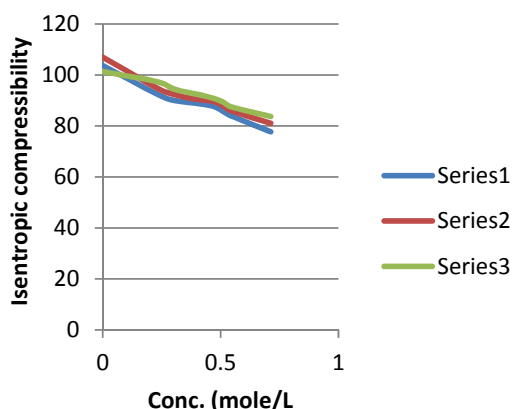| conc.(moles/L)	Z at 30°C	Z at 35°C	Z at 40°C
0	0.868	0.849	0.837
0.2384	0.965	0.949	0.934
0.2981	0.981	0.964	0.953
0.3726	0.988	0.978	0.961
0.4657	0.998	0.985	0.977
0.5118	1.015	1.001	0.99
0.5545	1.033	1.018	1.008
0.7127	1.113	1.077	1.049

Table:- 3 Conc. of solutions and their respective inter molecular free length values (Lf)

conc.(moles/L)	Lf(A°) at 30°C	Lf(A°) at 35°C	Lf(A°) at 40°C
0	0.6423	0.6581	0.6708
0.2384	0.6055	0.6186	0.632
0.2981	0.5988	0.6121	0.624
0.3726	0.5957	0.6065	0.619
0.4657	0.5912	0.6027	0.612
0.5118	0.5839	0.5965	0.606
0.5545	0.5782	0.59	0.6
0.7127	0.5562	0.5729	0.587

SERIES 1 at 30°C
SERIES 2 at 35°C
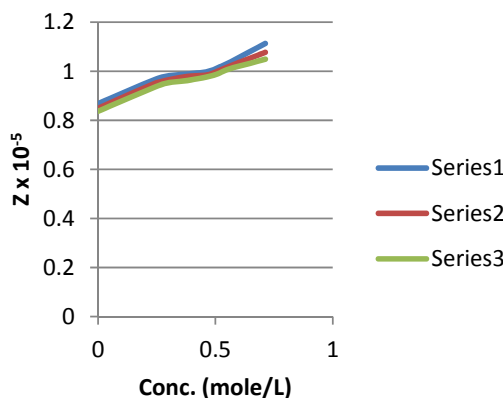**SERIES 3 at 40°C**

FIG. 4

SERIES 1 at 30°C
SERIES 2 at 35°C

Table:- 5 Conc. of solutions and their respective Molar sound velocity (R)

conc.(moles/L)	R at 30°C	R at 35°C	R at 40°C
0	774.53	775.85	778.54
0.2384	786.93	791.19	791.23
0.2981	803.65	807.66	807.3
0.3726	831.93	828.36	870.25
0.4657	867.25	884.24	882.73
0.5118	884.81	885.08	887.86
0.5545	887.13	888.98	888.51
0.7127	886.09	912.73	957.13

SERIES 1 at 30°C
SERIES 2 at 35°C
SERIES 3 at 40°C
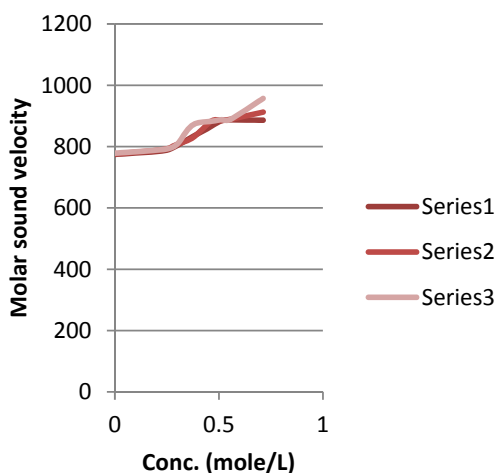
FIG. 5

4.References:

[1]. Singh D.P. and Bhatti S.S.,Accoustics Let., 8, 84 (1984)

[2]. Kalyansundram S. and Saraswathi S., Bull. Electro. Chem., 6, 311 (1990)

[3]. Singh D.P. and Kalsh S.C., Accoustics Let., 17, 206 (1991)

[4]. Venketesu P., Ramadevi R.S., and Prabhakara Rao M.V., J. Pure Appl. Ultrason., 18, 15 (1996)

[5]. Pandey J. D. and Akhtar Y., J. Pure Appl. Ultrason., 18, 108 (1966)

[6]. Srivastava T.N. and Singh R.P., Accoustics Let., 6, 152 (1983)

[7]. Srivastava T.N. and Singh R.P., Ind. J. Chem., 23 A, 227 (1984)

[8]. Saxena S.B., Srivastava S.K. and Jain S. , Orient. J. Chem., 15(2), 323 (1999)

[9]. Saxena S.B., Srivastava S.K. and Jain S. , J. Pure Appl. Ultrason., 586, (1999)

[10]. Saxena S.B., Srivastava S.K. and Jain S. , Orient. J. Chem., 16(1), 91-94 (2000)

[11]. Srivastava S.K., Jain Sharmila and Saxena S.B., SYNTH. REACT. INORG. MET. –ORG. CHEM., 28(9),1431-1444 (1998)

[12]. Srivastava S.K., Saxena S.B. and Jain S., IND. J. CHEM. 40A , 380-382 (2001)

[13]. Srivastava S.K., Saxena S.B. and Jain S., J. IND. CHEM. SOC., 78 , 362-363 (2001)

[14]. Hirschfelder J.O., Curtius and Bird R.B. , MOLECULAR THEORY OF GASES AND LIQUIDS, Joln. Wiley and sons, Inc. N.V. 1954, Chap. 12 & 13

[15]. Erying H. and Kincaid J. F. , J. Chem. Phys. (USA), 6 (1938), 620

[16]. Mednis L., AKust.,Zh. (USSR), 13(2) (1924) 24.

MODELLING SIMULATION AND KINEMATIC ANALYSIS BASED ON PRO/ ENGINEER FOR BOOM OF BACKHOE LOADER

Priyanka Goyal[1], Juber Hussain[2]
[1]PG Scholar, Dept. of Mechanical Engg., IPS-CTM, Gwalior
[2]Asst.Prof., Dept. of Mechanical Engg., IPS-CTM, Gwalior
Email: priyanka.goyal1594@gmail.com [1], juber.qur@gmail.com [2]

Abstract: Pro/Engineer is a parametric feature-based design of 3D software and capable to solve the motion dynamics of the motion, and the reactions at the constraints of the mechanisms can be used as the inputs for any Finite element program to understand the behavior of stresses and deformations of the individual component of the machine to estimate the working life of the machine elements designed for the application. .In this paper researcher describes, the Kinematic study of the Cad model of the Boom of machine is made for the worst case of the maximum load at the bucket (Breakout force) at different conditions.

Keywords: -Backhoe; Pro/Engineer; Model Simulation, Dynamic Analysis.

Introduction

An excavator is comprised of three planar implements connected through revolute joints known as the boom, arm, and bucket, and one vertical revolute joint known as the swing joint **[1]**. The backhoe loader is shown Figure1. Kinematics is the science of motion which treats motion without regard to the forces that cause it. Within the science of kinematics one studies the position, velocity, acceleration, and all higher order derivatives of the position variables (with respect to time or any other variables) **[2]**. The excavator linkage, however, is a complex link mechanism whose motion is controlled by hydraulic cylinders and actuators. To program the bucket motion and joint-link motion, mathematical model of the link mechanism is required to refer to all geometrical and/or time-based properties of the motion. Kinematic model describes the spatial position of joints and links, and position and orientation of the bucket **[3]**. The problem of link mechanism control requires both the direct and inverse kinematic models of the backhoe attachment of the excavator **[4]**. The derivatives of kinematics deal with the mechanics of motion with considering the forces that cause it.

Fig. 1: Excavator

Establishments and 3d Modelling of Boom

The Boom is the most stressed part of the backhoe loader. The drawing for the Boom with sectional width is shown in the Figure 2. All the plates welded are of 16 mm thickness, the fillet weld can be measured to be8 to 10 mm strong. The drawing for the Boom with sectional width is shown in the figure. All the plates welded are of 16 mm thickness, the fillet weld can be measured to be 8 to 10 mm strong. The consideration that the weld is stronger than the

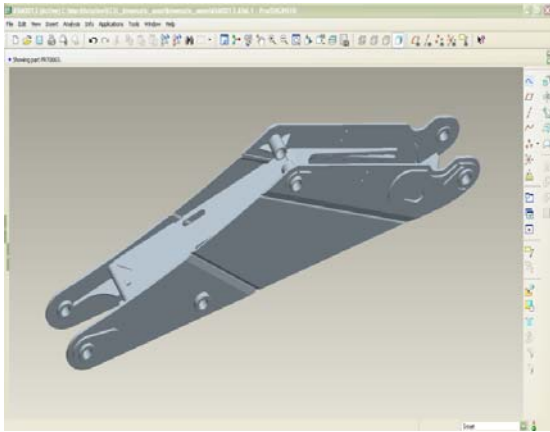base metal is kept in mind and thus the weld is not modelled in 3D.

Fig. 2: Cad model of boom

Kinematic & Dynamic Behavior study of Backhoe loader

In order to analyze excavator design in the real world by creating a virtual prototype, Pro/Mechanica was used to implement the excavator kinematic simulation and structure analysis **[5]** .To study the kinematic behavior of the components connected together, the assembly of all the components is done in Pro-E with the use of connection joints in the assembly module of pro-e. The motion is then analyzed in Pro-Mechanism module of pro-e.

Kinematic Analysis

The connections of Pin joint to different parts, to facilitate the motion of the system. While the linear motion of cylinders is done via use of slider mechanism constraint in the assembly mode of Pro-engineer standard module. The closed setting for cylinders is done in the mechanism to exteriorize the dependencies of motion constraint to facilitate the constraint of motions. First the motion of Bucket which is rotational motion to dipper connected joint and the linear motion is synthesized shown in the Figure 3.
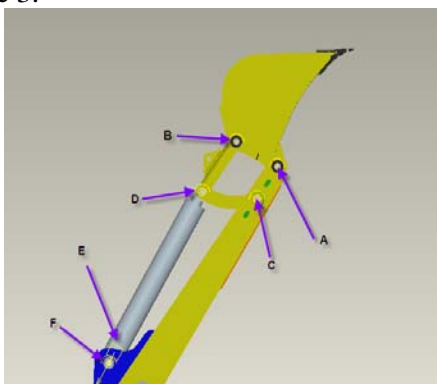
Fig. 4: Connections used in the synthesis of the bucket

The Figure 4 only shows the connections used in the synthesis of the bucket. The Connection "A" is a Pin joint connection in the Bucket and the dipper, connection "B" is in between the bucket and the link. Connection "C" is in between the link and the dipper, Connection "D" is in between the Hydraulic cylinder and the linkages. Connection "E" is the slider connection between the Piston and Cylinder of a Hydraulic Cylinder arrangement. Connection "F" is the Pin joint in between the cylinder and the dipper.
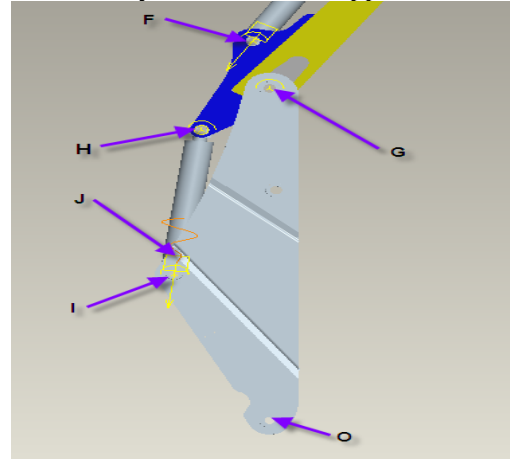
Fig. 4: Joint connections in the boom

The Figure 5 shows the joint connections in the boom, listed as "G" a pin joint connection connecting the dipper to the boom. Pin joint "H" is the connection of the cylinder to the dipper responsible for the motion of the dipper. Pin joint connection "I" will carry the reaction force via the cylinder to the boom. Joint "J" is the slider connection given to simulate the Hydraulic Cylinder. The Rotation motor input is given to the connection "A" for the rotation of the connection to visualize the kinematic synthesis of the bucket **[4].**
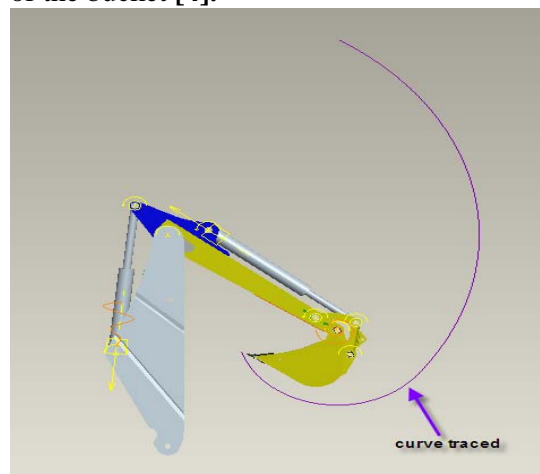
Fig. 5: Curve traced by the toe of bucket

Dynamic Analysis

The dynamic simulation in mechanism module of pro-e is done to calculate the results for forces in the joints at all time frame of the motion. The motion of the bucket is only analyzed and the reaction in the cylinder tilting the bucket was calculated via the force measures created in the mechanism module of pro-e [6]. The result window for the force analysis of the cylinder directly shifting the bucket is shown in the below figure for the force graph for the complete range of time.

Fig. 6: Result window for the force analysis of the cylinder

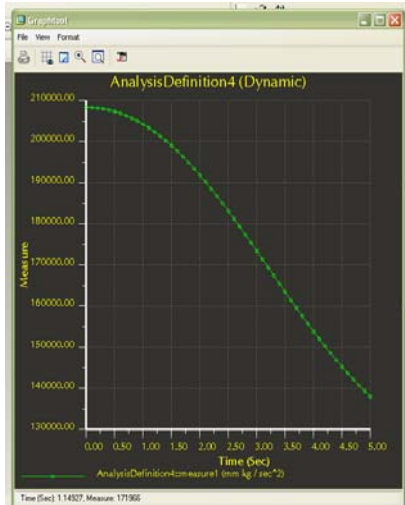The maximum force for the motion comes to 163435 N at the time of 3.5 sec. this can be cross-checked from the maximum pressure involved and the bore diameter of the cylinder. The Bore Diameter of the cylinder is 200 mm, the machine running pressure is 280 bar, while the maximum pressure for the machine is allowed to reach is 310 bar, after which the pressure relief valve connected in the circuit releases the oil to oil tank to maintain the pressure of max 310 bar in the machine. With 280 bars as the working pressure the maximum force a cylinder can develop will reach to 879645.9 N, the same is nearly 8 times the required force to tilt the bucket. Thus the force resulted via the mechanism is acceptable to us. The results of the force developed by the cylinder connected to the boom and the pin is given in the figure below. The Maximum force produces in this case is around 293215 N which is again nearly with factor of safety of 3 with the maximum force the cylinders can develop. The results of the system can be taken to Finite element package where boom can be analyzed for these results.

Conclusion

This study tells the optimization of the Boom for including the strength of welds where welds can be modelled with shell elements along with the boom to take moments can be done to predict the failure stresses of the welds. Localization and stress linearization of the weld can be simulated for calculating the factor of safety for weld strength.

References

[1] Cannon Howard N., "Extended Earthmoving with an Autonomous Excavator", Thesis of Master of Science, the Robotics Institute Carnegie Mellon University Pittsburgh, 1999.

[2] Craig John J., "Introduction to Robotics Machines and Control", Second Edition, Addison-Wesley Publishing Company, 1989, pp. 68.

[3] Mittal R. K., Nagtath I. J. (2008),'Robotics and Control', Tata McGraw-Hill Publishing Company Limited, 9th ed 2008, pp. 70

[4] Rao S. S., Bhatti P.K. (2001), 'Probabilistic approach to manipulator kinematics and dynamics', Reliability Engineering and System Safety, Elsevier Science, 2001,Vol. 3, No. 3,pp. 47-58.

[5] Patel Bhaveshkumar P. and Prajapati J.M. (2011),'A Review on Knematics of Hydraulics Excavator's Backhoe Attachment', International Journal of Engineering Science and Technology, Vol. No. 3, pp. 1990-1997.

[6] Vaha P. K., Skibniewski M. J. (1993), 'Dynamic Model of Excavator', Journal of Aerospace Engineering April 1993, Vol. 6, No. 2, pp.148-166.

[7] Yener Mehmet (2005), 'Design of a Computer Interface for Automatic Finite Element Analysis of an Excavator Boom', The Graduate School of natural and Applied Sciences of Middle East Technical University, M.S. Thesis, May 2005, pp. 1-4, 68-69.

[8] Greiner H.G. (1967) 'Data and Engineering Information used in the manufacture and applications of Cranes', Crane Handbook Design, 3rd ed 1967.

REVIEW ON FABRICATION AND MODAL ANALYSIS OF E-GLASS WOVEN ROVING COMPOSITE PLATE

Ganesh N. Sargule[1], A.A.Miraje[2], R.D.Patil[3], Sharayu U. Ratnaparkhi[4]

[1]P.G Scholar, M.E, Mechanical-Design Engineering, PVPIT, Budhgaon, Sangli.
[2]Associate Professor M.E.(Mech- Design) Ph.D.(Mech Engg) , PVPIT, Budhgaon, Sangli.
[3]Associate Professor M.E.(Mech- Design), PVPIT, Budhgaon, Sangli.
[4]Asst. Professor Mechanical, RMDSSOE, Warje, Pune

Abstract-Composites are one of the most widely used materials because of their adaptability to different situations and the relative ease of combination with other materials to serve specific purposes and exhibit desirable properties. Composite materials are used in the form of monocoque structures in which lamiae of fiber reinforced polymer are bonded to each other. Considering this, structures are being invented in addition to monocoque structures and used in many applications such as in the aeronautical, automobile industries, defence applications. Therefore it is very essential to analyse composites for vibration analysis.This is a review paper. This evolves extensive experimental works to find the free vibration of woven fiber Glass/Epoxy composite plates in free-free boundary conditions. Proposed work is relatyed with manufacturing of composite specimensby the hand-layup technique. Elastic parameters of the plate will also determine experimentally by tensile testing of specimens. An experimental investigation will be carried out using modal analysis technique, to obtain the Natural frequencies. There should be validation of results obtained from the FEA using Ansys. The effects of different parameters including no. of layers and aspect ratio of woven fiber composite plates will be studied in free free boundary conditions in details. This study may provide valuable information for researchers and engineers in design applications.

Keywords: fiber reinforced polymer, woven fiber Glass/Epoxy composite, free-free boundary

I. INTRODUCTION

The thin lamination structure with less than 6mm is an important option and has the ability to change the body covers of automobiles owing to its superior strength and stiffness along with low weight per unit area. In field of aerospace industry, better drape ability of thin sandwich formation is preferred over thick conventional sandwich composites. Truck bodies and trailers use assemblies and parts made from reinforced plastics to a great extent. The use of light metals, which lends itself to simple shapes and extrudable forms, is also found to be economical. The low heat transfer coefficient of composites enables their use in refrigerated units. Glass reinforced polyester has all the properties that make it ideal for this purpose and has become the standard material.

Fig no.1 Composite anatomy
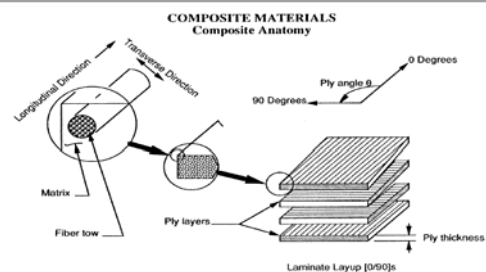
Most of the fiber reinforced polymer (FRP) composite materials are used in the form of monocoque structures in which lamiae of fiber reinforced polymer are bonded to each other.Realizing this, structures are being invented in addition to monocoque structures. These structures are found to be most influential in case of high stiffness and strength. Composites may be characterized as generally:

Anisotropic-There is no symmetric planes w.r.t the alignments of fibers. Fibers are arranged inthree- non mutual perpendicular direction

Monoclinic-There is one symmetric planes w.r.t the alignment of fibers.

Orthotropic -There are 3 mutually perpendicular symmetric planes w.r.t the alignment of fiber.

Isotropic-Every plane is a plane of symmetry. For example a composite containing a large no. of randomly oriented fibers behaves in an isotropic manner

II LITERATURE REVIEW

Cenk Aksoylar et al. (2011) [1] have discussed nonlinear transient analysis of FGM and FML plates under blast loads by experimental and mixed FE methods. Nonlinear transient behaviours' of fiber–metal laminated composite plates are investigated by both experimental and numerical techniques under non-ideal blast loads. In the experiments, three plates with different aspect ratios are tested and their responses are compared with both the developed mixed finite element method and the commercial software ANSYS. In the analyses with the developed mixed FEM, no condensation is performed hence time derivative of internal forces are also calculated. The results showed a good and reliable correlation between each other.

J. Suresh Kumar et al. (2011)[2] have investigated vibration analysis of composite laminated plates using higher-order shear deformation theory with zig-zagfunction. The ever increasing use of composite materials in advanced technology areas like aerospace, automotive, and sportsequipment's, have prompted to play a prominent role.

FarukFıratCalım (2009)[3] has intended to analyze free and forced vibrations of non-uniform composite beams in theLaplace domain. The free vibration is then taken into account as a special case of forced vibration. TheTimoshenko beam theory is adopted in the derivation of the governing equation. The material of therod is assumed to be homogeneous, linear elastic and anisotropic. The effects of shear deformation, rotaryinertia, non-uniformity of the cross-section are considered in the formulation.

K. Sepahvand et al. (2011)[4] have presented the theory and application of the generalized polynomial chaos expansion for the stochastic free vibration of orthotropic plates. Specifically, the stochastic analysis of orthotropic plates under the uncertainties in elasticity moduli is investigated. The uncertain moduli, Eigen-frequencies and Eigen-modes of the plates are represented by truncated polynomial chaos expansions with arbitrary random basis.

B. N. Singh (2009) [5] has developed composite plates to find out the non-linear free vibration response of composite laminates for different thickness and amplitude ratio. The used methodology is higher order deformation theory (HSDT) and MATLAB computation.

M. Barbato (2009) [6] has investigated a new simple and efficient two dimensional frame finite element able to accurately estimate the load carrying capacity of reinforced concrete beams flexurally strengthened with externally bonded fibre reinforced polymer(FRP) strips and plates. The input parameters were different loading conditions and output parameters were failure modes i.e. concrete crushing, reinforcing steel yielding, FRP rapture, FRP debonding. He was able to accurately simulate the response of RC beams flexurally strengthened with externally bonded FRP strips/ plates.

Thuc Phuong Vo et al. (2009) [7] have developed a geometrically nonlinear model to study the flexural–torsional behaviour of general thin-walled open-section composite beams with arbitrary lay-ups under various types of loadings. This model was capable of predicting accurately nonlinear flexural–torsional response for various configuration including boundary conditions and laminate orientation of thin-walled composite using incremental Newton–Raphson method, Von Karman formulation.

F. Moleiro et al. (2009)[8] have developed Layer wise finite element models, based on a mixed least-squares formulation for both static and free vibration analysis of multilayered composite plates. Input parameters were displacements, transverse stresses and in-plane strains. Used methodology was C° continuous function. Due to the least-squares formulation, the model for static analysis yields asymmetric positive definite system of linear equations, whereas the model for free vibration analysis yields a symmetric quadratic eigen value problem.

Zhigang Yu et al. (2010)[9] have developed Formulations of a multivariable hierarchical beam element for static and vibration analysis based on the generalized variational principle with two kinds of variables. The present method

has very high accuracy for the two kinds of independent variables simultaneously, especially for the generalized forces.

O.A. Ganilo (2010)[10] has discussed an analytical model for the vibration of composite plate containing an embedded periodic shape memory alloy structure. The work was presented in this paper an effective approximate analytical model has been developed and analysed, as well as a numerical solution generated for comparison purposes. The general solution obtained in this paper can be applied also in the case of time variant damping.

III PROBLEM DEFINATION

The literature review is devoted to the recently developed finite elements based on various laminated plate theories for the free vibrations and dynamics, buckling, post buckling analysis, geometric non linearity, large deformation analysis, damage analysis of composite material. Most structural composite structures are subjected to dynamic loading in their working life & maximum damage results from the resonant vibrations. Maximum amplitude of vibration must be limited for the safety of the structure. Hence vibration analysis has become very important in designing structure to know it's response in advanced and to take the necessary steps to control the structural vibrations.

Proposed Work-

A   Objectives
- A mathematical model is developed which is based on assumptions. The mathematical expressions based on differential equations and given conditions. These equations are very difficult to solve. Therefore the basic objective is to find out simple numerical solution technique.
- Composite materials are two or more distinct phase materials. Considering these to study the composite materials in depth is the objective.
- Fabrication method is the big concern related with the composite structures.

B.   Methodology
- Develop fabrication method to fabricate test specimen
⇩
- Proper experimental plan for testing
⇩
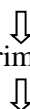
- Analytical study by using Ansys
⇩
- Theoretical and mathematical study to validate results
⇩
- DOE study to optimize result
⇩
- Validation of all results

IV CONCLUDING REMARK

Literature review is focused on the different types of analysis of composite materials. Due to the requirement of high performance material in aerospace and marine structures, the prospect of future research of composite material, such as FRP (Fibre Reinforced Plastic) is very bright. Analysis of natural frequency and properties of composite plate has started from 40 years ago.

The affects of different parameters on natural frequency is important analysis. The main factors or parameters which affect on vibration in case of composite laminated plates are unexplored.

As the composite material are made of two or more distinct phase materials. Manufacturing consideration plays an important role in design part. Therefore it is necessary to analyse the affect of different fabrication factors such as curing time, curing temperature and volume fraction ratio so as to optimise the fabrication process.

VI. ACKNOWLEDGMENT

REFERENCES
Journal papers:
[1] Cenk Aksoylar, Akin Omercikoglu, Zahit Mecitoglu, Mehmet H. Omurtag, "Nonlinear transient analysis of FGM and FML plates under blast loads by experimental and mixed FE methods",Composite Structures 94 (2012) 731–744.

[2] J. Suresh Kumar, T. Dharma Raju and K. Vijaya Kumar Reddy, "Vibration analysis of composite laminated plates using higher-order shear deformation theory with zig-zag function" Indian Journal of Science and Technology (Aug 2011), Vol. 4 No. 8

[3]Faruk Fırat Calım, "Free and forced vibrations of non-uniform composite beams", Composite Structures 88 (2009) 413–423.

[4]Sepahvand, S.Marburg, H.-J.Hardtke, "Stochastic free vibration of orthotropic plates using generalized polynomial chaos expansion", Journal of Sound and Vibration 331 (2012) 167–179.

[5] B. N. Singh, "Non-linear Free vibration analysis of composite plate with material uncertainties: A Monte Carlo simulation", Journal of sound and vibration 324 (2009) 126-138.

[6]M. Barbato, "Efficient finite element modeling of reinforced concrete beams retrofitted with fibre reinforced polymers", Composite structures 87 (2009) 167-176.

[7] Thuc Phuong Vo, Jaehong Lee, "Geometrically nonlinear analysis of thin-walled open-section composite beams", Computers and Structures 88 (2010) 347–356.

[8] F. Moleiro , C.M. Mota Soares , C.A. Mota Soares , J.N. Reddy , "Layerwise mixed least-squares finite element models for static and free vibration analysis of multilayered composite plates, Composite Structures 92 (2010) 2328–2338.

[9] Zhigang Yu, Xiaoli Guo, Fulei Chu, "A multivariable hierarchical finite element for static and vibration analysis of beams", Finite Elements in Analysis and Design 46 (2010) 625–631

[10] O.A. Ganilova , "An analytical model for vibration of composite plate containing an embedded periodic shape memory alloy structure", Journal of Composite structures, 92 (2010) 39-47.

Books:

[6] Robert M. Jones, Mechanics of composite material (Virginia Polytechnic Institute and state university, Taylor and Francis).

EFFECT OF AXIAL VISCOSITY VARIATION THROUGH AN ATHEROSCLEROTIC ARTERY: A NON-NEWTONIAN FLUID MODEL

Aditi Singh[1], Pushkar Singh[2], S. P. Singh[3]
[1,2]P.G Scholar, Department of Mathematics, D.E.I., Dayalbagh, Agra, India
[3]Asst. Prof., Department of Mathematics, D.E.I., Dayalbagh, Agra, India
Email: aditi.dei2014@gmail.com[1], pushkar19121992@gmail.com[2], shail.dei@gmail.com[3]

Abstract- **A mathematical model has been designed to study the effect of axial viscosity variation on various parameters of blood flow in an overlapping stenosed artery using Herschel-Bulkley fluid . This model has been undertaken to investigate the structure of the flow through an arterial segment with overlapping stenosis. The constitutive equations of the model are solved analytically using the initial conditions and given boundary conditions to get expressions for different parameters such as flow rate ,resistance to flow and wall shear stress . Variations of these flow parameters are analysed graphically.**

Keywords- **Blood flow, blood viscosity, overlapping stenosis, Herschel-Bulkley fluid, flow rate, resistance to flow, wall shear stress.**

I. INTRODUCTION

Mathematical modelling is the application of mathematics to explain and predict real world behaviour. It basically comprises of making an interpretation of certifiable issues into scientific issues, tackling the numerical issues and translating these arrangements in the dialect of real world. A new multidisciplinary science is now arising which bridges the gap and draws upon both the life science and physical science for help and support. This area is Biomechanics. The components in charge of the onset and advancement of vascular diseases have not been completely comprehended, and the related studies have turned into a predominated zone of multidisciplinary exploration.

Congenital and acquired cardiovascular diseases represent one of the most important causes of morbidity and mortality in the world. Among the acquired cardiovascular diseases, atherosclerosis is the most common manifestation which is often characterized by arterial narrowing and reductions in blood flow . While the risk factors of this disease such as nicotine, high cholesterol and familiar history are systemic , the manifestations (typically in the form of plaque deposits) are localized in areas of complex flow like the coronary, carotid, abdominal and femoral arteries. Hemodynamic quantities such as blood velocity, pressure and shear stress play a very important role in the localization of disease and in the efficacy of treatments. For both congenital and acquired cardiovascular diseases, a deep understanding of the altered blood flow conditions can enable the optimization of interventions employed to treat these conditions.

Stenosis in the arteries of mammals are a common occurrence and for many years researchers have endeavoured to model the flow of blood through stenosed arteries experimentally and theoretically. The deposition of cholesterol and proliferation of the connective tissues in the arterial wall form plaques which grow inward and restrict the blood flow. In order to have a fuller understanding of the development of these diseases, an accurate knowledge of the mechanical properties of the vascular wall together with the flow

characteristics of blood are indispensable. Thus relevant information is deemed to be of great help in the treatment of vascular diseases and also to bioengineers who are engaged in the design and construction of improved artificial organs. Perhaps the actual cause of abnormal growth in an artery is not completely clear to the theoretical investigators but its effect over the cardiovascular system has been determined by studying the flow characteristics of blood in the stenosed area.

The frequently occurring cardiovascular disease, stenosis or arteriosclerosis is the abnormal and unnatural growth in the arterial wall thickness that develops at various locations of the cardiovascular system under diseased conditions which occasionally results into serious consequences Srivastava [12].

To understand the effects of a single mild stenosis present in the arterial lumen, a good number of studies (Young[13] Shukla et al.[11]) on the blood flow through stenosed arteries have been performed. All these studies were made with the assumption that the flowing blood is Newtonian and the geometry of the stenosis is a smooth cosine function. However, it has been observed from experimental investigations that blood, being a suspension of cells, behaves like a non-Newtonian fluid at low shear rates in smaller arteries (Barnett and Han[1]). It is also realized that the Herschel-Bulkley model is a better model than Casson's model (Blair and Spanner[2]). Further, in small diameter tubes blood behaves like a Herschel-Bulkley fluid rather than power law and Bingham fluids (Chaturani and Samy [5]).

Misra et al.[10] developed a mathematical model(Herschel-Bulkley fluid model) for studying the non-Newtonian flow of blood through a stenosed arterial segment. The problem is investigated by a combined use of analytical and numerical techniques and it is noticed that the resistance of flow and the skin-friction increase as the stenosis height increases. Nallapu et al.[9] studied a two fluid model of Herschel-Bulkley fluid flow through tubes of small diameters and assumed that the core region consists of Herschel-Bulkley fluid and Newtonian fluid in the peripheral region and derived the analytical solutions for velocity, flowflux, effective viscosity, core hematocrit and mean hematocrit

and the effects of various relevant parameters on these flow variables have been studied.

In most of the recent literature about stenotic flow in either a rigid tube or a flexible artery, the stenotic geometry has been regarded as time-independent. Such a consideration may suit well for a rigid vessel but for a flexible vessel wall, the stenosis cannot remain static. Moreover, the problem becomes more acute in the presence of an overlapping stenosis in the arterial lumen instead of having a single (mild) stenosis as considered by aforesaid researchers. A consistent mathematical model for the unsteady flow of blood through an overlapping arterial stenosis was put forward first by Chakravarty and Mandal[4] in which the streaming blood was treated as a viscoelastic fluid and the flow was considered only in the axial direction.

Layek et al.[8] investigated the effects of an overlapping stenosis on flow characteristics considering the pressure variation in both the radial and axial directions of the arterial segment and treating blood as Newtonian . Gupta.S et al [6] investigated the effects of stenosis and radial variation of viscosity on the flow characteristics of blood considering laminar,incompressible and non-Newtonian flow of blood using Power-Law fluid model. Jain.N et al. [7] observed various flow characteristics of blood and effect of various parameters of stenosis using Herschel-Bulkley non-Newtonian fluid model considering steady,laminar,one-dimensional flow of blood through an axially non-symmetric but the radially symmetric atherosclerotic artery.

Motivated by these facts , we propose to study the "Effect of axial viscosity variation on blood flow in an overlapping stenosed artery when blood is considered as Herschel-Bulkley fluid ".

II.   FORMULATION OF THE MODEL

For the development of mathematical model, following assumptions are made :

●   Flow of blood is designed as laminar, steady and non-Newtonian in behaviour and the way of streaming blood is incompressible, homogeneous.
●   The flowing blood is not affected by any external force.

- Viscosity of blood varies along the axial direction and there exists a axial decrease in blood viscosity i.e., it is maximum at the axis and minimum near the wall.
- The stenosis in the artery is axially symmetric and depends upon the axial distance z and the height of its growth.
- Stenosis is taken overlapping.
- Radial velocity in the stenotic region is very small in comparison to the axial velocity Young [16].

The geometry of the stenosis, assumed to be manifested in the arterial segment is described (Chakravarty and Mandal [4]) in Fig. 1 as

$$\frac{R(z)}{R_o} = 1 - \frac{3\delta}{2R_o(l_o)^4}\{11(z-d)(l_o)^3 - 47(z-d)^2(l_o)^2$$
$$+ \quad 72(z-d)^3(l_o)$$
$$- 36(z-d)^4\} \quad ; \ d \le z \le d+l$$

$$= 1 \qquad \text{otherwise} \qquad (1)$$

where R_o is the radius of the artery (assumed to be a rigid circular tube) outside the stenosis, $R(z)$ is the radius of the stenosed portion of the arterial segment, l_o is the length of the stenosis, d indicates its location and δ is the maximum height of the stenosis into the lumen, appears at the two different locations: $z=d+l_o/6$ and $z=d+5\ l_o/6$ The height of the stenosis at $z=d+l_o/2$, called critical height is $3/4\ \delta$.

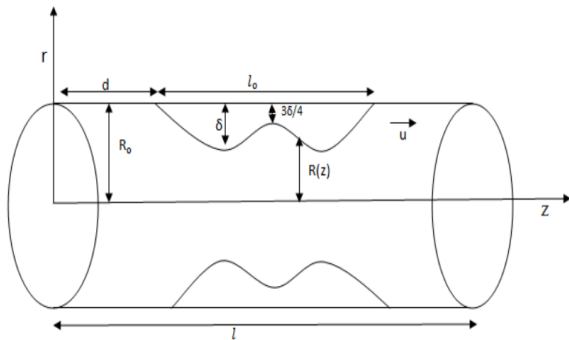
Fig.1 The flow geometry of an arterial overlapping stenosis

The Navier-Stoke equation [14] is

$$-\frac{\partial p}{\partial z} + \frac{1}{r}\frac{\partial}{\partial r}(r\tau) = 0 \quad (2)$$

where r and z be the radial and axial coordinates respectively, p is pressure and τ be shear stress.
The flow of blood is assumed to be steady, laminar and incompressible. No external force is being applied on the artery. The viscosity of blood is a function of z and is given by

$$\mu(z) = \mu_o\left(\frac{R(z)}{R_o}\right)^{-\alpha} \quad ; \quad d \le z \le d+l_o$$
$$= \mu_o \qquad ; \quad elsewhere \qquad (3)$$

where μ_o is the constant viscosity of the blood and $\alpha = 0,1,2,\ldots\ldots$ is any arbitrary constant parameter, which is the index of viscosity variation in the stenotic region. The form of viscosity variation assumed in equation (3) is very natural because accumulation of blood cells occurs in the stenotic region just before the minimum gap where radius also becomes minimum, but the viscosity becomes maximum.

The constitutive equation for Herschel-Bulkley fluid is given by

$$\tau = \mu\left(-\frac{\partial u}{\partial r}\right)^n + \tau_o \ ; \ \tau \ge \tau \qquad (4)$$

$$\frac{\partial u}{\partial r} = 0 \qquad ; \quad \tau < \tau_o \qquad (5)$$

where τ_o be the yield stress and μ be the viscosity coefficient of blood. The boundary conditions pertaining to the problem are :

At r = R(z), w = 0 and at r = 0, $\frac{\partial w}{\partial r} = 0$, (6)

Where w is axial velocity and n is the Herschel-Bulkley index number.

The equation of motion describing one-dimensional flow of blood treating as Herschel-Bulkley fluid whose viscosity varies along the z-axis may be expressed as

$$-\frac{\partial p}{\partial z} + \frac{1}{r}\frac{\partial}{\partial r}\left[r\left\{\mu(z)\left(-\frac{\partial w}{\partial r}\right)^n + \tau_o\right\}\right] = 0 \qquad (7)$$

Where τ_o is the yield stress , r and z is the radial and axial coordinate respectively, p is pressure and $\mu(z)$ is the viscosity of blood.

The expression for velocity profiles w ,by integrating equation (7) and using conditions (6), can be obtained as

$$w = A\left\{\left[\frac{R(z)\ P}{2} - \tau_o\right]^{1+1/n} - \left[\frac{r\ P}{2} - \tau_o\right]^{1+1/n}\right\} \qquad (8)$$

where $A = \dfrac{2}{P \ (1+1/n)[\mu(z)]^{1/n}}$ $\quad and \quad P = \dfrac{\partial p}{\partial z}$.

The **flow rate** Q is given by

$$Q = \pi \ \int_0^{R(z)} r^2 \left(-\dfrac{dw}{dr}\right) \ dr$$

$$= C \left[\dfrac{R(z)^2}{2}\left\{\dfrac{R(z) \ P}{2} - \text{T}_\text{o}\right\}^{1+1/n} - \right.$$

$$\dfrac{2 \ R(z)}{(2+1/n) \ P}\left\{\dfrac{R(z) \ P}{2} - \text{T}_\text{o}\right\}^{2+1/n} +$$

$$\dfrac{4}{(2+1/n)(3+1/n)P^2}\left[\left\{\dfrac{R(z) \ P}{2} - \text{T}_\text{o}\right\}^{3+1/n} - \right.$$

$$\left.\left. (-\text{T}_\text{o})^{3+1/n}\right]\right] \qquad (9)$$

Where $\quad C = \dfrac{4 \ \pi}{(1+1/n) \ [\mu(z)]^{1/n} \ P}$

The **pressure gradient** can be obtained as:

$$P = \dfrac{\partial p}{\partial z} = \dfrac{2 \ Q^n \ \mu(z)}{\pi^n I(r)^n} \qquad (10)$$

Where $I(r) = \int_0^{R(z)} r^2 \left[r - \dfrac{2 \ \text{T}_\text{o}}{P}\right]^{1/n}$

To obtain **pressure drop** (Δp), integrating equation (10) under the conditions:

$p = p_\text{o}$ at $z = 0$ $\quad$ and at $z = \ell$, $\quad p = p_\ell$ (11)

Integrating eq. (10) under boundary conditions (11), we get

$$\Delta p = p_\ell - p_\text{o} = \dfrac{2 \ Q^n}{\pi^n} \int_0^\ell \dfrac{\mu(z)}{I(r)^n} \ dz$$

Following Burton [3] and Young [13] , the **resistance to flow** is :

$$\lambda = \dfrac{\Delta p}{Q} = \dfrac{2 \ Q^n}{\pi^n} \int_0^\ell \dfrac{\mu(z)}{I(r)^n} \ dz$$

Now resistance to flow at $r = R(z)$ and at extreme stenosis height is

$$\lambda_\text{R} = \dfrac{2 \ Q^n}{\pi^n} \int_0^\ell \dfrac{\mu(z)}{I(R)^n} \ dz \quad at \quad z = d + \dfrac{\ell_\text{o}}{2}$$

For normal artery, the resistance to flow is is given by

$$\lambda_N = \dfrac{2 \ Q^n}{\pi^n} \int_0^\ell \dfrac{\mu(z)}{I(R_\text{o})^n} \ dz$$

Where $I(R) = \int_0^{R(z)} r^2 \left[r - \dfrac{2 \ \text{T}_\text{o}}{P}\right]^{1/n} dr$ and

$I(R_\text{o}) = \int_0^{R_\text{o}} r^2 \left[r - \dfrac{2 \ \text{T}_\text{o}}{P}\right]^{1/n} dr$.

Thus the ratio of resistance to flow is

$$\lambda' = \dfrac{\lambda_\text{R}}{\lambda_N}$$

The **wall shear stress** is given by

$$\text{T}_w = \mu(z)\left(-\dfrac{\partial w}{\partial r}\right)^n + \text{T}_\text{o} \quad at \ r = R(z)$$

$$= \dfrac{R(z)}{2}\dfrac{\partial p}{\partial z}$$

Now using equation (12), we have

$$\text{T}_w = \dfrac{R(z)Q^n \ \mu(z)}{\pi^n I(R(z))^n}$$

From it, wall shear stress at extreme stenosis height is

$$\text{T}_{ws} = \dfrac{R(z)Q^n \ \mu(z)}{\pi^n I(R(z))^n} \quad at \ z = d + \dfrac{\ell_\text{o}}{2}$$

For normal artery, the wall shear stress is given by

$$\text{T}_N = \dfrac{R_\text{o} \ Q^n \ \mu(z)}{\pi^n I(R_\text{o})^n}$$

So the ratio of wall shear stress is

$$\text{T}' = \dfrac{\text{T}_{ws}}{\text{T}_N} = \dfrac{R(z)}{R_\text{o}}\left(\dfrac{I(R_\text{o})}{I(R(z))}\right)^n$$

III. RESULTS AND DISCUSSION

The analytical expressions for flow rate, resistance to flow and wall shear stress have been derived and computed numerically. The numerical solutions are presented in graphical form.

Figs.2-7 reveals the variation of flow rate (Q) with stenosis height to radius ratio (δ/R_o) and axial distance to radius ratio (z/R_o) for different values of n, α and T_o . It is clear that increment in n, α and T_o decreases the flow rate with increment in stenosis height . Also on increasing axial distance ,the flow rate first decreases and then increases in the non stenotic region for different values of n, α and T_o.

Figs.8-10 shows that resistance to flow increases on increasing the stenosis height. It is clear that resistance to flow decreases on increment of

pressure gradient and it increases on increment of n and Υ_o .

Figs.11-13 shows that wall shear stress increases as the stenosis height increases for fixed values of n, P and Υ_o .

Fig.2 Profiles for Q against δ/Ro for different values of α

Fig.3 Profiles for Q against δ/Ro for different values of Υ_o .
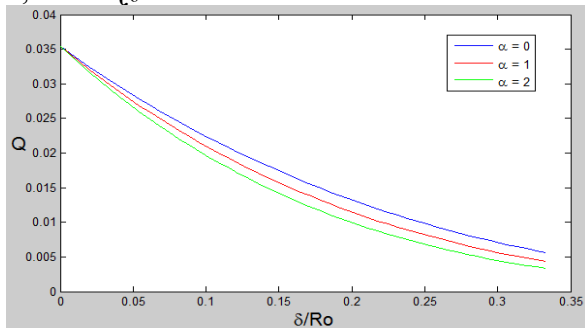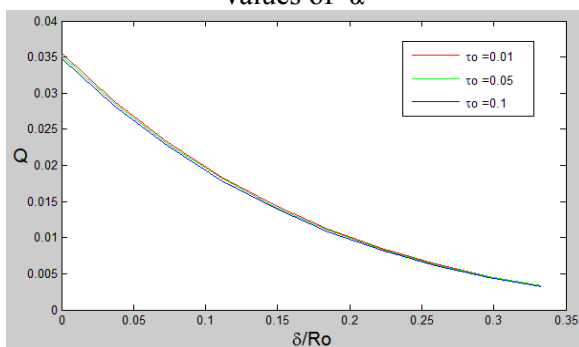

Fig.4   Profiles for Q against δ/Ro for different values of n .

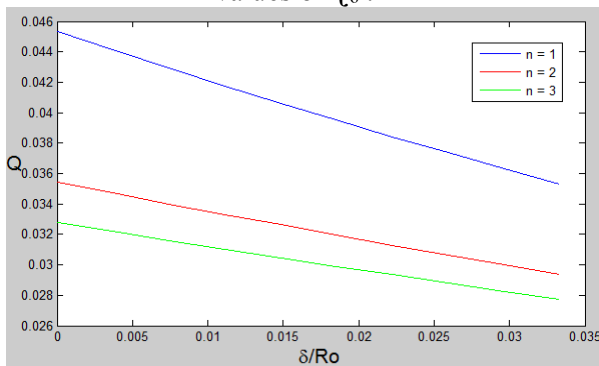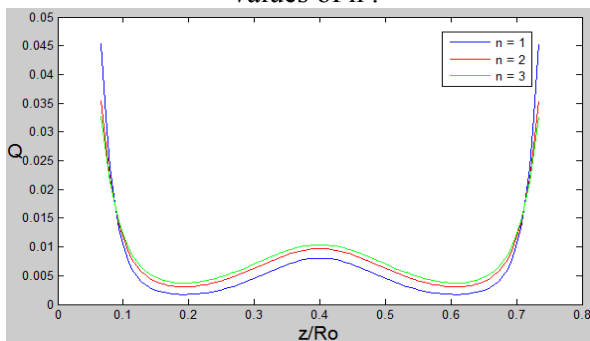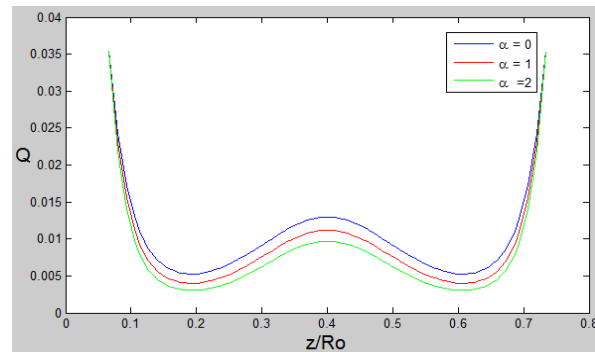
Fig.5 Profiles for Q against z/Ro for different values of n .

Fig.6 Profiles for Q against z/Ro for different values of α .

Fig..7 Profiles for Q against z/Ro for different values of Υ_o

Fig.8 Profiles for λ' against δ/Ro for different values of pressure gradient (P= $\frac{\partial p}{\partial z}$).

Fig.9 Profiles for λ' against δ/Ro for different values of n .

Fig.10 Profiles for λ' against δ/Ro for different values of Ƭₒ .

Fig.11 Profiles for Ƭ' against δ/Ro for different values of n.
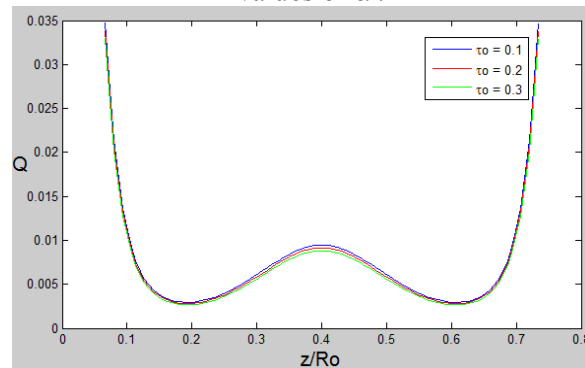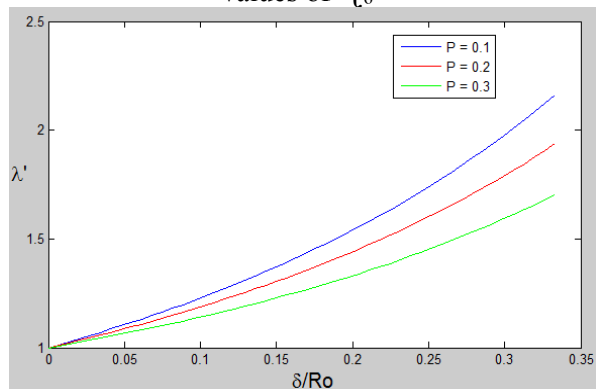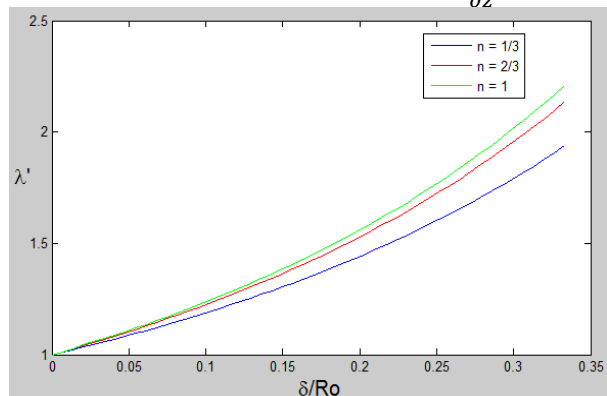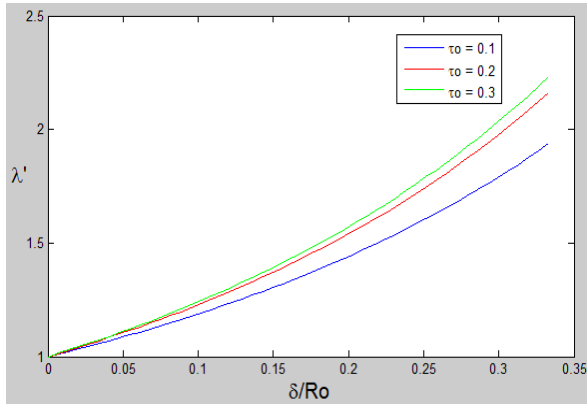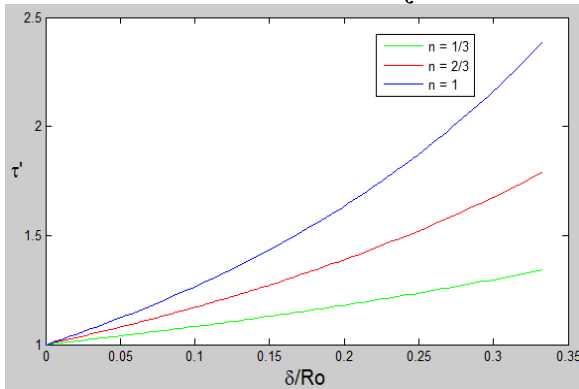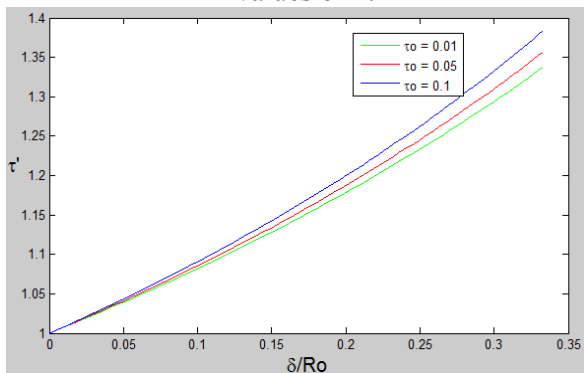

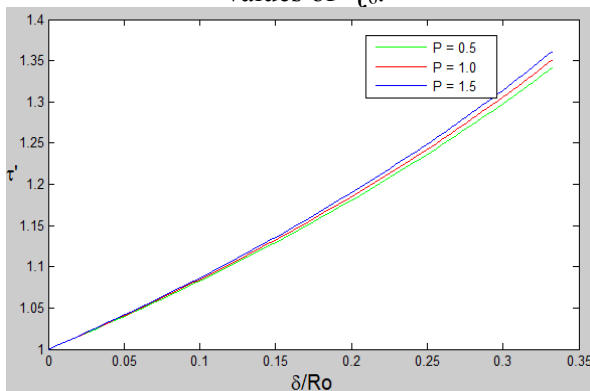Fig.12 Profiles for Ƭ' against δ/Ro for different values of Ƭₒ.

Fig.13 Profiles for Ƭ' against δ/Ro for different values of pressure gradient (P= $\frac{\partial p}{\partial z}$).

IV.   CONCLUSION

A non-Newtonian fluid (Herschel-Bulkley) model has been applied to investigate the effects on axial viscosity variation of blood flow due to the presence of an overlapping stenosis in arteries. The analytical expression is obtained for the flow rate, resistance to flow and wall shear stress and results are discussed on the basis of graphical presentation. It is found that flow rate decreases, resistance to flow increases and wall shear stress increases as the stenosis height is increased. Flow rate of the fluid first decreases as the axial distance increases and then it increases with the value of axial distance and attains its minimum value when stenosis size is maximum within the stenosis region. This study may be beneficial in the field of medical sciences as the medical scientists do not have precious information about various flow parameters of blood.

REFERENCES

[1]   Barnett, B. and Han, C.D.(1973) , Measurement of the rheological properties of biological fluids, In Rheology of Biological Systems, (Edited by H.L. Gabelnick and M. Litt), p. 195, Charles C. Thomas, Illinois.

[2]   Blair, G.W.S., Spanner, D.C.,(1974), An introduction to Biorheology.Elsevier., Amsterdam..

[3]   Burton, A.C. (1968): Physiology and Biophysics of the circulation, *Year Book Medical Publishers, Inc., Chicago*.

[4]   Chakravarty, S. and Mandal, P.K.,(1994), Mathematical modelling of blood flow through an overlapping arterial stenosis, Mathl. Comput. Modelling 19 (1) 59-70 .

[5]   Chaturani, P., PonnalagarSamy,R., (1985), A study of non-Newtonian aspects of blood flow through stenosed arteries and its applications in arterial diseases .Biorheol.,Vol.22,pp. 521-531.

[6]   Gupta, S., Gupta, M. and Singh, S.P. (2012): Effect of radial viscosity variation on non-Newtonian flow of blood in a stenosed artery, International Journal of Applied Mathematics and Mechanics, 8(2), pp. 51-61.

[7]   Jain, N., Singh, S.P. and Gupta, M. (2012): Steady flow of blood through an atherosclerotic artery: A non-Newtonian fluid model, International Journal of

Applied Mathematics and Mechanics, 8 (18), pp. 52-63.

[8] Layek, G. C., Mukhopadhyay, S. and Gorla, R. S. D. (2009). Unsteady viscous flow with variable viscosity in a vascular tube with an overlapping constriction. Int. J. Engng. Sci. 47, pp. 649-659

[9] Mishra, J.C. and Shit, G.C. (2005): Blood flow through arteries in a pathological state: A theoretical study, International Journal of Engineering Science, vol. 44, pp. 662-671.

[10] Nallapu S.,Radhakrishnamacharya G.,(2014),Herschel-Bulkley fluid flow through narrow tubes ,Central European Journal Of Physics,pp. 1-12

[11] Shukla JB, Parihar RS, and Gupta SP (1980). Effects of peripheral layer viscosity on blood flow through the artery with mild stenosis, Bulletin of Mathematical Biology 42, pp. 797-805.

[12] Srivastava, V. P. (1996). Two-phase model of blood flow through stenosed tubes in the presence of a peripheral layer: applications, Journal of Biomechanics, Vol. 29, pp. 1377-1382.

[13] Young, D.F. (1968),Effects of a time dependent stenosis on flow through a tube, Journal of Engineering for Industry,Vol. 90,Issue 1,pp. 248-254

PERFORMANCE AND COMPRESSION OF A NOVEL DESIGN WITH HYBRID LOGIC STYLE FOR ULTRA-LOW POWER

Atul kumar Pathak[1], Mukesh Kumar Silwat[2], Umesh Singh Sikarwar[3]
[1]Research Scholar, Electronics and Comm. Dept, NITM Gwalior India
[2]Research Scholar, Electronics and Comm. Dept, RJIT Tekanpur Gwalior India
[3]Assistant Professor, Electronics and Comm. Dept, SRIIT Gwalior India
Email: atulya_pathak@yahoo.co.in[1], mukesh.kumar971364@gmail.com[2],
umesh18sep@gmail.com[3]

Abstract

Full adder is the basic digital components for the region many improvements have been made to improve its architecture. In this paper, we present new adder logic style without losing the characteristic of the basic circuits with 8 transistors. The main design objectives for these adder cell modules are providing Low-Power dissipation, high speed with full-voltage swing without using extra elementary growth on design. In this design, we employed with 8 transistors. The utilizes dynamic change in the width Length ratio in order to get specified results new full adders with new methodology. This design is based on a different new approach which eliminates the need of XOR/XNOR gates for designing full adder cell; it provides high speed and Ultra Low-Power, as well as a full voltage swing without any extra component required. Many of the previously reported adders in literature suffered from the problems of extra elements required to full-fill the circuit recruitment like voltage-swing and speed when operated at low supply voltages. This new designs successfully operate at ultra low voltages. The studied circuits are optimized at 45nm and 90 nm PTM (Tanner). The comparison between these two novel circuits in terms of Power, Delay

Keywords: Propagation delay, Power consumption, Power-Delay-Product, 8T Novel Adder design, Hybrid design style.

1. Introduction

Addition is a very basic operation in arithmetic. Most of the operations based on addition. With these operations we need to minimize the power consumption and increasing speed of the system without further growth on the chip area, the low power requirement of VLSI system design have challenged the area of research towards technology, architectural design and methodology solution to allow reduce energy dissipation on CMOS Circuits. Since the full adder cell is performing regularity in the CMOS functional units, improving the performance of the 1-bit full adder is a major goal and has attracted much attention. A variety of full adders using different architectural designs and technologies have been reported in literature [1]

and they commonly aim to tradeoff between energy consumption and propagation delay. Adder performance affects the arithmetic system and functional units such as multiplier ALU etc. An optimized design is required to prevent any reduction in the output signal, consume less power, have less delay in critical path and be reliable even at low supply voltage as we scale towards nano-meter, layout regularity, and interconnect complexity are also primary concern. By scaling down the feature size of devices in nanometer, the supply voltage should be scaled down to avoid effects of hot carrier in CMOS circuitry. As a result, transistor size and static power playing main role in nano-scale circuits for efficient power control [2].

II Literature Review

Hybrid full adder

In this section shows an ultra Low-Power Hybrid full adder circuit with XOR-XNOR topology. SEMI-XOR gate generate the first four states and last four states generated by SEMI-XNOR gate of the SUM output. As depicted in Table 1, in order to design the SUM circuit, these SEMI XOR-XNOR gates employed with C_{in} input used as an enable signal. When C_{in} is equal to zero, the SEMI-XOR gate is similar to the SUM, and when C_{in} is equal to one, the SEMI-XNOR gate is the output of the SUM circuit. According to Fig. 1 the circuits of these gates and the table 1 shows the Truth-Table of these two gates When we connect the SEMI-XNOR gate output to the single NMOS transistor, where the source/ drain of this transistor is connected to SUM output and its drain/ source is connected to the C_{in} the high impedance states in the output will we set to the correct value. As shown in Fig. 2, in order to provide full-swing voltage at SUM and C_{out}, we take in the structure of this hybrid full adder cell. As it is apparent, this novel hybrid adder cell minimizes the static power consumption by improving W/L ratio and eliminating any possible direct path between V_{dd} and the ground due to the use of NMOSs and PMOSs in a complementary manner.
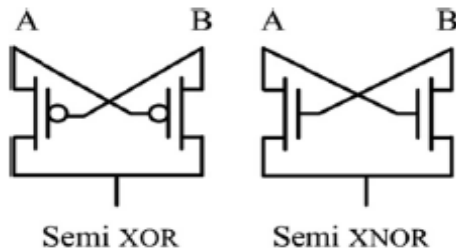
Fig. 1 Semi XOR and Semi XNOR Gate

By utilizing this technique, when one part of the circuit is on other one is in the off situation, so there is no short-circuit current.

A	B	SEMI XOR	SEMI XNOR
0	0	0	HZ
0	1	1	0
1	0	1	0
1	1	HZ	1

Table: 1 Truth Table of SEMI XOR and SEMI XNOR Gate
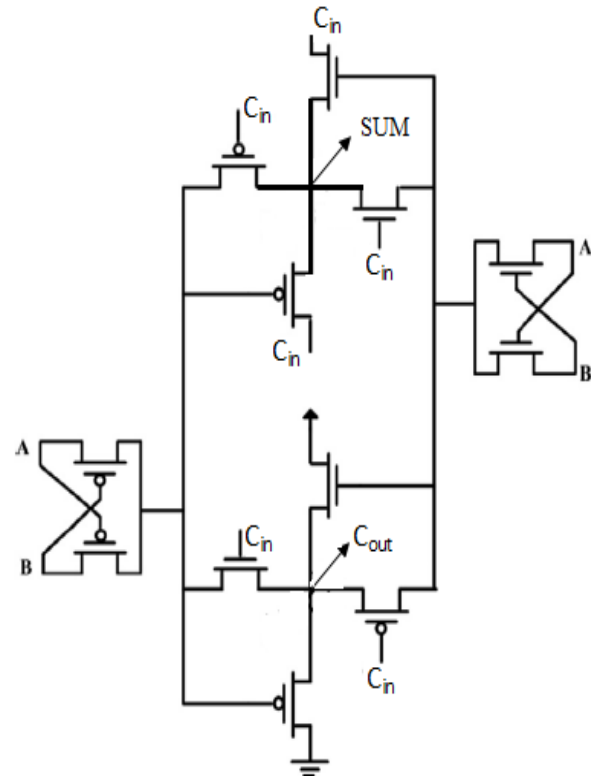
Fig. 2 hybrids Full Adder

This design uses 12 transistors with dynamic W/L of transistor. We are eliminating UPLD circuit from the design and utilize the basic property of the CMOS transistor in this proposed methodology has low energy dissipation and speed without extra circuitry use.

III Proposed Design

In this work, existing 8T full adder is modified to address their discharging problem with changing through dynamic width Length ratio output for the all combinations of the inputs. Before having a detailed understanding of working principle of proposed 8T full adder we need to be aware of the design and its working principle of the existing PRPOSE-8T full adder which is as shown in the Figure.3 and it is explained as follows. This full adder is designed using combination of transistors to get appropriate result. First block generate the out of input A and B as output of XOR between them and further XOR with C_{in} so we get output Sum but discharging are not in suitable value so next cycle of result not in get proper voltage level here we introduce third extra transistor to improve this discharging problem.

Performance of the 1-bit full adder cell is a significant goal. Thus in this work 8 transistors full adder is proposed which addresses the discharging problem at the output for the particular combinations of the inputs in the existing full adder design. The proposed 8T full adder is implemented using the 90nm and 45nm technology library and is simulated & verified. It observed from the simulation results that the proposed 8T full adder outperforms the other existing full adders in terms of power consumption, delay PDP (power delay product) and transistor count.
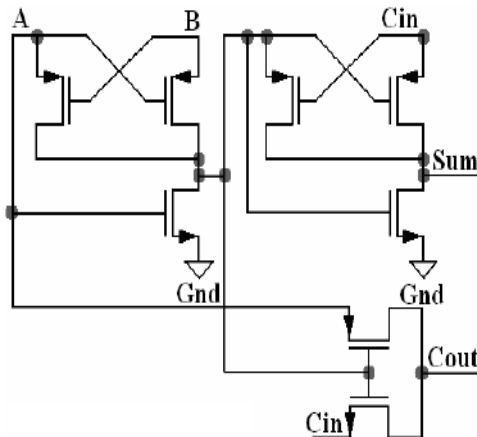
Fig. 3 PROSOSE-8T Full Adder

IV Simulation results and analysis

In this section, the proposed full adder cells shown in Fig. 8 is evaluated and compared to the ones chosen from the literature is shown in fig. 5 both the circuits are implemented using Tanner EDA and extracted using 90nm and 45 nm PTM CMOS technology.
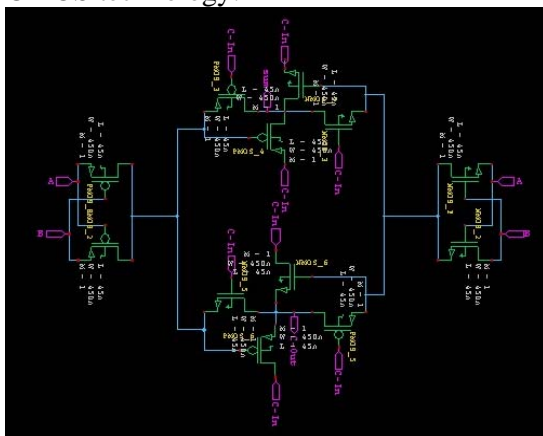
Fig. 5 Schematic Design of hybrid Full Adder
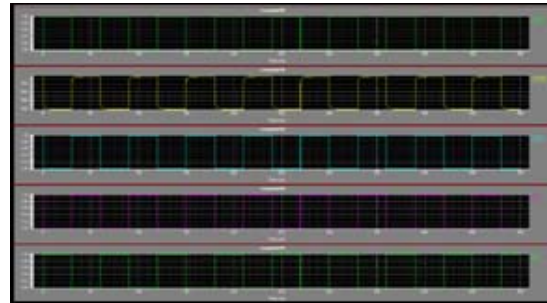
Fig. 6 Simulation Wave form of hybrid Full Adder at 45nm
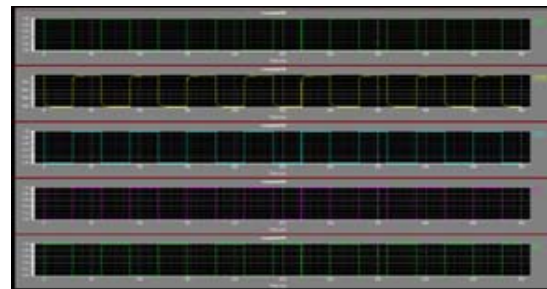
Fig. 7 Simulation Wave form of hybrid Full Adder at 90nm
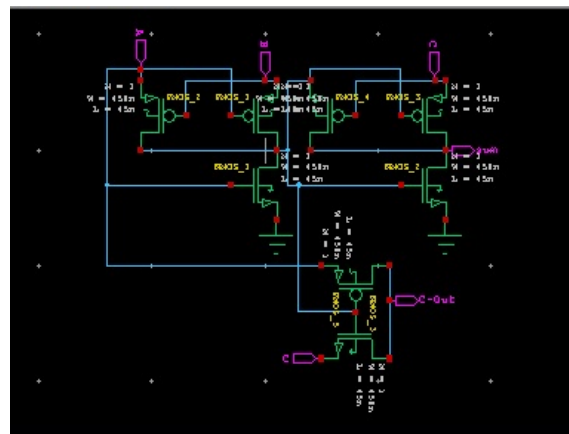
Fig. 8 Schematic Design of PROPOSE 8T Full Adder
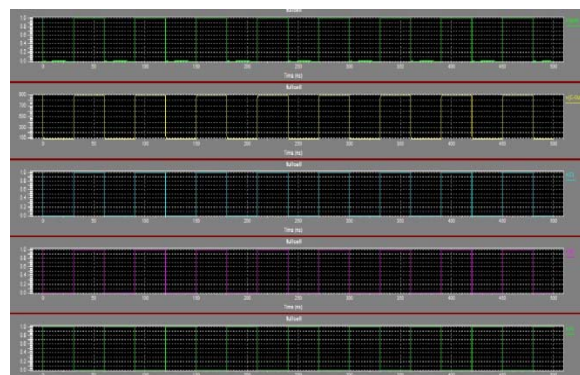
Fig. 9 Simulation Wave form of PROPOSE 8T Full Adder at 45nm
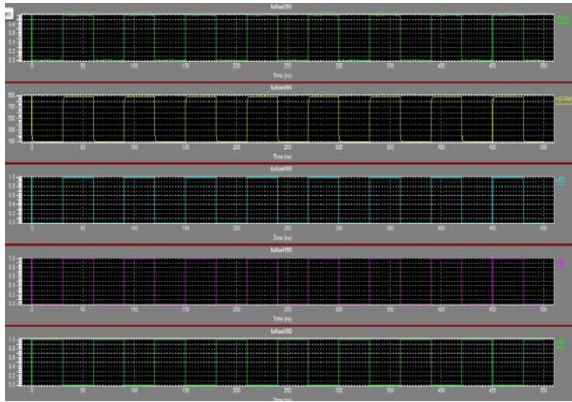
Fig. 10 Simulation Wave form of PROPOSE 8T Full Adder at 90nm

Design	Delay ($\times10^{-11}$s)	Power ($\times10^{-6}$W)	PDP ($\times10^{-17}$ J)	Vdd V
Hybrid	*2.080*	0.396	0.824	0.7
PROPSE-8T	*2.215*	0.322	0.714	0.7

Table: 3 Hybrid and PROPOSE-8T Results at 90nm

Design	Delay ($\times10^{-11}$s)	Power ($\times10^{-6}$W)	PDP ($\times10^{-17}$ J)	Vdd V
Hybrid	*1.877*	.360	0.675	0.7
PROPSE-8T	*2.012*	0.278	0.559	0.7

Table: 4 Hybrid and PROPOSE-8T Results at 45nm

According to Simulation results we are able to measure power delay product (PDP) through Delay and Power multiplication for Hybrid Full adder and PROPOSE-8T Full Adder. PROPOSE-8T provide better PDP, Voltage Swing Compare to Hybrid Full Adder but the same time PROPOSE-8T lacking on the Basis of Propagation

Delay

Delay by the hybrid full Adder technique. For each transition, the delay is measured from 50% of the input voltage swing to 50% of the output

voltage swing. It is apparent that among the existing full adders, the proposed full adder cell has the smallest delay because of just having two transistors in the critical path for driving the output. The PROPOSE-8T full adder follows the hybrid adder in outperforming the other four full adder cells in delay. Propose full adder in shows the least delay because of remving a XOR-XNOR design to produce internal signals, which is based on complementary pass transistor logic (CPL).The first half

Power

The proposed 8T full adder shows the best performance among the above mentioned full adders under varying supply voltages. The PROPOSE-8T- full adder utilizes PROPOSE-8T structure as its main cell which is proved in to be one of the lowest power consumer cells that not only is suitable for designing fast, Low- Power circuits but also improves logic level swing and static power characteristics. Hybrid full adder cell follows PROPOSE-8T full adder in outperforming the other full adder cells in power consumption. The Hybrid full adder cell consume slow static power due to removal of any direct path between Vdd and the ground by employing NMOSs and PMOSs in a complementary manner. The PROPOSE-8T full adder shows minimum power consumption at all supply voltages when compared to the Hybrid full adder.

Power-Delay-Product (PDP)

The PDP is a quantitative measure of the efficiency and a compromise between power dissipation and speed. PDP is particularly important when low power operation is needed. The Power-Delay- Product for Hybrid full adder in two full adder cells is evaluated under different supply voltages (0.8–1.4V) in 90nm and (0.6–1.2V in 45nm. Illustrate the values of PDP of the 1-bit adder based on each full adder cells. Tables 3 and 4 illustrate the values at 0.7V for 90 nm and 0.7 for 45nm. As shown the PROPOSE-8T full adder has the best PDP in comparison with its counterpart.

Conclusion

In this paper two novel full adder cells using PROPOSE-8T structure and hybrid CMOS logic style for Low-Power application are proposed. These two new designs successfully operate at low voltages with tremendous signal integrity and driving capability. The circuits being studied are optimized for energy efficiency at 90nm and

45nm PD SOI CMOS process technology. Simulations have been performed on PTM to evaluate the new designs. Hybrid full adder in and. A broad comparison to the state of the art designs cited in the VLSI literature illustrates a significant improvement in terms of power dissipation and Power- Delay product (PDP) parameter. The number of transistors used is significantly reduced resulting in a great reduction in switching activity and area. This considerable reduction in power by minimizing static and dynamic power dissipation as well as some techniques to enhance the speed of the design leads to the best PDP.

References

[1] R. Shalem, E.John, L.K.John, A novel low-power energy recovery full adder cell, in: Proceedings of the Great Lakes Symposium on VLSI, February 1999, pp. 380–383.

[6] R.X. Gu, M.-I.Elmasry, Power dissipation analysis and optimization of deep submicron CMOS digital circuits, IEEE Journal of Solid-State Circuits 31(5) (1996)707–713.

[3] V. Dessard, SOI Specific Analog Techniques for Low-noise ,High-temperature or Ultra-low Power Circuits, Ph.D. Thesis, UCL, Louvain, Belgium,2001.

[4] D. Hassoune, I.O Flandre, Connor, J.D.Legat, ULPFA: a new efficient design of a power-aware full adder, IEEE Transactions on Circuits and Systems—I: Regular Papers 57 (8) (2010).

[5] V. Kilchytska, D.Levacq, L.Vancaillie, D.Flandre, On the great potential of non- doped MOSFETs for analog applications in partially-depleted SOI CMOS process, Solid State Electronics 49 (5) (2005) 708–715.

[6] J.-M. Wang, S.-C.Fang, W.-S.Feng, New efficient designs for XOR and XNOR functions on the transistor level, IEEE Journal of Solid-State Circuits 29 (7) (1994) 780–786.

[7] Arkadiy Morgenshtein, A.Fish, Israel A.Wagner, Gate-diffusion input (PROPOSE-8T): a power-efficient method for digital combinatorial circuits, IEEE Transactions on VLSI Systems (2002) 566–581.

[8] Vahid Foroutan, Mohammad Reza Taheri, KeivanNavi, Arash Azizi Mazreah, Design of two Low-Power full adder cells using PROPOSE-8T structure and hybrid CMOS logic style, INTEGRATION, the VLSI journal 47(2014)48–61.

EFFECT OF HARDNESS ON TENSILE STRENGTH OF V-NOTCHED SUP 9A BAR

Adviteeya Gupta[1], Premanand S. Chauhan[2], Prabhu Dayal Arya[3]
[1]P.G Scholar, Dept. of Mechanical Engg.,IPS College of Technology and Management, Gwalior
[2]Prof., Dept. of Mechanical Engg., IPS College of Technology and Management, Gwalior
[3]Associate Prof., Dept. of Mechanical Engg., IPS College of Technology and Management, Gwalior
Email:adviteeya.gupta@gmail.com[1], prempunit@gmail.com[2]

Abstract-This article summarised the tensile test of notched bars manufactured from SUP 9A Spring Steel. The effects of notch and hardness on the tensile strength of this spring steel have been examined. The experimental results indicate that fracture initiate at the notched section. Experimental result also indicates that there is an impact of variation of hardness on the tensile strength of material. After increasing the hardness tensile strength of material has been increased. The experimental test is done on Universal Testing Machine.

Keywords- Hardness; Notch Bar; Tensile Strength; SUP 9A; UTM.

I. Introduction

SUP 9A is a spring steel used to manufacture torsion bar or stabilizer bar. The chemical compositions of this material are Carbon 0.56-0.64%, Silicon 0.15-0.35%, Manganese 0.7-1% and Chromium 0.7-1%. Spring steel is used in some of the smaller aircraft's landing gear due to its ability to absorb the shock from landing and also acts like damping. Typical uses include saw blades, tape measures, helical springs, and vehicle suspension elements. Spring steel alloys feature the unique characteristic of being able to withstand considerable twisting or bending forces without any distortion. Products made from this steel alloys can be bent, compressed, extended, or twisted continuously, and they will return to their original shape without suffering any deformation. This characteristic is defined as high yield strength and is the result of the specific composition and hardening of the steel alloy. The other alloy additives typically include manganese and silicone with silicone being the key component in high yield strengths.

Notch is a small cut that is shaped like V and U and that is made on an edge or a surface. The notch effect increases stress in an area of a component near a crack, depression, etc. or a change in section, such as a sharp angle. It can be enough to cause failure of the component although the calculated average stress may be quite safe. Carpinteri et al., (2006) examined the behaviour of a notched round bar with a part-through crack under both tension and bending. The Stress Concentration Factor (SCF) due to the circumferential groove has been computed. In order to obtain the Stress-Intensity Factor (SIF) distribution for different values of the SCF and crack geometries, a three-dimensional finite element analysis has been performed. The notch effect on the SIF is significant for any crack size and shape. Fatigue life for a notched bar is shorter than that for an unnotched bar in the case of tension, while the opposite occurs in the case of bending. Zappalorto et al., (2008) concluded the analytical expressions for the notch stress intensity factors as due to deep circumferential sharp V-notches under torsion loading have been found starting from the expressions of the theoretical stress concentration factor of a hyperbolic notch.

II. Process

A. Heat treatment

Heat treatment is an operation or combination of operations involving heating at a specific rate, soaking at a temperature for a period of time and

cooling at some specified rate. The aim is to obtain a desired microstructure to achieve certain predetermined properties (physical, mechanical, magnetic or electrical). Steels can be heat treated to produce a great variety of microstructures and properties. Generally, heat treatment uses phase transformation during heating and cooling to change a microstructure in a solid state. In heat treatment, the processing is most often entirely thermal and modifies only structure.

Quenching and Tempering: Martensitic transformation, more commonly known as quenching and tempering, is a hardening mechanism specific for steel. The steel must be heated above recrystallization temperature where the iron phase changes from ferrite into austenite, i.e. changes crystal structure from BCC (body-centered cubic) to FCC (face centered cubic). In austenitic form, steel can dissolve a lot more carbon. Once the carbon has been dissolved, the material is then quenched. It is important to quench with a high cooling rate so that the carbon does not have time to form precipitates of carbides. When the temperature is low enough, the steel tries to return to the low temperature crystal structure BCC. This change is very quick since it does not rely on diffusion and is called a marten sitictrans formation. Because of the extreme super saturation of solid solution carbon, the crystal lattice becomes BCT (body-centered tetragonal) instead. This phase is called marten site, and is extremely hard due to a combined effect of the distorted crystal structure and the extreme solid solution strengthening, both mechanisms of which resist slip dislocation.

Recrystallization Temperature:
0.5-0.7 T_m for recrystallization of alloy.

Where,
T_m is melting point in Kelvin of alloy.
B. Tensile Testing
The most common testing machine used in tensile testing is the universal testing machine. This type of machine has two crossheads; one is adjusted for the length of the specimen and the other is driven to apply tension to the test specimen. The machine must have the proper capabilities for the test specimen being tested. There are four main parameters: force capacity, speed, and precision and accuracy. Force capacity refers to the fact that the machine must be able to generate enough force

to fracture the specimen. The machine must be able to apply the force quickly or slowly enough to properly mimic the actual application. The test process involves placing the test specimen in the testing machine and slowly extending it until it fractures. During this process, the elongation of the gauge section is recorded against the applied force. The elongation measurement is used to calculate the engineering strain, ε, using the following equation

$$\epsilon = \frac{\Delta L}{L_0} \quad \text{………………...……………….……} (1)$$
$$\epsilon = \frac{L-L_0}{L_0} \text{……………………………….…… } (2)$$

Where,
ΔL is the change in gauge length,
L_0 is the initial gauge length,
L is the final length.
The force measurement is used to calculate the *engineering stress*, σ, using the following equation.
$$\sigma = \frac{F_n}{A} \text{…………………………………… } (3)$$
Where,
F_n is the tensile force
A is the nominal cross section of the specimen.
The machine does these calculations as the force increases.

III.   **Literature Review**

There are several types of experimental and research works have been developed to analyse the effect of hardness and notch on strength of alloy steels. In spite of the fact that the fracture tests on the notched bars have been conducted to analyse the effect of hardness on strength of bar but no studies have been found within the literature on SUP 9A. An extensive review and discussion of work have been done on the effect of hardness and of notch on strength of alloy steel. The details are as follows:

Nord et al., (1986) concluded stress intensity solutions for a surface flaw in a round bar and a threaded round bar. Loading cases include tension and pure bending. A finite element method, utilizing displacements in standard quadratic isoparametric elements adjacent to the crack edge, is used. The author presented results, in dimensionless format, which will be useful for determining fatigue life in various bolt and pin applications.

Zhang et al., (1992) concluded in terms of the spherical section by making an assumption, for an effective method for determining the local stress and limit load of a thick walled tube with an external hoop direction U shaped notch under tension, and discusses the relationships of the stress concentration factor with notch depth t, radius ϱ of the notch root and the internal radius of the tube. The expressions for the elastoplastic local stress and limit load are proposed.

Othman et al., (1993) studied constitutive equations in which the stress level dependence of creep rate is described by a sinh function, and two damage state parameters are used to model the tertiary softening caused by: (i) grain boundary cavity nucleation and growth, and (ii) the multiplication of mobile dislocations. These constitutive equations are applicable to polycrystalline nickel based super alloys and are used together with a continuum damage mechanics finite element based solver, DAMAGE XX, to study the behaviour of axis symmetrically notched tension bars and simulate the complex stress states that may be encountered at geometrical stress raisers in high temperature components. Numerical studies of such bars show that their behaviour can be accurately represented in terms of a 'skeletal effective stresses' located at a point within the notch throat, and the stress state at this point. Authors believe that this conclusion is valid not only for those materials that fail by grain boundary cavitation alone, but also for materials such as super alloys where grain boundary cavitation is accompanied by mobile dislocation multiplication.

Hayhurst et al., (1994) studied the range of applicability of the skeletal stress technique as a means of predicting the creep life time of a circumferentially notched tension bar subjected to steady load. The skeletal stress approach involves the quantification of the effective stress Σc and its ratio with the maximum principal tension stress Σl at a point, known as the skeletal point, at the throat of the notch. The stress Σc and stress state Σl/Σe at the skeletal point are assumed to remain constant and to determine the notched bar life time, which is determined by direct integration of the constitutive equations. It is also shown that the stress level applied to the bar, and the strength of the dislocations offending damage mechanism, denoted by a second damage variable ω1, also influences the above behaviour. Authors define

the bounds of applicability for the skeletal stress approach to life time prediction, and recommended the use of complete CDM finite element analysis for those situations where breakdown occurs.

Lin et al., (1998) studied fatigue crack growth for various cracks in both unnotched and notched round bars by using an automated numerical technique, which calculates the stress intensity factors at a set of points on the crack front through the three dimensional finite element method and then applies an appropriate fatigue crack growth law to this set of points to obtain a new crack front. This technique also has the capability of automatic remeshing so that the crack propagation can conveniently be followed. A surface crack in different semi circularly notched bars under both tension and bending, a surface crack initiated from the root of a V notched bar and an initially twin crack configuration within a smooth tension bar. Some fatigue growth characteristics relevant to each type of cracks are also revealed. It is demonstrated that the fatigue growth analyses of various cracks commonly occurring in bars can reliably be made by using the automated finite element technique proposed.

Tanaka et al., (1998) studied the *R*-curve method for predicting the fatigue thresholds of notched components was under combined loading of cyclic torsion and tension-compression. The prediction was compared with the experimental data obtained from thin-walled tubular specimen with a hole under the combination of cyclic torsion and axial loading. The experimental data agreed well with the prediction both for crack initiation and fracture. The measured length of non-propagating crack had some scatter and the maximum length agreed fairly well with the predicted line. The non-propagating crack length normalized with the hole radius at the threshold stress for fracture was predicted fairly constant without respect to the hole size, while it varies slightly with the loading condition. The effect of the in-phase combination of axial and torsional stress loadings on the fatigue threshold was predicted by assuming the crack direction perpendicular to the maximum principal stress.

Lin et al., (1999) studied the shape of the fronts of surface cracks in semi circularly notched round bars under fatigue loading by a numerical procedure developed by the authors. This

procedure utilizes a linear elastic three dimensional finite element analysis to estimate the stress intensity factor along the crack front, and then employs an experimental Paris type fatigue crack growth relation to calculate local crack advances at a few points along the crack front. Recreating a finite element model for the new crack front and repeating the calculation of the crack growth increment simulates further crack propagation. This method can avoid making the usually necessary assumption of crack shape during the fatigue life calculation for surface cracks in notched round bars. Both remote cyclic tension and bending loads are considered. Characteristics of the crack shape change are also investigated by examining deviations of the crack profiles from the widely assumed elliptical arc shape, and aspect ratio changes with crack growth.

Durmus et al., (2002) marked that circumferentially notched cylindrical specimens can be readily used for rapid determination of fracture toughness of metallic materials. Fracture toughness measurement of metallic materials by using circumferentially notched round specimens is observed to be an accurate and reliable procedure.

Carpinteriet al., (2004) studied the stress field in a structural component depends on the possible presence of a notch, and fatigue life may strongly be affected by geometric discontinuities. A circular-arc circumferential notch in a round bar is considered here, and the Stress Concentration Factor (SCF) related to both tension and bending is determined. Then, an elliptical-arc surface flaw is assumed to exist at the notch root and, for different values of SCF, the Stress-Intensity Factor (SIF) along the crack front is computed through a three-dimensional finite element analysis. The effect of the stress concentration on the SIF values is discussed for the considered crack configurations. Finally, the surface crack propagation under cyclic loading is examined through a numerical procedure which takes into account the computed SIF values.

Webster et al., (2004) studied and finite element calculations have been performed to obtain the creep stress distributions generated in circumferentially notched bar test-pieces. They have also been made to determine the relation between axial extension and notch throat diameter changes. It has been found that an approximate

skeletal point can be identified where the stress state is insensitive to the power law stress dependence of creep. Consistent trends in skeletal point stress ratios to those given in an existing Code of Practice for notch bar creep testing have been obtained. In contrast the link between extension and notch throat diameter changes has been found to depend on the creep stress index as well as the notch geometry. It is anticipated that the analysis can be used to establish the multi-axial creep stress deformation and rupture behaviour of materials.

Atzori et al., (2006) studied the multi-axial fatigue strength of notched specimens made of C40 carbon steel (normalised state), subjected to combined tension and torsion loading, both in-phase and out-of-phase (Φ=0 and 90°). Authors tested V-notched specimens under two nominal load ratios, R=−1 and 0, while keeping constant and equal to the unity the biaxiality ratio, $\lambda=\sigma_a/\tau_a$. All specimens have the same geometry, with notch tip radius and depth equal to 0.5 and 4 mm, respectively, while the V-notch angle is equal to 90°. The results determined are discussed together with those deduced under pure tension or torsion loading on plain and notched specimens as well as on small shafts with shoulders. The application of an energy-based approach allows all the fatigue data obtained from the notched specimens to be summarised in a single scatter band, in terms of the total strain energy density evaluated at the notch tip against cycles to failure.

Carpinteri et al., (2006) analysed the influence of a circular arc circumferential notch in a pipe. Firstly, the stress concentration factor (SCF) is determined. Then, an elliptical arc external surface crack is assumed to exist at the notch root, and the stress intensity factor (SIF) along the surface crack front is computed for four values of the dimensionless notch radius and for several opening stress distributions on the crack faces. The effect of stress concentration on the SIF values is discussed for both thick and thin walled pipes.

Hayhurst et al., (2008) studied and concluded that two sets of constitutive equations are used to model the softening which takes place in tertiary creep of Nimonic 80A at 750^0 C. Softening by multiplication of mobile dislocations is firstly combined, for low stress, with softening due to nucleation controlled creep constrained cavity growth; and secondly combined, for high stress,

with softening due to continuum void growth. The Continuum Damage Mechanics, CDM, Finite Element Solver DAMAGE XX has been used to study notch creep fracture. Low stress notch behaviour is accurately predicted provided that the constitutive equations take account of the effect of stress level on creep ductility. High stress notch behaviour is accurately predicted from a normalized inverse cavity spacing $d/2 = 6$, and an initial normalized cavity radius rhi = $3.16 \cdot 10\_3$, where 2 is the cavity spacing, and d is the grain size; however, the constants in the strain rate equation required recalibration against high stress notch data. A void nucleation mechanism is postulated for high stress behaviour which involves decohesion where slip bands intersect second phase grain boundary particles. Both equation sets accurately predict experimentally observed global failure modes.

Carpinteri et al., (2008) studied the fatigue growth of a surface crack in a metallic round bar under cyclic tension or bending. The fatigue behaviour of the cracked bar is numerically determined by a step-by-step procedure. The propagation of an initial surface crack under cyclic tension or bending loading acting perpendicular to the crack plane is examined. The crack front is assumed to be described by an elliptical arc.

Carpinteri et al., (2009) studied a sickle shaped surface crack, also called crescent-moon (or crescent) crack, is assumed to exist at the root of a circular arc circumferential notch in a round bar under tension and bending. For different notch sizes (i.e. different values of the stress concentration factor), the stress intensity factor along the crack front is computed through a three dimensional finite element analysis. Authors examined the effect of the stress concentration factor for several crack configurations. Finally, the surface crack growth under cyclic loading is analysed through a numerical procedure that employs the stress intensity factor values obtained.

Tanaka et al., (2009) studied fatigue tests for circumferentially notched bars of austenitic stainless steel, JIS SUS316L, under cyclic torsion with and without static tension. For the case of cyclic torsion without static tension, the fatigue life of notched bars was found to be longer than that of smooth bars and to increase with increasing stress concentration under the same amplitude of the nominal torsional stress. This notch-

strengthening effect is anomalous for the conventional fatigue design criterion. On the other hand, the fatigue life decreased with increasing stress concentration, when the static tension was superposed on cyclic torsion. For the case of cyclic torsion without static tension, the crack propagation life increased with increasing stress concentration, while the crack initiation life decreased. The anomalous behaviour of the notch effect was ascribed to the larger retardation of fatigue crack propagation by crack surface contact for sharper notches. The superposition of static tension reduced the retardation due to the smaller amount of crack surface contact, which gave rise well-known notch-weakening of the fatigue strength.

Wang et al., (2010) studied that on performing tensile tests at room temperature on 20 notched bars fabricated from constructional steel Q235 specified in Chinese National Standards. The effect of the notch radius, r, and that of the notch depth ratio, d/D, on the fracture model of the constructional steel is examined by the authors. The experimental results demonstrate that cracks initiate at the notched section. Specimens with a sharper notch radius (a smaller r) and a larger notch depth (a smaller d/D ratio) show poor ductility, but high fracture strength. The experimental data are further analysed using an elliptical yield model together with an elliptical fracture model originally proposed by the first author. The stress field computed from the numerical procedure indicates that the crack initiation occurs at the centre of the notched section which experiences the highest stress triaxially ratio (óm/óseq). As the stresses at the notched section reach the limiting values determined from the elliptical fracture model, macroscopic fracture failure in the notched bar occurs.

Wang et al., (2010) analysed the uniaxial tension tests for 20 notched bars fabricated from high strength steel Q345 specified in Chinese National Standards. The effects of the notch radius, r, and that of the notch depth ratio, d/D, on the ductility and fracture resistance of this high strength steel are examined. The experimental data are further analysed using a generalized yield model together with an elliptical fracture stress envelope originally proposed by the first author. The experimental results demonstrate that cracks initiate at the notched section, with the fracture

surface filled with many dimples and shearing marks. Specimens with a sharper notch radius (a smaller r) and a larger notch depth (a smaller d/D ratio) show poor ductility, but high fracture strength. The stress field computed from the numerical procedure including the generalized yield model indicates that the crack initiation occurs at the centre of the notched section which experiences the highest stress triaxiality ratio ($\sigma m/\sigma seq$). As the stresses at the notched section reach the limiting values determined from the elliptical fracture criterion, macroscopic fracture failure in the notched bar occurs.

Tanaka et al., (2010) studied the two specific subjects related to the fatigue strength and life of notched bars under combined torsional and axial loading. The first subject is the fatigue thresholds of materials with small defects. The fatigue threshold of materials with small defects or sharp notches is not controlled by the initiation of fatigue cracks, but by their propagation. Authors believe that the *R*-curve method is very useful to predict the fatigue thresholds of notched components. A small crack nucleated at the notch root becomes non-propagating when the applied stress intensity factor drops below the resistance of the material. It is important that the *R* curve is independent of loading conditions and only the applied stress intensity factor depends on loading conditions. In the present paper, the *R*-curve method was successfully applied to predict the fatigue thresholds of holed tubes made of carbon steels under in-phase and out-of-phase combinations of cyclic torsion and axial loading. The second subject is an anomalous phenomenon of notch strengthening found in torsional fatigue of circumferentially notched round bars of austenitic stainless steel. In torsional fatigue of circumferentially notched bars of austenitic stainless steel, the fatigue life of notched bars was found to be longer than that of smooth bars and to increase with increasing stress concentration under the same amplitude of the nominal torsional stress. On the basis of the electrical potential monitoring of the initiation and propagation of small cracks at the notch root, the crack initiation life decreased with increasing stress concentration, while the crack propagation life increased.

Ohkawa et al., (2011) studied notch effect in austenitic stainless steel under cyclic torsion depending on the superposition of static tension.

In pure torsion, the rubbing of the serrated factory roof type crack faces delays the crack growth along the notch root. Thus, the lifetime in notched specimen becomes longer than in smooth specimen. However, in cyclic torsion with static tension, the flat crack path and mean tensile stress reduce the influence of the crack face contact. Accordingly, shorter lifetime resulted from higher strain concentration at the notch root. Crack growth in low carbon steel under cyclic torsion is highly affected by the ferrite/pearlite banded microstructure besides the addition of static tension. Because of a small amount of the crack face contact, the reduction of lifetime in notched specimen is revealed irrespective of superposition of static tension.

Tanaka et al., (2014) studied circumferentially notched bars of austenitic stainless steel, SUS316L, and carbon steel, SGV410, with three different notch-tip radii and were fatigued under cyclic torsion without and with static tension. The torsional fatigue life of SUS316L was found to increase with increasing stress concentration under the same nominal shear stress amplitude. It is revealed that the crack initiation life decreased with increasing stress concentration, while the crack propagation life increased. The superposition of static tension on cyclic torsion causes notch weakening. The notch-strengthening effect in torsional fatigue was not found in carbon steels, SGV410. The difference in the crack path of small cracks near notch root between stainless steel and carbon steel gives rise to the difference in the notch effect in torsional fatigue. Under higher stresses, the fracture surface was smeared to be flat. The fracture surfaces of SG/V410 became smoother with increasing stress amplitude and notch acuity.

Chandra et al., (2014) studied modeling results for fatigue crack growths of a semi-elliptical surface crack in a V-shaped notchedround bar under uniform cyclic tension. All the analyses of modeling were carried out by using a software package featuring the boundary element method. The *J*-integral technique was used to compute the stress intensity factors (SIFs), and the NASGRO crack growth rate was chosen to simulate the fatigue crack growths. Mechanical and fracture properties of AZ-6A-T5 magnesium alloy were used for this analysis. Crack shape evolutions for different crack aspect ratios and the corresponding SIFs may be correlated to study the behaviour of

crack growths. An unstable crack growth was observed when the evolving crack aspect ratio was between 0.6and 0.7.

Luo et al., (2015) studied the brazed structures having geometrical discontinuities like fillets working as notches. These notches have great effect on creep crack initiation and propagation. The notch effect on creep damage for HastelloyC276-BNi2 brazed joint, and the effects of notch type, notch radius and notch angle on creep damage have been investigated. The results show that the creep damage initiates in the filler metal. Different notch types bring different stress states, and generate different stress triaxialities and equivalent creep strains (CEEQs), leading to different creep damages. The maximum creep damage is generated in the notch tip for V-type notch. For U-type notch, the location of the maximum creep damage moves from the notch tip to the inside gradually as the not chradius increases. With the increase of notch radius and notch angle, the failure time of creep damage increases for U-type and V-type notches. The creep failure is prone to happen to V-type notch because it belongs to sharp notch.

Review revealed that several works has been done on austenitic stainless steel, SUS 316L, carbon steel, SGV410, and AZ-6A-T5 magnesium alloy. The researchers mainly focused on FEM and FDM analysis. In the analysis the fracture testing and fatigue testing is mainly focused. It has been observed in literature review that the analysis of hardness on the SUP 9A notched bar has not been performed that's why it is been observed that the analysis is needed to be done in this area. In this literature review, the relevant informations are summarized, including: the definition, development and application of notched bar, the mechanical properties of SUP 9A steels is analysed.

IV. Experimental Work

In this experimental work, the specimens with V notch (Figure 1) and after conducting heat treatment on electric furnace (Figure 2)is analysed on UTM (Figure 3) by conducting fracture test. The material of specimen is SUP 9A. The test is conducted on these specimens with v notch and hardness to analyse the effect of hardness and notch on strength of material. The specimens are manufactured with the details as mentioned in table 1.

V. Specification of Experimental Setup

The most common testing machine used in tensile testing is the universal testing machine. This type of machine has two crossheads; one is adjusted for the length of the specimen and the other is driven to apply tension to the test specimen. The machine must have the proper capabilities for the test specimen being tested. There are four main parameters: force capacity, speed, and precision and accuracy. Force capacity refers to the fact that the machine must be able to generate enough force to fracture the specimen. The machine must be able to apply the force quickly or slowly enough to properly mimic the actual application. The test process involves placing the test specimen in the testing machine and slowly extending it until it fractures. During this process, the elongation of the gauge section is recorded against the applied force.

Machine Specifications are as follows:

Model: AMT 20 UTM
Capacity: 20 Tonnes
Load Range: 0-20 kN
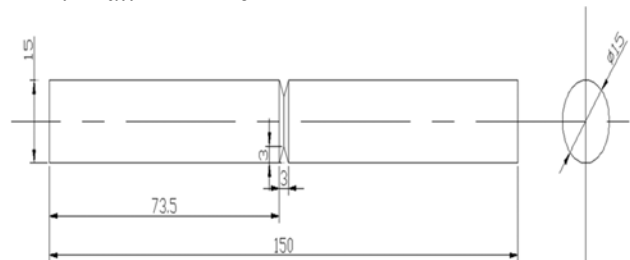Least Count: 0.02 kN
Max. Dia.:   20mm
Min. Dia.:   6mm

Figure 1: Specimen with V Notch

Figure 2: Electric Furnace

Figure 3: Experimental setup of fracture test

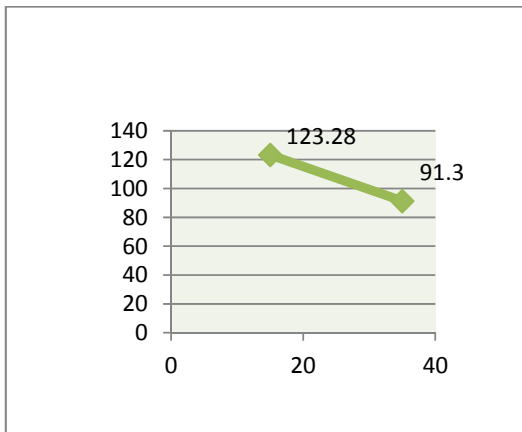| S. N o.	Speci men V Notch	Hardn ess (HRC)	Load (kN)	Displace ment (mm)
1	√	15	123.28	40.59
2	√	35	91.30	42.48

Table 1

Figure 4: Relation between Hardness and Tensile Strength

VI. Conclusion

After conducting experiments, it can easily be concluded that there is impact of change of hardness on tensile strength of material. Graph (figure 4) shows that after increasing the hardness of notched SUP 9A turned bar, tensile strength of bar is decreased. This paper may be helpful for industry and research & development department to analyse the effect to hardness on notched bar.

References

1. Atzori, B., Berto, F., Lazzarin, P., &Quaresimi, M. (2006). Multi-axial fatigue behaviour of a several notched carbon steel. *International Journal of Fatigue, 28*(5–6), 485-493.

2. Carpinteri, A. (1993). Shape change of surface cracks in round bars under cyclic axial loading. *International Journal of Fatigue, 15*, 21-26.

3. Carpinteri, A., Brighenti, R., &Vantadori, S. (2003). Circumferentially notched pipe with an external surface crack under complex loading. *International Journal of Mechanical Sciences, 45*(12), 1929-1947.

4. Carpinteri, A., Brighenti, R., &Vantadori, S. (2006). Surface cracks in notched round bars under cyclic tension and bending. *International Journal of Fatigue*, *28*(3), 251-260.

5. Carpinteri, A., &Vantadori, S. (2008). Surface cracks in round bars under cyclic tension or bending. *Key Engineering Materials*, *378-379,* 341-354.

6. Carpinteri, A., &Vantadori, S. (2009). Sickle-shaped surface crack in a notched round bar under cyclic tension and bending. *Fatigue & Fracture of Engineering Materials & Structures, 32*(3), 223-232.

7. Couroneau, N., & Royer, J. (1998). Simplified model for the fatigue growth analysis of surface cracks in round bars under mode I. *International Journal of Fatigue, 20*(10), 711-718.

8. Durmus, A., Bayram, A., &Uguz, A. (2002). Rapid determination of the fracture toughness of metallic materials using circumferentially notched bars. *Journal of Materials Engineering and Performance, 11*(5), 571-576.

9. Hayhurst, D. R., Dimmer, P. R., & Morrison, C. J. (1984). Development of continuum damage in the creep rupture of notched bars. *Philosophical Transactions of the Royal Society of London. Series A, 311*(15-16), 103-129.

10. Hayhurst, D. R., Dyson, B. F., & Lin, J. (1994). Breakdown of the skeletal stress technique for lifetime prediction of notched tension bars due to creep crack growth. *Engineering Fracture Mechanics, 49*(5), 711-726.

11. Hayhurst, D. R., Lin, J., &Hayhurst, R. J. (2008). Failure in notched tension bars due to high-temperature creep: Interaction between nucleation controlled cavity growth and continuum cavity growth. *International Journal of Solids and Structures*, *45*(7-8), 2233-2250.

12. Lin, X. B., & Smith, R.A. (1998). Fatigue growth simulation for cracks in notched and unnotched round bars. *International Journal of Mechanical Sciences, 40*(5), 405-419.

13. Lin, X. B., & Smith, R. A. (1999). Shape evolution of surface cracks in fatigued round bars with a semi-circular circumferential notch. *International Journal of Fatigue*, *21*(9), 965-973.

14. Levan, A., & Royer, J. (1993). Part-circular surface cracks in round bars under tension, bending and twisting. *International Journal of Fatigue, 61*, 71-99.

15. Ng, L., &Zarrabi K. (2008). On creep failure of notched bars. *Engineering Failure Analysis, 15*(6), 774-786.

16. Nord, K. J., & Chung, T. L. (1986). Fracture and surface flaws in smooth and threaded round bars. *International Journal of Fatigue, 30*, 47-55.

17. Othman, A. M., Hayhurst, D. R., & Dyson, B. F. (1993). Skeletal point stresses in circumferentially notched tension bars undergoing tertiary creep modelled with physically-based constitutive equations. *The Royal Society of London. 441*, 343-358.

18. Ohkawa, C., &Ohkaw, I. (2011). Notch effect on torsional fatigue of austenitic stainless steel: Comparison with low carbon steel. *Engineering Fracture Mechanics, 78*(8), 1577-1589.

19. Tanaka, K., Akiniwa, Y., Morita, K., &Wakita, M. (1998). Resistance-Curve Method for Predicting Propagation Threshold of Short Fatigue Cracksat Notches. *Engineering Fracture Mechanics, 30*(6), 863-876.

20. Tanaka, K., Hashimoto, A., Narita, J., & Noboru. E. (2009). Fatigue Life of Circumferentially Notched Bars of Austenitic Stainless Steel under Cyclic Torsion with and without Static Tension. *Journal of the Society of Materials Science Japan, 58*(12), 1044-1050.

21. Tanaka, K. (2010). Small fatigue crack propagation in notched components under combined torsional and axial loading. *Procedia Engineering, 2*(1), 27-46.

22. Tanaka, K. (2014). Crack initiation and propagation in torsional fatigue of circumferentially notched steel bars. *International Journal of Fatigue, 58*, 114-125.

23. Wang, W. Z., Liu, W. F., & Wang, X. T. (2010). Fracture Test and Analysis of Notched Bars Fabricated from Q235 Steel at Room Temperature. *Applied Mechanics and Materials, 34-35,* 1406-1414.

24. Wang, W., Qian, X., Su, R., &Wang, X. (2010). Tensile tests and analyses of notched specimens fabricated from high strength steels using a generalized yield model. *Fatigue & Fracture of Engineering Materials & Structures, 33*(5), 310 -319.

25. Webster, G. A., Nikbin, K. M., &Biglari F. (2004). Finite element analysis of notched bar skeletal point stresses and dimension changes due to creep. *Fatigue & Fracture of Engineering Materials & Structures, 27*(4), 297-303.

26. Zhang, Q. Y., & Liu, Y. (1992). Determining local stress and limit load in a thick walled tube with a hoop direction U-shaped notch under tension. *International Journal of Pressure Vessels and Piping*, *51*(3), 361-372.

27. Chandra, D., Purbolaksono, J., Nukman, Y., Liew, H., Singh, R.,& Hassan, M. (2014). Fatigue growth of a surface crack in a V-shaped notched round bar under cyclic tension. *J Zhejiang Univ-Sci A (ApplPhys&Eng) 15*(11), 873-882.

28. Luo, Y., Jiang, W., Zhang, W., Zhang, Y. C., Woob, W., &Tuc, S. T. (2015). Notch effect on creep damage for Hastelloy C276-BNi2 brazing joint. *Materials and Design, 84,* 212–222.

COMPARATIVE STUDY OF FUNCTIONAL GROUPS IN NATURAL FIBERS: FOURIER TRANSFORM INFRARED ANALYSIS (FTIR)

Muhammad Khusairy Bin Bakri[1], Elammaran Jayamani[2]

[1,2]Faculty of Engineering, Computing and Science, Swinburne University of Technology Sarawak Campus, Jalan Simpang Tiga, 93350, Kuching, Sarawak, Malaysia.

Email: elammaranj@gmail.com[2]

Abstract — Throughout this research, the fundamental characterization of functional groups bond structure and the behavior of natural fiber before and after treatment were understood. Fibers were obtained by extracting it from the bamboo, betel nut and hemp plants. The Infrared spectrum of natural fiber were obtained and tested using Fourier transform infrared (FTIR) spectroscopy in the range of 400 cm^{-1} to 4000 cm^{-1} for untreated and alkali treated fibers. It was prepared quantitatively and qualitatively according to ASTM E168-06 and ASTM E1252-98 standards. Based on the Infrared spectral, the functional groups of the plant fiber were then collected and classified. The effect of chemical treatment was evaluated and discussed. Based on the result obtained, the bond structure of certain functional groups (i.e. hemicellulose, cellulose, and lignin) was removed and changed due to the alkaline treatment.

Index Terms—Natural Fiber, Alkaline Treatment, Infrared Spectral, Qualitative and Quantitative Anaysis.

I. INTRODUCTION

Fourier transform infrared (FTIR) spectroscopy is used to obtain infrared (IR) spectra of inorganic and organic materials. This technique measured the IR radiation absorption or transmittance by the sample material against its wavelength or wavenumbers. IR radiation causes the molecule structure to vibrate as the material being exposed to it. According to Mosiewicki et al. [1], the dipole moment of molecule in the material must be changed in order for a motion of vibration to be IR active. The total internal energy of a molecule can be resolved into the sum of vibrational, rotational and electronic energy levels. Furthermore, FTIR can also be used to determine the interactions between matter and electromagnetic fields in the IR region. The molecular components and structures can be identified through the IR absorption bands. The higher the changes in the magnitude of the molecule, the higher the intensity of the band created. The IR absorption

bands are used to understand the characteristic of polymer interfaces and modified natural fibers in composite materials [1]. In general, a frequency will be strongly absorbed if its photon energy coincides with the vibrational energy levels of the molecule. IR spectroscopy is therefore a very powerful technique which provides fingerprint information on the chemical composition of the sample. FTIR spectrometer is found in most analytical laboratories.

A basic IR spectrum is essentially a plotted graph of infrared light absorbance or transmittance (vertical axis) vs. frequency or wavelength (horizontal axis). Typical frequency units used in IR spectra are reciprocal centimeters (it is also called as wavenumbers), with the symbol cm^{-1}. The IR wavelength units are commonly given in micrometers (formerly called "microns"), symbol μm, which are related to wavenumbers in a reciprocal way. According to Stuart [2], the IR spectrum is divided into three sub-regions: the near-IR, approximately 14000 cm-1 – 4000 cm^{-1} (0.8 μm – 2.5 μm

wavelength), the mid-IR approximately 4000 cm^{-1} – 400 cm^{-1} (2.5 μm – 25 μm wavelength) and the far-IR approximately less than 400 cm^{-1} – 10 cm^{-1} (25 μm –1000 μm wavelength). Besides that, based on Stuart [2] and Mosiewicki et al. [1], majority of analytical FTIR applications used are in mid-IR range, which is approximately around 4000 cm^{-1} – 400 cm^{-1}. The higher-energy near-IR can excite overtone or harmonic vibrations. The mid-IR may be used to study the fundamental vibrations and associated rotational-vibrational structure. The far-IR lying adjacent to the microwave region has low energy and may be used for rotational spectroscopy. The names and classifications of these sub-regions are pacts, and are only roughly estimated based on the relative molecular or electromagnetic properties.

Based on the research made by Ramadevi et al. [3], FTIR can be used to analyze the potential existing chemical bonding for the treated and untreated fibers. According to Rowell et al. [4], at 3400 cm^{-1} inside the large band, it is normally related due to the bonded O-H group stretching vibrations in the presence of carbohydrate (cellulose + hemicellulose) and hydroxyl groups. As for abaca fiber alkaline-treated, the removal of the hemicellulose component causes the 3347 cm^{-1} band assigned to the alcohol group to be reduced. Another peak due to the presence of alcohol group of cellulose OH deformation that appeared at 1310 cm-^{1} was reduced due to alkaline treatment. The FTIR can be used to investigate the bonding characteristics between natural fiber and matrices in the natural composite material. Based on the research made by Muniandy et al. [5], it showed that the formation of a bond between the silane coupling agents gives better interaction between the rubber matrix and rattan fiber. These peaks can be found in the region of 1586 cm^{-1} and 1172 cm^{-1} which corresponds to Si-O-C silanes and C-N stretching.

FTIR spectroscopy test on plantain fiber and composites are normally done to determine the strength of the composites and fiber before and after treatment. According to Ihueze et al. [6], there is a characteristic of O-H hydrogen bond stretching and vibration at a strong peak of 3406.40 cm^{-1}. Based on Ihueze et al. [6], this high peak of O-H stretching is due to the presence of intermolecular hydrogen bonding that tends to shift higher absorbance. The result obtained by Ihueze et al. [6] is coherent with the result observed by earlier works done by Clemsons et al. [7] and Rowell [8]. In this research, the fundamental behavior of natural fiber of bamboo, betel nut and hemp, before and after treatment were investigated. Respectively, all experiments were carried out using FTIR spectroscopy by quantitative and qualitative method and technique.

II. MATERIALS

Bamboo and betel nut were obtained from small local traditional agricultural and industrial factory in Kuching, Sarawak, Malaysia. Betel nut (*areca catechu*) was grown vastly in rural area of Sarawak typically and mainly Borneo Island. The fibers were extracted from the betel nut fruit rind (shells cover the nut of the fruits). Each betel nut fruit can produce around 2.5 - 2.8 g of fiber approximately depending on the size of the betel nut. Bamboo (*bambusa shrep*) is widely and wildly available in Sarawak forest. Bamboo is commonly used as a cooking utensil for preparing '*Pansuh Ayam*' (local Sarawak delicacy). The steam explosion technique was used in order to extract the fibers from raw bamboo trees. Hemp fibers were obtained from the skin or bark (or bast) of hemp (*cannabis sativa*) that imported from the local China market. Hemp is usually used to produce oil and create textile base products.

Sodium hydroxide (NaOH) with product code 'S/4920/AP1' was supplied by Fisher Scientific, UK. It is caustic soda pellet forms highly alkaline, odorless and completely soluble when react with water. Universal Indicator Solution was supplied by Fisher Scientific, UK.

III. METHOD

Fibers obtained were divided into two parts; untreated and treated fibers. For the treated fiber, the fiber underwent treatment using alkaline solution. The alkaline solution was prepared by mixing 5wt % of sodium hydroxide with distilled water. The solution was stirred vigorously to ensure the caustic soda completely soluble in water. The alkaline solution was then

poured into a beaker filled with fiber. The solution and fiber were stirred properly and were left for 30 min for reaction to occur. The fibers were filtered and wash with distilled water till the pH is neutralized. Universal Indicator Solution was used to test the pH level. Meanwhile, for the untreated fibers, the fibers were washed with distilled water to remove any dirt or impurity. Both untreated and treated fibers were then dried up in the oven at 60 °C for 48 hours to remove the moisture. The drying oven with model name 'ECOCELL EC55' with brand name 'MMM Group' equipped by Fisher Scientific, UK. The dried untreated and treated fibers were then blended into powder form. The samples were kept under 24±3 °C in temperature, 65 % in relative humidity and 101 kPa in pressure for 24 hours before testing. The composites were conditioned according to ASTM E41-92 [9] standards.

IV. FOURIER TRANFORM INFRARED (FTIR) SPECTROSCOPY TESTING

FTIR spectroscopy was used to understand the functional groups and its molecular bond structure in the range of 4000 cm^{-1} to 400 cm^{-1}. The FTIR spectroscopy with a model name of 'IRAffinity-1' was used and equipped by Shimadzu (Japan) Corporation. Approximately 0.5 mg of powder sample was mixed with approximately 100 mg of dry powder, potassium bromide (KBr) in a small agate pestle to create a sample pellet for FTIR spectroscopy. Then, the mixture sample pellet was then taken into the sample holder inside the spectroscopy. Vacuum pressure was applied onto the mixture sample pellet inside the spectroscopy. The vacuum pressure causes the removal of moisture inside spectroscopy. IR spectrum bands were obtained when laser of infrared projected onto the mixture pellets. All the information obtained was analyzed according to ASTM E168-06 [10] and ASTM E1252-98 [11] standards.

V. RESULTS AND DISCUSSION

A. BAMBOO FIBERS

Figure 1 shows the FTIR spectra of untreated and treated bamboo fibers. In Figure 1, the region of the broad absorption band at 3500 cm^{-1} to 3300 cm^{-1} for untreated and treated fibers are characterized with O-H stretching and H-

bonded bond structure that mostly contains major functional groups of phenols, alcohols and waters. The O-H stretching and H- bonded broad absorption band in the region is decreased after alkaline treatment. These are due to decrease in functional group of phenolic or aliphatic hydroxyl in the fiber due to reaction with sodium hydroxide that promotes free hydroxyl that caused the addition of extra peak in free hydroxyl bond structure at 2873.06 cm^{-1} and 3597.24 cm^{-1}. A small peak at 2895.15 cm^{-1} for the untreated and 2912.51 cm^{-1} for the treated was attributed to the C-H stretching and O-H stretching bond structure that contains a functional group of alkanes (cellulose and lignin) and carboxylic acids. According to Khalil et al. [12], small peak in the region of the C-H stretching bond structure can also include a functional group of methyl (CH$_3$), methylene (CH$_2$), and aliphatic saturated (CH).
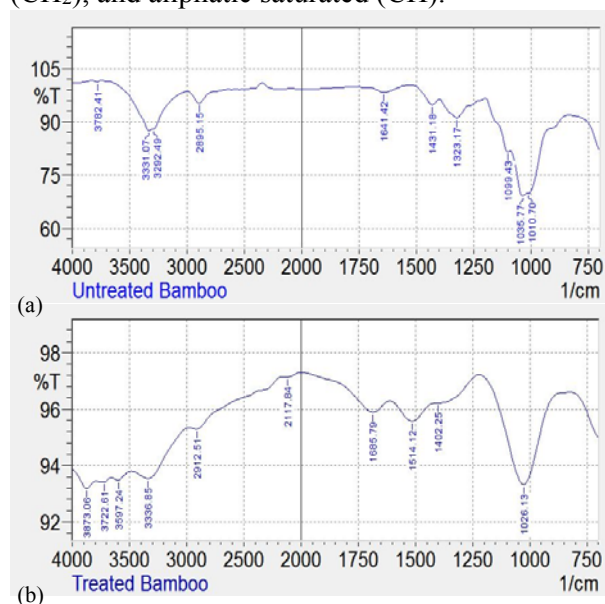

Figure 1 Fourier transform infrared spectroscopy analysis of (a) untreated bamboo fiber; and (b) treated bamboo fiber.

Table 1 shows the characterization of untreated and treated bamboo fibers as extracted from Figure 1. For untreated agarwood fiber, it shows the small peak band at 2117.84 cm^{-1}, are characterized as the C≡C stretching and C≡N stretching bond structure that contain functional group of nitriles and alkynes groups, the small peak at 1641.42 cm^{-1} is characterized as the C=C stretching bond structure from the functional group of alkenes (lignin), the peak at 1431.42 cm^{-1} is characterized as the C-H bending bond

from the functional group of alkanes (cellulose, hemicellulose and lignin), and the peak at 1099.43 cm^{-1}, 1035.77 cm^{-1} and 1010.70 cm^{-1} are characterized as the C-O stretching bond structure from the functional group of alcohol (cellulose, hemi-cellulose and lignin), carboxylic acids, esters and ethers.

Table 1 Characterization spectral analysis of bamboo fiber

Bond - Functional Group	Untreated bamboo fiber (wavenumber, cm^{-1})	Treated bamboo fiber (wavenumber, cm^{-1})
O-H stretching, Free hydroxyl - Alcohol, Water, Phenols	3782.41	3873.06, 3722.61, 3597.24
O-H stretching, H-bonded - Alcohol, Water, Phenols	3331.07, 3292.49	3336.85
C-H stretching, O-H stretching - Alkanes (CH; CH$_2$; CH$_3$), Carboxylic Acids	2895.15	2912.51
C≡C stretching, C≡N stretching – Nitriles, Alkynes	2117.84	-
C=C stretching - Alkenes (lignin)	1641.42	1685.79
C-H bending - Alkanes (cellulose; hemi-cellulose; lignin)	1431.42	1514.12, 1402.25
C-O stretching - Alcohol (cellulose; hemi-cellulose; lignin), Carboxylic Acids, Esters, Ethers	1099.43, 1035.77, 1010.70	1026.13

It is noticed that alkaline treatment caused the peak band at 2117.84 cm^{-1} to be disappeared. The disappearing of the peak may be due to the breaking of the triple bond structure of C≡C stretching from the functional group of nitriles and C≡N stretching bond structure of the functional group of alkynes into the double bond structure C=C and C=N. By compared with treated fibers, there was reduced in the intensity of the bands at 1099.43 cm^{-1} characterized as the C-O stretching band structure of the functional group of alcohol due to alkaline treatment. Furthermore, there are combinations of two different small peak band of 1035.77 cm^{-1} and 1010.70 cm^{-1} that form a single peak 1026.13 cm^{-1} after the alkaline treatment. According to Cao et al. [13] and Hinterstoisser et al. [14], the peaks band located in the region of 1100 cm-1 to 1000 cm^{-1} are also characterized as the C-O stretching bond structure of the functional group of glycosides linkage. The result obtained agreed with study reported by Xu et al. [15].

B. BETEL NUT FIBERS

Figure 2 shows the FTIR spectra of untreated and treated betel nut fibers. In Figure 2, the region of the broad absorption band at 3500 cm^{-1} to 3000 cm^{-1} for the untreated and treated fiber are characterized with O-H stretching and H-bonded bond structure that mostly contains major functional groups of phenols, alcohols and waters. The O-H stretching and H- bonded broad absorption band in the region is increased and the peak reduced after alkaline treatment. These are due to breaking of certain bond structure in functional group such as alkenes which forming O-H or H- bonded structure in the fiber after treatment. According to Ramadevi et al. [3], the O-H stretching, H- bonded and free hydroxyl were due to the presence of carbohydrates (hemicellulose and cellulose). The results obtained were also reported in Dwivedi and Mehta [16]. A small peak at 2906.73 cm^{-1} for the untreated and 2939.52 cm^{-1} for the treated was attributed to the C-H stretching and O-H stretching bond structure that contains groups of

alkanes (cellulose and lignin) and carboxylic acids.
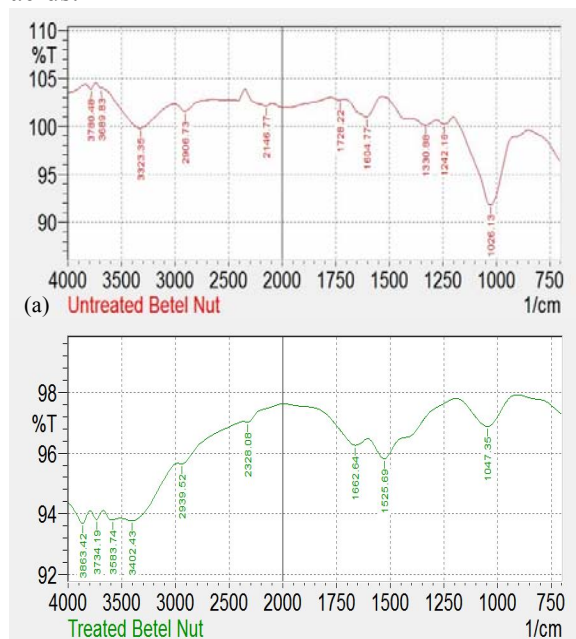

(a) Untreated Betel Nut

Treated Betel Nut

Figure 2 Fourier transform infrared spectroscopy analysis of (a) untreated betel nut fiber; and (b) treated betel nut fiber.

Table 2 shows the characterization of untreated and treated betel nut fibers as extracted from Figure 2. For untreated betel nut fiber, it shows the small peak band at 2146.377 cm⁻¹ are characterized as the C≡C stretching and C≡N stretching bond structure from the functional group of nitriles and alkynes, the small peak at 1728.22 cm⁻¹ and 1604.77 cm⁻¹ is characterized as the C=C stretching bond structure from the functional group of alkenes (lignin), the small peak at 1330.88 cm⁻¹ and 1242.16 cm⁻¹ is characterized as the C-H bending bond structure of the functional group of alkanes (cellulose, hemicellulose and lignin), and the peak at 1026.13 cm⁻¹ are characterized as the C-O stretching bond structure of the functional group of alcohol (cellulose, hemi-cellulose and lignin), carboxylic acids, esters and ethers.

Table 2 Characterization spectral analysis of betel nut fiber

Bond - Functional Group	Untreated betel nut fiber (wavenumber, cm⁻¹)	Treated betel nut fiber (wavenumber, cm⁻¹)
O-H stretching, Free hydroxyl - Alcohol, Water, Phenols	3780.48, 3689.83	3863.42, 3734.19, 3583.74
O-H stretching , H-bonded - Alcohol, Water, Phenols	3323.35	3402.43
C-H stretching, O-H stretching - Alkanes (CH; CH₂; CH₃), Carboxylic Acids	2906.73	2939.52
C≡C stretching, C≡N stretching – Nitriles, Alkynes	2146.77	2328.08
C=C stretching - Alkenes (lignin)	1728.22, 1604.77	1662.64, 1525.69
C-H bending - Alkanes (cellulose; hemi-cellulose ; lignin)	1330.88, 1242.16	-

Compared with the treated fibers, there was reduced in the intensity of the bands at 1330.88 cm⁻¹ and 1242.16 cm⁻¹ characterized as the C-H bending bond structure of the functional group of alkanes due to alkalization treatment. The alkaline treatment caused the breaking of the C-H bending bond structure of functional group alkanes that promote to H- bonding and free hydroxyl bond structure. Thus, this promotes extra band in that functional group of alcohol, water and phenols.

C. HEMP FIBERS

Figure 3 shows the FTIR spectra of untreated and treated hemp fibers. In Figure 3, the region of the broad absorption band at 3500 cm⁻¹ to 3000 cm⁻¹ for the untreated and treated fiber are characterized with O-H stretching and H-bonded bond structure that mostly contains major functional groups of phenols, alcohols and waters. The O-H stretching and H- bonded bond

structure of the broad absorption band in the region is decreased after alkaline treatment. These are due to decrease in functional group of phenolic or aliphatic hydroxyl in the fiber due to reaction with sodium hydroxide. A small peak at 2893.22 cm^{-1} for the untreated and 2893.22 cm^{-1} for the treated was attributed to the C-H stretching and O-H stretching bond structure that contains a functional group of alkanes (cellulose and lignin) and carboxylic acids.
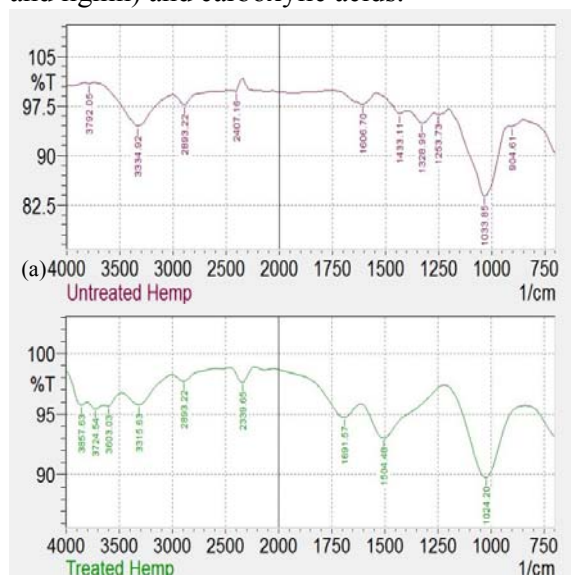

Figure 3 Fourier transform infrared spectroscopy analysis of (a) untreated hemp fiber; and (b) treated hemp fiber.

Table 3 shows the characterization of untreated and treated hemp fibers as extracted from Figure 4. For untreated hemp fiber, it shows the small peak band at 2407.16 cm^{-1} is characterized as the C≡C stretching and C≡N stretching from the functional group of nitriles and alkynes, a peak at 1606.70 cm^{-1} is characterized as the C=C stretching from the functional group of alkenes (lignin), small peak at 1433.11 cm^{-1}, 1328.95 cm^{-1} and 1253.73.11 cm^{-1} characterized as the C-H bending bond structure from the functional group of alkanes (cellulose, hemicellulose and lignin), the peak at 1033.85 cm^{-1} are characterized as the C-O stretching bond structure from the functional group of alcohol (cellulose, hemi-cellulose and lignin), and the small peak at 904.61 cm-1 characterized as C-H "oop" bond structure of the functional group of aromatic (lignin). The results obtained were reported almost similar to Garside and Wyeth [17].

Table 3 Characterization spectral analysis of hemp fiber

Bond - Functional Group	Untreated hemp fiber (wavenumber, cm^{-1})	Treated hemp fiber (wavenumber, cm^{-1})
O-H stretching, Free hydroxyl - Alcohol, Water, Phenols	3792.05	3857.63, 3724.54, 3603.03
O-H stretching, H-bonded, Free hydroxyl - Alcohol, Water, Phenols	3334.92	3315.63
C-H stretching, O-H stretching - Alkanes (CH; CH$_2$; CH$_3$), Carboxylic Acids	2893.22	2893.22
C≡C stretching, C≡N stretching – Nitriles, Alkynes	2407.16	2339.65
C=C stretching - Alkenes (lignin)	1606.70	1691.51, 1504.48
C-H bending - Alkanes (cellulose; hemi-cellulose; lignin)	1433.11, 1328.95, 1253.73	-
C-O stretching - Alcohol (cellulose; hemi-cellulose; lignin), Carboxylic Acids, Esters, Ethers	1033.85	1024.20
C-H "oop" – Aromatic (lignin)	904.61	-

By compared with treated fibers, there was reduced in the intensity of the bands at 1433.11 cm^{-1}, 1328.95 cm^{-1} and 1253.73.11 cm^{-1} characterized as the C-H bending from the functional group of alkanes due to alkalization treatment. Furthermore, there was a reduction in the intensity of the bands at 904.61 cm^{-1} characterized as C-H "oop" bond structure of functional group of aromatic. This caused disappearing of smell from the hemp fibers.

D. EFFECT OF ALKALINE TREATMENT

Sodium hydroxide (NaOH) was used widely in treatment of natural fibers. Its helps in modify the natural cellulose fiber either by bond structure or its functional groups. Alkaline treatment caused the increase in the amount of amorphous cellulose than crystalline cellulose. H-bonded bond structure in the fiber network structure was removed due to alkaline treatment. However, not all fibers tend to interact when reacted with sodium hydroxide. Alkaline treatment or mercerization is the most common method to produce quality fibers [18]. The mercerization is a process that allows natural fibers such as vegetable, wood and etc. to interact with low concentrated solution from strong base [19]. The process caused swelling structure due to changes in fine structure, morphology, mechanical and dimension properties [19].

Due to alkaline treatment, the alkaline sensitive hydroxyl groups (O-H bond structure) present in the natural fiber molecules were broken. It then react with water, phenols or alcohols molecules groups (H-O-H bond structure) and move in or out from the fiber structure depending on the characteristic of fiber toward the reaction of alkaline. Thus, the remaining of the reactive molecules indirectly forms the fiber cell of -O-Na bond structure between the cellulose molecular chains [20]. Thus, some hydrophilic hydroxyl groups are reduced and the fibers moisture resistance properties are increased. Some of the impurity, pectin, hemicelluloses, hemi-cellulose, lignin, wax and oil that covering were removed from the fibers as due to alkaline treatment [21]. Alkaline treatment also caused fibrillation that breaks the composites fiber bundle into smaller fibers and reduces the fiber diameter. Increase in the aspect ratio of the fiber lead to enhanced interface adhesion between fiber and matrix due to higher surface roughness. The sound absorption, mechanical, water absorption and thermal behaviors of the composites are improved significantly by this treatment. According to Kabir et al. [22], the treated fibers are known to have lower lignin content than the untreated fibers. Furthermore, the chemical treatment also partially removes the oil and wax that cover fibers and distension of crystalline cellulose order [22].

VI. CONCLUSIONS

Based on the result obtained, the bond structure in certain functional groups (this includes hemicellulose, cellulose, and lignin) was removed and changed due to the alkaline treatment. Furthermore, change in the bond structure of carbon and hydrogen gave an effect on the absorption properties of fiber. It is known that alkaline treatment removed the smell of the fiber and change the absorption properties of fiber. It becomes stronger and rougher than the untreated fibers. By understand the natural fiber characteristics; it can help improve the mechanical, acoustical, thermal and morphological properties of composites or related materials.

REFERENCES

[1] M.A. Mosiewicki, N.E. Marcovich, and M.I. Aranguren, "In Interface Engineering of Natural Fibre Composites for Maximum Performance," N. Zafeiropoulos, Eds. Woodhead Publishing: Cambridge, vol. 1, chapter 4, pp. 117-145, Feb 2011.

[2] B.H. Stuart, "In Infrared Spectroscopy: Fundamentals and Applications," B.H. Stuart, Eds. Wiley: New York, vol. 1, chapter 3, pp. 45-70, June 2004.

[3] P. Ramadevi, D. Sampathkumar, C.V. Srivasa, and B. Bennehalli "Effect of Alkali Treatment on Water Absorption of Single Cellulosic Abaca Fiber," Bioresources, vol. 7, no. 3, pp. 3515-3524. August 2012,

[4] J.S. Han, and J.S. Rowell, "Paper and Composites from Agro-based Resources," R.M. Rowell, R.A. Young, J.K. Rowell, Eds. CRS Press: Boca Raton, vol. 1, chapter 5 pp. 105-131, October, 1997.

[5] K. Muniandy, H. Ismail, and N. Othman, "Studies on Natural Weathering of Rattan Powder-Filled Natural Rubber Composites," Bioresources, vol. 7, no. 3, pp. 957-971, August 2012.

[6] C.C. Ihueze, C.E. Okafor, and C.I. Okoye "Natural Fiber Composite Design and Characterization for Limit Stress Prediction in Multiaxial Stress State," Journal of King Saud Uniersity – Engineering Science, vol. 27, no. 2 pp. 193-206, July 2015.

[7] C. Clemsons, R.A. Young, and R.M. Rowell, "Moisture Sorption Properties of Composite Boards from Esterified Aspen Fiber" Wood and Fiber Science, vol. 24, no. 3, pp. 353-363, July 1992.

[8] R.M. Rowell "International Encyclopedia of Composites," S.M. Lee, Eds, Wiley: New York, vol. 5, chapter 1-12, pp.1-548. June 1991.

[9] ASTM E41-92, "Terminology Relating to Conditioning," ASTM International, West Conshohocken, PA, vol. 14, pp. 1-2. 2010.

[10] ASTM E168-06, "Standard Practices for General Techniques of Infrared Quantitative Analysis," ASTM International, West Conshohocken, PA, vol. 13, pp. 1-17, 2015.

[11] ASTM E1252-98, "Standard Practice for General Techniques for Obtaining Infrared Spectra for Qualitative Analysis" ASTM International, West Conshohocken, PA, vol. 13, pp.1-13, 2013.

[12] A.S. Khalil, A.A. Rahim, K.K. Taha, and K.B. Abdallah, "Characterization of Methanolic Extracts of Agarwood Leaves," Journal of Applied and Industrial Science, vol. 1, no. 3, pp. 78-88, August 2013.

[13] Cao, Y. and H. Tan. "Structural characterization of cellulose with enzymatic treatment," Journal of Molecular Structure, vol. 705, no. 1-3, pp. 189-193, November, 2004.

[14] B. Hinterstoisser, M. Åkerholma, and L. Salména, "Effect of Fiber Orientation in Dynamic FTIR Study on Native Cellulose," Carbohydrate. Research, vol. 334, no.1, pp. 27-37, August 2001.

[15] G. Xu, L. Wang, J. Liu, and J. Wu, "FTIR and XPS Analysis of the Changes in Bamboo Chemical Structure Decayed by White-rot and Brown-rot Fungi," Applied Surface Science, vol. 280, no. 1, pp. 799-805, September 2013,.

[16] B.K. Dwivedi, and B.K. Mehta, "Chemical Investigation of Aliphatic Compounds of Piper Betle (Leaf Stalk)" Journal of Natural Product and Plant Resource, vol. 1, no. 2, pp. 18-24, 2011.

[17] P. Garside, and P. Wyeth, "Identification of Cellulosic Fibres by FTIR Spectroscopy: Differentiation of Flax and Hemp by Polarized ATR FTIR," Studies in Conservation, vol. 51, no. 3, pp. 205-211, 2006.

[18] D. Ray, B.K. Sarkar, A.K. Rana, and N.R. Bose, "Effect of alkali treated jute fibres on composite properties" Bulletin of Materials Science vol.24, no. 2, pp. 129-135, April 2001.

[19] A.K. Bledzki, and J. Gassan, "Composites reinforced with cellulose based fibres," Progress in Polymer Science, vol. 24, no. 2, pp. 221-274, May 1999.

[20] M.J. John, and R.D. Anandjiwala, "Recent Developments in Chemical Modification and Characterization of Natural Fiber-reinforced Composites," Polymer Composites, vol. 29, no. 2, pp. 187-207, December 2008.

[21] X. Li, L.G.; Tabil, and S. Panigrahi, "Chemical Treatments of Natural Fiber for Use in Natural Fiber-Reinforced Composites: A Review," Journal of Polymer and the Environment, vol. 15, no.1, pp. 25-33, January 2007.

[22] M.M. Kabir, H. Wang, K.T. Lau, and F. Cardona, "Chemical Treatments on Plant-based Natural Fibre Reinforced Polymer Composites: An Overview," Composites Part B: Engineering vol. 43, pp. 2883-2892, October 2012.